SOAR TECH

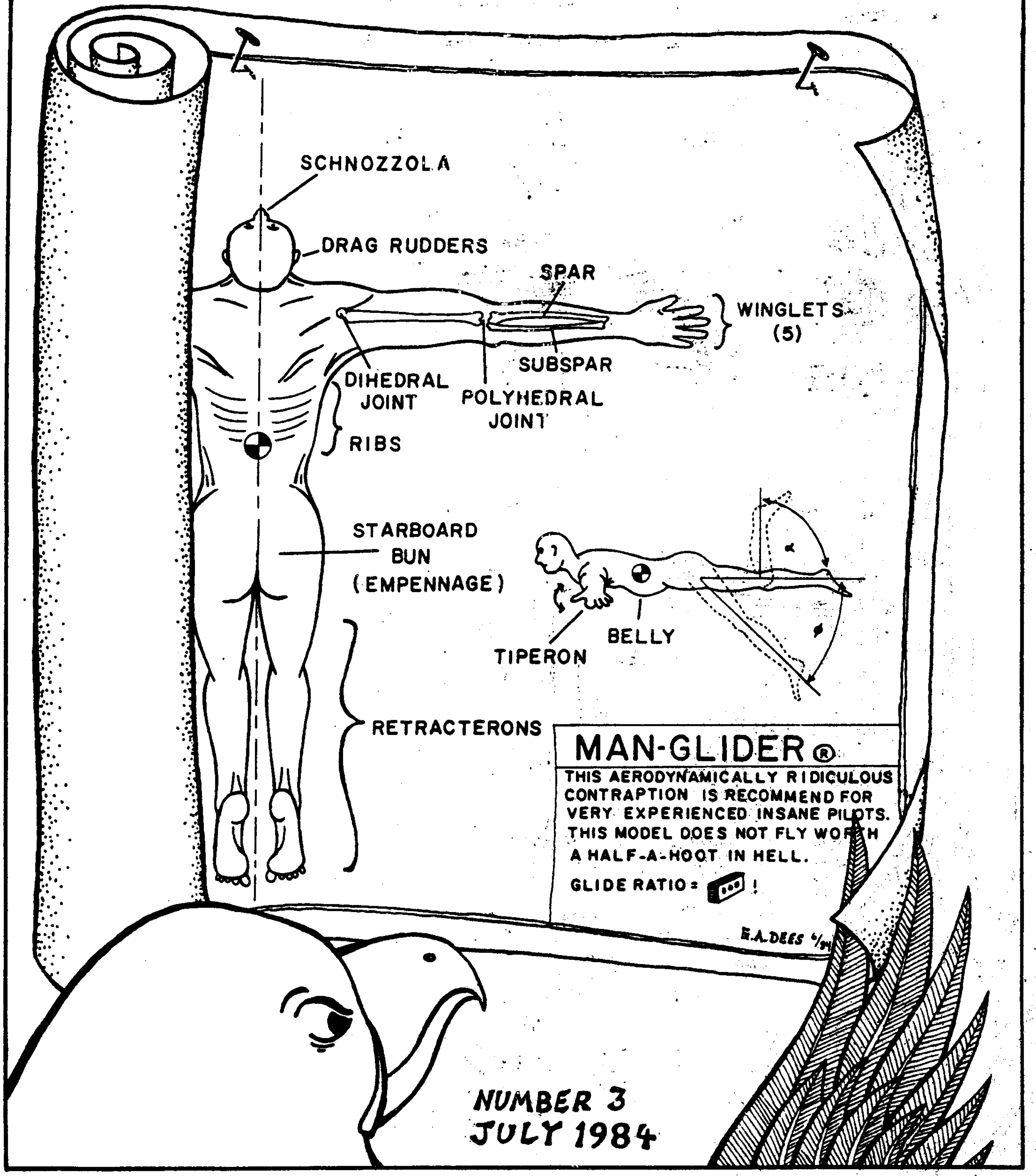

NUMBER 3
JULY 1984

July 1984

Dear Subscriber,

This third offering of Soartech is smaller than the first two. I promised to try to get them together faster, and the preparation is much simpler when I reduce its size. When I offered no. 2, I asked those of you who were interested in continuing to receive Soartech to send along an additional sum of $5 ($10 for foreign airmail). If you like getting Soartech, and think the cost is worth it, send another equal amount, and I'll mail you #4 when it is ready.

Soartech is published without profit to the editor or the writers of the material published. Our intention is to provide a forum for material that is too long or technical for the model press or for newsletters. I recognize that this kind of publication is not for everyone who flys model sailplanes. For those who do find this interesting, I am pleased to tell you that we have a good reservoir of new material to publish in future issues. It is nice to know that our well hasn't gone dry.

It may interest you who didn't write me, to know that "Soartech" no. 2 encountered a six month printing delay. The fact that it was so large strained our copying resources almost to the breaking point. I made a few copies for selected supporters and distributed them before I sent the master for printing. The news that it was out then appeared in certain publications, and many of you wrote me wondering where yours might have gone. Sorry for that delay, I'm going to have an easier time with these smaller issues. I hope you found no. 2 worth waiting for.

Herk Stokely
editor

SOARTECH #3 CONTENTS AND AUTHORS

"Soartech" is a NO-PROFIT English Language journal which provides technical information on the subject of Radio controlled Soaring and Sailplanes. The papers included have been provided freely by their authors, and should be used freely by others. Copying and further use of this material is encouraged. Common courtesy indicate that where it is used in other publications, the author and the source be given credit. Contributions are requested, and the editor asks that you correspond with him on any of the material that is included.

H. A. (Herk) Stokely
1504 Horseshoe Circle
Virginia Beach, Va. 23451 USA

PAPERS INCLUDED IN THE THIRD ISSUE

THE DRAG OF SAILPLANES

Bob Said, the editor of "Soaring" explains the significance of this paper in his introductory comments. Its contents apply to model sailplanes as fully as they do to manned aircraft and it should tell us clearly, how drag reduction efforts will pay off in our design and building efforts. Oran W. Nicks is a noted researcher (Deputy Director of NASA's Langley Research Center at the time of his retirement), and an excellent sailplane pilot as well. He is now a member of the faculty of Texas A&M University, where he is continuing his aeronautical research.

This paper is published with the permission of Mr. Nicks and "Soaring" (the magazine of the Soaring Society of America).

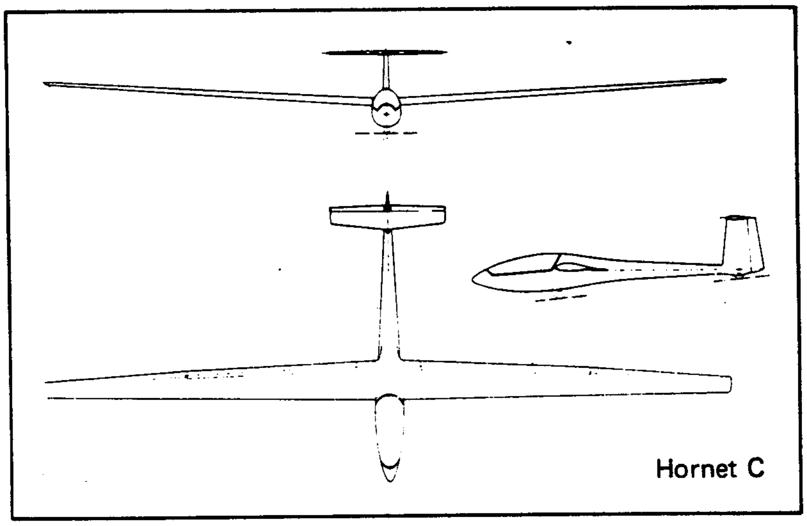

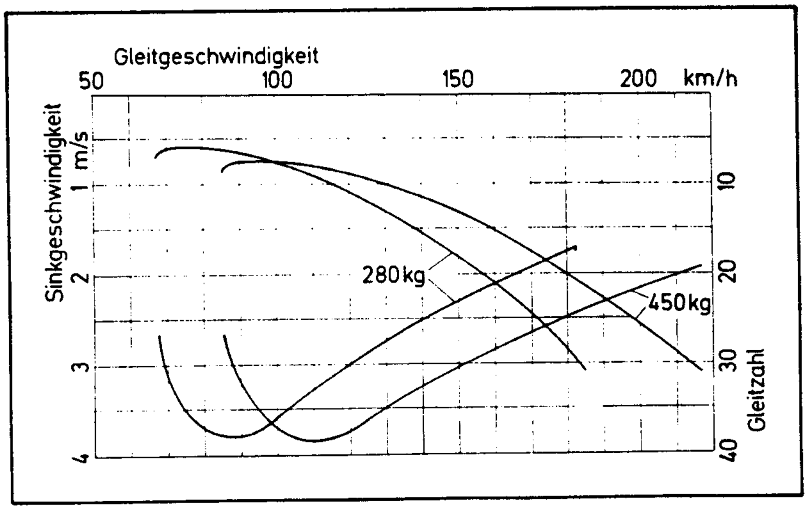

DRAG AWARENESS

In Simple English, The Lowdown on Slowdown

by ORAN W. NICKS

Two kinds of people talk about drag: those who don't know any more about it than you do, and those who know so much more that they can talk only in equations, coefficients, vector diagrams, Greek letters and other mystifying symbols. Here is an unusual discussion of drag by a man who knows a whole lot more about it than most of us, but who contrives to explain it in terms that even a glider pilot can understand. Want to know how many pounds of penalty drag is causing you, where and how, and what to do to cut it down? Read on. The author spent 12 years with North American and Chance Vought, 20 years with NASA (half of them as Deputy Director of the Langley Research Center) and the last four running the wind tunnel program at Texas A&M University. He is Chairman of the Technical Board of the SSA, and an active pilot of his own LS-1f. -Ed.

All soaring enthusiasts are aware of the importance of drag. Experts who make scientific studies of soaring speak of it in terms of coefficients, variations with Reynolds number, dynamic pressure and other expressions having vague or unknown meanings to most of us. Since drag needs to be understood by all who soar, there ought to be some way to relate its causes and effects in terms more easily understood.

The problem of learning to speak "Aerodynamics" before discussing drag with an aerodynamicist is somewhat like having to learn French before conversing with a Frenchman. Perhaps, if we are lucky, the Frenchman has already learned English and is able to communicate in that form. With that simile in mind, why, then, can't an aerodynamicist who also speaks English translate for us? At the risk of speaking "Aerodynamics" with a bad accent, I've decided to give it a try.

First, let's discuss the drag on a sailplane as a total force, measured in pounds, that is trying to hold us back. In a glide, we are always going "downhill", and like the kid on the skateboard, the steeper the hill the faster the speed. Of course, the less the drag, the faster we can go a given slope—the kid with bad bearings will have to find steeper hills to go as fast as he would like. Similarly, the more drag we have, the steeper our glide and the quicker the flight is over at the bottom of the "hill".

Figure 1

DRAG ACCOUNT BY COMPONENT—15 METER SPAN WINGS LEVEL

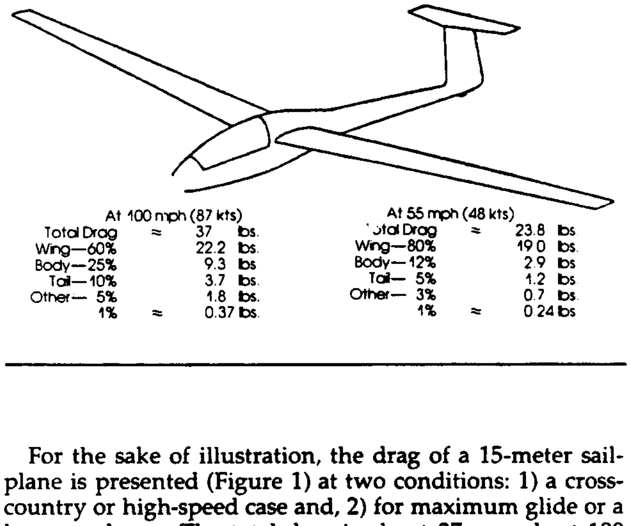

At 100 mph (87 kts)			At 55 mph (48 kts)		
Total Drag	≈	37 lbs.	Total Drag	≈	23.8 lbs.
Wing—60%		22.2 lbs.	Wing—80%		19.0 lbs.
Body—25%		9.3 lbs	Body—12%		2.9 lbs
Tail—10%		3.7 lbs.	Tail— 5%		1.2 lbs.
Other— 5%		1.8 lbs.	Other— 3%		0.7 lbs.
1%	≈	0.37 lbs.	1%	≈	0.24 lbs

For the sake of illustration, the drag of a 15-meter sailplane is presented (Figure 1) at two conditions: 1) a cross-country or high-speed case and, 2) for maximum glide or a low-speed case. The total drag is about 37 pounds at 100 mph and is reduced to about 23.8 pounds at 55 mph. You probably expected it to be less at a lower speed, for after all, we are familiar with the change in resistance as we change speeds. It's very important when swimming in a fluid called water that our resistance is greater as we go faster, and believe it or not, air is a fluid that behaves in accord with the same laws as water at the speeds sailplanes fly.

Drag Breakdown By Component

Figure 1 shows the contributions of major components to the drag. In cruise flight the wing contributes 60% of the total drag or 22.2 pounds. Of course the wing provides th lift to make flight possible, and its size is determined by the weight of the glider and the speeds to be flown. If we could always fly fast the wing could be smaller and its drag would be less, but we have to be able to fly slowly to thermal and to land safely, so the wing size is greater than required for cruise.

The body is just a streamlined fairing around the pilot and payload, but its cross-sectional area and its surface or "wetted" area are important parameters affecting drag. The supine seating in high performance sailplanes helps to reduce both the cross-section and the wetted areas.

Vertical and horizontal tails are necessary to meet the requirements for stability and control, which determine tail sizes and therefore tail drag. For optimum cruise conditions we could almost do without them, but alas, we must haul them around so that they will be available when we want to manuever, change speeds, change center of gravity or balance conditions, and deal with turbulence and gust disturbances. On most airplanes, the "tail group" contributes about 10% of the total drag during cruise. When the wing is doing a lot of lifting at low speeds, the tail drag percentage is less only because of the increase in wing drag.

When drag values for all major components are added together, they total somewhat less than the drag measured for the complete sailplane. Things like tail skids, total energy probes, air vents and such have to be included in a category called "other".

Figure 2

DRAG BREAKDOWN BY CAUSE—15 METER SPAN WINGS LEVEL

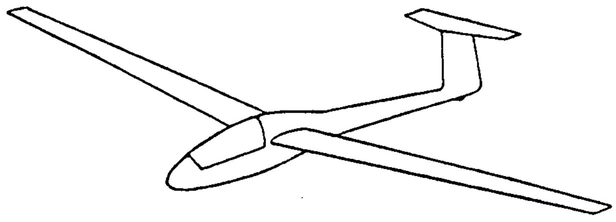

	At 100 mph (87 kts)		At 55 mph (48 kts)	
Friction	53%	19.6 lbs.	29%	6.8 lbs.
Pressure	32%	11.8 lbs.	9%	2.2 lbs.
Induced	10%	3.7 lbs.	57%	13.6 lbs.
Interference	5%	1.9 lbs.	5%	1.2 lbs.
TOTAL	100%	37.0 lbs.	100%	23.8 lbs.

The main point to be gained from this account is the obvious fact that as far as sailplane drag is concerned, "the wing's the thing!" As we will see later, in addition to the effect of area already mentioned, its airfoil profile, its planform, and its aspect ratio (span divided by chord) are especially important to drag.

Drag Breakdown by Cause

Now let us look at the drag account from another viewpoint—just what are the causes for drag and how much is each contributing? For now we will examine the drag causes for the entire sailplane (**Figure 2**) and afterward we will go into more detail about each.

At high speeds, friction is the big one at 53%, almost 20 pounds. This is a function of surface area, so the smaller the sailplane, the smaller friction drag would be. It is also very much affected by surface shape and smoothness.

Pressure drag is caused by the fact that the sailplane pushes air out of the way as it passes through, making the air turbulent, "stealing" energy from the moving object. If the object passing through air didn't cause flow turbulence or separation, pressure drag would be zero.

Induced drag is a term applied to the drag effects caused by lifting surfaces. Sometimes it is called "the drag due to lift." They say you can't get something for nothing; the drag that is caused by the production of lift is a price paid by a wing. Actually the induced drag is determined by how hard the wing is having to work to produce lift. If you water ski, you know how hard the rope pulls your arms when you're going very slowly. The drag is greater because the angle of the skis is greater in order to keep you from sinking. A wing has the same problem—it must be inclined at a greater angle of attack at low speeds to produce enough lift to balance the weight, which is the same at all speeds. This accounts for the almost four-fold increase in induced drag at 48 knots over that at 87 knots.

Where the wing joins the body and where tails join together, turbulence is created by interference, which causes additional drag. Its effects are usually more like pressure drag, but interference also affects friction drag when it triggers laminar flows and makes them transition to turbulent flows. Interference also can be manifested as induced drag. A classic case exists when the wing and tail are "lifting" in opposite directions. This is generally the case, for a requirement of stability is that the tail must push down for balance when the wing center of lift is anywhere aft of the center of gravity. The down-load on the tail forces the wing to provide even more lift, in order to offset the weight plus the tail down-load. Designers try to set wing and tail incidences to optimize balance for stability over a range of conditions, but this form of trim drag is hard to avoid entirely.

Perhaps your curiosity is now whetted enough to want to know more about why the things happen that we have just discussed. I remember an old saying that "The guy who knows how will always have a job, but he will always be working for the guy who knows why!" Perhaps knowing "why" will help you become a better pilot. I'll try to keep this part as simple as the accounting comments, but it will be tougher.

Friction Drag

If you were pulling a bobsled along snow and came to an icy place on the road, you would expect it to pull easier. If the snow had melted and you came to bare ground, you would expect more drag. Friction is at work! What if you could pull your sled onto a cushion of air; there would not seem to be any drag—but there would be. It would just be a good deal less.

Streamlined shapes seem to move so easily through air that we are fooled, but you may be sure that the fluid (air) scrubbing past the surfaces of a wing or body produces drag. If air were more viscous, like honey, you would believe it created friction; again I remind you that air *is* a fluid and at low speeds behaves according to the same basic laws as liquids.

Friction drag is affected by the density and viscosity of the air, as well as its speed along surfaces, but the three big things affecting the friction drag of sailplanes are:

1. The length of surface contact where scrubbing occurs.
2. The roughness of the surface that is being scrubbed by the air.
3. The waviness or local contours which may cause variations in the pressure field along the surfaces.

It has been determined experimentally that air flowing along a perfectly smooth, flat plate will "transition" from laminar flow to turbulent flow after a finite distance. No matter how smooth the surface, there is friction and the air scrubbing the surface finally slows more and more along the length until it becomes turbulent and builds up on the surface. If the surface is roughened, this happens in a shorter distance. Slowing the air is the cause of drag, so naturally friction produces more drag the longer the air and surface are in contact.

Waviness effects simply tend to thicken the thin layer of air near the surface as the flow cannot follow the ups and downs. This thickening of the boundary layer at the surface encourages the earlier transition to turbulent flow, much like the effects of roughness.

Pressure Drag

Stirring iced tea with a spoon creates eddies and mixing because of the turbulence, and of course, creates drag on the spoon. An object moving through air tends to do the same. If you move the tea spoon very rapidly, the disturbance effects are obviously greater; thus pressure drag increases with speed. In fact, drag varies greatly with speed changes; for example, the drag is doubled when speed changes from 52 knots to 74 knots.

What is happening when the object is moved through the fluid is that the pressure builds up on the upstream side. If the flow around the body filled in immediately around it without turbulence, there would only be friction drag. But unless the shape is ideally streamlined and no friction exists, there will be some separation and eddying produced by the body. You know from experience that streamlining greatly reduces drag, but we hope to give you some quantitative feel for the significance of streamlining.

Ways of Reducing Friction and Pressure Drag

In the real world it is impossible to separate friction and pressure drag effects on a sailplane; two examples are offered to put them in better perspective. To do this I will first compare familiar shapes **(Figure 3)** and show experimental results of actual drag measurements.

(1) *Streamlining*:

For comparison I have taken one-foot lengths of three familiar shapes:

Figure 3

STREAMLINING REDUCES DRAG
These Sections Have Same Drag at 100 mph (87 kts)
0.32 lbs. Per Foot of Length

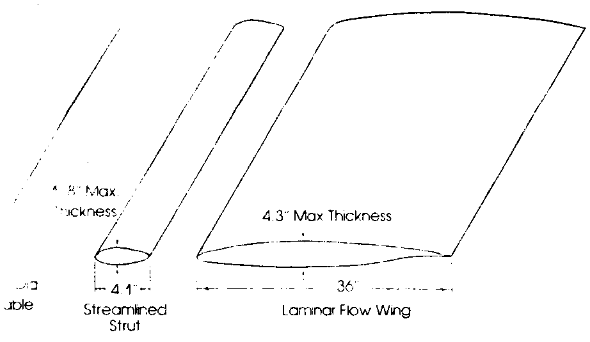

Figure 4

LAMINAR FLOW REDUCES DRAG
Wing Profile Drag at 100 mph (87 kts)
Combined Friction and Pressure Drag
12% Thick, 36 Inch Chord Section

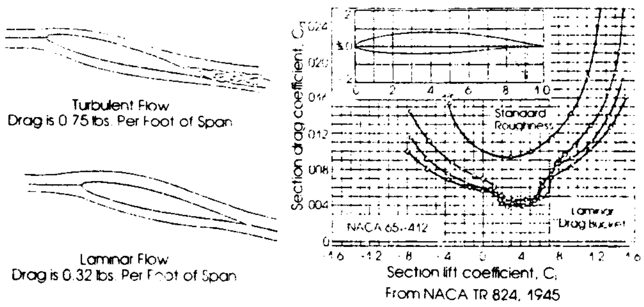

1. A stranded cable
2. A streamlined strut
3. A laminar flow wing

From drag data obtained and verified over the years by many experimenters, we find that the same lengths of a 1/8 inch diameter stranded cable, a four-inch chord streamlined strut, and a three-foot-chord section of laminar flow wing have the very same drag at 100 mph or 87 knots. Using the experimentally obtained drag data shows that a foot of each produces about a third of a pound of drag at 100 mph, and lower but roughly equal amounts at lower speeds.

(2) *Laminar Flow*

In the case of the wing section, laminar flow is a big help in reducing drag. During the 1940's researchers at NACA Langley found an amazing effect they named a "drag bucket" while testing airfoil sections of different shapes in a wind tunnel **(Figure 4)**. The facility had been carefully designed to produce almost undisturbed flows past their models, and aptly named "The Low Turbulence Pressure Tunnel." The term "drag bucket" was coined because the drag coefficient plotted against lift coefficient showed extremely low values over a certain range of lift values, making a plot that looked like it might hold water as shown in Figure 4. They also found that when they artificially roughened their models, the drag increased dramatically; in fact the "drag bucket" disappeared and drag more than doubled for some lift values. These new airfoil sections were named "laminar flow airfoils" because it was shown that the large extent of laminar flow was the cause for their drag reduction. While most sections used on gliders today are slightly different, they are descendants of the family of NACA-developed laminar flow shapes that have been tailored to sailplane conditions.

Induced Drag

As already mentioned, induced drag, the drag due to lift, is affected by such things as the span-to-chord ratio (aspect ratio) of the wing, the planform, the wing twist and the shape of the tips. All of these also influence the distribution of lift along the wing. The wing designer takes these factors into account, making tradeoffs between aerodynamic performance, weight, cost, and maneuverability. Most of the induced drag effects are evidenced as vortex flows around wing tips, so long slender wings with relatively small tips tend to cause less induced drag. Tip shape is also important

Figure 5

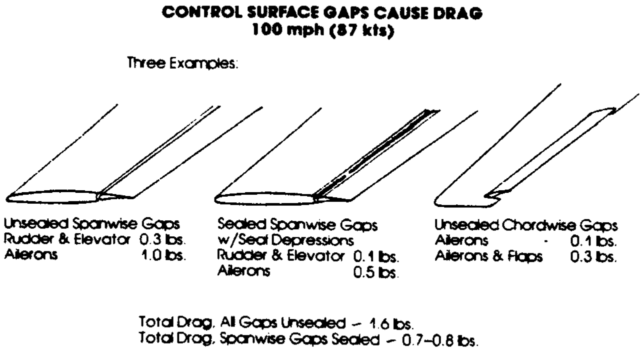

because it is high pressure air leaking from the lower surface to the upper surface which causes vortices to form. This "stirring" of the air by the wing tip transfers energy to the air which is dissipated—this loss is induced drag.

Interference Drag

In addition to the interactions between wing, body and tails, moveable control surfaces, spoilers, and air vent systems also cause drag. Some of these interferences are inherent in the design and some may be affected by the pilot. Control surface and flap gaps may create interference drag which can be reduced by sealing. Some sample data are provided in **Figure 5** to give an idea of the importance of these sources to sailplane drag.

One of the most insidious forms of drag in soaring is caused by air leaks. Because air is invisible, there are no obvious indications of flows into or out of sailplane canopy cracks, or around wing roots and spoilers, except for hissing sounds. Pilots must have cooling air inside their glass cages or they would melt, so some form of "controlled" leaks into

Figure 6

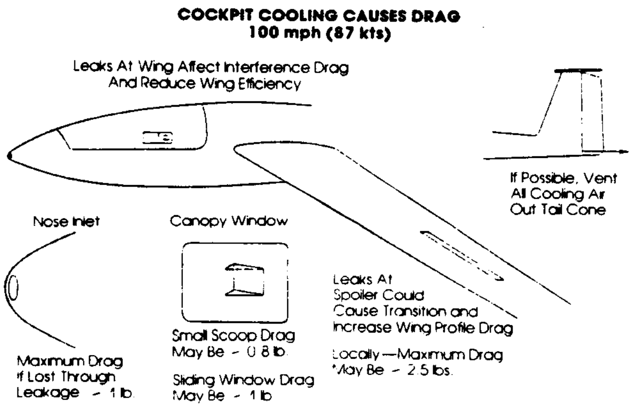

and out of the cockpit is necessary. It is extremely difficult to quantify the drag due to all possible leaks, but a look at some of the classical cases may be informative. **Figure 6** illustrates these effects.

The cooling air system with the lowest drag would take in air at a place where the inlet would not disturb external flows, gradually diffuse and pass the air through the body at very low speeds, and exhaust it at the tail of the sailplane through a duct sized to bring the flow back to free stream velocity. This idealized system would still produce some drag, but not nearly as much as most cooling systems. The nose is a good place to take in air, although some designers have worried about disturbances the inlet might cause to laminar flow over the body and have located inlets aft under the wing.

Figure 7

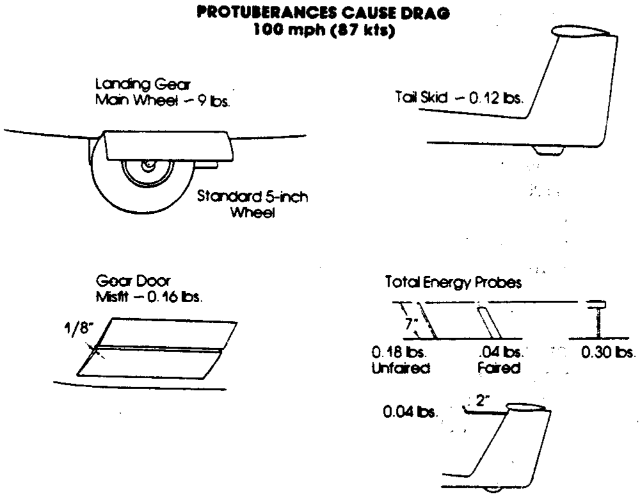

A more serious concern is cockpit sealing to prevent flows in or out of the sailplane at places other than specifically intended. Pressure variations along a fuselage, over a wing root or past a wheel well door can cause circulative flows into and out of the ship which interfere with the normal airflow along the surfaces. These create a momentum exchange drag and may also cause disturbances in the external flow field. For example, if the air taken in at the nose exhausted out the edges of the canopy through leaks, about one pound of drag would result. This does not even take into account interference effects caused by boundary layer disturbances. Leaks through the wing and exhausting around spoilers could be more devastating. They could cause boundary layer separation and turbulence over 10-15% of the wing span, seriously increasing drag locally, perhaps adding 2.5 pounds of drag.

It is common knowledge that protuberances like tail skids, landing gear, total energy probes, antennas and such cause drag; but from the number of these "drag items" seen on sailplanes, it is worth looking at the values for some of them. In **Figure 7** several typical items are shown, indicating the drag penalties that might be associated with them.

Finally, changes in the sailplane flight loading conditions should be mentioned for they can cause significant changes in drag. Increases in gross weight resulting from the addition of water or other ballast obviously change the lift requirements for the wing. Since induced drag is proportional to the square of the lift value, induced drag is increased significantly with an increased loading. For example, if the weight were to increase 10%, the induced drag at a given speed would increase 20%. Also important is the center of gravity position, as this affects the trim requirements and may result in larger tail down loads for balance. The drag variation caused by a shift from a forward CG to an aft CG may amount to about one pound at cruise conditions. This is approximately a three per cent variation in total drag, a number which may be highly significant to the racing pilot.

Maneuvering Drag

Another effect of significance in soaring is the drag caused by maneuvering, the most common maneuver being a simple turn. **Figure 8** summarizes the nature of these effects. Because of centrifugal forces, the wing has to provide lift in a turn greater than the weight of the sailplane, thus increasing the induced and control surface drags required to maintain the turning attitude. At a 45° bank angle, the lift must be increased to about 1.4 times the value required in a wings-level glide at the same speed; this causes the drag to increase to about 1.7 times what it would be for a wings-level glide at the same speed. The reasons are: 1) the induced drag is increased at greater lift values, 2) the trim drag is increased to maintain balance with the greater lift, 3) aileron and rudder misalignments are used to maintain attitude during the turn, and 4) there is a high probability of some slipping or skidding in a turn which increases drag. Serious pilots may want to do some experiments and simple calculations concerning the effects of turning on lift and drag.

Designers have reported that for design optimizations they assume that average bank angles of about 40 to 45 degrees are common. Since the sailplane drag at 48 knots in a wings-level glide is about 23.8 pounds and increases to 40.7 pounds in a 45 degree bank angle glide, it is obvious why pilots who are able to climb straight ahead do better than they would in circling flight.

Figure 8

TURNING INCREASES DRAG

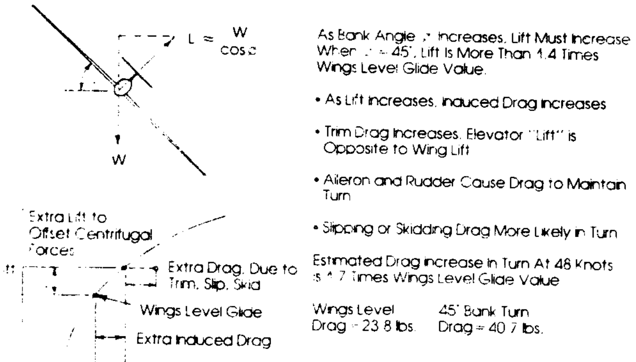

Summary

Drag is obviously "the enemy" in soaring flight. Not only are the design characteristics and the physical condition of the sailplane important, but the ways we prepare and operate the craft influence its drag. Of the major components, the wing is by far the largest contributor to drag, and its airfoil profile, aspect ratio and surface condition are critical to total sailplane drag. Streamlining is not only a matter of aesthetically pleasing shapes but also a product of sealing leaks, proper venting of air and treatment of interference regions. Air leaks are common causes of drag that can be reduced with owner attention. Finally we see that the way we fly can have a dramatic impact on drag. The most pronounced variation due to piloting is the effect of maneuvers on induced drag.

Yes, an awareness of the causes and effects of drag should be ever present in soaring. With a bit of study and with a reasonable application of TLC, we should all glide a little bit farther, faster or longer—and maybe all three!

REFERENCES

1. "Aerodynamic Drag," Sighord F. Hoerner: *Otterbein Press*, 1951.
2. "Summary of Airfoil Data," Ira H. Abbott, Albert E. VonDoenhoff and Louis S. Stivers, Jr.: *NACA Report No. 824*, 1945.
3. "Engineering Aerodynamics," Walter H. Diehl: *Roland Press*, 1942.
4. "Proceedings of the NASA/Industry/University General Aviation Drag Reduction Workshop": Jan Roskam, editor, 1975.
5. "Review of Drag Cleanup Tests in Langley Full Scale Tunnel," Paul L. Coe, Jr.: *NASA Technical Note D-8206*, 1975.
6. "Proceedings of the 1st International Symposium on The Technology and Science of Motorless Flight," James L. Nash-Webber, Editor: MIT, Cambridge USA, October 1972.
7. "Motorless Flight Research, 1972," James L. Nash-Webber, Editor: *NASA CR-2315*, 1973.
8. "Science and Technology of Low Speed and Motorless Flight," Perry W. Hansen, Compiler: *NASA Conference Publication 2085*, 1979.
9. "Influence of Systematic Variations on the Drag Polar of the Sailplane RJ-5," August Raspet: *Soaring*, September-October, 1951.

All of the numbers generated in this presentation were based on sound experimental and analytical data; however, in the process of generalizing and simplifying, the numbers necessarily become more qualitative than exact. Please consider them for the insight they provide—as "representative" only—and not as directly applicable to your specific sailplane. For those who wish to delve more deeply, a list of references is provided after the article.

—*Oran W. Nicks*

OPTIMIZING MODEL SAILPLANES

In the previous "Soartech" issues we published performance analysis and optimization studies that put into our hands the methods we need to zero-in on improved models. This paper, which takes on the popular two-meter class model sailplane, has a surprising conclusion. Martin Simons has thoroughly worked out the performance of the two-meter model and documented the whole process in detail. It puts the cap on his previous papers dealing with performance analysis. Taking on the two meter was a very good choice. It's hard to optimize the performance of models, because the range in which we fly them makes bigger models better. Any attempt to optimize without limits means that, basically, the biggest model has the best performance. Limiting span stops that process at a point, and by optimizing the rest of the dimensions, Martin Simons shows that we should do much better with lower aspect ratios.

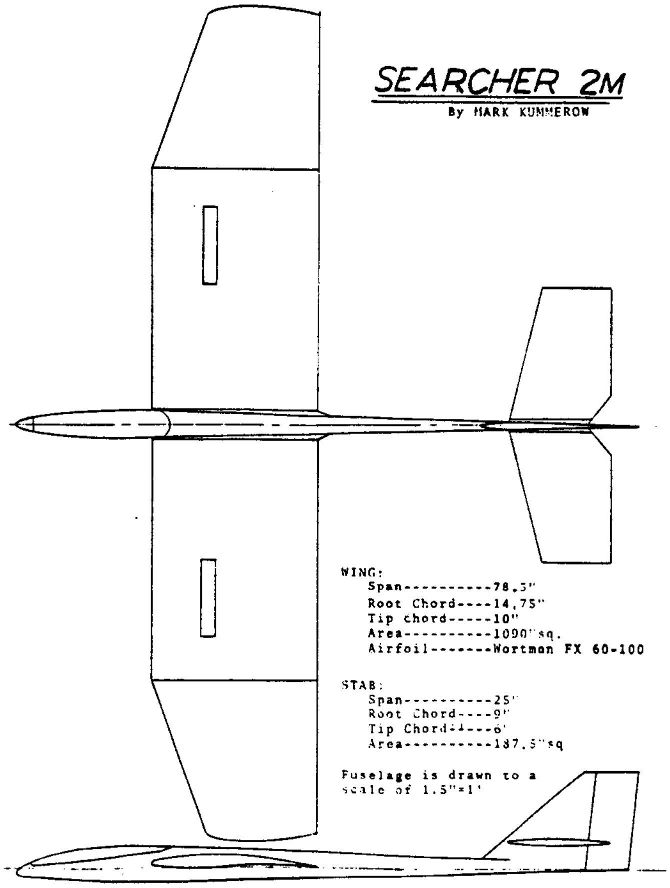

THE TWO METRE SAILPLANE

By Martin Simons

The Two Metre Sailplane

In Australia now the two metre span, radio controlled sailplane, seems to be recognised as a competition class and regulations have stabilised so that it is possible to do some theoretical work. Any future changes in the regulations will tend to invalidate the findings presented here.

Briefly, under the Australian rules, the two metre sailplane is to be controlled by rudder and elevator only or, if a V tail is used, by the usual 'ruddervators'. Ailerons, flaps, spoilers and radio-operated tow release hooks are disallowed. The standard methods of launching, hand towline or winch, are to be used with the usual limitations on line length, winch dimensions, etc.

Ballast is permitted but the contestant is not allowed to change the mass of the sailplane during a round. In other words, the two tasks, 'A' and 'B', constituting a round, have to be flown with the same ballast, but this may be changed between rounds. Anyone putting too much ballast in may thus suffer a disadvantage in task 'A' while gaining some benefit in task 'B', and vice versa if too little ballast is used. Task 'A' is the normal six minute duration task, with points deducted for times either less than or greater than six minutes. A spot landing may be added at the discretion of the contest organisers. Task 'B' is a speed task similar to that used for the FAI international F3B championships, four runs over a 150 metre course at right angles to two parallel sighting lines, line 'A' and line 'B'. The start is made by crossing line A, flying as fast as possible to cross and turn at line B, flying back to line A and turning again, to complete the task by flying again to B and turning back to cross line A. The task requires three high speed turns, which makes the exercise a good deal more interesting, from the theoretical point of view, than the former two lap, one turn speed course.

Whether or not a spot landing is required is of some importance in deciding what ballast to carry, because a heavier, faster-flying model without spoilers, is much harder to get down safely on the designated spot than a light, slower model. This is one of the factors the pilot must consider when making the decision, before a round, about ballast.

The ability to fly the turns efficiently in the speed task, is also of great importance. The direction of flight has to be reversed completely three times without the sailplane either slowing down too much or flying too far beyond the turning point. Without ailerons it is unlikely that pilots will be able to adopt the half roll and inverted 'pull through' diving technique used by some international champions. This method, if well judged, ensures that the sailplane accelerates, rather than slowing down, at each end of the lap. In the normal turn likely to be used in two metre competitions, a heavy load of ballast will tend to force the sailplane to turn on a large radius, adding distance to the task with some penalty showing on the timer's clock. The alternative is to steepen the turn to a large angle of bank, which reduces the radius of turn but causes a sharp increase of drag, especially wing tip vortex drag, which slows the aircraft down. The ability of the pilot to time the turns is most important and the theorist cannot help much here. Obviously the turn should begin before reaching the mark, so that, ideally, the aircraft will cross the line only for an instant and start the return journey immediately. In some contests observed by the author (we shall say nothing about those in which he has actually flown), the winning times were achieved, not by those with the fastest sailplanes, but by those who judged the turns best. Some models spent more time turning outside the course than actually flying between the lines.

The combined effect of all the FAI general rules governing contest aircraft models, and the two metre span limitation, presents us with a flight 'envelope' of the type shown in Figure 1. The maximum total, projected, area of all wing and tail (or other similar) surfaces must not exceed 150 sq dm or 1.5 sq metres. Unless we build a tailless aircraft, the true effective wing area will always be less than the FAI area by an amount equal to the area of the tailplane or other stabilising surface. It is assumed for present purposes that the stabiliser will be 10% of the wing, so the maximum wing area in practice is 1.35 sq m. Small deviations caused by slightly larger or smaller tailplanes will make only marginal differences to the performance. They may have more important effects on the stability of the sailplane, but 10% is a fairly typical stabiliser area for a competition model. The FAI area limit determines the lower limits for the wing aspect ratio. This ratio is found by dividing the square of the span by the wing area, so for a two metre sailplane the lowest possible value of 'A' (aspect ratio) will be:

$$2 \times 2 - 1.35 = 2.963$$

Along the top edge of the diagram is a scale of aspect ratio. The corresponding wing areas and FAI total areas are also shown. There is no legal limit at the right hand side. We can build a model with as high an aspect ratio as we choose, but as the aspect ratio rises, the wing chord becomes narrower. As will be shown, there are grave disadvantages with a fixed, two metre span, if the wing chord is too small.

Down the left hand edge of the flight envelope is the FAI loading scale. Using the combined areas of wing and stabilising surfaces, the FAI confines contest models between the loadings of 12 and 75 grammes per sq dm. Allowing for the 10% tailplane area, these become effective wing loadings between 1.32 and 8.25 kg per sq m. (Full sized sailplanes commonly fly with wing loadings between 30 and 45 or 50 kg per sq m.) There is a further restriction of 5 kg on total all up mass, which appears in Figure 1 as a slanting line across the top left corner.

The modeller has a wide range of choices. The main variables are the wing aspect ratio, which controls area and chord, and the mass, which controls wing loading. Aspect ratio is a matter of design, and once the model is built, it cannot be changed much. To decide on this single figure is one of the chief preoccupations of the sailplane designer. The mass and hence flying weight of the model, can be varied to some extent on the field by adding or removing ballast, so although the designer can provide for ballast to be fitted, preferably in a way that adds strength to the wing as well as mass, the decision as to how much to carry has to be made by the pilot before each contest round. To use the ballast in such a way that it adds strength and stiffness to the wing, can be done if the ballast itself is in the form of a steel rod or rods passing right through the fuselage and wing roots, adding greatly to the strength of the aircraft in this critical region. This method has been used with success by the Australian F3B team and should be applied also to the two metre sailplane. When all ballast has been removed, the structural weight of the sailplane will depend on its construction and the kind of radio gear used. By very careful weight control techniques and using ultra light radio equipment, a two metre sailplane could be made to have the FAI minimum wing loading. This, however, might create serious difficulties in practice. The stresses set up during a winch launch are quite severe and depend far more on the wing span and the strength of the line used on the winch, than on the other features of the sailplane. A delicate structure would also tend to break if the model landed badly when carrying ballast. These problems should not be overlooked when considering the theoretical arguments which follow. In the flight envelope of Figure 1, the lowest part of the unshaded area is more or less excluded for these structural and operational reasons.

The slanting, curved lines on Figure 1 indicate, very approximately, the Reynolds numbers at which models of this class fly when soaring. The Re number is one of the most important factors in all model aircraft design. Without going into detailed physical explanations, it expresses the relationship of the size and speed of the wing (or any other part of an aircraft) to the density and viscosity of the air. The larger and faster the aircraft, the larger the Re number. The wing tip of a full-sized sailplane near stalling speed, operates at Re about 400 000, and a model sailplane at its maximum velocity in a speed task, may reach this figure at the wing root. When the model is flying slowly, as it will be when soaring in thermals, the Re is much lower and since the speed, at this trim, is determined mainly by the wing area and flying weight, the Re is low for lightweight, high aspect ratio aircraft and somewhat higher for heavier, low aspect ratio types.

As the Re number falls, the effects of the air's viscosity become more pronounced and the drag of the wing profile increases in importance, relative to the size and weight of the aircraft. A crude way of expressing this is to say that the air becomes more 'treacly' to the smaller and slower wing. Ultra light aeroplanes and full-sized sailplanes suffer from this effect, but model aircraft much more so. With the kind of wing sections commonly used for radio controlled sailplanes, at Re numbers below about 60 000, there is often a very marked breakdown of the airflow, so that the wing stalls prematurely. It is very important to avoid any part of a wing reaching its 'critical' Re figure, and it must be remembered that the chord at a point on the span, is what counts. If a tapered wing has a Re number of 80 000 at the root, the tip, which is narrower, may be operating at less than 60 000, very close to or below the critical value. (The figure varies from one wing section to another.) In a turn, the inner wing tip will be moving slower through the air than the outer tip, so the Re number there will be lower again. Generally, therefore, a successful and legal two metre sailplane will lie in the unshaded area of the envelope, to the left of the sketched Re 60 000 line, and preferably should be flying at no less than Re 100 000 to ensure a safe margin. In any case, the higher the Re, the more efficient the wing section will be.

(Free flight models often operate below Re 60 000. To achieve efficient flight, they require specialised aerofoil sections which are usually very thin, and may be fitted with turbulators and other devices to prevent the sub-critical flow breakdown. Such thin profiles are not really suitable for radio controlled sailplanes which have to fly speed tasks as well as soaring, and which require fairly deep spars to withstand the loads involved in launching and high speed turns.)

The Re depends on chord as well as flying speed, and chord depends on the aspect ratio. The lower the aspect ratio is, the more efficiently the wing profile will work. However, at low flying speeds, i.e., when soaring, the most important source of drag is not the wing profile but the wing tip vortex. Since there is a difference in pressure between the lower and upper surfaces of any lifting wing (or tail), the air tends to flow round the tip from lower to upper side. A strong, rotating vortex or 'swirlwind' forms behind and slightly inboard of each tip, and trails off, spiral fashion, downstream. Much energy is lost in this way, and at high angles of attack, as in slow speed trim, the drag resulting totals MORE THAN HALF the total drag of the entire sailplane. The most effective way of reducing these losses is to increase the aspect ratio. Tapering the wing in plan, preferably giving it a perfectly elliptical outline, can save a few percent more. The special wing tip vanes or 'winglets' seen on some modern aeroplanes may also be used to reduce the strength of the vortex and can save a little more drag at high angles of attack. These may prove useful for two metre models. If the winglet is vertical there is no increase in projected span. Their design and angular twist setting require a good deal of care. In any case, at high flight speeds vortex drag is much less significant than parasitic drag and the winglets which reduce drag in soaring become parasitic items at high speeds.

Against the benefits of low aspect ratio for the sake of lower profile drag, we have to set the benefits of high aspect ratio for lower vortex drag. Against the benefits of tapering the wing to reduce vortex drag, we have to set the dangers of a low Re at the tips. Against the advantages of winglets (which require very careful design and positioning), must be set their extra drag at high speeds. The final outcome has to be a compromise between all these factors and this is where some calculation can be of help.

The methods used in what follows are standard and have been described elsewhere. The work required is only simple arithmetic and can be done by anyone. A computer is used only to save time. In this case, the program is that devised some years ago for the full-sized 'Sigma' project, by Nick Goodhart. When the computed performance of some full-sized sailplanes was checked against their actual behaviour in flight, the Sigma program proved extremely accurate. The program has been adapted for models by Tom Nemeth. The great advantage of this program is that it allows the use of wind tunnel test results rather than relying entirely on theoretical aerofoil work. Perhaps the most important feature of the calculations is that wind tunnel data over a wide range of Reynolds numbers are employed, rather than relying on a single test at one Re. A good many authors in the past, with all respect to their enthusiasm, have overlooked the point that a model wing operates at quite different Re as its flying speed varies. Performance estimates not allowing for this are very unreliable. The Goodhart program takes wind tunnel data at four different Re numbers and, having first worked out the flight speed of the sailplane at a given trim, and knowing the average wing chord, interpolates wing profile drag figures for the appropriate Reynolds number. A simplified version of this method has been described by the present writer in a previous article in Soartech 1. In other words, supposing always that the actual model wing is accurately made and smooth, the performance should be close to that predicted by the Sigma program. Wind tunnel models themselves are not quite perfect, so the practical modeller can at least aim to achieve similar results, whereas the mathematically perfect aerofoil curves coming from the computer but not proved in the wind tunnel, remain to be demonstrated in practice.

Figure 2 shows the effects of ballast. The performance of an example sailplane has been worked out and plotted in the usual way as a polar curve. This shows, at each trimmed flying speed, the rate of sink of the model through the air. For this diagram, the model is supposed to have an aspect ratio of 10 and the wing profile is the well known Eppler 193. This profile is used, not because it is necessarily the best available, but because it has been well tested in the Stuttgart wind tunnel and has also been amply proved in practical model flying. There has not been sufficient time to run the program with other wing profiles, although this may be done some day.

As the various different curves show, adding ballast to the model tends to shift the entire performance curve to the right, higher speed side of the chart, but also flattens the curve. There are no great surprises here. It will be noticed that the curve representing the lightest condition has some irregularities at the low speed end, and although this light model has a very low minimumn sinking speed, the curve is quite sharply peaked. These features of the polar are caused almost entirely by the low Reynolds number effects mentioned above. As indicated, the average Re of the wing, at this weight and trimmed for least sink, is only 68 000. The airflow is already beginning to separate on the upper surface of this wing, and in practice it is very doubtful if the model would ever achieve its 'peak' soaring performance. The peak is so narrow that a small piloting error or gust would move the model off it, either to the higher speed side of the curve, or to the stall. Increasing the weight to 1.3 kg brings the Re to a much safer average near 100 000, and while there is some penalty in both sinking speed and turn radius, the model would be much more tolerant.

Polar curves representing sailplanes of weights intermediate between those actually plotted, may be estimated fairly well by interpolating between the lines on the diagram. There are no anomalies or oddities arising.

Not only does ballast increase the rate of sink in straight flight, as shown on these polars, but it also increases the radius of turn at any given angle of bank. If a thermal is narrow, to remain within it the sailplane must turn on a small radius. The light model can do this with a relatively gentle angle of bank, so the sinking speed in the turn is increased only slightly above that for the straight glide. A heavier sailplane can achieve the required small turn radius only by banking steeply, and the effect on sinking speed is quite serious. This may not matter if the thermal, once caught, is strong, but a narrow, weak thermal presents the pilot of a heavy model with real difficulties. The choice lies between circling with small angle of bank, which then probably takes the sailplane out of the thermal altogether, or circling tightly with large angle of bank, which will probably increase the sinking speed so much that the model will not climb. The only escape in such conditions, is for the pilot of the heavy model to use the good high speed performance of the aircraft to explore a larger area in search of a better thermal. There may not be one.

The advantage of the heavily ballasted sailplane for high speed flight, is probably clear enough. A rough measure of this is to note the flying speed at which each curve crosses the line representing a glide ratio of 1 : 10. Still, the effect of the additional mass, and speed, on the racing turns, mentioned above, must not be overlooked.

Figure 3 summarises in one chart, all these effects, so far as that can be done in a single diagram. The lowest line on this graph shows how additional mass causes the radius of turn, with a 30 degree angle of bank, to rise. The rate of sink in a turn increases, so the two central curves in the diagram show this effect, again based on a carefully flown, 30 degree banked turn. (Of course, every turn must be flown with the correct angle of bank. To try to turn 'flat' as some pilots do, is to cause considerable outward skidding in the turn, with consequent high drag and greater sink.) The uppermost curve shows how the speed at which the model flies when trimmed for minimum sink, rises with weight.

The question now arises as to whether the aspect ratio chosen for the example, 10, is the best compromise. The next diagram indicates that it is not. In Figure 4, polars have been plotted for three sailplanes all built and ballasted to the same flying weight, but with aspect ratios 4, 6, 10 and 14. Naturally the A = 10 curve is the same as that of the previous figures, and is included for comparison.

To the right appears the polar of a model weighing 1.3 kg with an aspect ratio of 14. Vortex drag has been cut, but at the cost of lower Re numbers. The curve shows a very sharp peak and the same sort of irregularity we have learned to associate with low Re conditions. Not only this, but the best rate of sink, even if the model could be trimmed accurately enough to achieve it, is less than that of the original A = 10 example. By increasing the aspect ratio we have made the model harder to trim, it will require a larger turn radius, and will not perform so well in Task A. The high aspect ratio curve improves relatively at high speeds, but more will be said about this later.

The polar curves for A = 4 and 6 are particularly interesting. Although such low aspect ratios imply high vortex drag, which is usually very bad for a soaring sailplane, the Re number for these wide chord wings is higher. The improvement in profile drag counteracts the extra vortex drag. The minimum sinking speed is very similar to that for A = 10, at the same total weight. (The wing loading, of course, is less.) What is probably much more important is that this low sinking speed is reached at a low flying speed, and these polars are remarkably free from sharp peaks and irregularities. This means that the low A model will be tolerant of rough air, easier to trim, and capable of turning on small radii at shallow angles of bank. For soaring, these are very important features. It is also very encouraging to see that, because of the generally flat nature of the low A curves, the glide ratio does not deteriorate very rapidly as the forward speed increases. At velocities around 8 and 9 metres per second, the two low aspect ratio aircraft would 'penetrate' through sinking air, or make headway against the wind, just as well as the A = 10 sailplane. the A = 6 model maintains its superiority up to flying speeds of 11 m/sec. For general soaring and for exploring the air to find sources of lift, such a model would be excellent.

For the speed task, the light wing loading of the lower A model is against it to some extent. The polar curves cross over again as the velocity rises. The higher wing loadings of the high aspect ratio models, now at sufficient Re numbers for the narrow wings to be working well, gives them an apparent advantage.

It is therefore of some interest to compare low and high aspect ratio sailplanes at the same wing loadings. To achieve this, ballast would be added to the low A sailplanes and mass would have to be subtracted from the high A aircraft. The stalling speed, which depends mainly (not entirely, because of Re effects on lift coefficients) on the wing loading, should be very similar in all cases. The high aspect ratio wing, because of low vortex drag, should exhibit a better minimum rate of sink, so should have some advantage in the duration task. The low aspect ratio wing, because of its better Re numbers and because vortex drag is almost negligible at low angles of attack, might be expected to do better at high speed. Figure 5 shows what happens. The most interesting point about the curves here is that, while the A = 10 sailplane does indeed show better minimum sink, its superiority is confined to a very narrow range, close to the stall. The A = 14 polar has virtually collapsed. The reason is that, to get this wing to the same wing loading as the others, the flying weight has to be reduced. This brings the Re number down quite drastically to critical values. Such a model would be very unsatisfactory. The advantage of the lower aspect ratio at high speed is quite clear. The A = 6 sailplane is evidently a better compromise than A = 4, because its soaring performance and penetration remain excellent with very little given away to the lower A type at the highest velocities. It will occur to the reader that a low aspect ratio sailplane with intermediate ballast, to bring its wing loading up near but not equal to, the equivalent high A type, should be capable of both out-climbing and out racing, the high aspect ratio model. How much ballast to carry on a given occasion, remains for the pilot to decide on the day, or at the hour.

These facts are summarised in the next diagram, Figure 6, where the influence of mass and aspect ratio on the flying speeds at steep glide ratios, is shown. The speed task will probably be flown at a glide ratio of about 1 : 5. This assumes a reasonably high start and efficient turning technique. The A = 14 model, at all weights, reaches this glide ratio at a higher flight speed than the lower aspect ratio aircraft. However, some of the models represented on this diagram would be disqualified because they fall outside the FAI limits. For instance, the A = 14 sailplane, would be loaded to the FAI maximum of 7.5 kg/sq m if it were flying at slightly over 2 kg all up. Its 1 : 5 glide speed would be surpassed by an A = 6 model loaded to about 3 kg, and this would be quite legal. Needless to say, to ballast any two metre model to this extent would prove a severe penalty in the duration task, but the point is probably sufficiently made.

It is also important to recognise some other advantages of the low aspect ratio. To taper the wings of a high A sailplane, with the two metre span restriction, brings the tips quickly into the critical Re zone and so it is unadvisable. Rectangular planforms are better for the two metre, high A, type. But if aspect ratio is reduced, the critical Re problem is avoided and the wing can safely be tapered. This helps, a little, to offset the high vortex drag. It also allows the wing roots to be both broader and deeper. The wing may then be built lightly, so the low aspect ratio model may, in weak conditions, truly be capable of soaring and winning task A when higher aspect ratio aircraft cannot stay up at all. Then although the speed task may have to be flown at a relatively slow speed, the final score may still be good enough to win. In the next round, when thermals pick up and a wind rises, the model may be able to carry ample ballast to win the speed task and still do well enough in task A. The final choice remains with the pilot, but the low aspect ratio sailplane seems to offer a greater range of possibilities. Figure 7 is equivalent to Figure 2, showing the polars for an A = 6 sailplane at the same flying weights. By tracing these curves and laying them one by one over the earlier figure, a fair comparison can be made.

In conclusion, it is emphasised again that this study has used only one aerofoil section and it remains to be found how a change of this important aspect of a design, affects the results. The author believes, from previous experience of similar studies, that the outcome will remain in favour of considerably lower aspect ratios than have been seen hitherto on two metre sailplanes. A further point worth making is that, throughout the above study, certain assumptions have been made about such things as parasitic drag, fuselage size, tailplane and vertical tail surface areas and drag coefficients and so on. Any and all of these may be in error to some extent, but the fact is, even if they are all removed from the calculations, the benefits of the lower aspect ratio still appear. The final diagram illustrates this. In computing sailplane performance, it is possible to work out the polar curve for the wing alone, and even to make unrealistic assumptions, such as, that the wing has the perfect, elliptical lift loading distribution giving minimum vortex drag. It is then fairly safe to assume that the best wing, fitted to a standard type of fuselage with a normal stabiliser and tail unit in proportion to the wing area, will produce the best sailplane. Figure 8 shows the results of such a theoretical exercise. It is obvious that all the polars improve a good deal, which is to be expected. Yet apart from a very narrow zone of flight, close to the stalling speed, the A = 6 wing outperforms the others and gets better and better, relatively, as the velocity increases.

In practice the low aspect ratio sailplane offers some ways of reducing parasitic drag which have not been allowed for at all, yet. For instance, with a broad and deep wing root, some, if not all, the radio gear can be housed in the wing itself and the fuselage reduced to a very slender form, which will have less drag, especially at high speeds. This in its turn suggests the possibility of eliminating the fuselage altogether and attaching the elevators directly to the trailing edge of the mainplane. The resulting, apparently tailless, sailplane, would have a very light wing loading when unballasted, so the usual disadvantage of the tailless type, poor soaring ability, would be largely overcome. At high speeds, where parasitic drag becomes so important, the performance should be extremely good and, if control difficulties in the lateral sense can be overcome, the 'all wing' two metre model might prove to be a winner.

All this applies only to the two metre contest sailplane. There is no substitute for span, and larger aircraft will, other things being equal, always fly better than small ones. The two metre contest sailplane will become, under the influence of the Australian rules, highly specialised. Perhaps few people other than the keen competitors, will choose to fly such aircraft when allowed to employ something larger. What we have found is that a particular set of competition rules, is likely to lead to the development of sailplanes which will be efficient for their particular purposes, but which will still be outperformed by aircraft of larger dimensions and orthodox appearance.

Another point is, of course, to wonder whether this kind of sailplane is exactly what the rule makers had in mind when they searched for the ideal BEGINNERS' competition sailplane. What, we may ask, was wrong with the old 100 inch or 2.54 metre span, two control, so-called 'Standard Class"? The author of this article thinks there was nothing wrong with it at all, for beginners, and would like to see it back in the contest calendar.

Figure 1

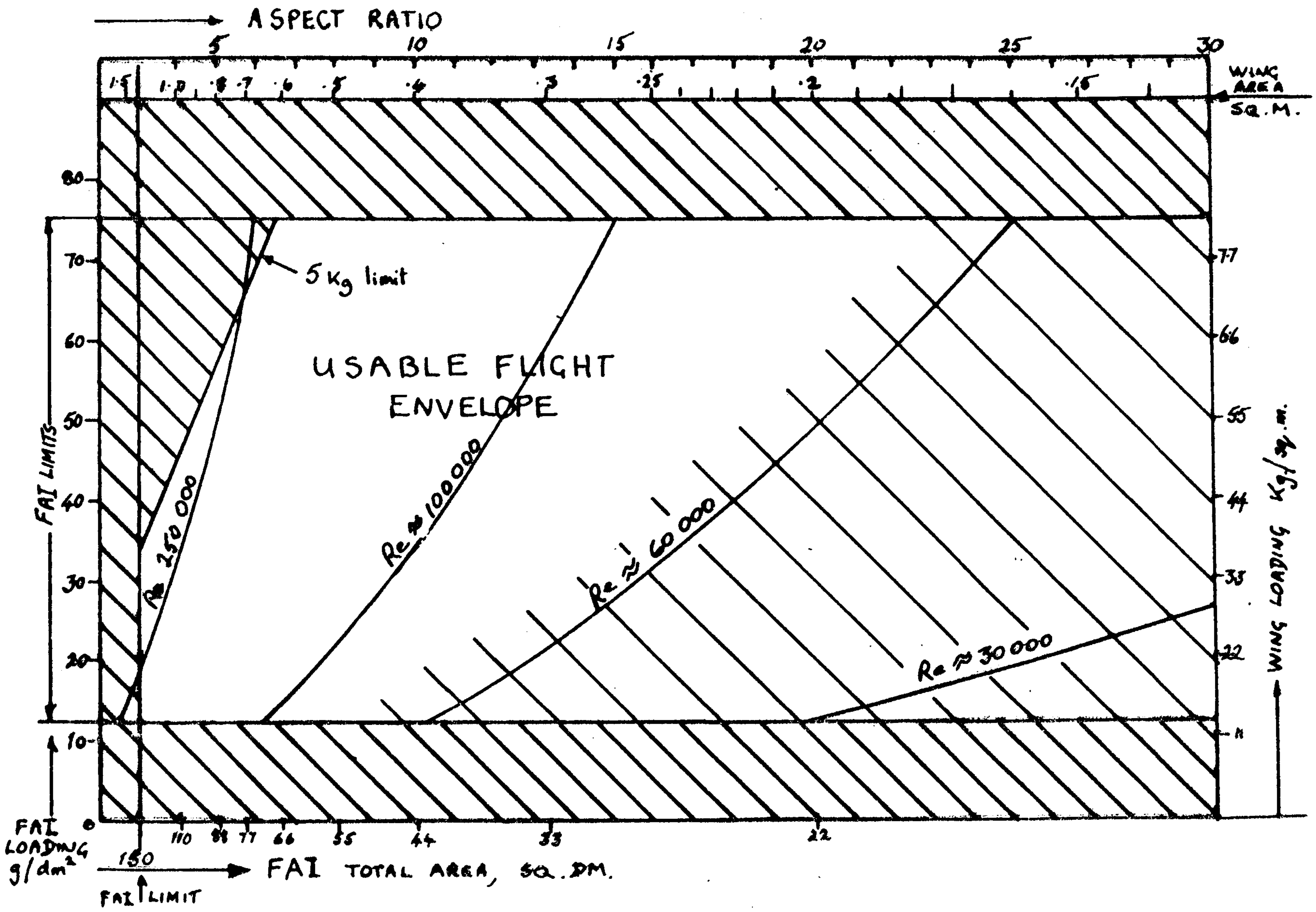

ASPECT RATIO
5
10
15
20
25
30
WING AREA SQ.M.
1.5
1.0
.8
.7
.6
.5
.4
.3
.25
.2
.15
80
70
60
50
40
30
20
10
0
FAI LIMITS
FAI LOADING g/dm²
5 Kg limit
USABLE FLIGHT ENVELOPE
Re ≈ 250 000
Re ≈ 100 000
Re ≈ 60 000
Re ≈ 30 000
77
66
55
44
33
22
11
WING LOADING Kg/sq.m.
150
110
88
77
66
55
44
33
22
FAI TOTAL AREA, SQ. DM.
FAI LIMIT

Figure 2. The effects of ballast on a two metre sailplane with aspect ratio 10

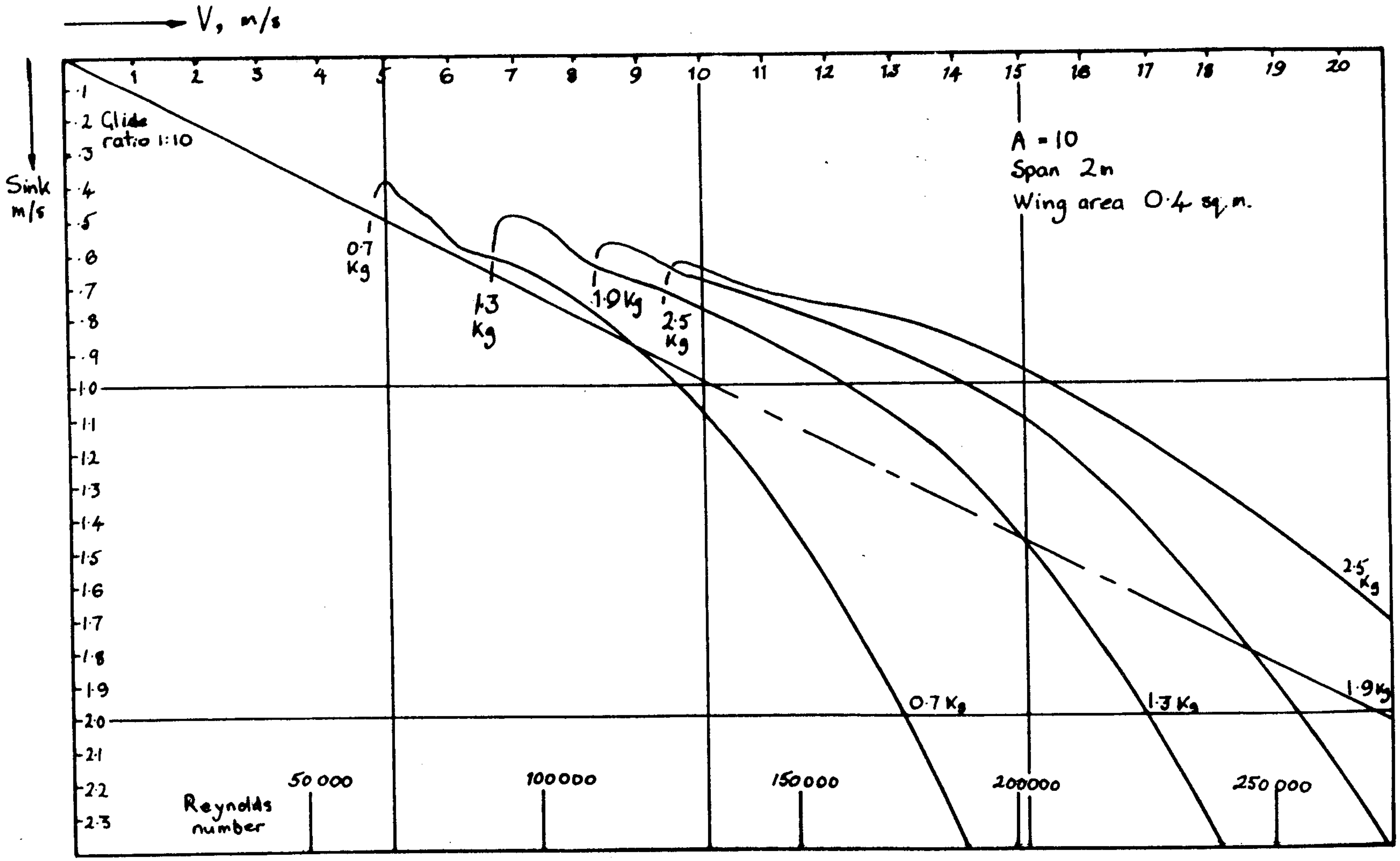

Figure 3
Summary diagram showing effects of ballast on turn radius and on sinking speed in turns

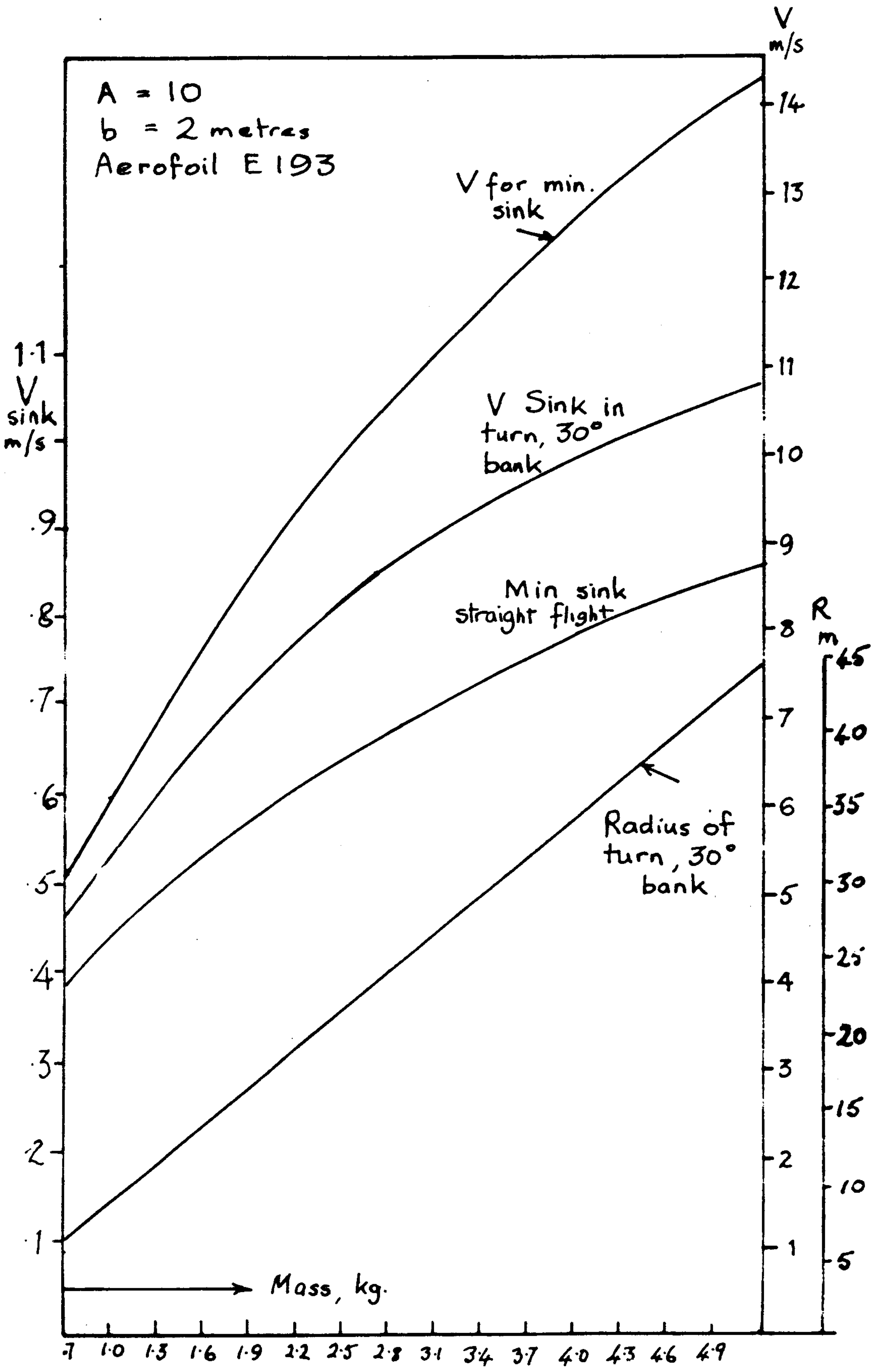

Figure 4. The effects of changing aspect ratio with two metre span sailplane of constant mass 1.3 kg.

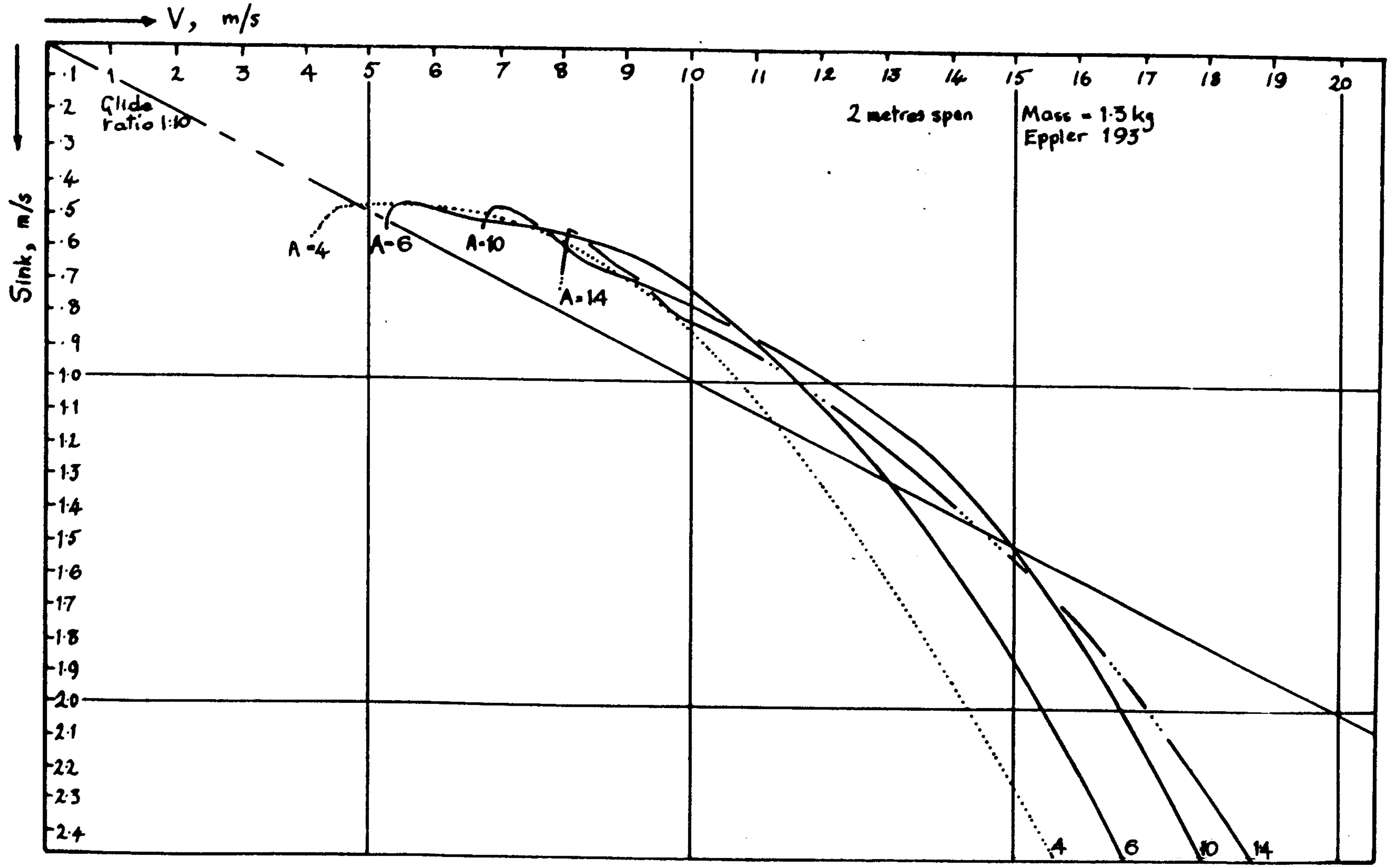

Figure 5 Changing the aspect ratio with ballast adjusted to keep wing loading constant

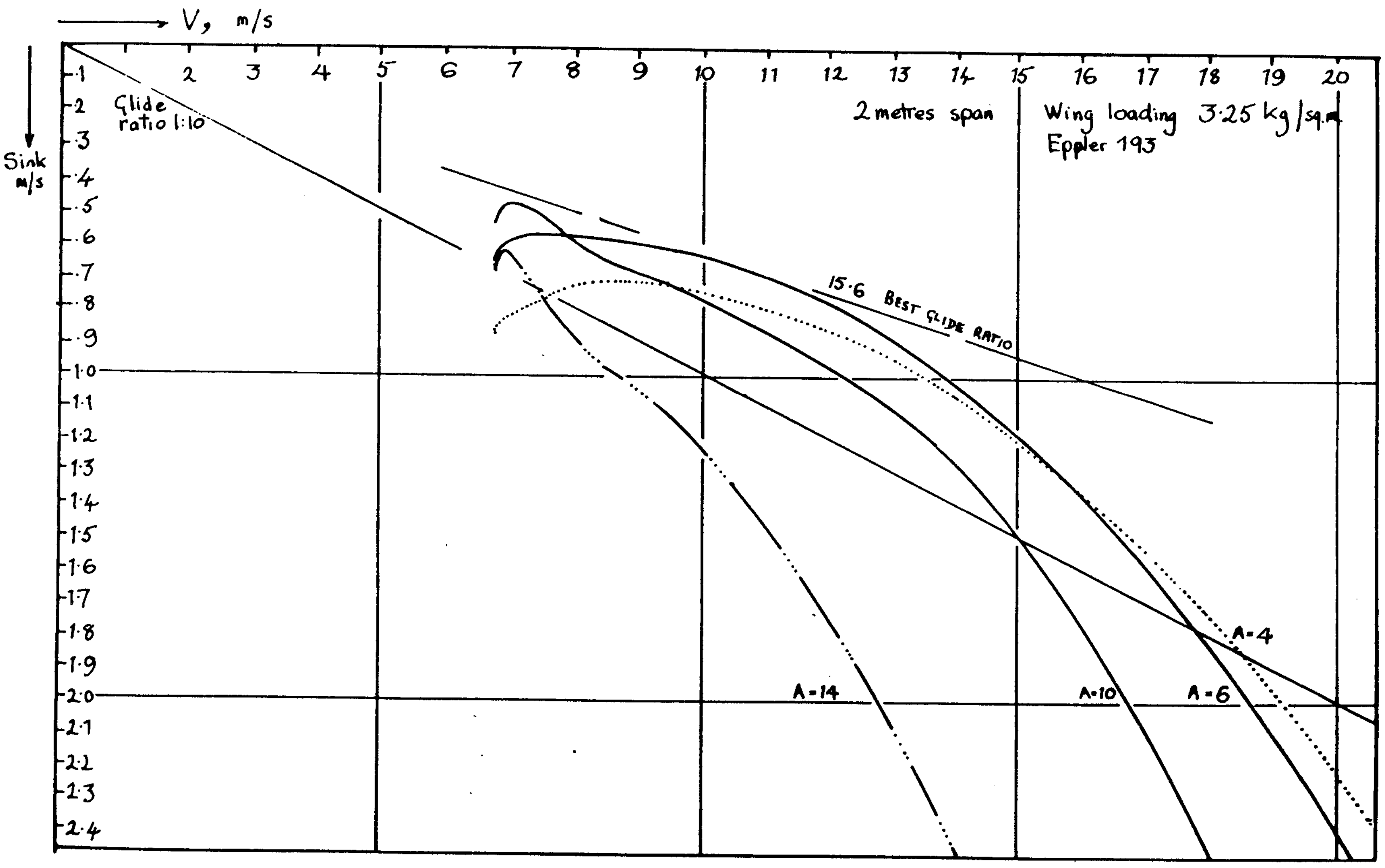

Figure 6. The effects of ballast and aspect ratio on high speed performance

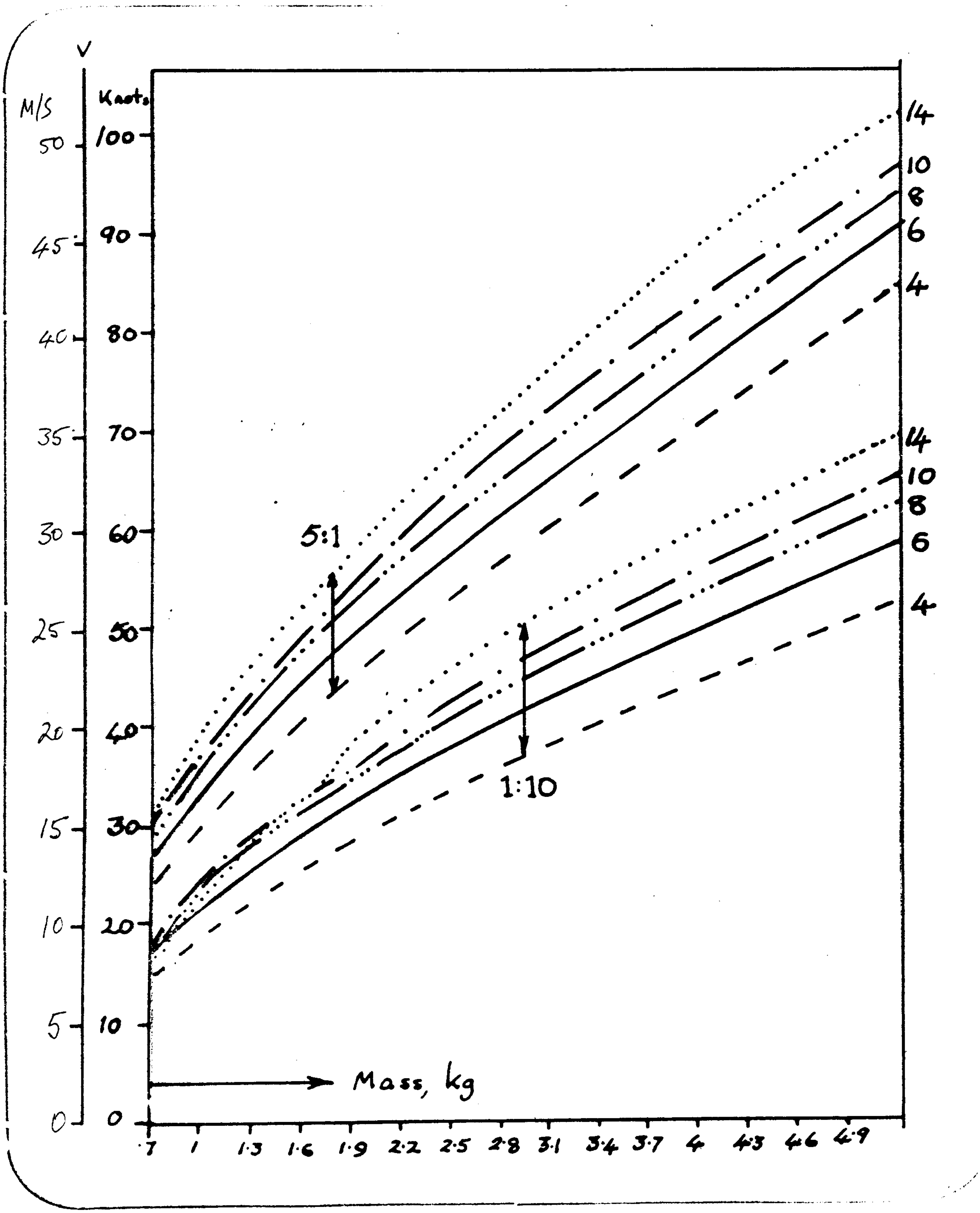

Figure 7. The polars of a two metre sailplane with aspect ratio 6, ballasted to various total flying weights. Compare with Figure 2.

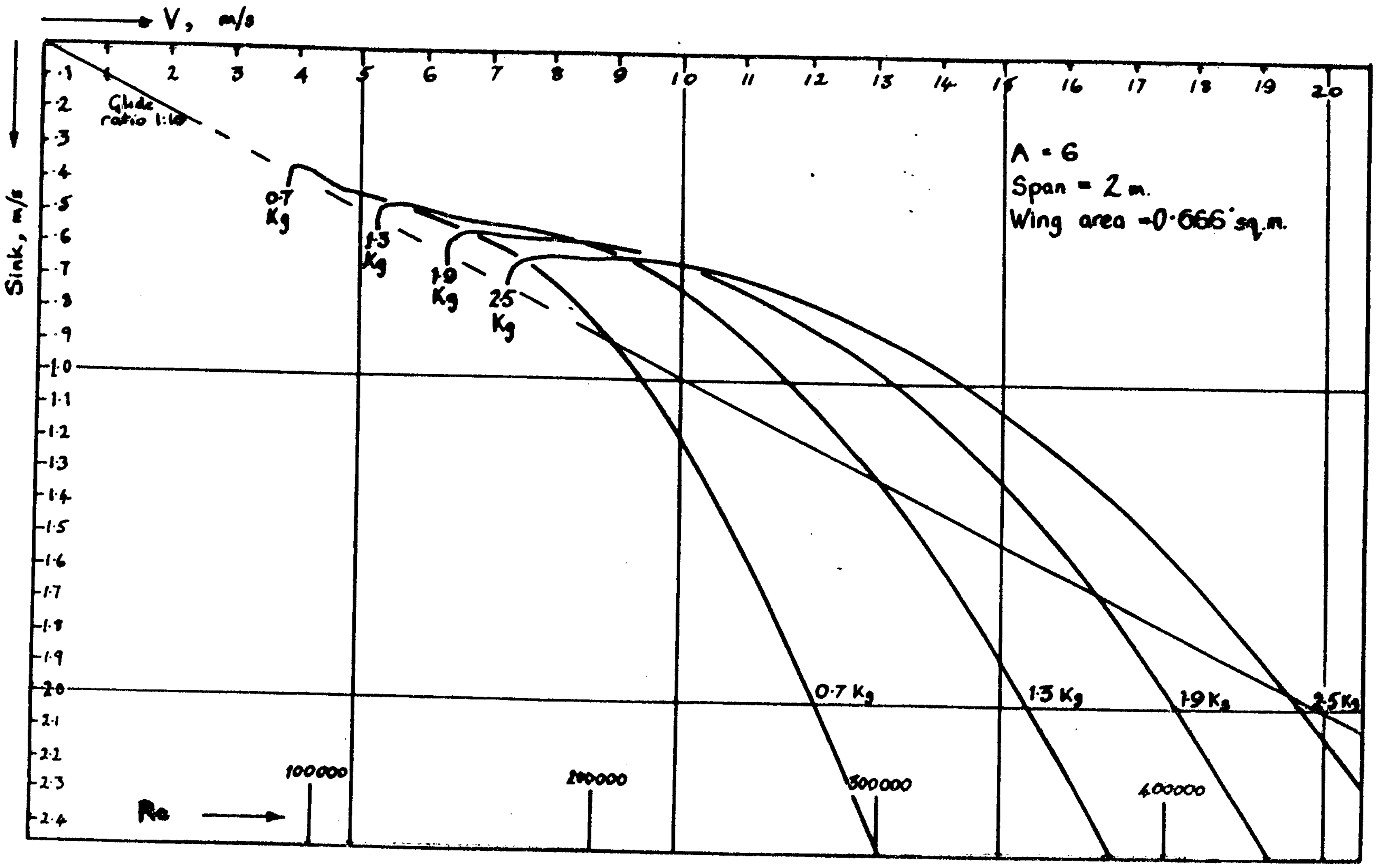

Figure 8. Polars for an idealised two metre wing without parasitic drag or other defects.

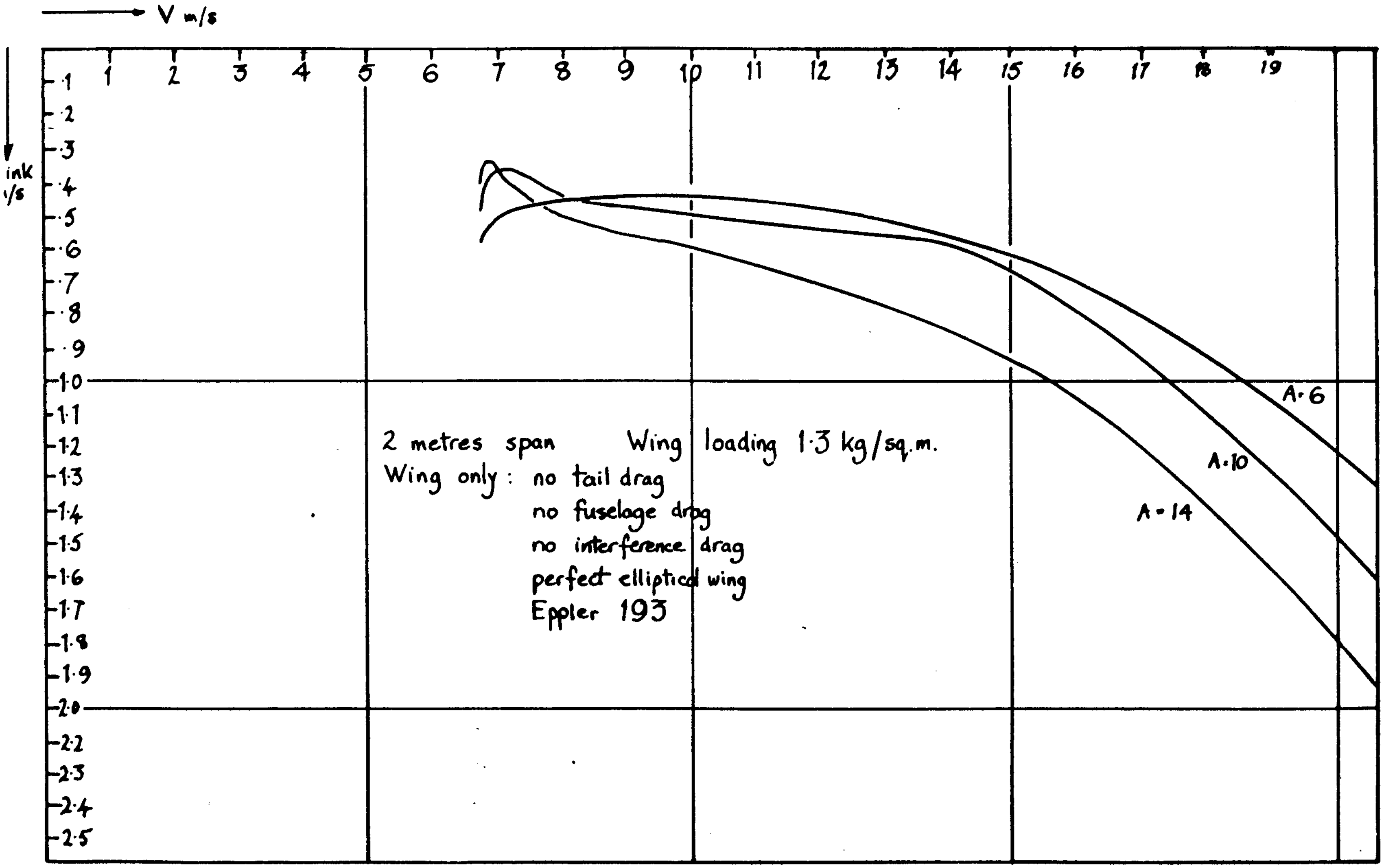

AIRFOIL DESIGN

This paper was entered by Michael Selig in a competition which was sponsored by the American Institute of Aeronautics and Astronautics. Although you might not think that a paper which referenced only model aircraft parameters was primary AIAA material, he won first place in the competition. Michael became skilled in .using the Eppler airfoil design program during his undergraduate studies at the University of Illinois. Although a number of modelers have made use of the Eppler method to study and develop model airfoils, none that I am aware of, have gone to the depth that Michael explores in this paper. The conclusions that he has reached about the peculiarities of designing for models are important and unique. I hope that they point out useful directions for others who are studying airfoil development; and I'm sure that his designs and advice will help others to build superior sailplanes.

Michael is transferring his Aerospace studies to the graduate school at Princeton University this fall. He has been granted a position as a research assistant there where he will be working toward his Master's in Aerospace Engineering. He has also been sponsored by AIAA to present this paper at their national conference in Reno Nevada this fall.

THE DESIGN OF AIRFOILS AT LOW REYNOLDS NUMBERS

Presented at the 1984 AIAA Student Paper Conference

Sponsored by

Purdue University AIAA Student Chapter on March 23-24, 1984

By

MICHAEL S. SELIG

B. S. 1984
AERONAUTICAL AND ASTRONAUTICAL ENGINEERING
UNIVERSITY OF ILLINOIS AT URBANA-CHAMPAIGN

May 20, 1984

ABSTRACT

This report focuses on the design of airfoils at low Reynolds numbers (100,000 < Re < 500,000), specifically those applicable to radio-controlled model sailplanes. Two common types of airfoil lift and drag hysteresis are illustrated and explained in terms of the behavior of the upper-surface laminar separation bubble which is commonly present at these low Reynolds numbers. The theoretical section characteristics of several airfoils predicted by the Eppler computer program for the design and analysis of low-speed airfoils were compared with the recent data of Dieter Althaus. Good correlation was found between the type of hysteresis and the type of upper-surface pressure recovery. Also, the validity of the predicted section characteristics is discussed for this Reynolds number regime. From the comparisons, the desirable qualities of a low Reynolds number airfoil were determined. Based on these qualities, several airfoils for radio-controlled model sailplanes were subsequently designed and analyzed using the Eppler computer program.

INTRODUCTION

Increasing interest has been given to airfoils operating at chord Reynolds numbers (Rn) below 500,000. Radio-controlled (R/C) sailplanes, being the author's hobby and motivation for this study, fly in this Rn regime. Additional applications include the following: remotely piloted vehicles at low speeds or high altitudes, inboard sections of helicopter blades, human-powered aircraft, windmill blades, slats and flaps of high-lift, multi-element airfoils, struts on light aircraft, and turning vanes in air supply ducts.

This report focuses on the design of airfoils at low Reynolds numbers, specifically those applicable to R/C sailplanes. The approach taken in this report was to compare for several airfoils the theoretical section characteristics predicted by the Eppler computer program [1,2] with the experimental data of Althaus [3]. From these comparisons, the desirable qualities of a low Rn airfoil were determined. Based on these comparisons, several R/C sailplane airfoil were designed and analyzed using the Eppler computer program.

AIRFOILS AT LOW REYNOLDS NUMBERS

For airfoils at low Rn's, the phenomena of a laminar separation bubble and turbulent separation significantly increase the drag and decrease the lift which both contribute to low lift-to-drag ratios. Increasing the Rn will reduce the length of the laminar separation bubble and the extent of turbulent separation. Correspondingly, the lift-to-drag ratios increase. For the upper surface of the airfoil at positive incidence, the boundary layer is laminar along the upper-forward surface of the airfoil. This laminar flow then separates upon entry into an adverse pressure gradient of sufficient magnitude, and then quickly undergoes transition to turbulent flow in the separated shear layer. Depending on the severity of the adverse pressure gradient, this separated turbulent boundary layer may or may not reattach to the airfoil's surface. The region of recirculating air enclosed by the laminar separation point and the turbulent reattachment point is called a laminar separation bubble. With reattachment, the turbulent boundary layer may then separate ahead of the trailing edge. For the lower surface at positive incidence, typically the boundary layer has little tendency to separate and commonly is entirely laminar. Figure 1 illustrates an airfoil with attached turbulent flow followed by turbulent separation on the upper surface and laminar flow on the lower surface.

If the Rn is low enough such that reattachment does not occur, increasing the Rn to some value, known as the critical Rn, causes reattachment of the turbulent boundary layer, which can be identified by a dramatic increase in the lift-to-drag ratio and a lift curve that is approximately linear with angle of attack, i.e. straight. Clearly, the possibility of both laminar and turbulent separation should be considered in the design of airfoils in this low Rn regime.

See Appendix I for a brief discussion of the Rn.

Hysteresis

As an airfoil is cycled through increasing angles of attack up to stall, the laminar separation point progresses forward. At some angle of attack, reattachment cannot occur, causing the laminar separation bubble to "burst." This bursting is manifested as a stall. Through decreasing angles of attack, the bubble, in general, does not behave in the same manner as for increasing angles of attack, thus accounting for the phenomenon of hysteresis shown in experimental lift and drag curves. Two common types of hysteresis will now be discussed.

Figure 2 illustrates the section characteristics of an airfoil that exhibits a common type of hysteresis which, for this discussion, will be called high-lift hysteresis. For this case, increasing the angle of attack causes the laminar separation point and turbulent reattachment point to both move forward toward the leading edge with the reattachment point moving forward at a slightly greater rate such that the bubble decreases in length. Eventually, a short bubble exists only on the leading edge of the airfoil. Further increasing the angle of attack causes this short leading edge bubble to "burst," resulting in a leading edge stall characterized by a sharp drop in lift. Upon decreasing the angle of attack, the leading edge bubble reattaches at an angle of attack lower than that of the stall for increasing angles of attack. The airfoil then behaves as it did for increasing angles of attack.

Figure 3 illustrates the section characteristics of an airfoil that exhibits another common type of hysteresis which, for this discussion, will be called moderate-lift hysteresis. For this case, increasing the angle of attack causes the laminar separation point to progress forward, as it did for the case of high-lift hysteresis. In contrast to a airfoil with high-lift hysteresis the reattachment point moves backward toward the trailing edge forming a bubble of increasing length. As this happens, the lift curve begins to flatten out and the drag curve quickly increases. Up to this point, the process can be thought of as a soft trailing-edge stall. Increasing the angle of attack further unstalls the airfoil by causing the long bubble to collapse into a short bubble near the leading edge. This occurence can be identified by a sharp increase in the lift and a dramatic decrease in the drag. Increasing the angle of attack further causes the airfoil to fully stall. When decreasing the angle of attack, a sharp drop in lift is noted due to reformation of the long bubble at an angle of attack lower than that at which the sharp increase was noted with increasing angles of attack. For some airfoils, the contraction and reformation of the long bubble occur at the same angle of attack. Several popular Eppler airfoils exhibit this type of hysteresis as will be shown later.

Airfoils with moderate-lift hysteresis tend to show a high drag knee, that is, an increase in drag through the middle of the drag polar. Airfoils with high-lift hysteresis, on the other hand, do not exhibit a knee and generally have lower drag. Because of this, airfoils that exhibit high-lift hysteresis are favored for low Reynolds number applications.

INFLUENCING TRANSITION

The formation of the laminar separation bubble is due to the inability of the boundary layer to make a natural transition to turbulent flow before it attempts to negotiate an adverse pressure gradient of sufficient magnitude to cause laminar separation [4]. If it were possible at low Rn´s for the boundary layer to make a transition before the adverse pressure gradient, the bubble and its drag could be eliminated. Several parameters which influence transition [5] are as follows:

1. Boundary-layer suction and blowing
2. Disturbances in the free-stream flow
3. Surface roughness
4. Pressure distribution (velocity distribution)

Although advantageous at low Rn´s, boundary-layer suction and blowing [6] are of little practical value to the modeler because of the complexity of such a suction or blowing device and for this reason, will not be discussed here. Also, disturbances in the free-stream flow will not be discussed as they are not applicable in the case of R/C sailplanes.

Surface roughness has some application for low Rn airfoils. It is a common practice for free flight modelers to place a turbulator along the upper-forward surface. If effectively positioned, this turbulator artifically causes transition of the boundary layer to occur before the adverse pressure gradient and thereby eliminates the bubble and its drag.

The foremost disadvantage of the turbulator is its fixed position. While a turbulator may improve the overall performance of an airfoil at low Rn´s, at higher values, the turbulator causes transition earlier than needed which results in more drag than necessary. Therefore, one can understand why this method of influencing transition is employed mostly on free-flight models that operate at very low Rn´s about which there are minimal fluctuations.

The influence of the pressure distributions on transition will be discussed in a later section.

COMPARISONS OF THEORETICAL AND EXPERIMENTAL PERFORMANCE

The Eppler Computer Program

The theoretical section characteristics of several airfoils were computed using the Eppler computer program which has the following three capabilities: (1) potential flow design, (2) potential flow analysis, and (3) boundary-layer analysis. For the design method, the potential flow velocity distribution about an airfoil is specified. From this, the airfoil contour is determined by conformal mapping. In the analysis method, the velocity distribution for a given airfoil is determined by a panel method. To compute the section characteristics, the boundary-layer routines of the program incorporate an empirical transition criterion, and empirical skin friction, dissipation, and shape factor laws.

For Rn´s greater than those considered in this report, the theoretical section characteristics compare favorably with experimental measurements. As will be shown, however, the program does not accurately predict the section characteristics of airfoils at low Rn´s since it makes the assumption that if the flow undergoes laminar separation before transition, the flow quickly reattaches as turbulent flow - the assumption of a short bubble. For higher Rn´s, corresponding to those in the full-size sailplane regime, this quick reattachment is characteristic of the flow; but, for lower Rn´s, this assumption is not valid since the bubble can extend over 20-30% of the upper surface of an airfoil. If the program predicts a laminar separation bubble longer than 0.03c, this is listed in the output summary as a warning that the theoretical section characteristics may not be indicative of the actual section characteristics. As one might expect, this warning commonly appears for airfoils analyzed at low Rn´s.

The limitations of the program should be realized. Due to the incorporation of the short-bubble assumption, the present version of the program does not account for the additional bubble drag. If the program predicts turbulent separation, a small approximate drag penalty is added. Also, the program includes a correction for the pitching-moment and lift coefficients due to turbulent separation; however, it does not include a correction for a bubble. Despite this latter exclusion, the theoretical maximum lift coefficient is in most cases indicative of the experimental maximum lift coefficient. With these limitations in mind, the theoretical section characteristics should be cautiously interpreted in this low Rn regime. This interpretation is discussed in further detail in a later section.

Althaus´ Experimental Work

Several problems are incountered in obtaining reliable experimental lift and drag measurements of an airfoil in the low Rn regime. First, the ambient turbulence, tunnel noise, model vibration, and model surface contaminations all cause transition to occur earlier on the test model than in actual use. This has profound consequences - namely, it produces a shorter bubble and hysteresis which is less pronounced than that found in actual use to such an extent that the airfoil appears better than it actually is. Second, accurately measuring the extremely small lift and drag forces presents many difficulties. These problems combined make it difficult to reliably conclude anything based on comparing the data of an airfoil tested in different wind tunnels.

In order that a self-consistent set of experimental data is considered, this paper will only examine data taken at a single facility. In particular, the author chose the data taken in 1980 by Althaus at the University of Stuttgart.

Comparisons

To represent a broad range of behavior, eleven airfoils were chosen for comparison of the theoretical and experimental section characteristics. For this report, however, only six of the eleven airfoils will be discussed. This is done without sacrafice to the clarity of the report or the conclusion which follow this section. These six airfoils may be grouped as follows:

1. Airfoils with high-lift hysteresis-
   FX63-137 and GOE801
2. Airfoils with moderate-lift hysteresis-
   E193 and E201
3. Airfoils without hysteresis-
   NACA0009 and FX60-100

The CLARK-Y, FX63-137, E392, GOE795, and FX60-100 were compared and are discussed in detail in reference [8].

For all airfoils compared, except those of Eppler, the original coordinates published in Althaus's book [3] had to be smoothed using a cubic spline smoothing program. This was done because the original coordinates caused irregularities or oscillations in the velocity distributions as shown in Figs. 4 and 5. The velocity distributions for the smoothed and unsmoothed FX60-100 are shown in Fig. 6. Since the boundary-layer routines are highly sensitive to such irregularities, the theoretical section characteristics computed from the original coordinates are meaningless. For most coordinates, the difference between the original and smoothed coordinates was less than 0.0004c. In the case of wind tunnel models, it is probably true that these coordinates are similarly smoothed in the construction of the models.

To compare the drag polars, each airfoil was analyzed at the test Rn's used by Althaus, at a Rn of 400,000, and in some cases at a Rn of 600,000. Analyzing each airfoil at a common Rn of 400,000 inables one to compare the theoretical data of one airfoil with another. In order to make comparisons of the lift vs. drag data, Althaus's experimental data is co-plotted with the theoretical data. In some instances, Althaus's experimemtal data could not be co-plotted for a particular Rn because of the limits of the drag coefficient axis, this is indicated by the words "NOT SHOWN" on the graph. Commonly, due to a high drag knee at the lower test Rn's of Althaus ($60,000 < Rn < 100,000$), only a few experimental data points could be co-plotted at the high- and low-lift ends of the drag polar. In these cases, only those data points at the low-lift end were co-plotted. Also, Althaus' experimental lift curves are shown to illustrate the lift hysteresis of the airfoil. A theoretical lift curve is co-plotted with the experimental lift curves to show, in some cases, discrepencies which will be discussed in a later section.

The airfoil velocity distributions were plotted for angles of attack relative to the zero-lift line in increments of one or two degrees. The increment that was used can be distinguished by the relative differences in spacing between two adjacent velocity distributions.

A Theoretical Boundary-Layer Summary Table is presented that should be used as a guide when evaluating the theoretical section characteristics. When a "*" appears it indicates that the program predicts a laminar separation bubble longer than 0.03c. For these cases, the predicted drag is most likely too low since the program does not account for the additional bubble drag. When a "O" appears it indicates that the predicted bubble is shorter than 0.03c. In these cases, agreement between the theoretical and experimental section characteristics should be expected. If the predicted bubble is shorter than 0.03c and transition occurs before 0.05c, a "●" indicates this. Agreement, for these cases, generally is good. When a "-" appears it indicates separation without reattachment - a stall. The symbol "+" has been placed beside the angles of attack relative to the zero-lift line which are within the low-drag range of the drag polar.

Discussed next is the agreement or lack thereof between the theoretical and experimental section characteristics. Following this several conclusion are drawn.

Symbols are defined in Appendix II.

1. Airfoils with high-lift hysteresis. Airfoils in this group are the FX63-137 and GOE801, shown in Figs. 7-8 and 9-10. Agreement between the theoretical and experimental drag at a Rn of 200,000 is relatively good for both airfoils. This suggests that at this Rn, the bubble is short. For the FX63-137 at Rn's greater than critical Rn near 85,000, the theoretical and experimental lift curves are in poor agreement. In contrast, for the GOE801 at Rn's greater than critical, the lift curves are in fairly good agreement. These two airfoils differ greatly in the amounts of aft loading with, the FX63-137 having the larger amount. For these airfoils at a Rn of 400,000, the program does not predict a laminar separation bubble at high angles of attack within the low-drag range of the drag polar. Notice that these airfoils have a have a convex velocity distribution recovery. This is in contrast to the next group of airfoils.

2. Airfoils with moderate-lift hysteresis. Airfoils in this group are the E193 and E201, shown in Figs. 11-12 and 13-14. Again,

agreement between the theoretical and experimental drag is good at a Rn of 200,000. At a Rn of 100,000 which is above the critical value of 60,000, these airfoils show a high drag knee between the lift coefficients of 0.5 and 1.0, which suggests the presence of an attached bubble of increasing length for increasing angles of attack. The theoretical and experimental lift curves are in fairly good agreement. For both airfoils at a Rn of 400,000, a laminar separation bubble is predicted on the upper surface for angles of attack within the low-drag range of the drag polar. These Eppler airfoils are similar in that the velocity distribution is characterized at a particular angle of attack by a constant velocity rooftop (shown in Fig. 11), followed by a slightly concave velocity recovery.

While not compared in this paper, when tested by T. J. Mueller and L. J. Pohlen [7] at the University of Notre Dame, the Miley M06-13-128 airfoil [4], which has a very concave velocity distribution with no aft loading, demonstrated this type of hysteresis for Rn's less than 150,000.

3. Airfoils without hysteresis. Airfoils in this group are the NACA0009 and FX60-100, shown in Figs. 15-16 and 17-18. These airfoils have a critical Rn below 60,000. Agreement for the NACA0009 is inconsistent; but, as expected for thin airfoil with no camber, it does have low drag. The FX60-100 has aft loading which does not result in steep adverse pressure gradients at the trailing edge like that present in the case of the FX63-137. Agreement between the lift curves for both airfoils is good. Like the first group of airfoils with high-lift hysteresis, these airfoils have convex recovery regions.

Appendix III presents the theoretical section characteristics and a discussion of several popular R/C sailplane airfoils.

LOW REYNOLDS NUMBER AIRFOIL DESIGN CONSIDERATIONS

At low Rn´s it is desirable to have the flow transition early allowing for quick reattachment and thereby avoiding a long laminar separation bubble. As discussed previously, a turbulator effectively achieves this but results in a drag greater than necessary at higher Rn´s. In designing airfoils specifically for R/C sailplanes operating in the Rn regime from 100,000 (C_ℓ=1.2) to 600,000 (C_ℓ=0.1), it is desirable on the upper surface to have transition occur early at low Rn´s (high C_ℓ´s) and later at high Rn´s (low C_ℓ´s). The AQUILA airfoil, presented in Appendix III, illustrates this movement of the theoretical upper surface transition point. This movement can only be achieved by the proper design of the velocity distribution along the upper-forward surface of the airfoil so that a laminar separation bubble is not predicted. Also, this type of design shows a theoretical drag which slowly increases with increasing lift coefficients rather than a theoretical drag which quickly increases like the designs of Eppler.

Here the comment should be made that while the Eppler airfoils are excellent in that they have low drag and wide drag polars at Rn´s above around 200 000, they suffer from large laminar separation bubbles at Rn´s below this. Because of this, the Eppler airfoils perform well on F3B type models but not so well on soaring type models which typically operate at Reynolds number less than 200,000. Not surprisingly with the increasing popularity of the Eppler sections, there has been a trend to increase the chord lengths and wing loadings both of which increase the Reynolds number. Also, there seems to be a consensus among modelers that the Eppler sections must be flown "on step," i.e. fast. This too increases the Reynolds number.

From the comparisons, it is concluded that the type of velocity recovery employed should be linear to convex in order to prevent moderate-lift hysteresis.

As demonstrated in the comparisons, the theoretical and experimental lift and drag coefficients are in poor agreement for airfoils with large amounts of aft loading, or thick trailing edges which result in steep adverse pressure gradients on the upper surface near the trailing edge. Such a gradient likely leads to turbulent separation on the upper surface that extends further upstream than can be predicted by conventional boundary-layer methods. Examples of airfoils with large amounts of aft loading are the FX63-137 and E214 shown in Appendix III.

SOME NEW AIRFOILS DESIGNED FOR R/C SAILPLANES

Based on the previously discussed low Rn airfoil design considerations, several airfoils were designed by the author using the Eppler computer program - the same program that Eppler used to design the E193, E201, E392, etc..

The author's airfoil nomenclature is as follows: the first four digits are unique to each individual airfoil, larger numbers being later designs; the next three digits indicate the section thickness ratio times 1000; and the last two digits designate the year of design.

S2046-090-83, Figs. 19-20 - This 9% thick airfoil is based on the HQ2.5/9 shown in Appendix III. The velocity distributions of the HQ2.5/9 show that it pulls a suction peak (shown in Fig. 62) on the leading edge of the lower surface for angles of attack less than four degrees. This suction peak increases the bias toward laminar separation on the lower surface at low angles of attack. In redesigning the HQ2.5/9, emphasis was placed on mantaining the same section thickness and drag polar structure while mitagating the lower surface suction peak. The resulting airfoil is slightly thicker than the HQ2.5/9 along the lower-forward surface. The new airfoil should out-perform the HQ2.5/9.

S2091-101-83, Figs. 21-22 - This airfoil is based on the AQUILA airfoil. Because of the flat-bottom contour of the AQUILA airfoil, it performs poorly at low angles of attack such that an R/C sailplane utilizing this airfoil suffers from poor wind penetration as a result of high drag at low angles of attack. The new airfoil has an extended low-lift, low-drag range, which allows for better penetration, without comprising the high-lift capability of the AQUILA airfoil. This airfoil is a good example of convex recovery with no steep pressure gradients on the upper surface near the trailing edge. As indicated in the Theoretical Boundary-Layer Summary Table, this airfoil is expected to perform as predicted. The author highly recommends it for use on a precision/duration type R/C sailplane.

S3002-099-83, Figs. 23-24-25 - This airfoil was designed for used with flaps. For zero flap deflection at a Rn of 100,000, its performance at high lift coefficients compares with that of the 2046 and

2091. Notice that the aft loading does not lead to steep adverse pressure gradients near the trailing edge. Figure 25 clearly illustrates the advantage of using flaps - that being a.wider operating range. At the low lift coefficients (near C_l=0.1, δ_f =-5 deg), the lower surface shows some separation; however, here the Rn of an R/C sailplane is much higher than 200 000. Therefore, this separation is of little concern for this application. At the high lift coefficients (near C_l= 1.1, δ_f =+5 deg), little separation is predicted. For lift coefficients less than 1.1 at positive five degrees flap deflection, both the lower and upper surfaces show separation at the low Rn's, and for this reason, excessive positive flap deflection at low lift coefficients and low Rn's is not desirable. Large positive flap deflections are suggested only for towing purposes, while small positive flap deflections are suggested for soaring in light lift.

S2027-145-83, Figs. 26-27 - This airfoil likely has a very soft stall as indicated by the smooth progression of the separation point on the upper surface. Close inspection of the airfoil reveals that both the upper and lower aft surface contours are concave rather than convex like the MB253515 and the thick low Reynolds number Eppler airfoils. This convexity should not be neglected in constructing a wing using this airfoil. Also, no attempt should be made to sharpen the leading edge, as such modification would lead to permature separation at the leading edge and lower the maximum lift.

S3010-103-84, Figs. 28-29 - In viewing the Theoretical Boundary Layer Summary Table, the S3010 is expected to operate efficiently at very low Reynolds numbers. Because of this, it is well suited for R/C hand launch gliders.

S3021-095-84, Figs. 30-31 - At a glance, the semi-flat-bottomed S3021 looks very much like the famed E205 airfoil. The major difference between the two is at the high lift coefficients. Unlike the E205, at high lift coefficients, the upper surface transition point of the S3021 progresses gradually towards the leading edge with increasing angle of attack. The result is improved performance at high lift (since the laminar separation bubble is shorter) while the integrity of the Eppler section at low lift is mantained.

S4022-113-84, Figs. 32-33 - Since this airfoil has large amounts of aft loading, its theoretical lift and drag coefficients probably would not agree with experimental data. The actual performance of the S4022 is most likely similar to the FX63-137 with the exception that its drag polar is narrower by virtue of the S4022 being thinner than the FX63-137.

S4053-089-84, Figs. 34-35 - The author was motivated to design this airfoil at the request of Stan Watson who wished to have a "thinned out E193." The S4053 designed like an Eppler section will perform like one; it must be flown at Rn´s near 200,000.

S4061-096-84, Figs. 36-37 - This airfoil would be an excellent choice for a cross-country sailplane where high lift-to-drag ratios are of most importance.

S4110-084-84, Figs. 38-39 - By smoothing the upper surface velocity distributions of the S2046 and combining it with the lower surface of the S2091, the S4110 results. Since the low drag range is so narrow like the HQ2.5/9, it is suggested that flaps be used on this airfoil.

S4158-109-84, Figs. 40-41 - The unique S4158 must be considered strictly experimental. At the low lift and high Rn's, the flow on the upper surface is predicted to transition around 68% of the chord where it then incounters a steep adverse pressure gradient similar the a low drag stratford recovery. To promote transition at this point a turbulator could be place slightly ahead at 60%. At intermediate lift coefficients, this airfoil probably has a high drag knee and, therefore, should be flown at high Rn's to avoid this added drag.

S4180-098-84, Figs. 42-43 - The S4180 was designed primarily for soaring. Its ability to penetrate equals that of the AQUILA airfoil. According to the Theoretical Boundary-Layer Summary Table, this airfoil should out-perform the AQUILA in distance and duration.

S4233-136-84, Figs. 44-45 - This airfoil is a thinner, lower drag version of the S2027.

S4310-109-84 and S4320-094-84, Figs. 46-47 and 48-49 - Like the S3021 these airfoils are expected to be improvements over the Eppler sections.

As discussed, the selection of an airfoil should not be based solely on comparisons of the theoretical section characteristics predicted by the Eppler computer program. In addition, the velocity distributions, Theoretical Boundary-Layer Summary Table, and movement of the theoretical transition point should all be carefully examined before final selection.

CONCLUDING REMARKS

In designing airfoils for low Rn´s, a convex recovery is favored over a concave recovery, thus preventing moderate-lift hysteresis and its associated lift and drag penalties. Large amounts of aft loading which result in steep adverse pressure gradients should be avoided, and the transition point should be designed to progress forward toward the leading edge with increasing angles of attack in order to minimize the areas of laminar and turbulent separation that are detrimental to airfoil performance. Some new airfoils have been designed with these considerations and should prove to be successful specifically in application to R/C sailplanes. To use the Eppler computer program for the design and analysis of low Rn airfoils, the limitations of the boundary-layer analysis, as discussed, must be considered when designing and choosing an airfoil for use in the R/C sailplane Rn regime.

ACKNOWLEDGEMENTS

The author expresses special thanks to Dr. Mark D. Maughmer, Professor of Aerospace Engineering at Pennsylvania State University (formerly of the University of Illinois), for making available the Eppler computer program. In addition, the author especially thanks him for their many discussions throughout the course of this work.

APPENDIX I

The Reynolds number is defined as

$$R_n = \frac{Vc}{\nu} \qquad (I-1)$$

where

c = wing chord
V = velocity
ν = kinematic viscosity

At standard sea level conditions

$$\nu = 1.5723 \times 10^{-4} \ ft^2/sec \qquad (I-2)$$

Thus

$$R_n = 6360 \ Vc \ , \ sec/ft^2 \qquad (I-3)$$

The lift produced by the sailplane is given as

$$L = \tfrac{1}{2} \rho V^2 S C_L \qquad (I-4)$$

where

ρ = air density
S = wing area
C_L = total aircraft lift coefficient

For steady, level flight the lift is equal to the weight.

$$W = L \qquad (I-5)$$

Substituting equation (I-5) into (I-4) gives

$$W = \tfrac{1}{2} \rho V^2 S C_L \qquad (I-6)$$

Solving for the velocity yields

$$V = \sqrt{\frac{2 \ W/S}{\rho \ C_L}} \qquad (I-7)$$

where W/S is termed the wing loading.

Using equation (I-7), (I-3) may be expressed as

$$R_n = 6360\sqrt{\frac{2W/S}{\rho C_L}}\ C \qquad \text{(I-8)}$$

From equation (I-8) it is seen that increasing the wing loading and the chord length increase the Reynolds number and increasing the aircraft lift coefficient decreases the Reynolds number. It should be pointed out the the aircraft lift coefficient is commonly less than the wing lift coefficient. And the wing lift coefficient is typically less than the airfoil lift coefficient.

APPENDIX II

Symbols

c	airfoil chord, ft
C_{ℓ}	airfoil lift coefficient
C_d	airfoil drag coefficient
$C_{m\,c/4}$	airfoil pitching-moment coefficient at quarter-chord point
Rn	Reynolds number based on free-stream conditions and airfoil chord, for airfoil at standard sea level conditions, 6380VC where [VC]=[ft /sec]
t	airfoil thickness ratio
V	local velocity, ft/sec
V_{∞}	free-stream velocity, ft/sec
V/V_{∞}	nondimensional velocity
x	airfoil abscissa, ft
x/c	percent chord
α	angle of attack, degrees
α_o	zero-lift angle of attack relative to chord line - zero-lift line, degrees

Abbreviations

T.	boundary-layer transition point
S.	boundary-layer separation point
U.	upper surface of airfoil
L.	lower surface of airfoil

APPENDIX III

The following airfoils have been used on R/C sailplanes with much success. Of course, this success depends not only on the airfoil, but also, on the sailplane and ,most importantly, the skills of the pilot.

ANTARES, Figs. 50-51 - This airfoil, used on the Antares sailplane designed by Scott Christensen of Top Flite, is a "composite" airfoil. The upper surface is from the E193 and the lower surface from the E205. The resulting hybrid appears no different than the designs of Eppler.

AQUILA, Figs. 52-53 - This flat-bottom airfoil is used on the Airtronics Aquila R/C sailplane (now out-of-production) designed by Lee Renaud. Close inspection of the airfoil reveals that the upper-surface contour was borrowed from the E205. It is interesting to note that the upper-surface contour does not yield the same velocity distributions as the E205. The Theoretical Boundary-Layer Summary Table shows that at several angles of attack within the drag bucket, a laminar separation bubble is not predicted.

E205, E211, E214 and E374, Figs. 54-55, 56-57, 58-59, and 60-61 - These airfoils are designs of Eppler.

HQ2.5/9, Figs. 62-63 - Designed by Dr. Helmut Quabeck this airfoil was used by Ralf Decker of West Germany to win the 1983 R/C Soaring Championships held in York, England. By design, this airfoil is flown with flaps.

MB253515, Figs. 64-65 - This 15% thick ai foil, designed by Michael Bame, is thick enough to allow for use with powerful winches. Despite its thickness it has proven to be formidable airfoil in F3B competition. The waviness of the velocity distribution is characteristic of airfoils drawn with french curves as this one was. Note the convex recovery region.

REFERENCES

1. Eppler, Richard and Somers, Dan M., "A Computer Program for the Design and Analysis of Low-Speed Airfoils," NASA TM-80210, August, 1980.

2. Eppler, Richard and Somers, Dan M., "Low Speed Airfoil Design and Analysis " Proceedings of the NASA Advanced Technology Airfoil Research Conference, NASA CP-2045, Part 1, March 1978.

3. Althaus, Dieter, Profilpolaren Fur Den Modellflug, Villingen-Schwennigen: Necker-Verlag, 1980.

4. Miley, S. J., "On the Design of Airfoils for Low Reynolds Numbers," Proceedings of the Second International Symposium on the Technology and Science of Low-Speed Motorless Flight, The Soaring Society of America, Inc. September 1974.

5. Schlichting, Herman, Boundary-Layer Theory, 7th ed. Trans. by J. Kestin, New York: McGraw-Hill, 1979.

6. Horstmann, K. H., Quast, A., "Reduction of Section Drag by Blowing Through Rows of Holes in Areas of Laminar Separation Bubbles," Technical Soaring, Vol. VII, No. 1, September 1981.

7. Mueller, T. J. and Pohlen, L. J., "Boundary Layer Characteristics of the Miley Airfoil at Low Reynolds Numbers," AIAA-83-1795, July 1983.

8. Selig, Michael S., "The Design of Airfoils at Low Reynolds Numbers," Paper presented at the AIAA 1984 Student Paper Conference held at Purdue University on March 23-24, 1984.

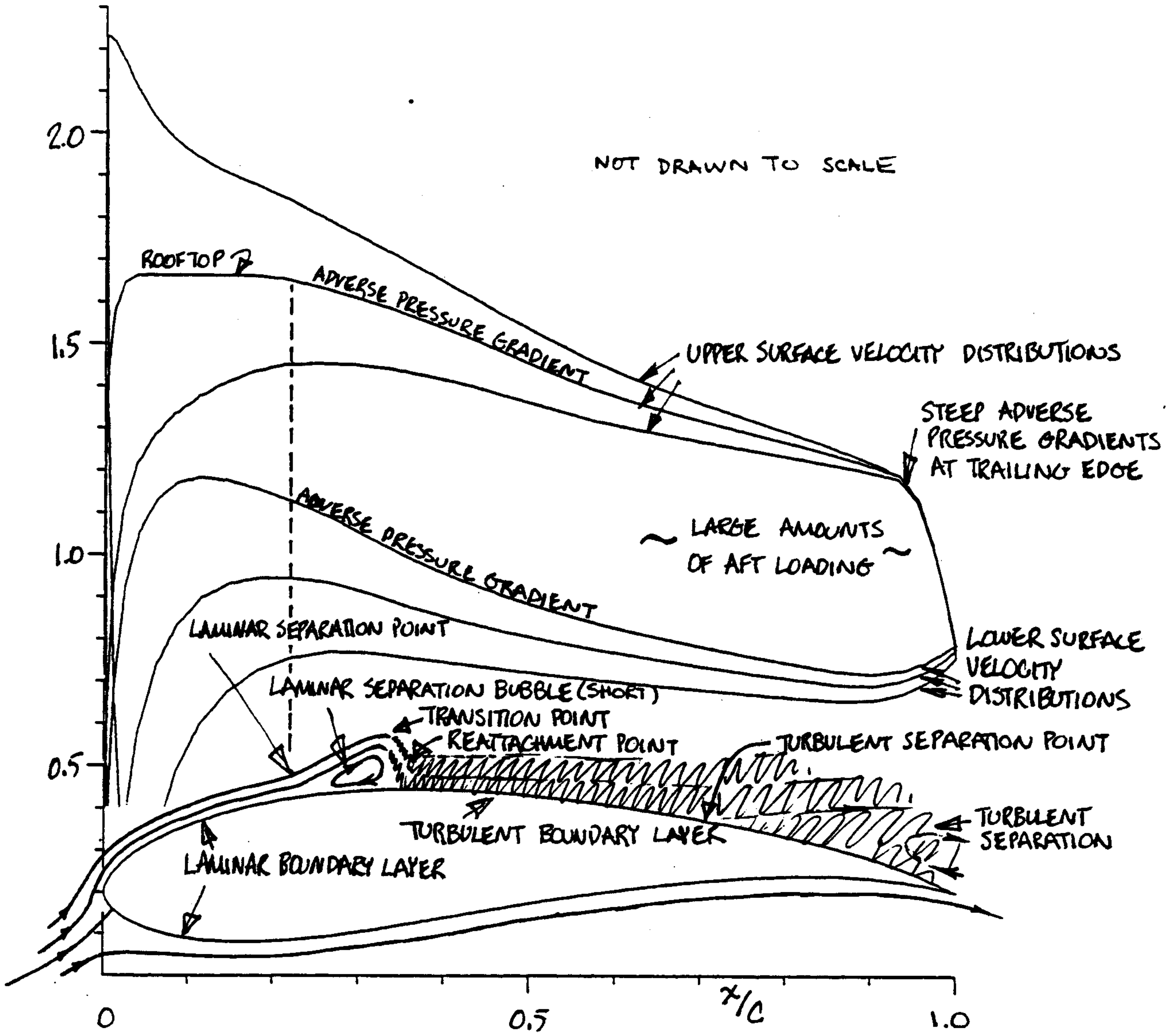

FIGURE 1.- ILLUSTRATION OF ATTACHED FLOW, FOLLOWED BY TURBULENT SEPARATION ON UPPER SURFACE WITH LAMINAR FLOW ON LOWER SURFACE.

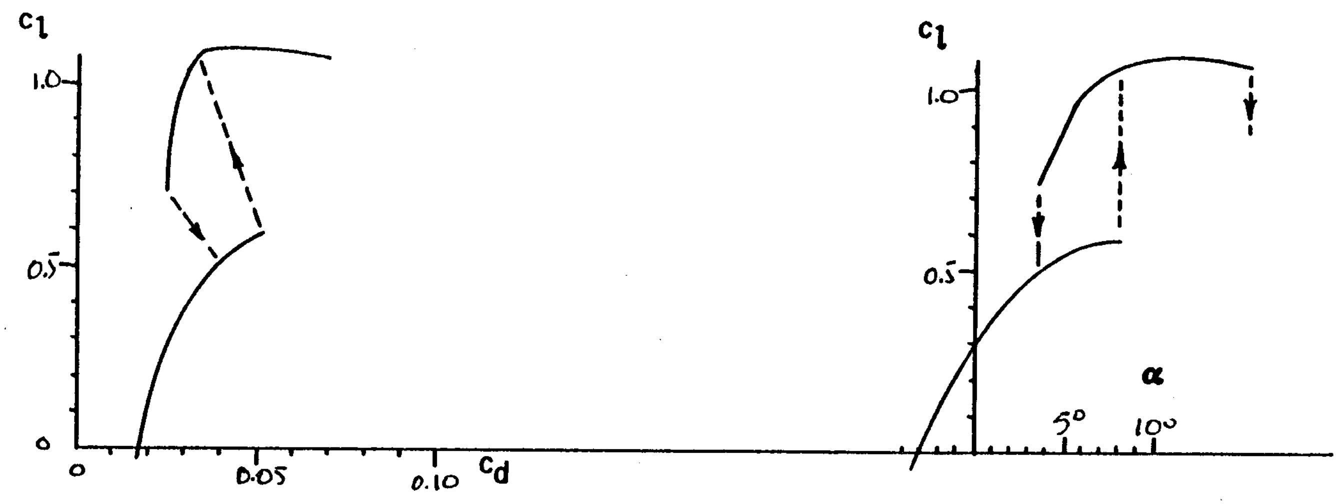

FIGURE 3.- TYPICAL SECTION CHARACTERISTICS OF AN AIRFOIL THAT EXHIBITS MODERATE-LIFT HYSTERSIS.

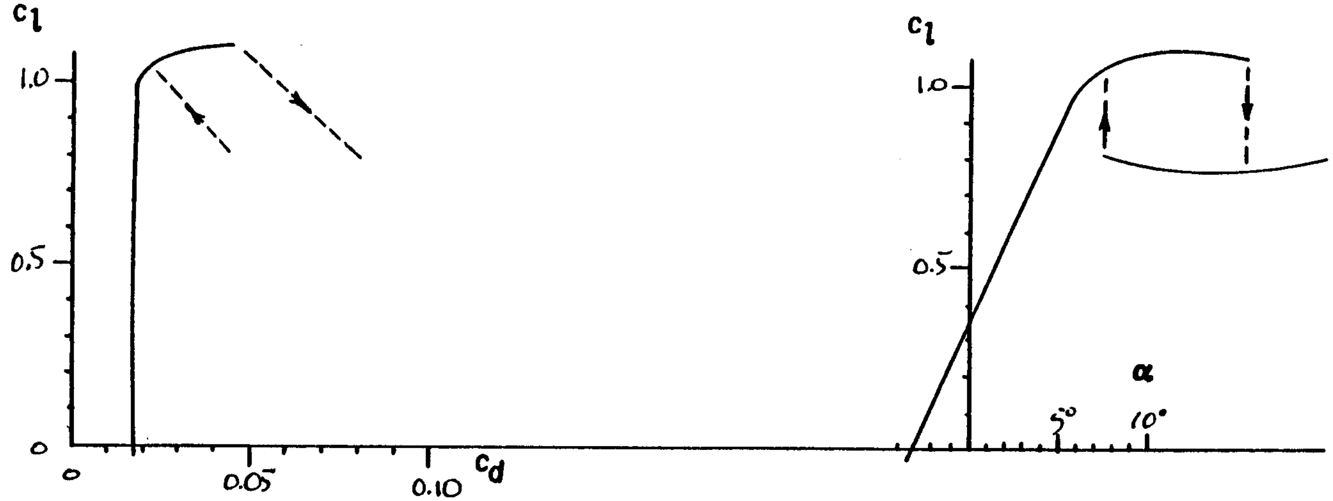

FIGURE 2.- TYPICAL SECTION CHARACTERISTICS OF AN AIRFOIL THAT EXHIBITS HIGH-LIFT HYSTERSIS.

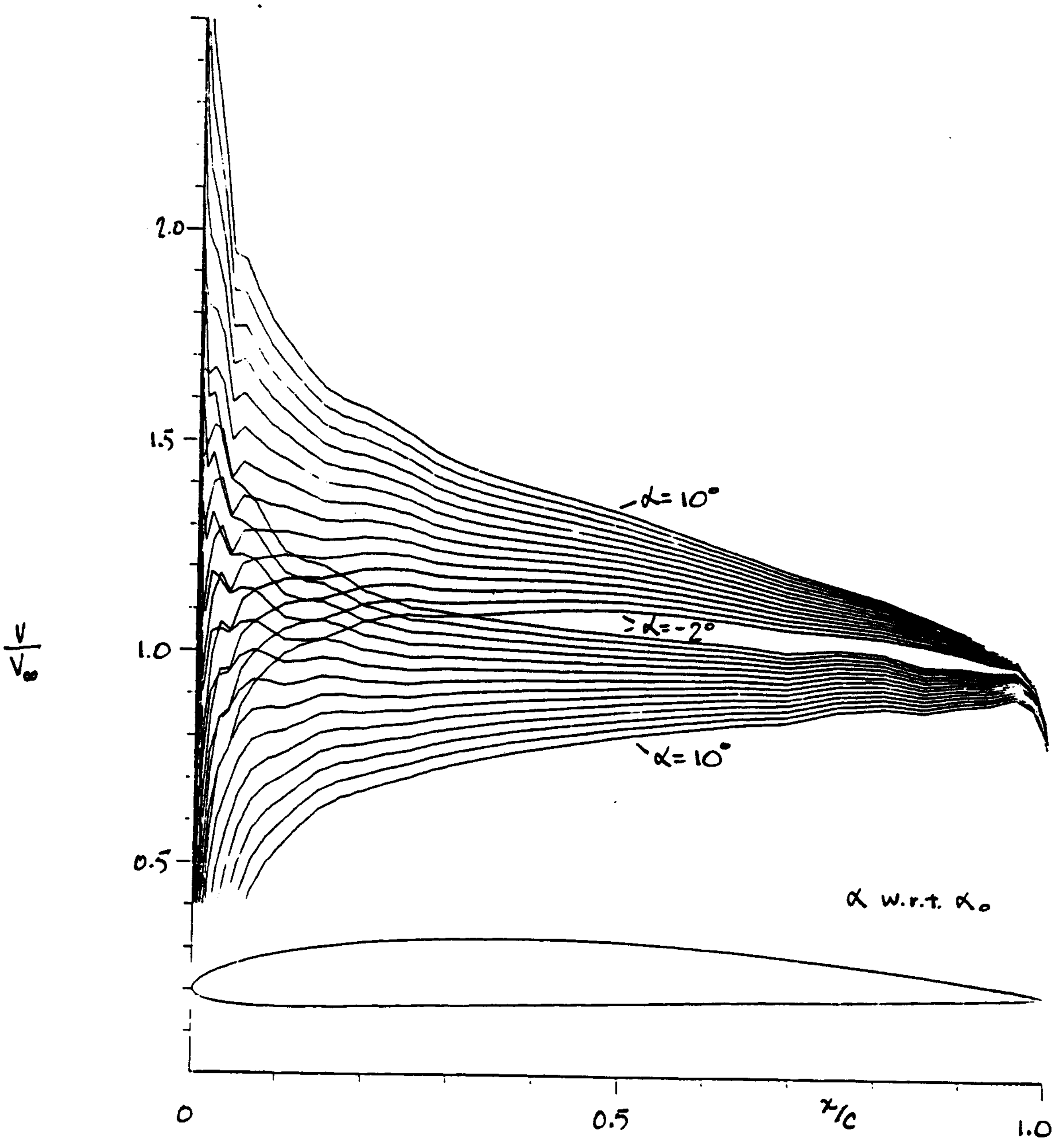

FIGURE 4.- VELOCITY DISTRIBUTIONS FOR THE ORIGINAL GOE 795 COORDINATES.

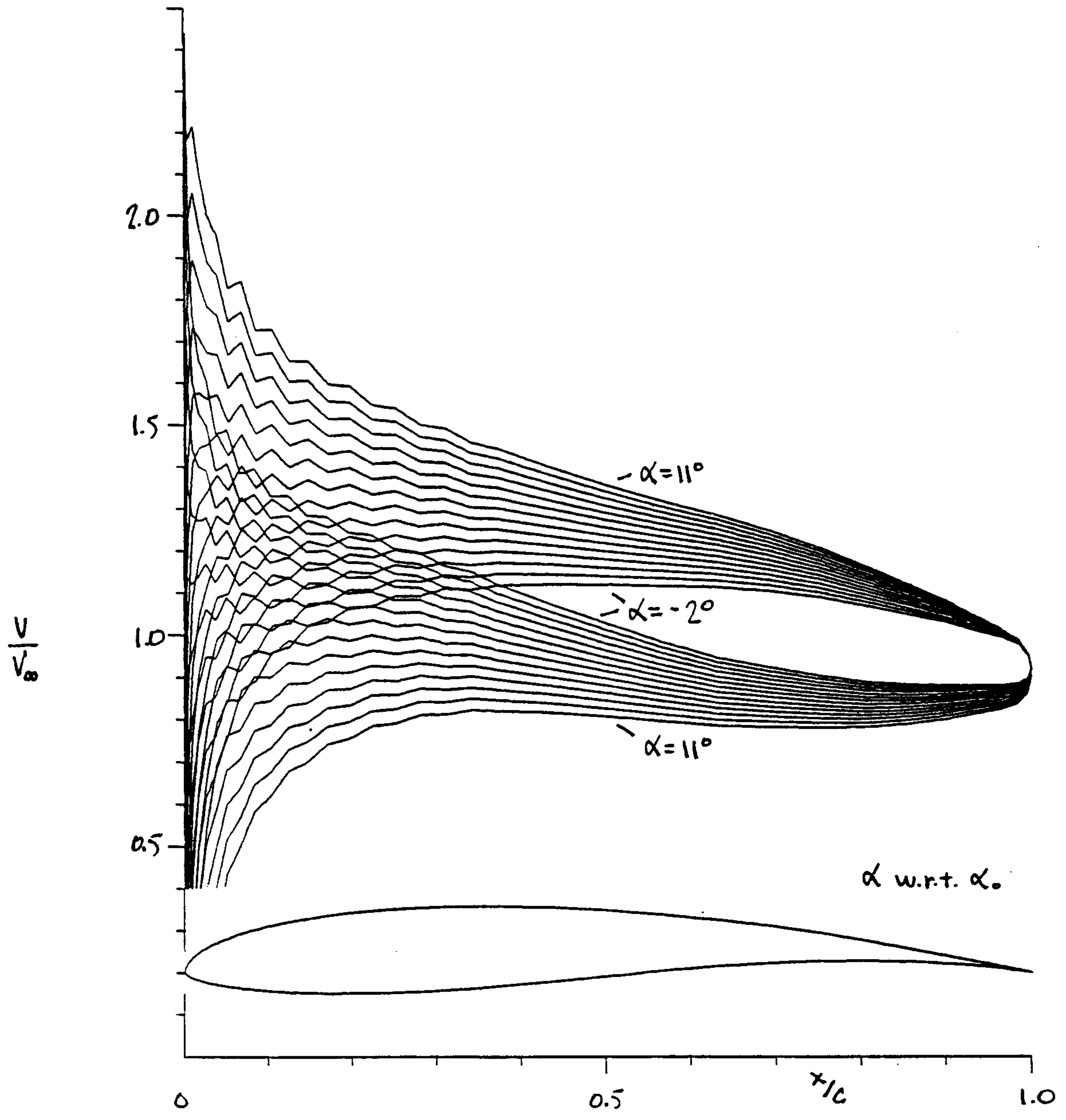

FIGURE 5.- VELOCITY DISTRIBUTIONS FOR THE ORIGINAL FX 60-100 COORDINATES.

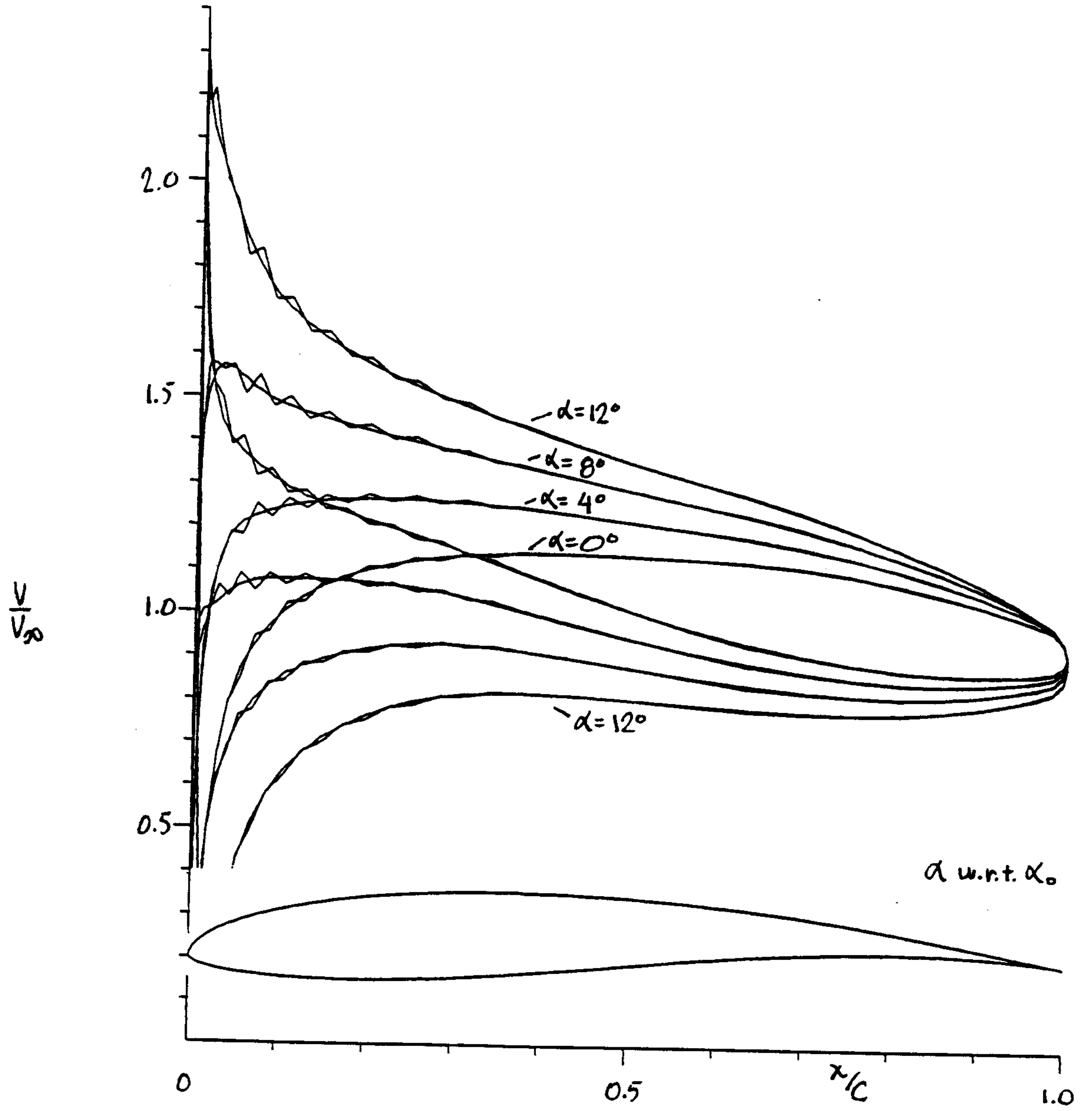

FIGURE 6.- VELOCITY DISTRIBUTIONS FOR THE ORIGINAL AND SMOOTHED FX 60-100 COORDINATES.

THEORETICAL BOUNDARY-LAYER SUMMARY TABLE										
AIRFOIL CLARK-Y	*-LAMINAR SEPARATION BUBBLE WARNING O-NO SEPARATION BUBBLE WARNING ●-NO BUBBLE, TRANSITION BEFORE 0.05C --SEPARATION AT LEADING EDGE (STALL) +-ANGLE OF ATTACK WITHIN DRAG BUCKET									
ALPHA (deg)	REYNOLDS NUMBER									
	60000		100000		200000		400000			
	us	ls	us	ls	us	ls	us	ls	us	ls
-1	-	-	-	-	*	*	*	●		
0	-	-	*	*	*	*	*	●		
1	*	*	*	*	*	●	*	●		
+ 2	*	*	*	*	*	*	*	●		
+ 3	*	*	*	*	*	*	*	*		
+ 4	*	*	*	*	*	*	*	*		
+ 5	*	*	*	*	*	*	*	*		
+ 6	*	*	*	*	*	*	*	*		
+ 7	*	*	*	*	*	*	*	*		
+ 8	*	*	*	*	*	*	O	*		
+ 9	*	*	*	*	*	*	O	*		
+10	*	*	*	*	*	*	O	*		
11	*	*	*	*	●	*	●	*		
12	*	*	*	*	●	*	●	*		

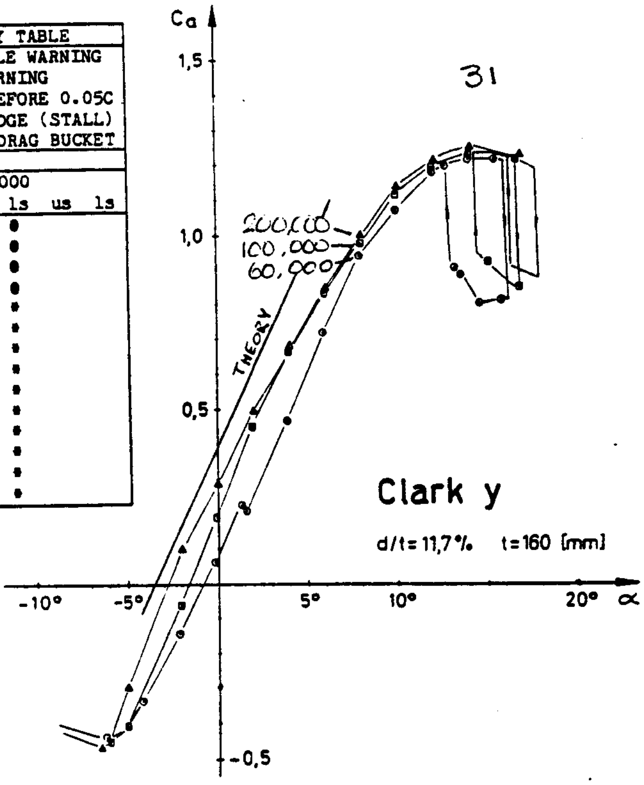

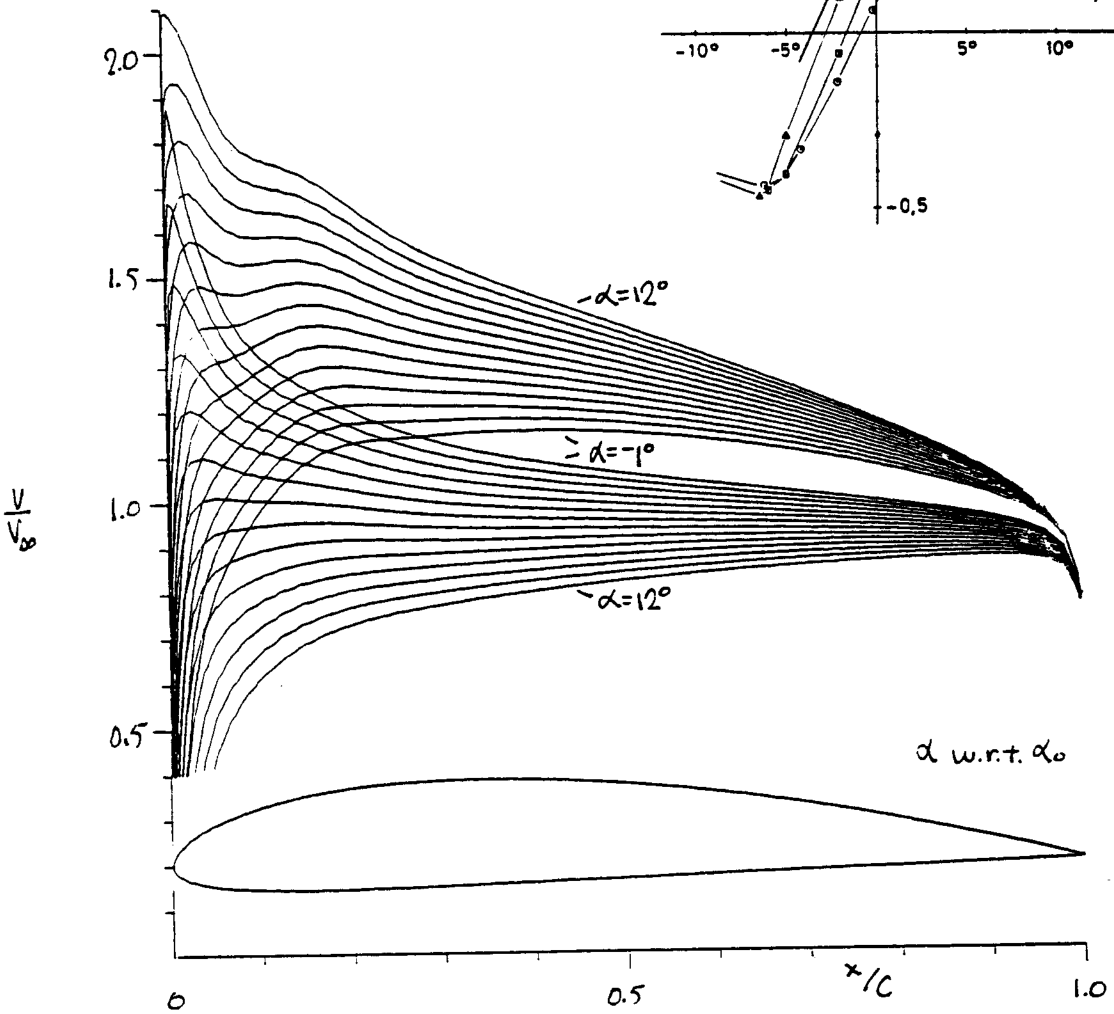

FIGURE7. - VELOCITY DISTRIBUTIONS FOR THE CLARK-Y AIRFOIL.

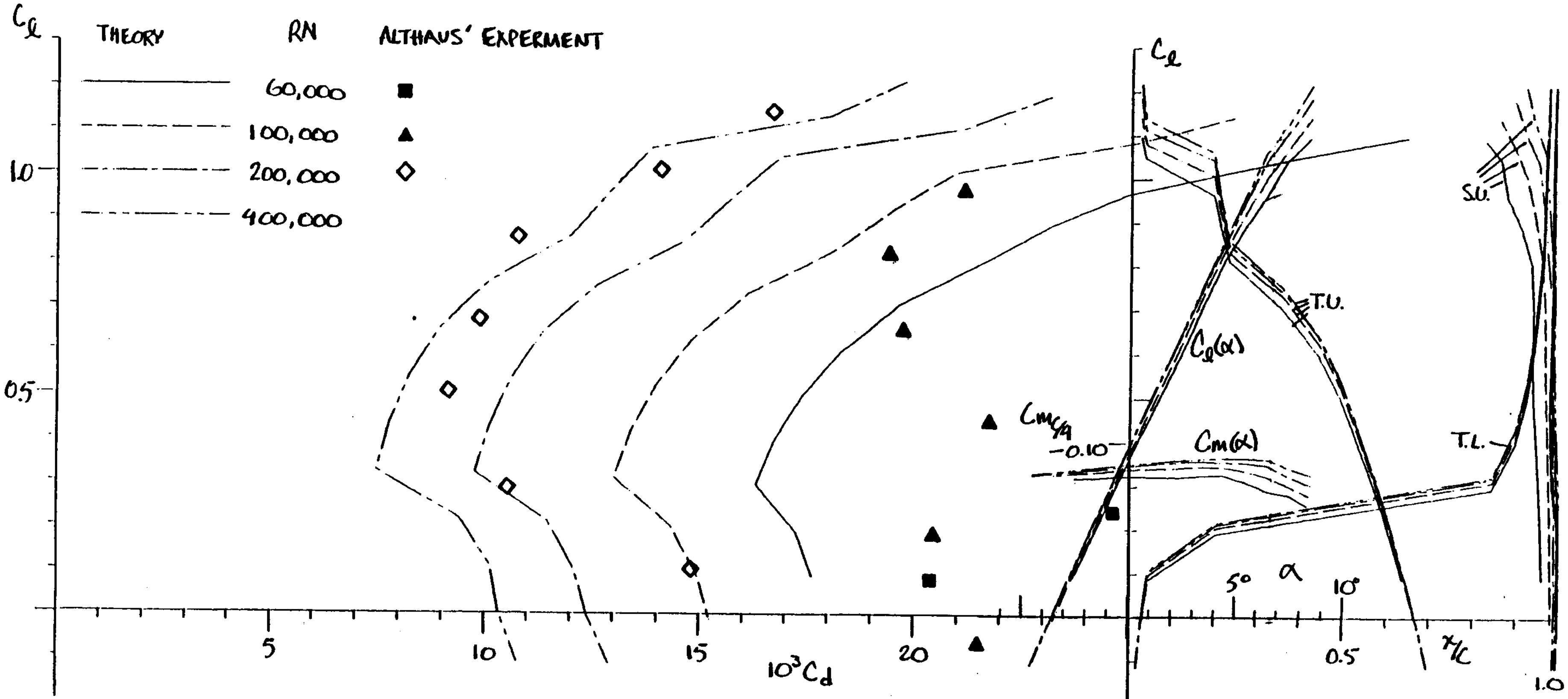

FIGURE 8.- COMPARISON OF THE THEORETICAL AND EXPERIMENTAL SECTION CHARACTERISTICS FOR THE CLARK-Y AIRFOIL.

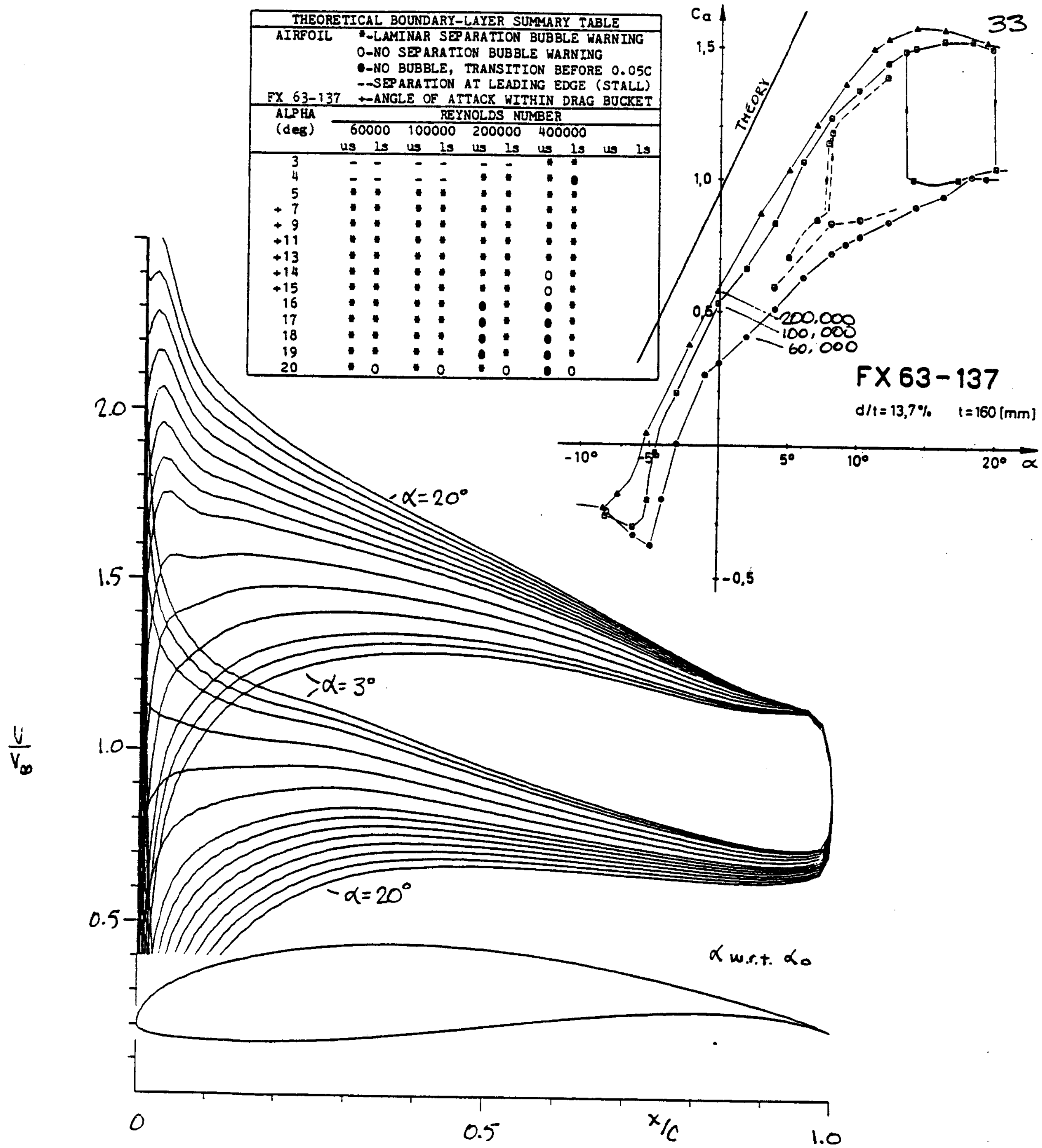

THEORETICAL BOUNDARY-LAYER SUMMARY TABLE										
AIRFOIL FX 63-137	*-LAMINAR SEPARATION BUBBLE WARNING O-NO SEPARATION BUBBLE WARNING ●-NO BUBBLE, TRANSITION BEFORE 0.05C --SEPARATION AT LEADING EDGE (STALL) +-ANGLE OF ATTACK WITHIN DRAG BUCKET									
ALPHA (deg)	REYNOLDS NUMBER									
	60000		100000		200000		400000			
	us	ls	us	ls	us	ls	us	ls	us	ls
3	-	-	-	-	-	-	*	*		
4	-	-	-	-	*	*	*	●		
5	*	*	*	*	*	*	*	*		
+ 7	*	*	*	*	*	*	*	*		
+ 9	*	*	*	*	*	*	*	*		
+11	*	*	*	*	*	*	*	*		
+13	*	*	*	*	*	*	*	*		
+14	*	*	*	*	*	*	O	*		
+15	*	*	*	*	*	*	O	*		
16	*	*	*	*	●	*	●	*		
17	*	*	*	*	●	*	●	*		
18	*	*	*	*	●	*	●	*		
19	*	*	*	*	●	*	●	*		
20	*	O	*	O	*	O	●	O		

FIGURE 9.- VELOCITY DISTRIBUTIONS FOR THE FX 63-137 AIRFOIL.

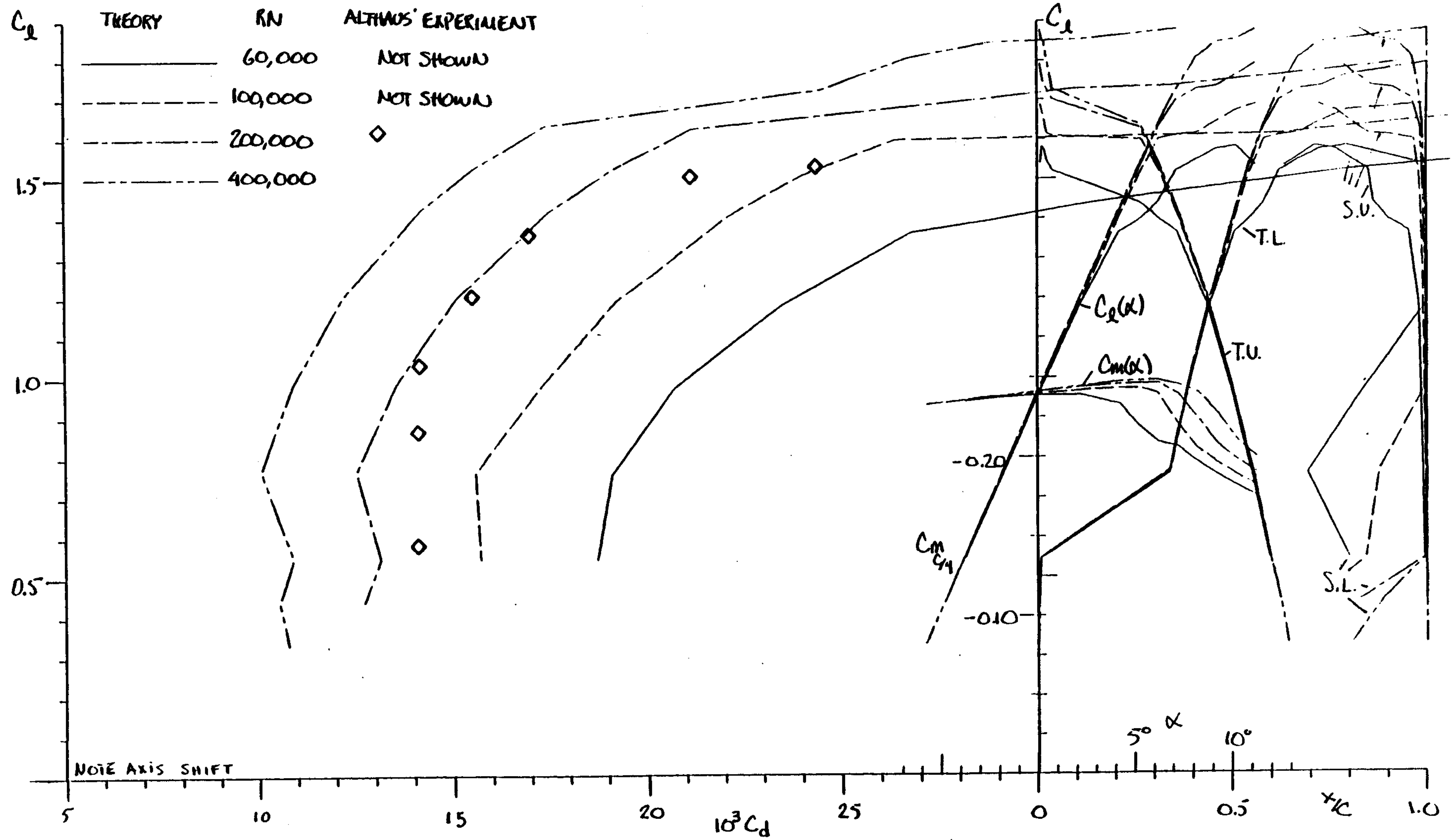

FIGURE 10.- COMPARISON OF THE THEORETICAL AND EXPERIMENTAL SECTION CHARACTERISTICS FOR THE FX 63-137 AIRFOIL.

THEORETICAL BOUNDARY-LAYER SUMMARY TABLE										
AIRFOIL E 193	*-LAMINAR SEPARATION BUBBLE WARNING O-NO SEPARATION BUBBLE WARNING ●-NO BUBBLE, TRANSITION BEFORE 0.05C --SEPARATION AT LEADING EDGE (STALL) +-ANGLE OF ATTACK WITHIN DRAG BUCKET									
ALPHA (deg)	REYNOLDS NUMBER									
	60000		100000		200000		400000			
	us	ls	us	ls	us	ls	us	ls	us	ls
-1	-	-	-	-	-	-	*	*		
0	-	-	*	*	*	*	*	●		
1	*	*	*	*	*	●	*	●		
+ 2	*	*	*	*	*	*	*	*		
+ 3	*	*	*	*	*	*	*	*		
+ 4	*	*	*	*	*	*	*	*		
+ 5	*	*	*	*	*	*	*	*		
+ 6	*	*	*	*	*	*	*	*		
+ 7	*	*	*	*	*	*	*	*		
+ 8	*	*	*	*	*	*	*	*		
+ 9	*	*	*	*	*	*	*	*		
+10	*	*	*	*	*	*	*	*		
11	-	-	●	*	●	*	●	*		
12	-	-	-	-	-	-	●	*		

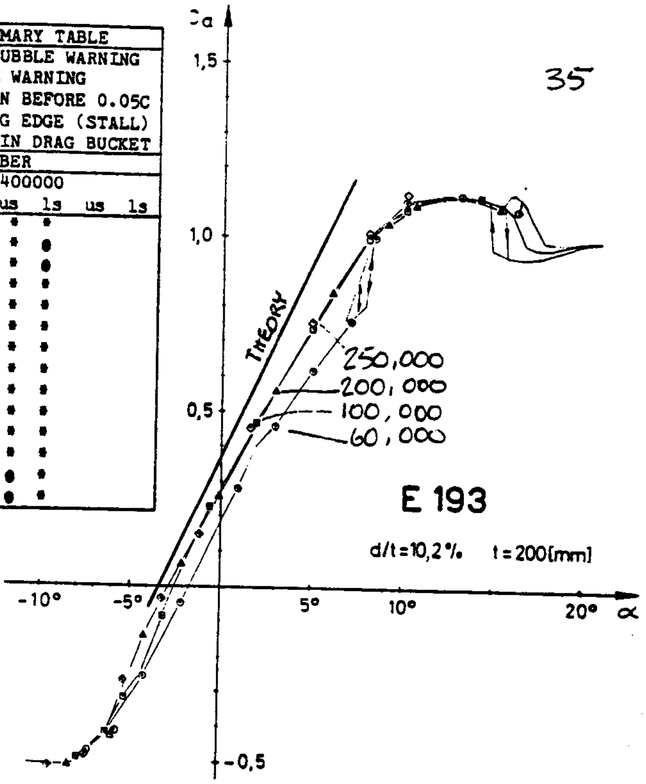

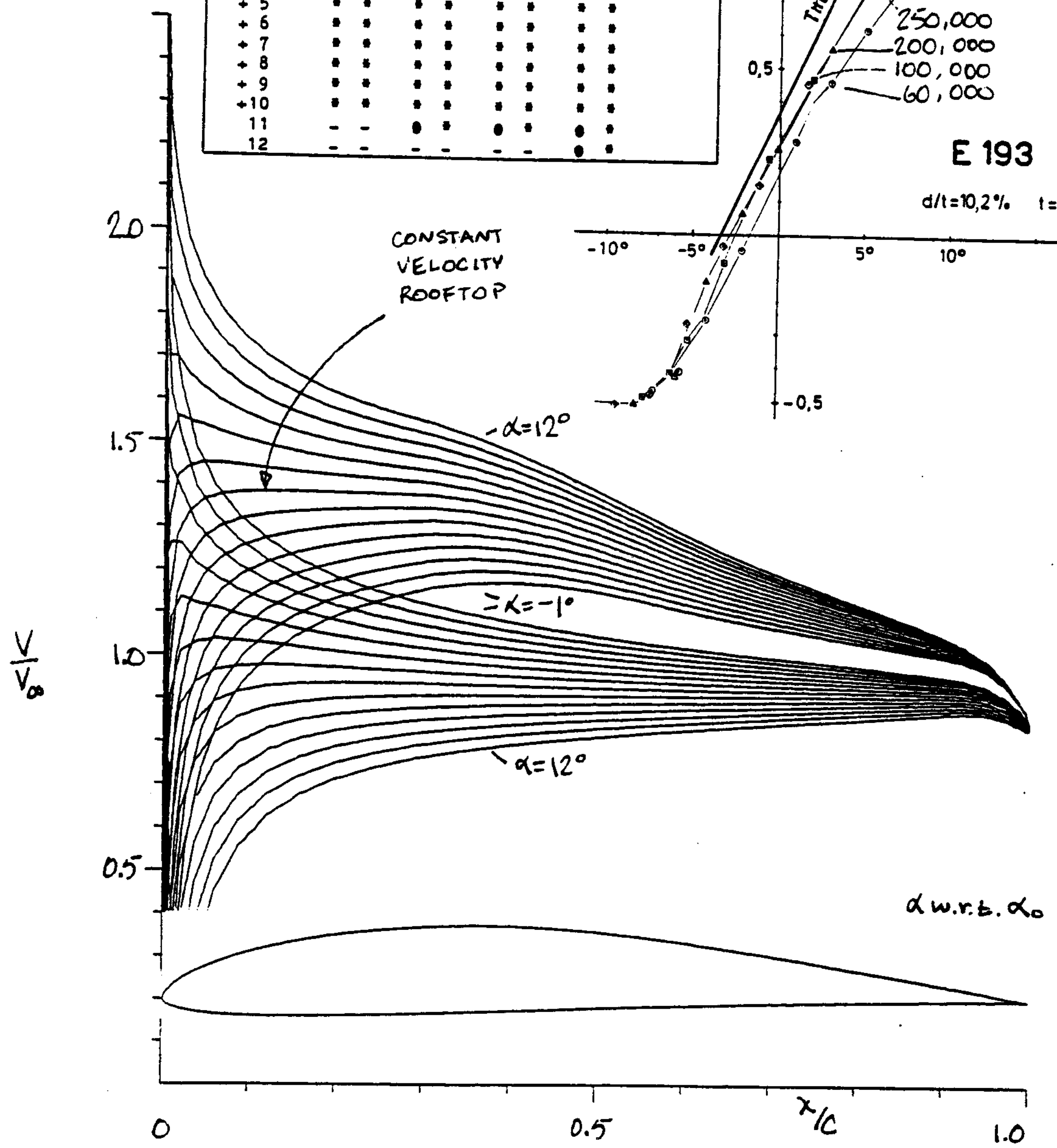

FIGURE 11.- VELOCITY DISTRIBUTIONS FOR THE E193 AIRFOIL.

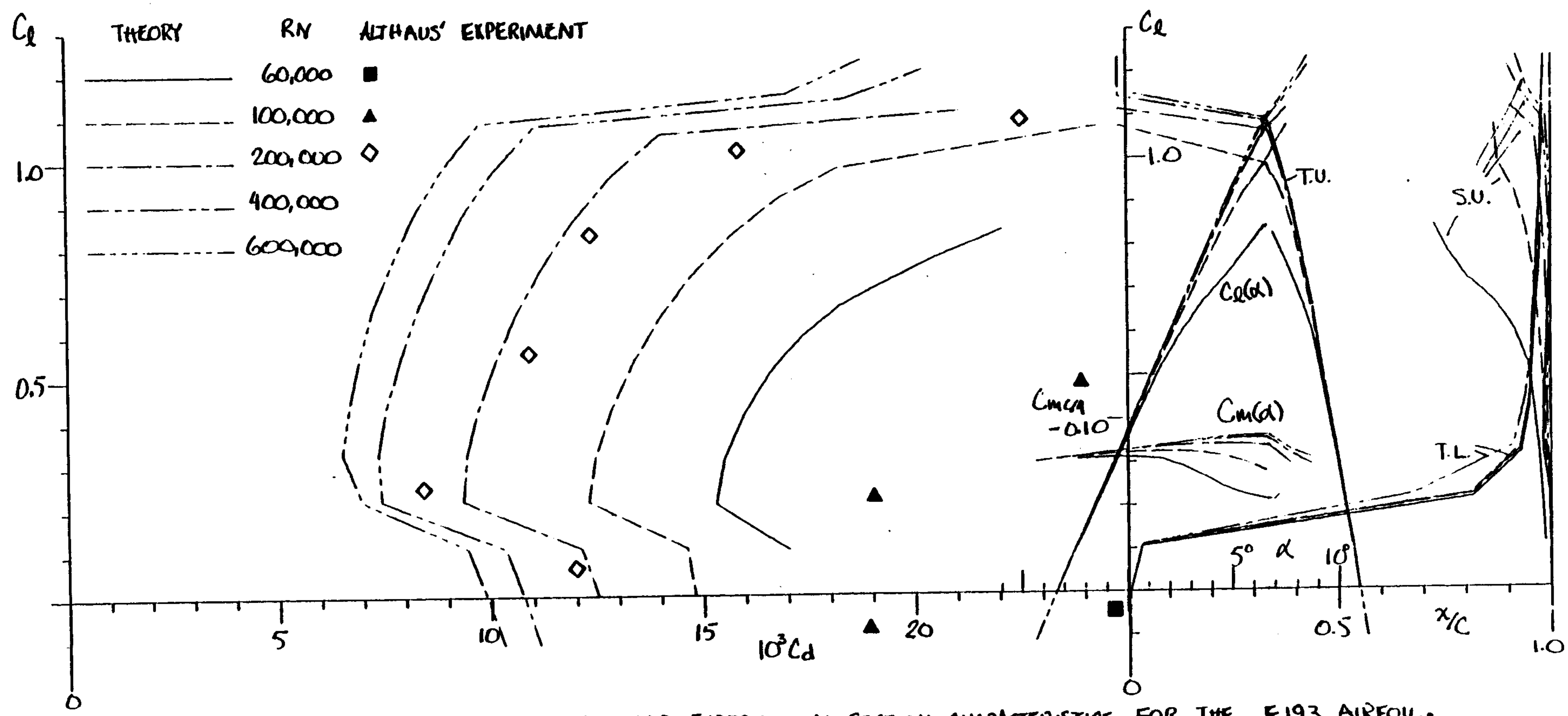

FIGURE 12.- COMPARISON OF THE THEORETICAL AND EXPERIMENTAL SECTION CHARACTERISTICS FOR THE E193 AIRFOIL.

THEORETICAL BOUNDARY-LAYER SUMMARY TABLE										
AIRFOIL E 201	*-LAMINAR SEPARATION BUBBLE WARNING O-NO SEPARATION BUBBLE WARNING ●-NO BUBBLE, TRANSITION BEFORE 0.05C --SEPARATION AT LEADING EDGE (STALL) ←ANGLE OF ATTACK WITHIN DRAG BUCKET									
ALPHA (deg)	REYNOLDS NUMBER									
	60000		100000		200000		400000			
	us	ls	us	ls	us	ls	us	ls	us	ls
-2	-	-	-	-	-	-	*	●		
-1	*	*	*	*	*	●	*	●		
+ 0	*	*	*	*	*	*	*	O		
+ 1	*	*	*	*	*	*	*	*		
+ 2	*	*	*	*	*	*	*	*		
+ 3	*	*	*	*	*	*	*	*		
+ 4	*	*	*	*	*	*	*	*		
+ 5	*	*	*	*	*	*	*	*		
+ 6	*	*	*	*	*	*	*	*		
+ 7	*	*	*	*	*	*	*	*		
+ 8	*	*	*	*	*	*	*	*		
+ 9	*	*	*	*	*	*	*	*		
+10	*	*	*	*	*	*	*	*		
11	*	*	●	*	●	*	●	*		

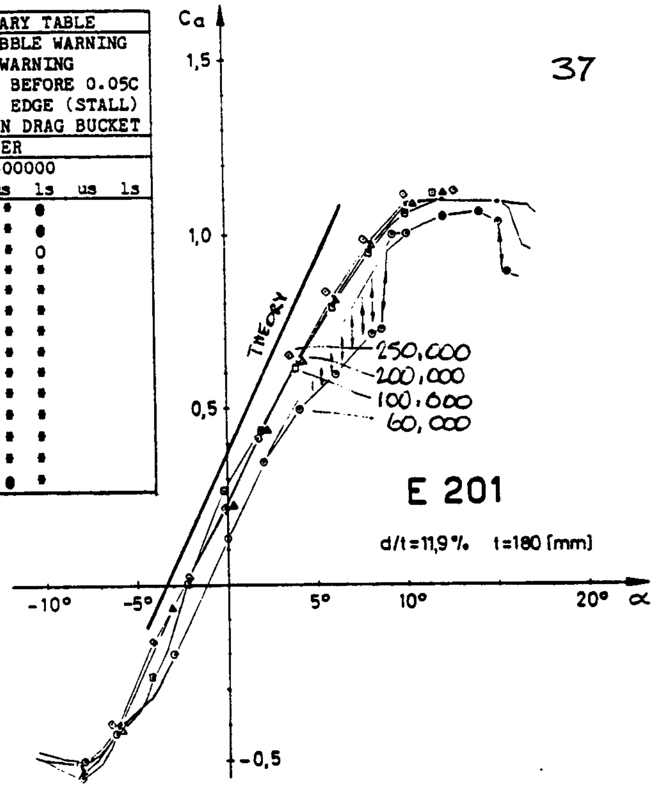

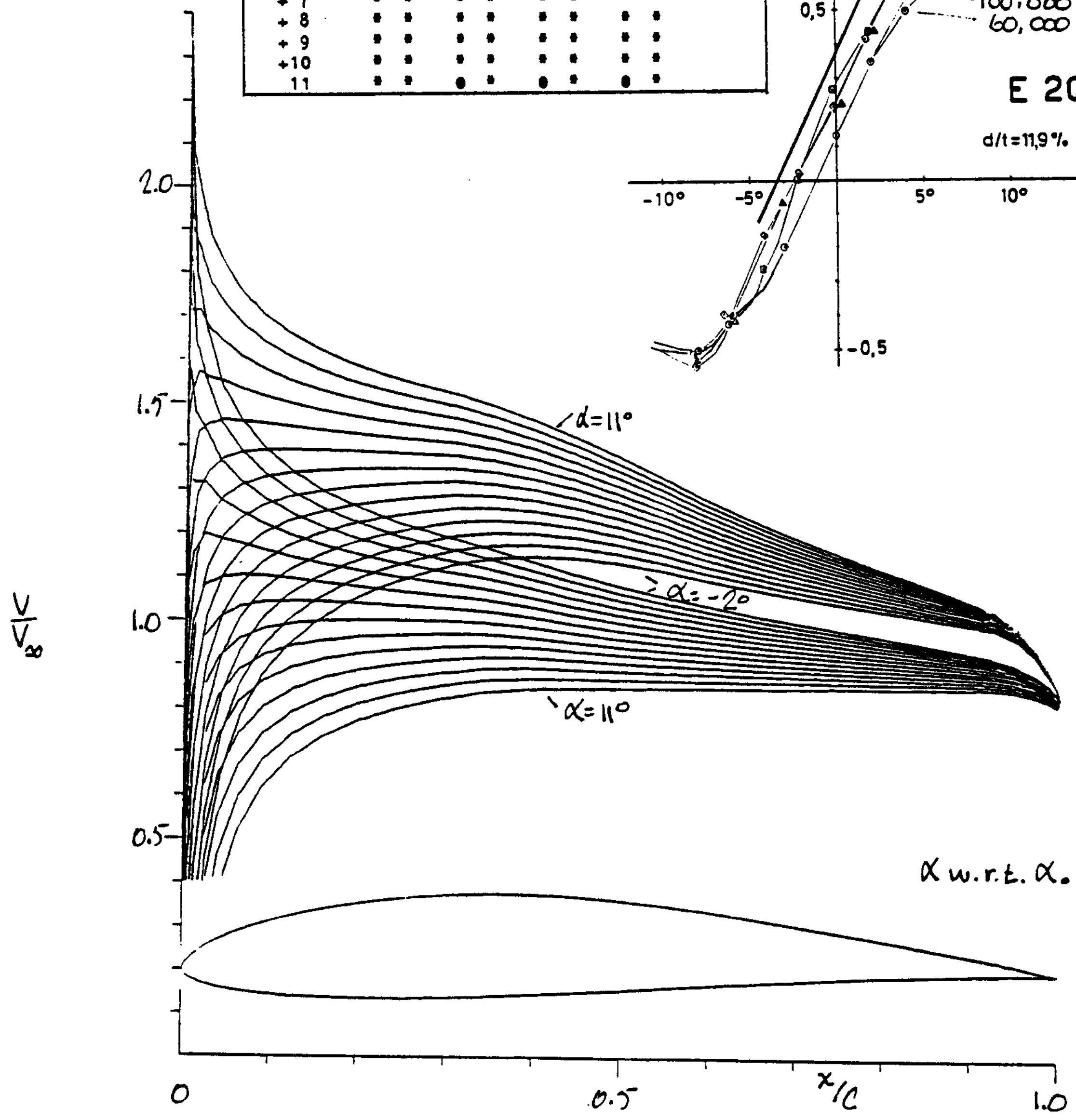

FIGURE 13.- VELOCITY DISTRIBUTIONS FOR THE E201 AIRFOIL.

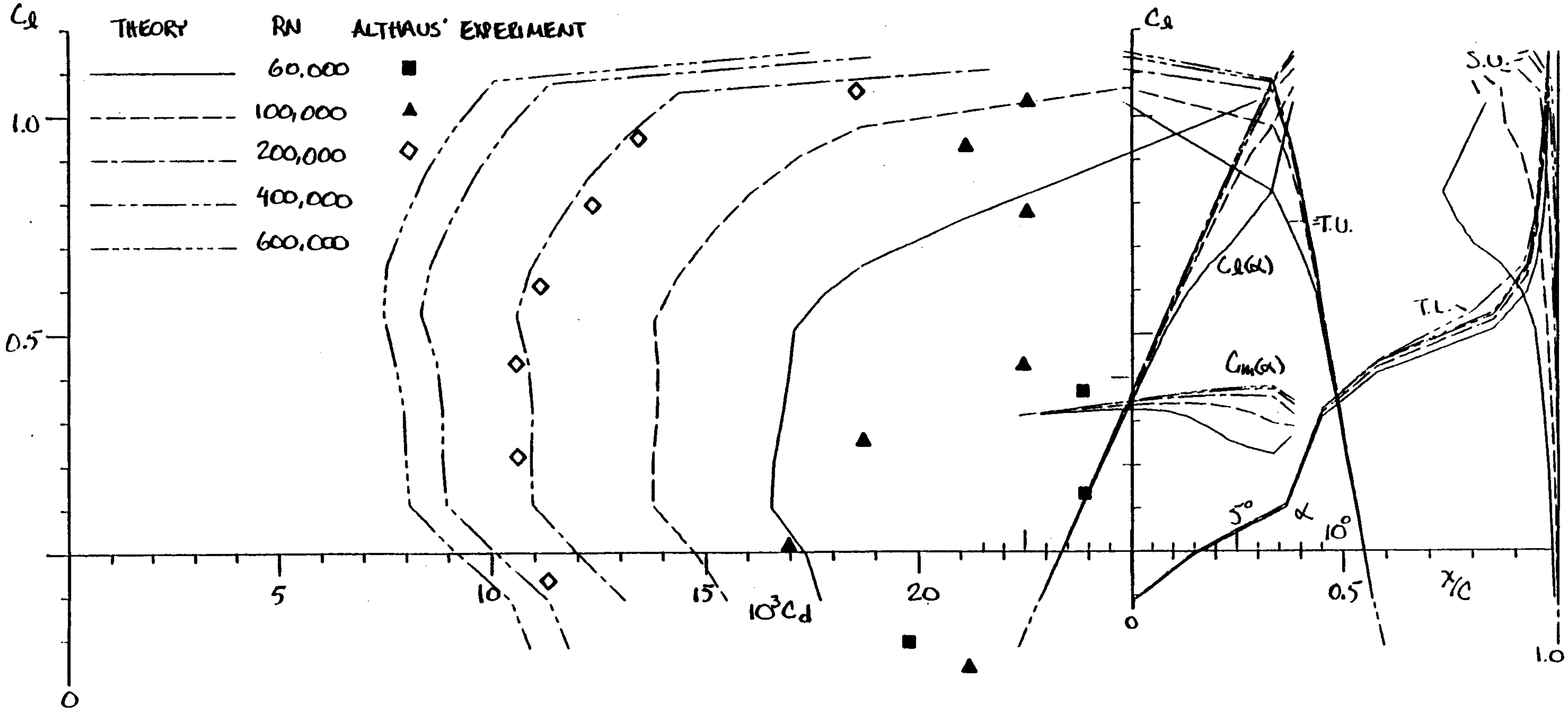

FIGURE 19.- COMPARISON OF THE THEORETICAL AND EXPERIMENTAL SECTION CHARACTERISTICS FOR THE E201 AIRFOIL.

THEORETICAL BOUNDARY-LAYER SUMMARY TABLE										
AIRFOIL NACA0009	*-LAMINAR SEPARATION BUBBLE WARNING O-NO SEPARATION BUBBLE WARNING ●-NO BUBBLE, TRANSITION BEFORE 0.05C --SEPARATION AT LEADING EDGE (STALL) +-ANGLE OF ATTACK WITHIN DRAG BUCKET									
ALPHA (deg)	REYNOLDS NUMBER									
	60000		80000		150000		400000			
	us	ls	us	ls	us	ls	us	ls	us	ls
+ 0	*	*	*	*	*	*	*	*		
+ 1	*	*	*	*	*	*	*	*		
+ 2	*	*	*	*	*	*	*	*		
+ 3	*	*	*	*	*	*	*	*		
4	*	*	*	*	●	*	●	*		
5	*	*	*	*	*	*	*	*		
6	-	-	-	-	*	*	●	*		
7	-	-	-	-	-	-	●	*		
8	-	-	-	-	-	-	●	*		

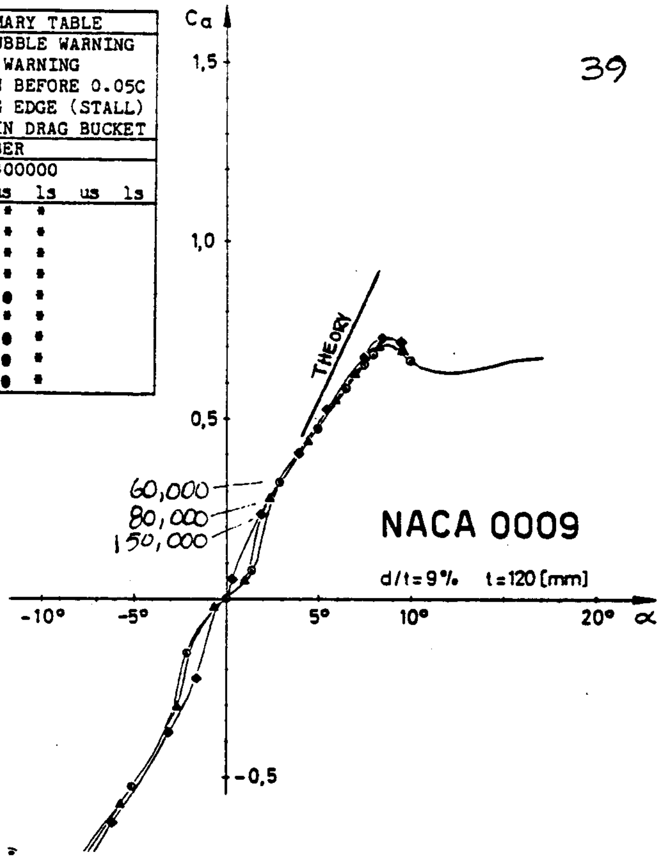

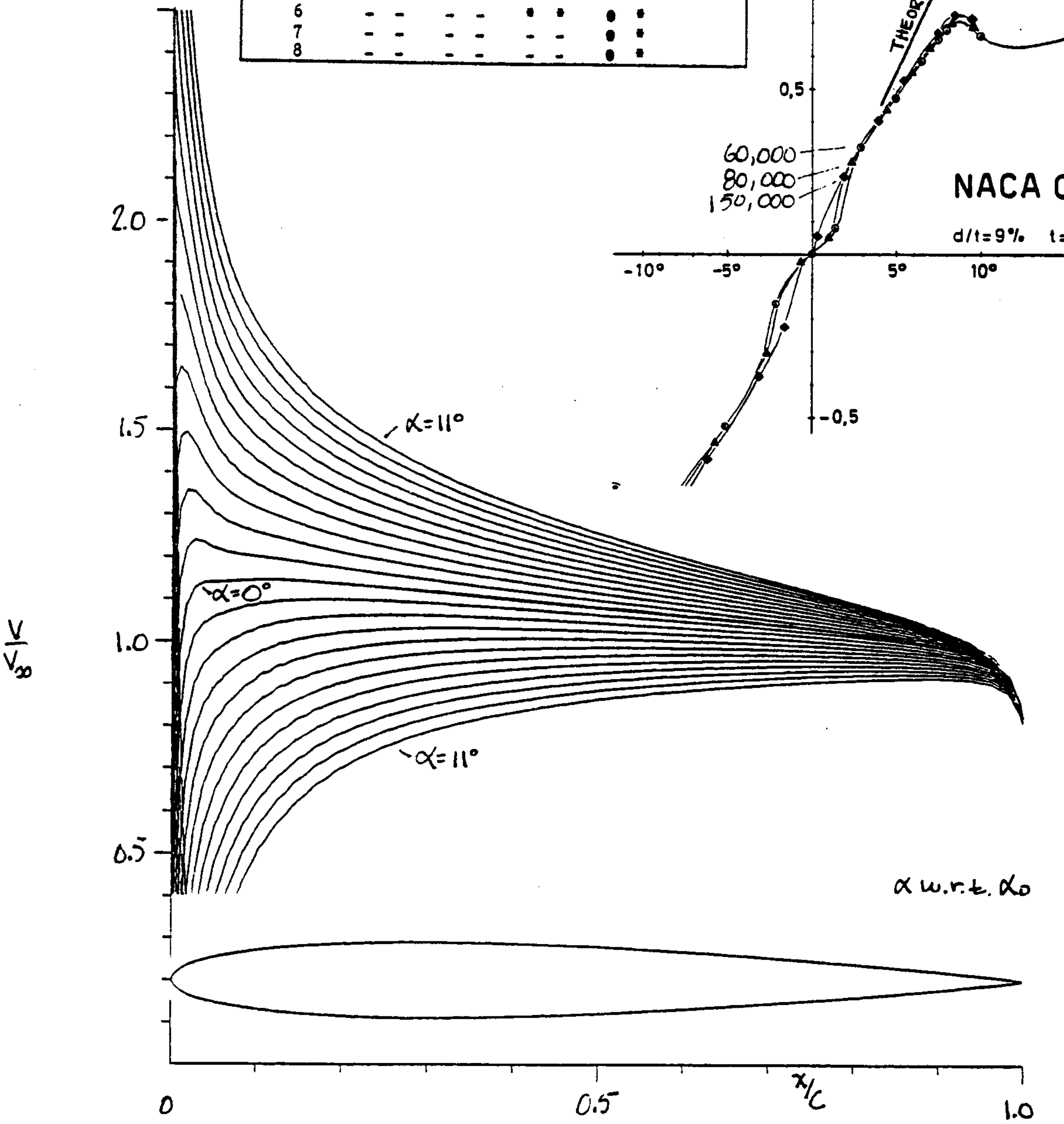

FIGURE 15.- VELOCITY DISTRIBUTIONS FOR THE NACA 0009 AIRFOIL.

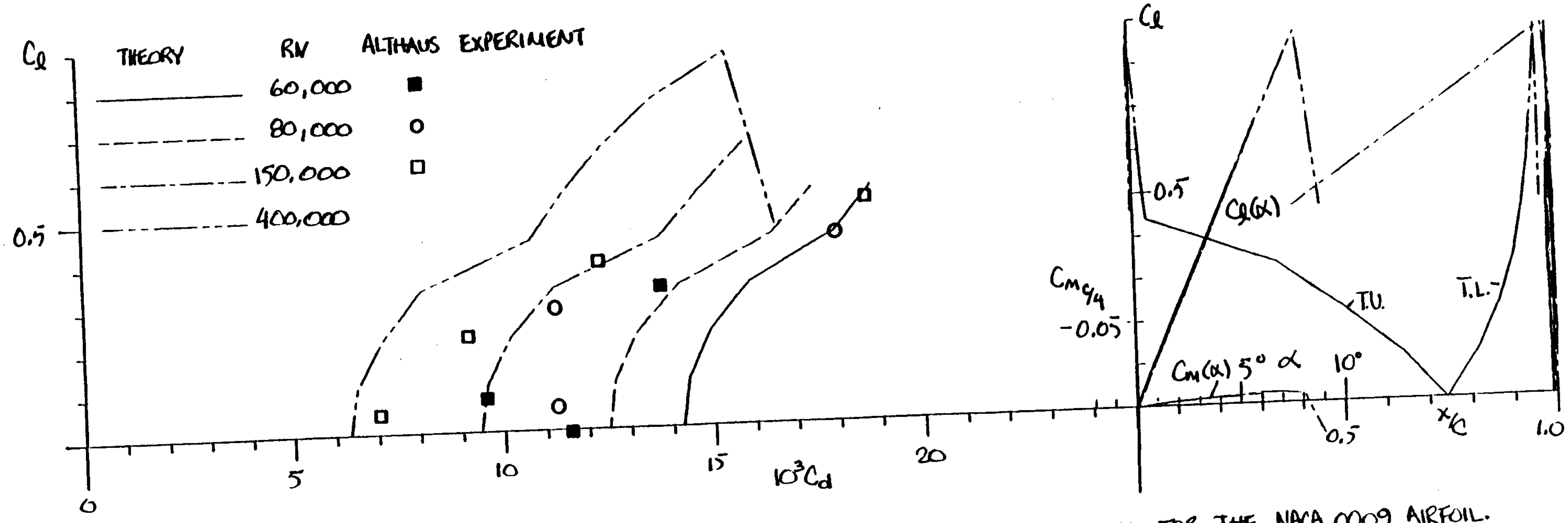

FIGURE 16.- COMPARISON OF THE THEORETICAL AND EXPERIMENTAL SECTION CHARACTERISTICS FOR THE NACA 0009 AIRFOIL.

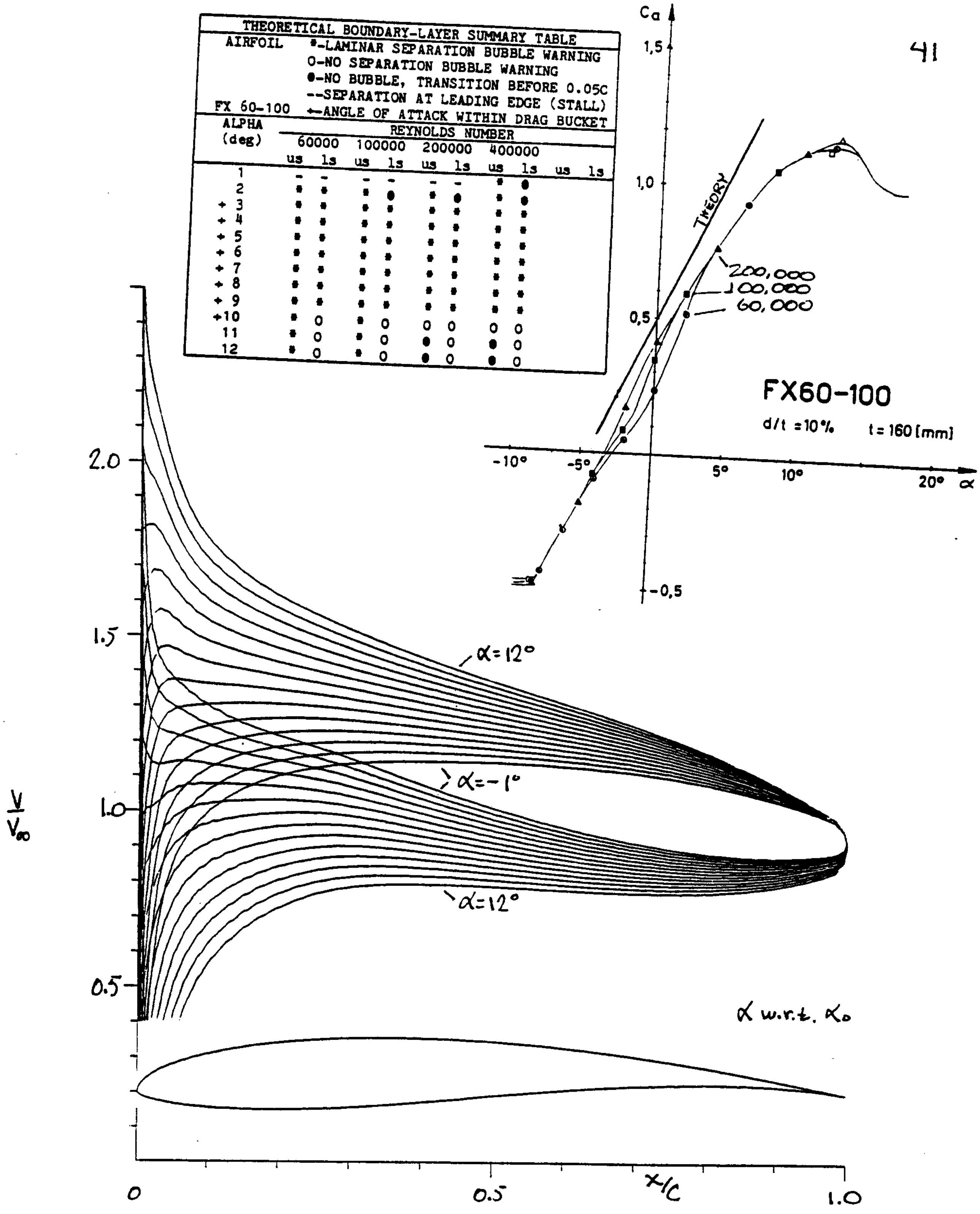

THEORETICAL BOUNDARY-LAYER SUMMARY TABLE										
AIRFOIL FX 60-100	*-LAMINAR SEPARATION BUBBLE WARNING O-NO SEPARATION BUBBLE WARNING ●-NO BUBBLE, TRANSITION BEFORE 0.05C --SEPARATION AT LEADING EDGE (STALL) ←ANGLE OF ATTACK WITHIN DRAG BUCKET									
ALPHA (deg)	REYNOLDS NUMBER									
	60000		100000		200000		400000			
	us	ls	us	ls	us	ls	us	ls	us	ls
1	-	-	-	-	-	-	*	●		
2	*	*	*	●	*	●	*	●		
← 3	*	*	*	*	*	*	*	*		
← 4	*	*	*	*	*	*	*	*		
← 5	*	*	*	*	*	*	*	*		
← 6	*	*	*	*	*	*	*	*		
← 7	*	*	*	*	*	*	*	*		
← 8	*	*	*	*	*	*	*	*		
← 9	*	*	*	*	*	*	*	*		
←10	*	O	*	O	O	O	O	O		
11	*	O	*	O	●	O	●	O		
12	*	O	*	O	●	O	●	O		

FIGURE 17. - VELOCITY DISTRIBUTIONS FOR THE FX 60-100 AIRFOIL.

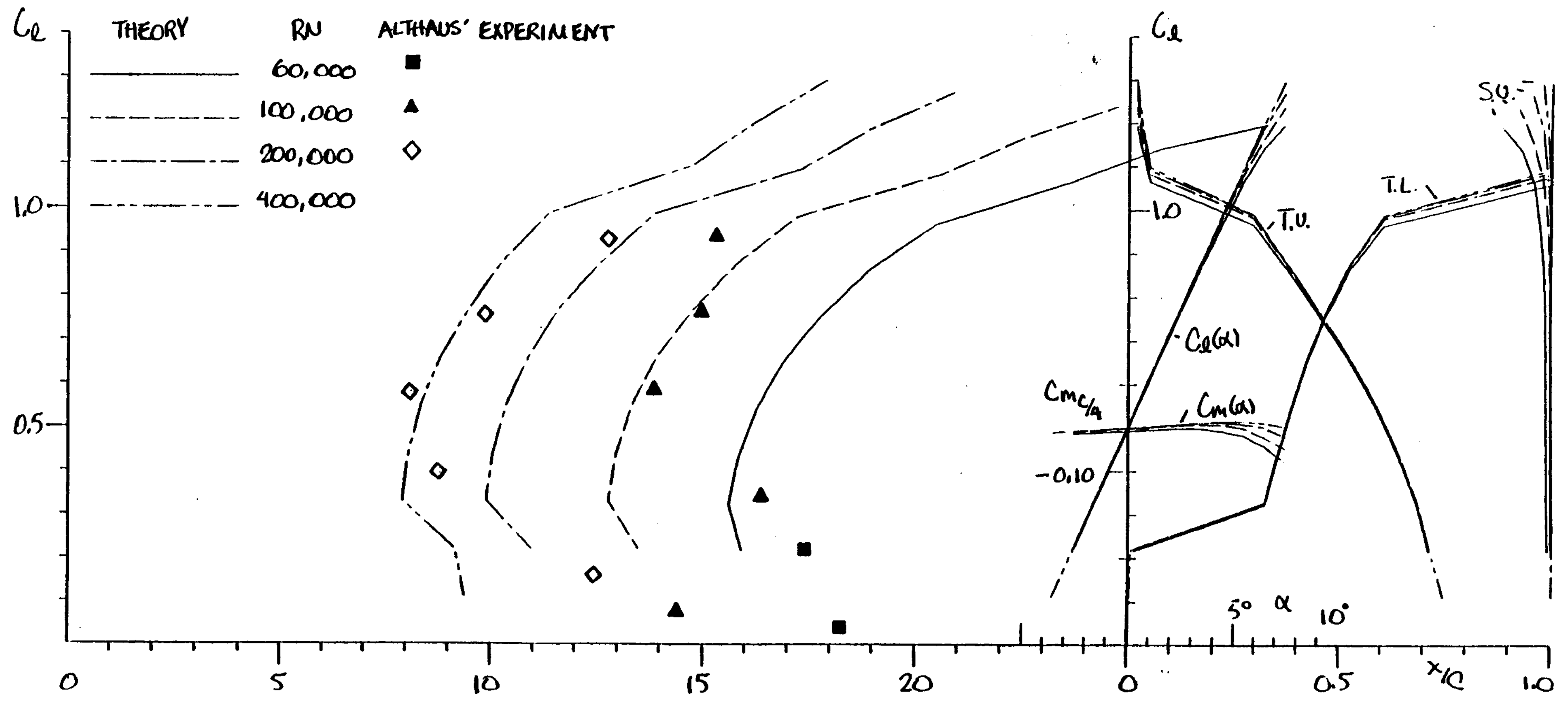

FIGURE 18. - COMPARISON OF THE THEORETICAL AND EXPERIMENTAL SECTION CHARACTERISTICS FOR THE FX 60-100 AIRFOIL.

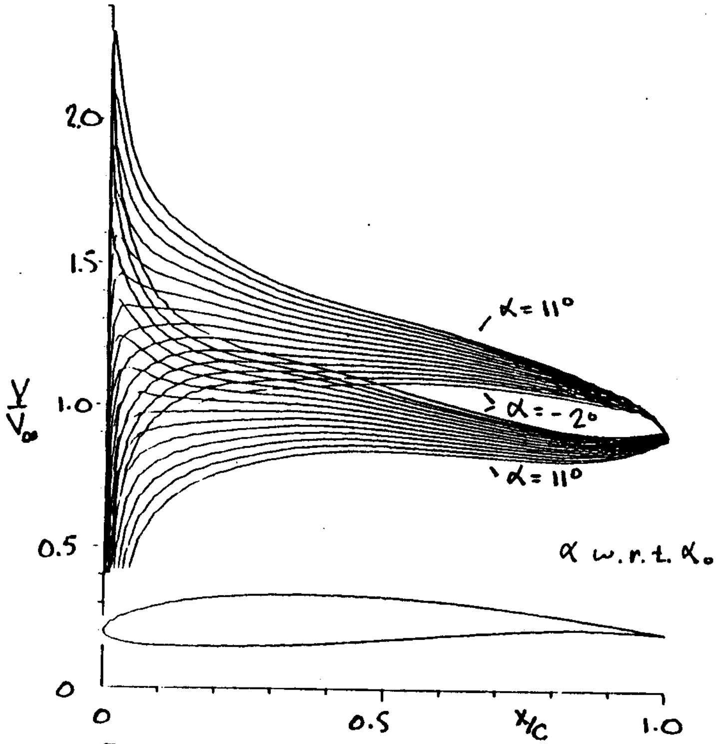

FIG. 19 - VELOCITY DISTRIBUTIONS FOR THE S2046-090-83.

THEORETICAL BOUNDARY-LAYER SUMMARY TABLE										
AIRFOIL 2046-090-83	*-LAMINAR SEPARATION BUBBLE WARNING O-NO SEPARATION BUBBLE WARNING ●-NO BUBBLE, TRANSITION BEFORE 0.05C --SEPARATION AT LEADING EDGE (STALL) +-ANGLE OF ATTACK WITHIN DRAG BUCKET									
ALPHA (deg)	REYNOLDS NUMBER									
			100000		200000		400000		600000	
	us	ls	us	ls	us	ls	us	ls	us	ls
-2			-	-	*	*	*	●	*	●
-1			*	*	*	●	*	●	*	●
0			*	*	*	●	*	●	*	●
+ 1			*	*	*	*	*	O	*	O
+ 2			*	*	*	*	*	*	*	*
+ 3			*	*	*	*	*	*	*	*
+ 4			*	*	*	*	*	*	*	*
+ 5			*	*	*	*	*	*	*	*
+ 6			*	*	*	*	*	*	*	*
+ 7			*	*	*	*	O	*	O	*
+ 8			*	*	*	*	O	*	O	*
9			*	O	●	O	●	O	●	O
10			*	O	●	O	●	O	●	O
11			*	O	*	O	●	O	●	O

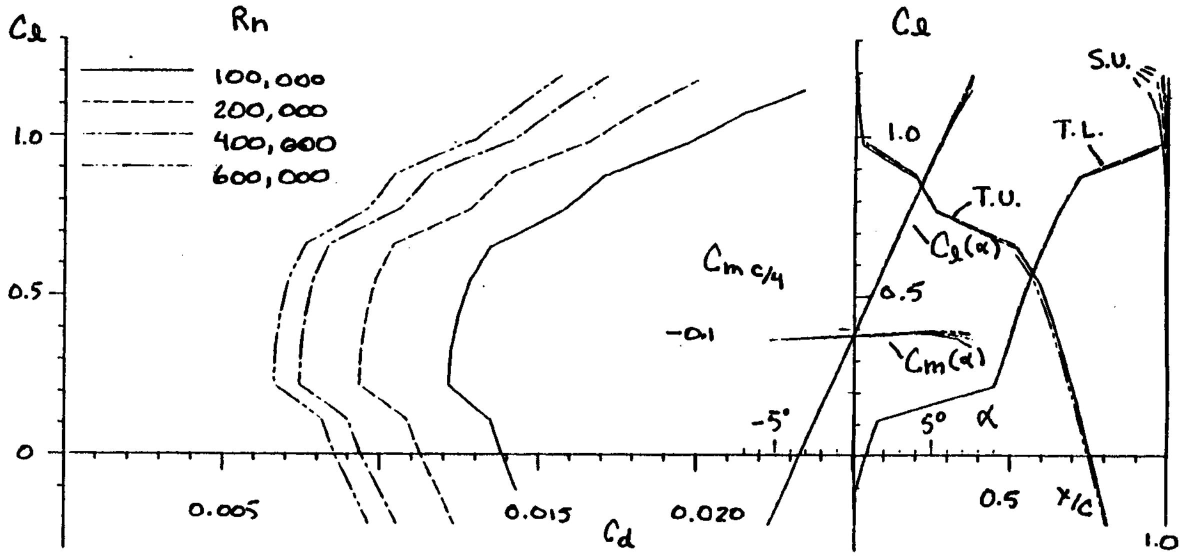

FIG. 20 - THEORETICAL SECTION CHARACTERISTICS FOR THE S2046-090-83.

x	y
1.00000	0.00000
.99684	.00049
.98756	.00202
.97263	.00462
.95247	.00812
.92737	.01233
.89786	.01717
.86379	.02256
.82624	.02835
.78552	.03433
.74211	.04029
.69650	.04603
.64915	.05136
.60053	.05608
.55108	.06005
.50122	.06316
.45137	.06540
.40203	.06676
.35374	.06732
.30703	.06700
.26243	.06577
.22040	.06357
.18129	.06031
.14539	.05600
.11291	.05071
.08406	.04462
.05912	.03795
.03838	.03089
.02209	.02352
.01036	.01588
.00307	.00813
.00003	.00077
.00192	-.00536
.00922	-.01059
.02154	-.01535
.03875	-.01919
.06092	-.02200
.08807	-.02383
.12001	-.02492
.15629	-.02542
.19647	-.02538
.24002	-.02481
.28644	-.02373
.33514	-.02206
.38567	-.01967
.43769	-.01655
.49083	-.01284
.54465	-.00876
.59863	-.00461
.65213	-.00068
.70446	.00276
.75491	.00546
.80269	.00717
.84689	.00768
.88649	.00710
.92073	.00578
.94909	.00412
.97129	.00249
.98721	.00116
.99679	.00030
1.00000	-.00000

S2046-090-83 COORDINATES

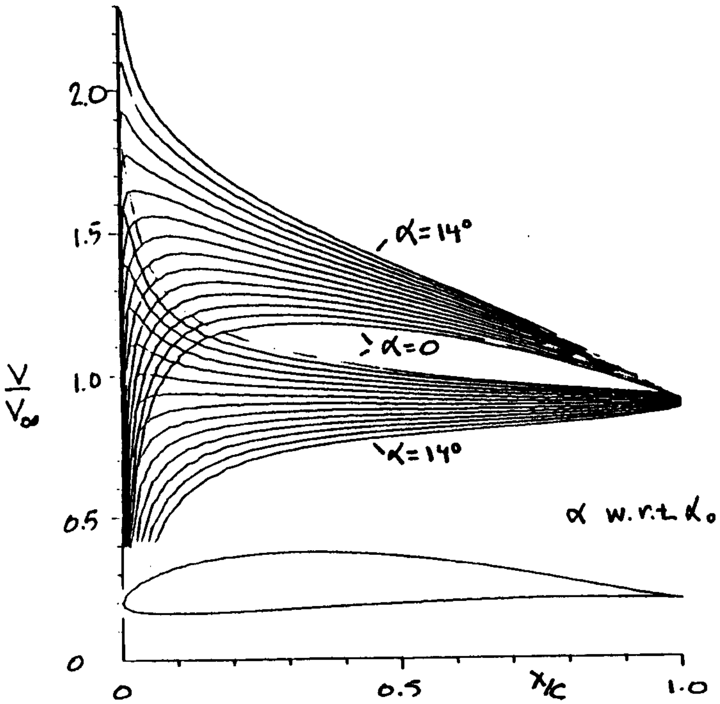

FIG. 21 - VELOCITY DISTRIBUTIONS FOR THE S2091-101-83.

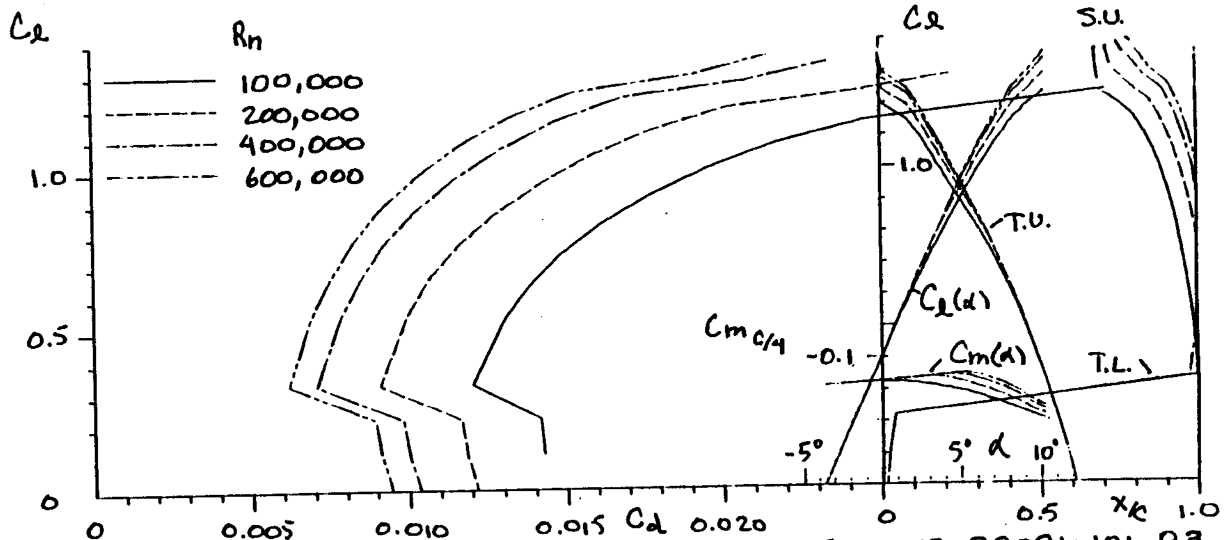

FIG. 22 - THEORETICAL SECTION CHARACTERISTICS FOR THE S2091-101-83.

THEORETICAL BOUNDARY-LAYER SUMMARY TABLE										
AIRFOIL 2091-101-83	*-LAMINAR SEPARATION BUBBLE WARNING O-NO SEPARATION BUBBLE WARNING ●-NO BUBBLE, TRANSITION BEFORE 0.05C --SEPARATION AT LEADING EDGE (STALL) +-ANGLE OF ATTACK WITHIN DRAG BUCKET									
ALPHA (deg)	REYNOLDS NUMBER									
			100000		200000		400000		600000	
	us	ls	us	ls	us	ls	us	ls	us	ls
0			*	*	*	*	*	●	*	●
1			*	*	*	*	*	●	*	●
+ 2			*	*	*	●	*	●	*	●
+ 3			*	*	*	*	*	*	*	*
+ 5			*	O	*	O	*	O	*	O
+ 6			*	O	*	O	*	O	O	O
+ 7			*	O	*	O	*	O	O	O
+ 8			*	O	*	O	*	O	O	O
+ 9			*	O	*	O	O	O	O	O
+10			*	O	*	O	O	O	O	O
+11			*	O	*	O	O	O	O	O
+12			*	O	O	O	O	O	O	O
13			●	O	●	O	●	O	●	O
14			*	O	●	O	●	O	●	O

x	y
1.00000	0.00000
.99674	.00035
.98707	.00150
.97126	.00367
.94970	.00699
.92292	.01150
.89147	.01713
.85594	.02373
.81693	.03107
.77501	.03888
.73070	.04689
.68454	.05479
.63700	.06231
.58856	.06920
.53965	.07526
.49073	.08029
.44220	.08416
.39450	.08677
.34805	.08805
.30323	.08794
.26043	.08644
.22002	.08356
.18232	.07934
.14765	.07382
.11622	.06708
.08823	.05927
.06384	.05060
.04320	.04130
.02645	.03168
.01374	.02205
.00517	.01269
.00077	.00401
.00058	-.00312
.00575	-.00864
.01662	-.01315
.03263	-.01645
.05397	-.01844
.08063	-.01936
.11236	-.01939
.14883	-.01873
.18960	-.01750
.23417	-.01581
.28205	-.01374
.33271	-.01142
.38555	-.00894
.43995	-.00643
.49526	-.00398
.55086	-.00171
.60605	.00025
.66005	.00162
.71216	.00296
.76168	.00367
.80795	.00397
.85036	.00391
.88834	.00354
.92140	.00295
.94911	.00222
.97109	.00144
.98705	.00073
.99674	.00020
1.00000	-.00000

S2091-101-83 COORDINATES

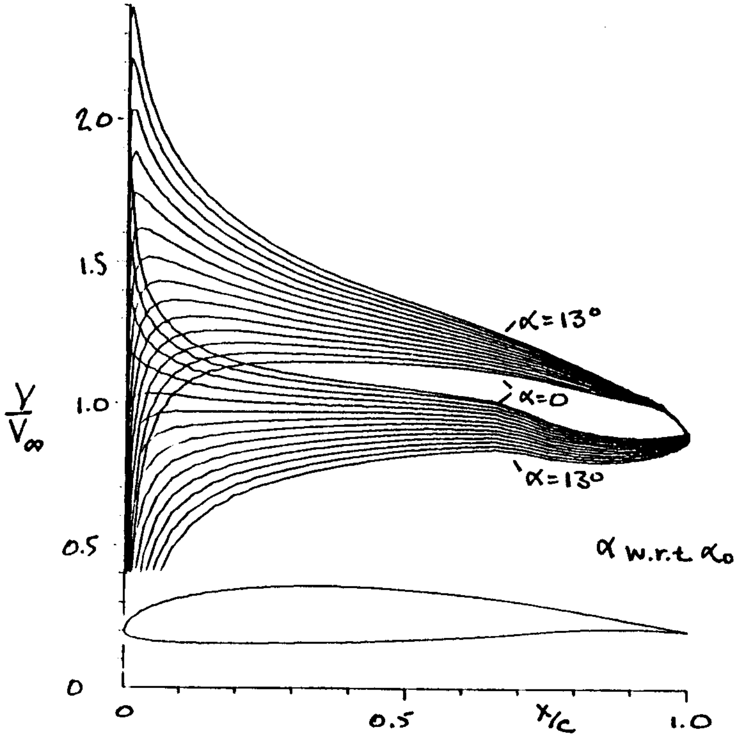

FIG. 23 - VELOCITY DISTRIBUTIONS FOR THE S3002-099-83.

THEORETICAL BOUNDARY-LAYER SUMMARY TABLE									
AIRFOIL	*-LAMINAR SEPARATION BUBBLE WARNING O-NO SEPARATION BUBBLE WARNING ●-NO BUBBLE, TRANSITION BEFORE 0.05C --SEPARATION AT LEADING EDGE (STALL) +-ANGLE OF ATTACK WITHIN DRAG BUCKET								
3002-099-83									
ALPHA (deg)	REYNOLDS NUMBER								
			100000		200000		400000		600000
	us	ls	us	ls	us	ls	us	ls	us	ls
0			*	●	*	●	*	●	*	●
1			*	*	*	*	*	●	*	●
+ 2			*	*	*	*	*	*	*	*
+ 3			*	*	*	*	*	*	*	*
+ 4			*	*	*	*	*	*	*	*
+ 5			*	*	*	*	*	*	*	*
+ 6			*	*	*	*	*	*	*	*
+ 7			*	*	*	*	*	*	O	*
+ 8			*	*	*	*	O	*	O	*
+ 9			*	*	*	*	O	*	O	*
+10			*	*	O	*	O	*	O	*
+11			*	*	●	*	●	*	●	*
12			*	*	●	*	●	*	●	*
13			*	*	●	*	●	*	●	*

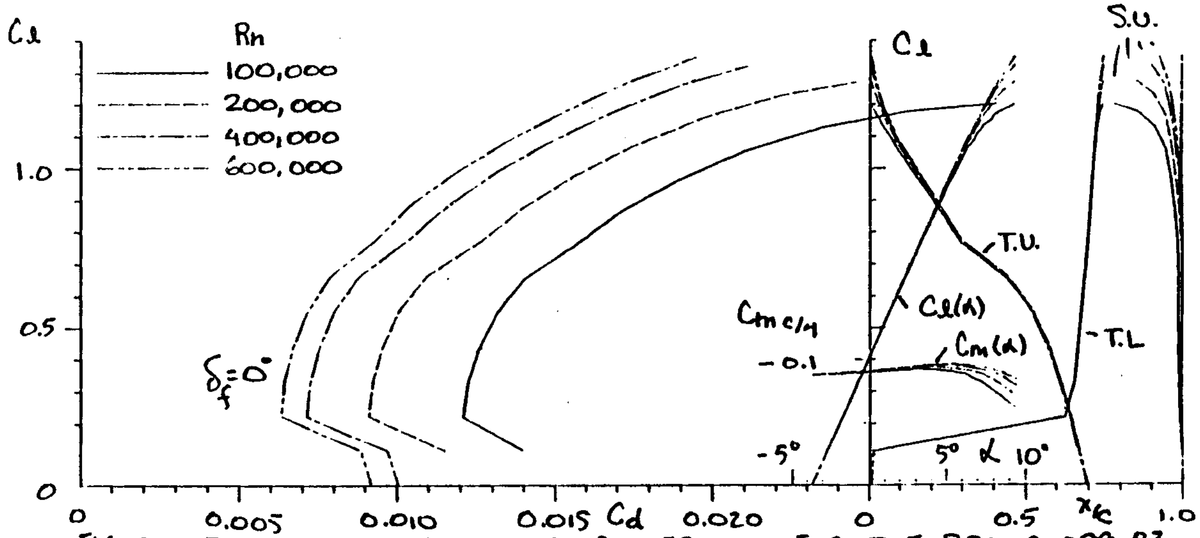

FIG. 24 - THEORETICAL SECTION CHARACTERISTICS FOR THE S3002-099-83.

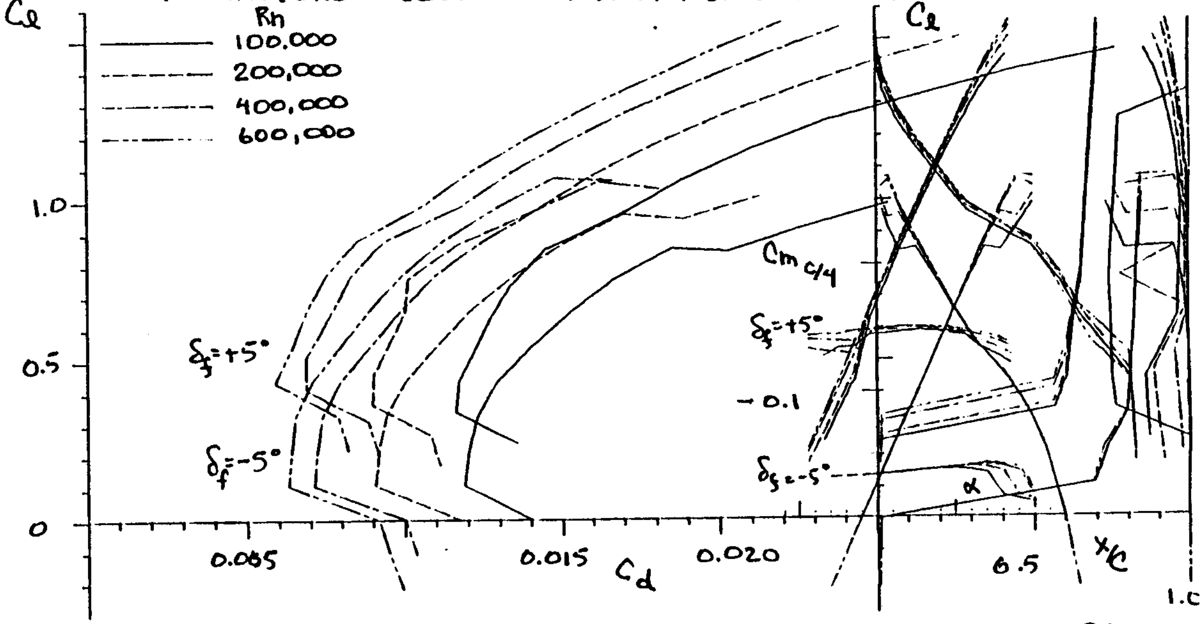

FIG. 25 - THEORETICAL SECTION CHARACTERISTICS FOR THE S3002-099-83 AT A FLAP DEFLECTION OF $\delta_f = +5°$ AND $\delta_f = -5°$.

x	y
1.00000	0.00000
.99676	.00048
.98723	.00205
.97191	.00463
.95131	.00867
.92576	.01330
.89553	.01862
.86104	.02463
.82286	.03124
.78161	.03825
.73787	.04538
.69214	.05226
.64481	.05868
.59634	.06441
.54711	.06930
.49758	.07328
.44820	.07627
.39944	.07823
.35178	.07915
.30572	.07900
.26173	.07776
.22026	.07537
.18165	.07181
.14619	.06711
.11417	.06135
.08583	.05460
.06135	.04701
.04087	.03873
.02450	.03000
.01234	.02105
.00440	.01211
.00048	.00360
.00051	-.00333
.00602	-.00831
.01778	-.01223
.03507	-.01544
.05763	-.01796
.08522	-.01976
.11761	-.02087
.15449	-.02145
.19537	-.02159
.23976	-.02136
.28711	-.02078
.33684	-.01988
.38835	-.01869
.44102	-.01717
.49424	-.01527
.54750	-.01294
.60027	-.01020
.65199	-.00697
.70250	-.00311
.75186	.00081
.79932	.00382
.84366	.00550
.88373	.00590
.91863	.00527
.94770	.00402
.97052	.00257
.98688	.00125
.99672	.00033
1.00000	-.00000

S3002-099-83 COORDINATES

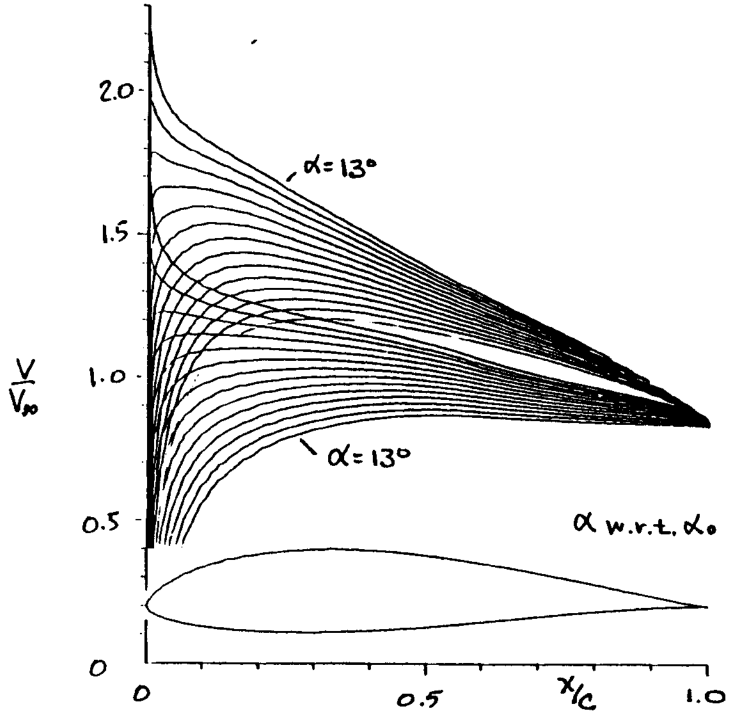

FIG. 26 - VELOCITY DISTRIBUTIONS FOR THE S2027-145-83.

THEORETICAL BOUNDARY-LAYER SUMMARY TABLE										
AIRFOIL	*-LAMINAR SEPARATION BUBBLE WARNING O-NO SEPARATION BUBBLE WARNING ●-NO BUBBLE, TRANSITION BEFORE 0.05C --SEPARATION AT LEADING EDGE (STALL) +-ANGLE OF ATTACK WITHIN DRAG BUCKET									
2027-145-83										
ALPHA (deg)	REYNOLDS NUMBER		100000		200000		400000		600000	
	us	ls	us	ls	us	ls	us	ls	us	ls
-3			*	*	*	*	*	*	*	●
-2			*	*	*	●	*	●	*	●
-1			*	●	*	●	*	●	*	●
+ 0			*	*	*	*	*	*	*	*
+ 1			*	*	*	*	*	*	O	*
+ 3			*	*	*	*	*	*	O	*
+ 5			*	*	*	*	*	*	O	*
+ 7			*	*	*	*	*	*	O	*
+ 8			*	*	*	*	*	*	O	*
+ 9			*	*	*	*	O	*	O	*
+10			*	*	*	*	O	*	O	*
+11			*	O	*	O	O	O	O	*
+12			*	O	*	O	O	O	O	O
13			●	O	●	O	●	O	●	O

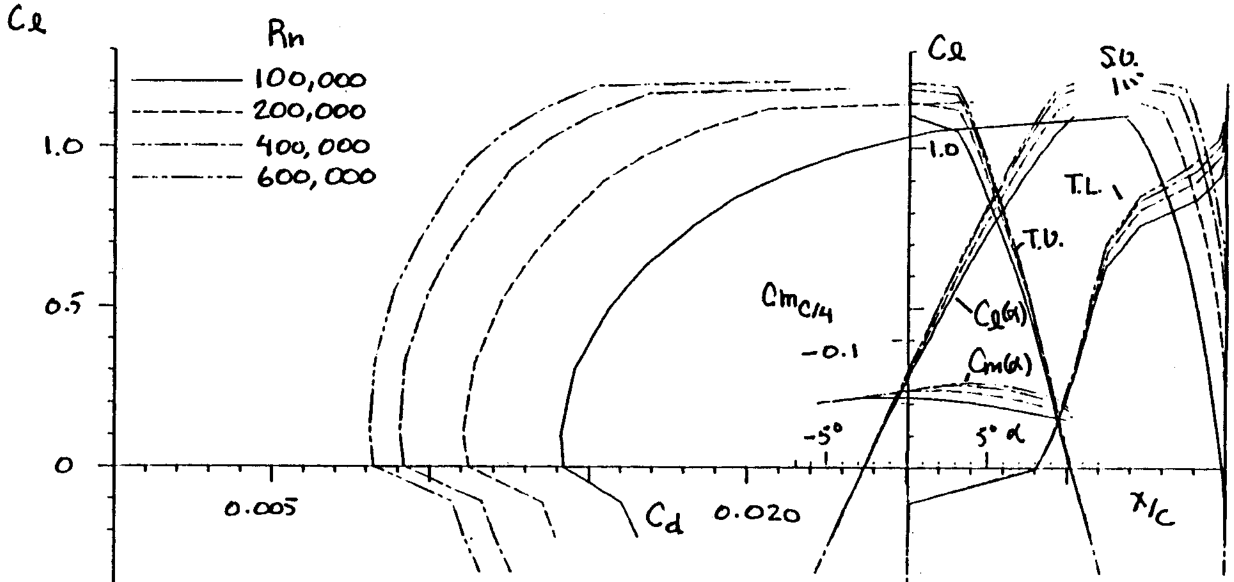

FIG. 27- THEORETICAL SECTION CHARACTERISTICS FOR THE S2027-145-83.

x	y
1.00000	0.00000
.99647	.00037
.98604	.00164
.96916	.00413
.94635	.00798
.91825	.01321
.88548	.01970
.84870	.02725
.80852	.03560
.76553	.04444
.72028	.05346
.67332	.06236
.62516	.07084
.57628	.07865
.52717	.08554
.47831	.09130
.43016	.09571
.38310	.09857
.33747	.09978
.29361	.09929
.25186	.09709
.21254	.09321
.17589	.08769
.14216	.08064
.11153	.07224
.08419	.06274
.06033	.05240
.04012	.04159
.02380	.03064
.01156	.01992
.00357	.00980
.00004	.00090
.00226	-.00627
.01078	-.01262
.02476	-.01894
.04376	-.02486
.06752	-.03027
.09581	-.03497
.12833	-.03890
.16474	-.04200
.20467	-.04420
.24773	-.04546
.29350	-.04574
.34154	-.04504
.39139	-.04338
.44256	-.04076
.49465	-.03721
.54723	-.03285
.59994	-.02792
.65225	-.02282
.70342	-.01790
.75270	-.01340
.79932	-.00946
.84257	-.00617
.88176	-.00360
.91625	-.00174
.94545	-.00055
.96864	.00005
.98597	.00020
.99646	.00009
1.00000	-.00000

S2027-145-83 COORDINATES

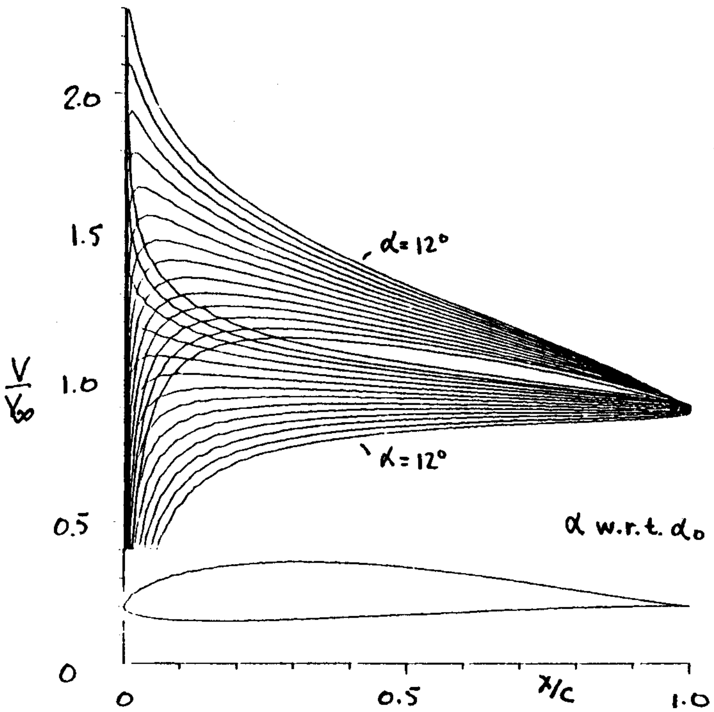

FIG. 28 - VELOCITY DISTRIBUTIONS FOR THE S3010-103-84.

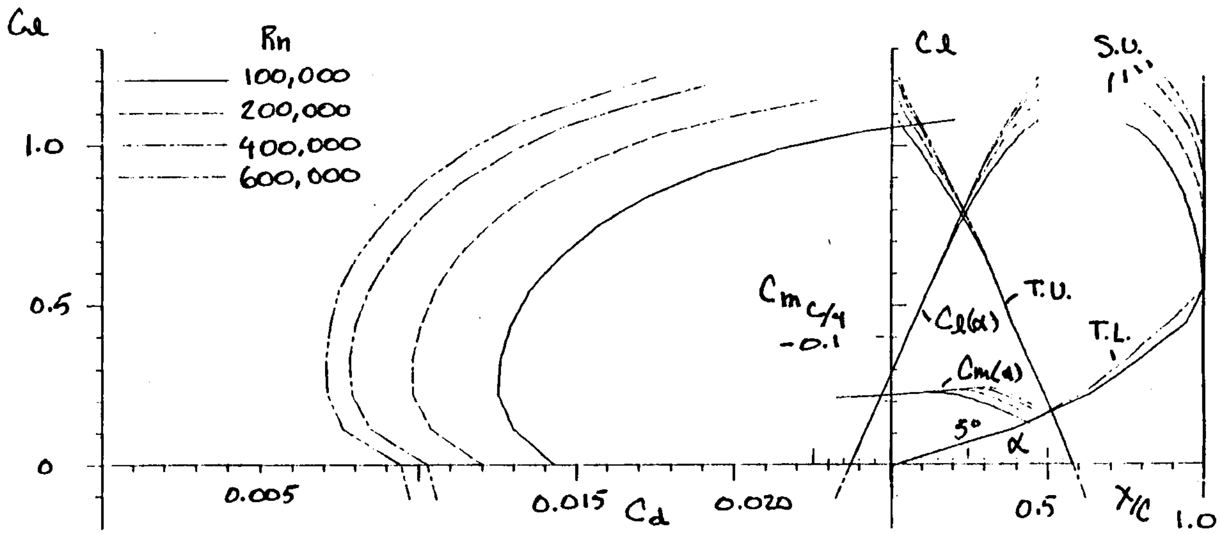

FIG. 29 - THEORETICAL SECTION CHARACTERISTICS FOR THE S3010-103-84.

THEORETICAL BOUNDARY-LAYER SUMMARY TABLE										
AIRFOIL	*-LAMINAR SEPARATION BUBBLE WARNING									
	O-NO SEPARATION BUBBLE WARNING									
	●-NO BUBBLE, TRANSITION BEFORE 0.05C									
	--SEPARATION AT LEADING EDGE (STALL)									
3010-103-84	+-ANGLE OF ATTACK WITHIN DRAG BUCKET									
ALPHA (deg)	REYNOLDS NUMBER									
			100000		200000		400000		600000	
	us	ls	us	ls	us	ls	us	ls	us	ls
-1			*	-	*	-	*	●	*	●
0			*	●	*	●	*	●	*	●
+ 1			*	*	*	*	*	*	*	*
+ 2			*	*	*	*	*	*	*	*
+ 3			*	*	*	*	*	*	*	*
+ 4			*	*	*	*	*	*	O	*
+ 5			*	O	*	O	*	O	O	O
+ 6			*	O	*	O	O	O	O	O
+ 7			*	O	*	O	O	O	O	O
+ 8			*	O	*	O	O	O	O	O
+ 9			*	O	O	O	O	O	O	O
+10			*	O	O	O	O	O	O	O
11			*	O	●	O	●	O	●	O
12			*	O	●	O	●	O	●	O

x	y
1.00000	0.00000
.99674	.00027
.98706	.00118
.97122	.00293
.94959	.00564
.92264	.00936
.89090	.01405
.85493	.01960
.81531	.02585
.77261	.03259
.72739	.03958
.68021	.04658
.63158	.05337
.58203	.05971
.53204	.06541
.48213	.07029
.43275	.07422
.38438	.07706
.33750	.07870
.29250	.07902
.24970	.07796
.20944	.07556
.17206	.07184
.13785	.06689
.10706	.06076
.07990	.05360
.05655	.04556
.03713	.03683
.02173	.02766
.01042	.01835
.00319	.00927
.00005	.00100
.00181	-.00543
.00932	-.01048
.02239	-.01506
.04061	-.01894
.06381	-.02203
.09180	-.02427
.12435	-.02567
.16119	-.02625
.20200	-.02610
.24635	-.02531
.29376	-.02399
.34371	-.02221
.39565	-.02009
.44899	-.01769
.50312	-.01514
.55743	-.01252
.61127	-.00994
.66399	-.00749
.71495	-.00526
.76350	-.00332
.80901	-.00172
.85087	-.00051
.88651	.00031
.92140	.00075
.94905	.00086
.97104	.00072
.98703	.00042
.99674	.00013
1.00000	-.00000

S3010-103-84 COORDINATES

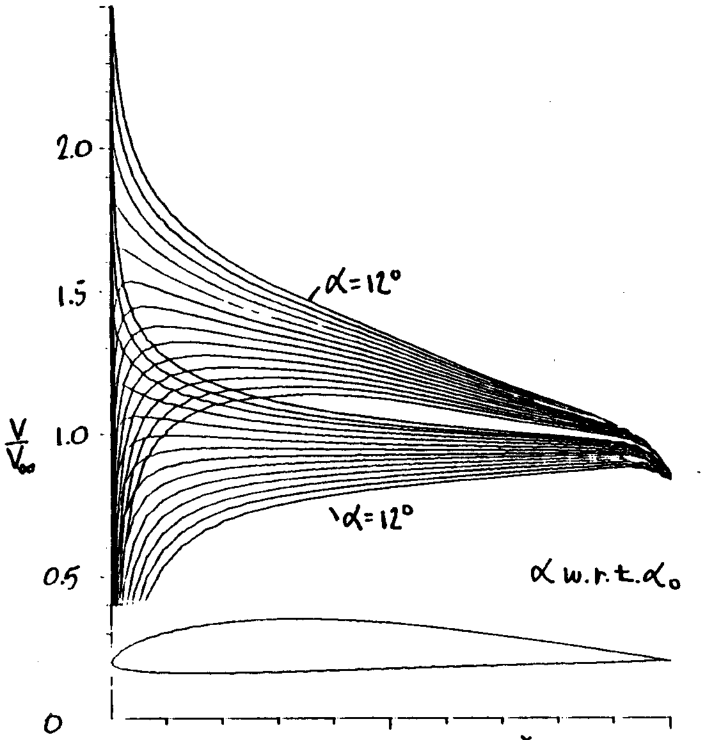

FIG. 30- VELOCITY DISTRIBUTIONS FOR THE S3021-095-84.

THEORETICAL BOUNDARY-LAYER SUMMARY TABLE										
AIRFOIL	*-LAMINAR SEPARATION BUBBLE WARNING O-NO SEPARATION BUBBLE WARNING ●-NO BUBBLE, TRANSITION BEFORE 0.05C --SEPARATION AT LEADING EDGE (STALL) +-ANGLE OF ATTACK WITHIN DRAG BUCKET									
3021-095-84										
ALPHA (deg)	REYNOLDS NUMBER									
			100000		200000		400000		600000	
	us	ls	us	ls	us	ls	us	ls	us	ls
-1			*	-	*	-	*	●	*	●
0			*	*	*	●	*	●	*	●
+ 1			*	*	*	*	*	*	*	*
+ 2			*	*	*	*	*	*	*	*
+ 3			*	*	*	*	*	*	*	*
+ 4			*	*	*	*	*	*	*	*
+ 5			*	*	*	*	*	*	*	*
+ 6			*	*	*	*	*	*	*	*
+ 7			*	*	*	*	*	*	O	*
+ 8			*	*	*	*	O	*	O	*
+ 9			*	*	*	*	O	*	O	*
+10			*	*	O	*	O	*	O	*
11			●	*	●	*	●	*	●	*
12			*	*	●	*	●	*	●	*

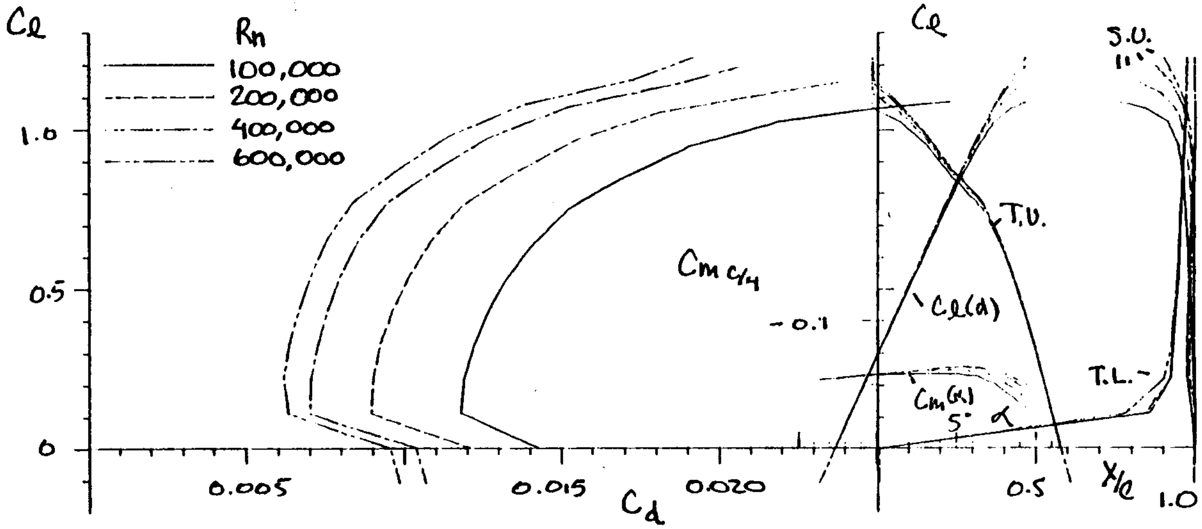

FIG. 31 - THEORETICAL SECTION ~~CHARACTERISTICS~~ CHARACTERISTICS FOR THE S3021-095-84.

x	y
1.00000	0.00000
.99663	.00039
.98679	.00172
.97104	.00419
.94996	.00769
.92398	.01193
.89336	.01670
.85840	.02199
.81959	.02776
.77748	.03394
.73266	.04039
.68572	.04695
.63730	.05342
.58801	.05955
.53839	.06505
.48891	.06964
.43996	.07312
.39191	.07537
.34513	.07632
.29999	.07596
.25685	.07433
.21611	.07151
.17816	.06753
.14331	.06243
.11182	.05631
.08393	.04930
.05983	.04157
.03968	.03329
.02358	.02472
.01160	.01615
.00374	.00799
.00008	.00099
.00191	-.00427
.00984	-.00852
.02320	-.01232
.04178	-.01547
.06542	-.01789
.09394	-.01957
.12712	-.02053
.16464	-.02085
.20613	-.02059
.25118	-.01986
.29928	-.01876
.34988	-.01742
.40237	-.01592
.45611	-.01433
.51046	-.01273
.56475	-.01115
.61833	-.00963
.67055	-.00821
.72078	-.00690
.76839	-.00571
.81282	-.00462
.85354	-.00365
.89004	-.00278
.92186	-.00193
.94875	-.00107
.97046	-.00035
.98659	.00003
.99660	.00006
1.00000	-.00000

S3021-095-84 COORDINATES

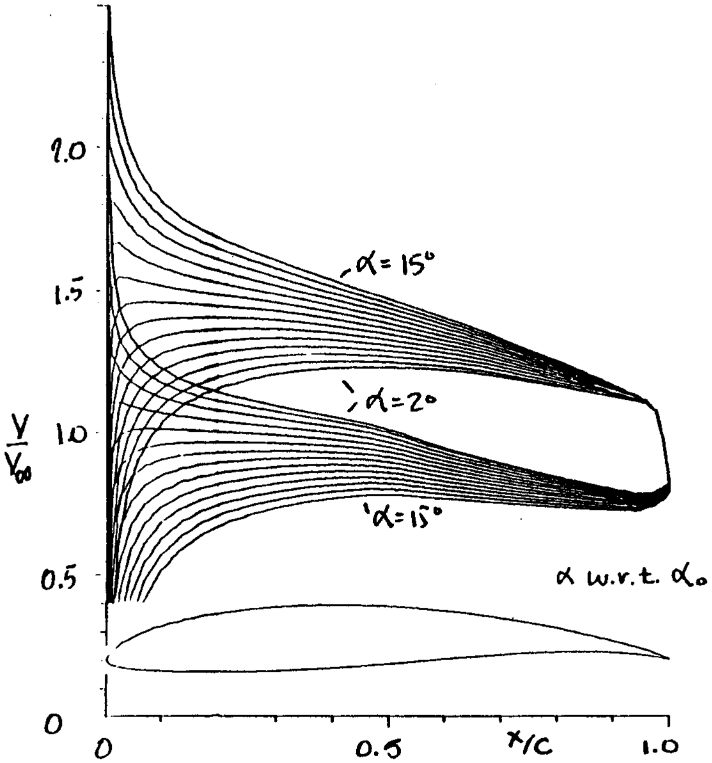

FIG. 32 - VELOCITY DISTRIBUTIONS FOR THE S4022-113-84.

THEORETICAL BOUNDARY-LAYER SUMMARY TABLE										
AIRFOIL 4022-113-84	*-LAMINAR SEPARATION BUBBLE WARNING O-NO SEPARATION BUBBLE WARNING ●-NO BUBBLE, TRANSITION BEFORE 0.05C --SEPARATION AT LEADING EDGE (STALL) +-ANGLE OF ATTACK WITHIN DRAG BUCKET									
ALPHA (deg)	REYNOLDS NUMBER									
			100000		200000		400000		600000	
	us	ls	us	ls	us	ls	us	ls	us	ls
2			*	-	*	-	*	*	*	*
3			*	*	*	*	*	-	*	-
+ 4			*	*	*	*	*	*	*	*
+ 5			*	*	*	*	*	*	*	*
+ 6			*	*	*	*	*	*	*	*
+ 7			*	*	*	*	*	*	*	*
+ 8			*	*	*	*	*	*	*	*
+ 9			*	*	*	*	*	*	*	*
+10			*	*	*	*	*	*	*	*
+11			*	*	*	*	*	*	O	*
+12			*	*	*	*	*	*	O	*
+13			*	*	*	*	O	*	O	*
14			*	*	●	*	●	*	●	*
`5			●	O	●	O	●	O	●	O

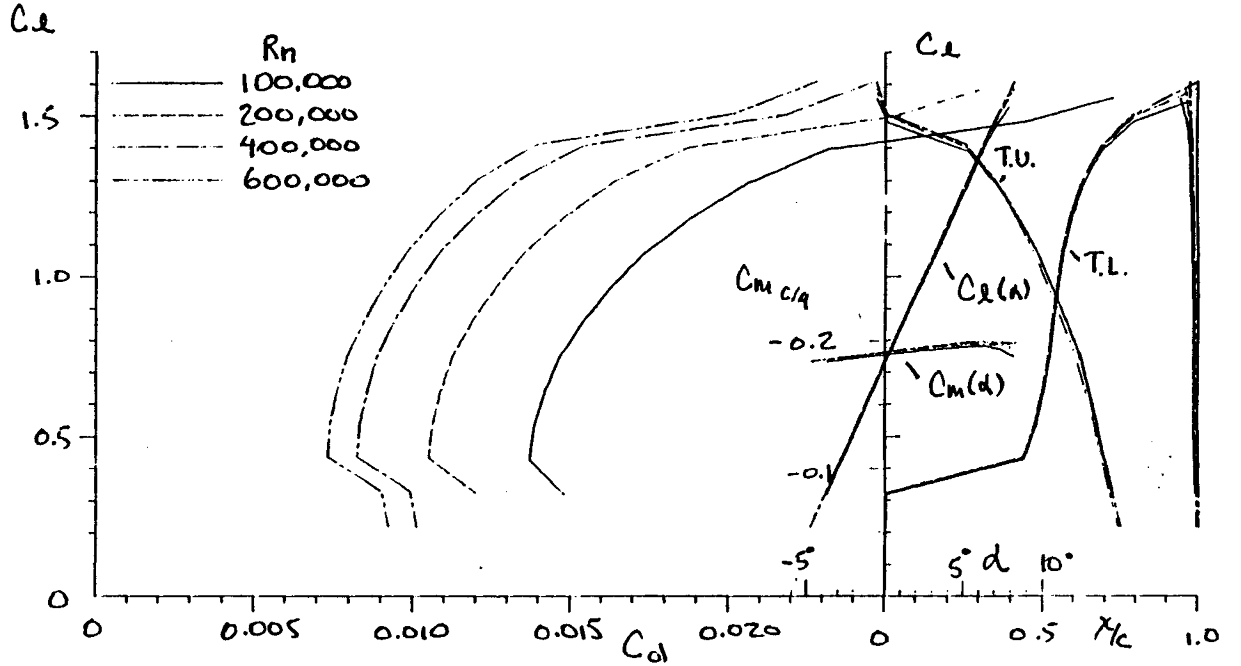

FIG. 33 - THEORETICAL SECTION CHARACTERISTICS FOR THE S4022-113-84.

1.00000	0.00000
.99679	.00128
.98795	.00501
.97456	.01036
.95658	.01638
.93381	.02295
.90652	.03009
.87510	.03768
.83996	.04557
.80158	.05358
.76043	.06152
.71703	.06914
.67185	.07619
.62532	.08241
.57782	.08760
.52975	.09167
.48158	.09453
.43371	.09608
.38660	.09628
.34064	.09512
.29623	.09258
.25373	.08871
.21350	.08361
.17587	.07741
.14120	.07023
.10980	.06225
.08196	.05361
.05792	.04451
.03789	.03515
.02206	.02575
.01050	.01649
.00313	.00776
.00001	.00038
.00246	-.00502
.01117	-.00919
.02553	-.01287
.04522	-.01594
.07000	-.01834
.09959	-.02006
.13368	-.02111
.17189	-.02152
.21378	-.02129
.25888	-.02044
.30669	-.01897
.35670	-.01685
.40838	-.01409
.46124	-.01061
.51493	-.00635
.56931	-.00152
.62394	.00324
.67803	.00747
.73071	.01084
.78110	.01311
.82829	.01415
.87139	.01390
.90955	.01242
.94190	.00982
.96749	.00648
.98569	.00321
.99645	.00085
1.00000	.00000

S4022-113-84 COORDINATES

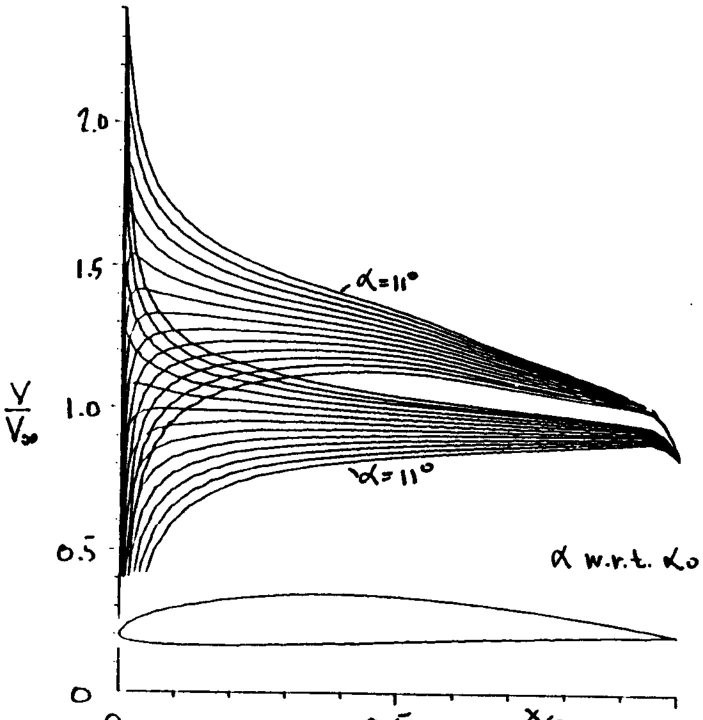

FIG. 34 - VELOCITY DISTRIBUTIONS FOR THE S4053-089-84.

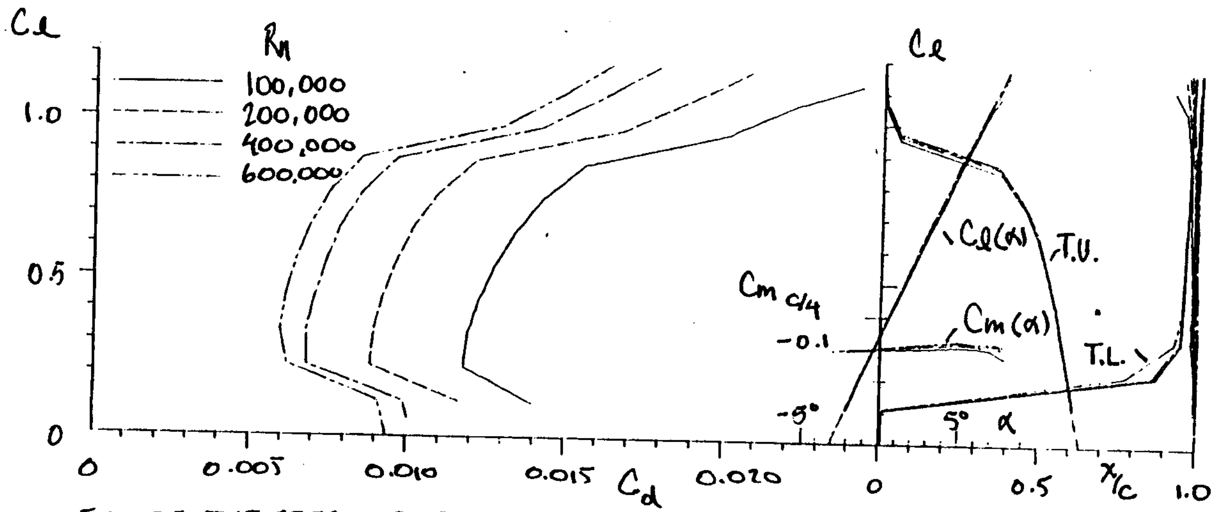

FIG. 35 - THEORETICAL SECTION CHARACTERISTICS FOR THE S4053-089-84.

THEORETICAL BOUNDARY-LAYER SUMMARY TABLE										
AIRFOIL	*-LAMINAR SEPARATION BUBBLE WARNING O-NO SEPARATION BUBBLE WARNING ●-NO BUBBLE, TRANSITION BEFORE 0.05C --SEPARATION AT LEADING EDGE (STALL) +-ANGLE OF ATTACK WITHIN DRAG BUCKET									
4053-089-84										
ALPHA (deg)	REYNOLDS NUMBER									
			100000		200000		400000		600000	
	us	ls	us	ls	us	ls	us	ls	us	ls
-1			*	-	*	-	*	-	*	-
0			*	-	*	-	*	-	*	●
1			*	*	*	●	*	●	*	●
+ 2			*	*	*	*	*	*	*	*
+ 3			*	*	*	*	*	*	*	*
+ 4			*	*	*	*	*	*	*	*
+ 5			*	*	*	*	*	*	*	*
+ 6			*	*	*	*	*	*	*	*
+ 7			*	*	*	*	*	*	*	*
+ 8			*	*	*	*	*	*	O	*
+ 9			*	*	O	*	O	*	O	*
10			*	*	●	*	●	*	●	*
11			*	*	●	*	●	*	●	*

X	Y
1.00000	0.00000
.99662	.00053
.98686	.00231
.97153	.00538
.95119	.00935
.92601	.01381
.89611	.01877
.86192	.02422
.82393	.03011
.78266	.03632
.73869	.04271
.69260	.04911
.64500	.05531
.59647	.06102
.54753	.06592
.49853	.06973
.44977	.07232
.40160	.07366
.35444	.07383
.30868	.07280
.26476	.07066
.22310	.06749
.18409	.06333
.14813	.05828
.11551	.05243
.08655	.04588
.06147	.03879
.04053	.03131
.02388	.02360
.01163	.01564
.00377	.00823
.00013	.00131
.00152	-.00392
.00876	-.00781
.02165	-.01116
.03990	-.01388
.06334	-.01592
.09177	-.01729
.12494	-.01808
.16249	-.01840
.20391	-.01829
.24875	-.01771
.29661	-.01671
.34698	-.01541
.39927	-.01392
.45286	-.01231
.50711	-.01064
.56136	-.00896
.61507	-.00731
.66752	-.00579
.71809	-.00443
.76614	-.00328
.81105	-.00236
.85226	-.00165
.88923	-.00113
.92145	-.00075
.94854	-.00041
.97028	-.00003
.98646	.00018
.99655	.00010
1.00000	.00000

COORDINATES FOR THE S4053-089-84

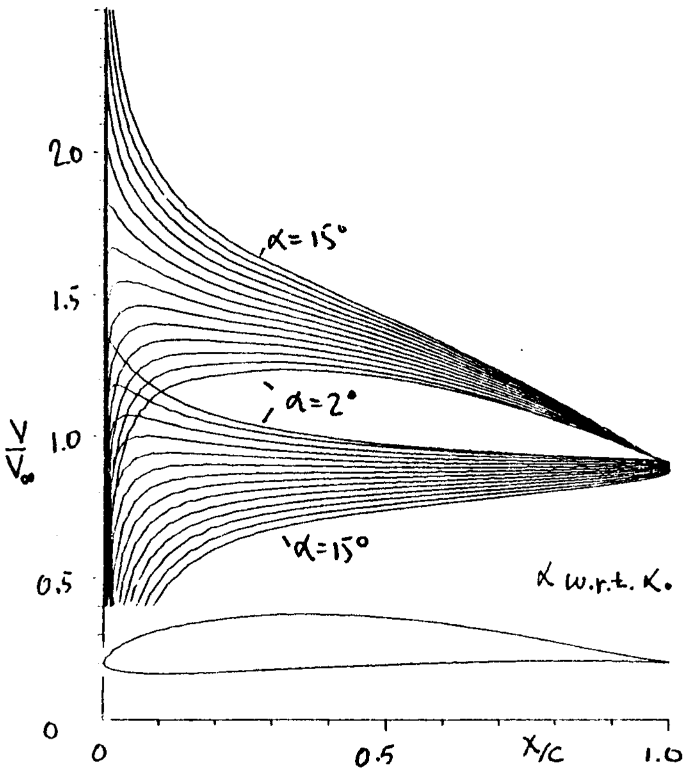

FIG. 36- VELOCITY DISTRIBUTIONS FOR THE S4061-096-84.

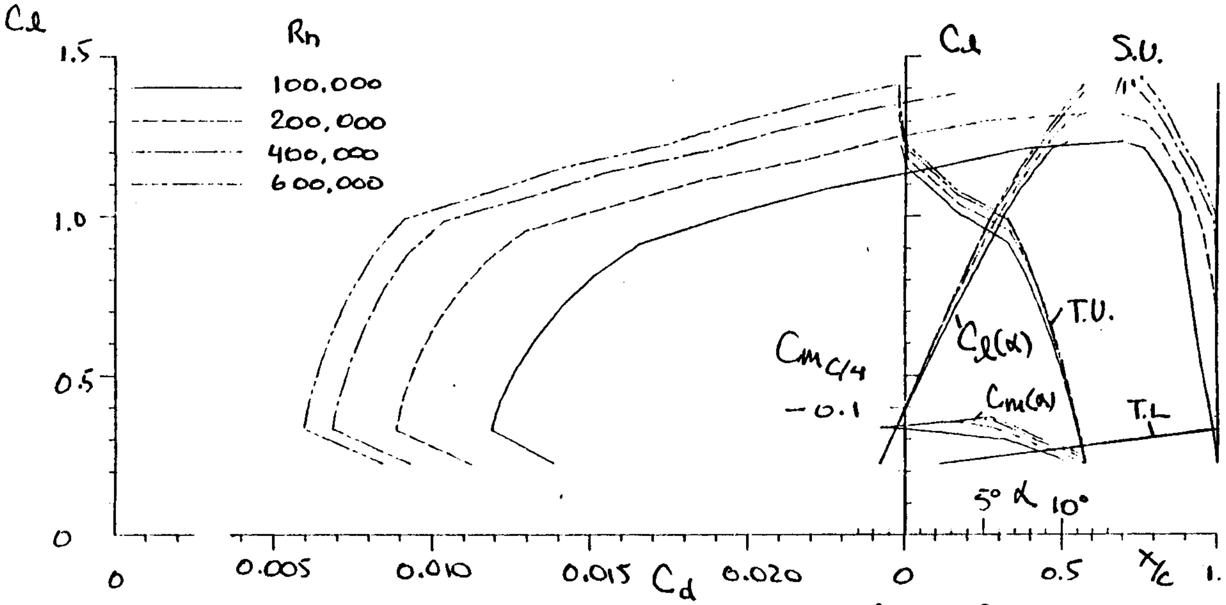

FIG. 37- THEORETICAL SECTION CHARACTERISTICS FOR THE S4061-096-84.

THEORETICAL BOUNDARY-LAYER SUMMARY TABLE										
AIRFOIL 4061-096-84	*-LAMINAR SEPARATION BUBBLE WARNING O-NO SEPARATION BUBBLE WARNING ●-NO BUBBLE, TRANSITION BEFORE 0.05C --SEPARATION AT LEADING EDGE (STALL) +-ANGLE OF ATTACK WITHIN DRAG BUCKET									
ALPHA (deg)	REYNOLDS NUMBER									
			100000		200000		400000		600000	
	us	ls	us	ls	us	ls	us	ls	us	ls
2			*	*	*	*	*	O	*	O
+ 3			*	*	*	*	*	*	*	*
+ 4			*	O	*	O	*	O	*	O
+ 5			*	O	*	O	*	O	*	O
+ 6			*	O	*	O	*	O	O	O
+ 7			*	O	*	O	*	O	*	O
+ 8			*	O	*	O	*	O	*	O
+ 9			*	O	*	O	*	O	O	O
+10			*	O	*	O	O	O	O	O
+11			*	O	O	O	O	O	O	O
12			*	O	●	O	●	O	●	O
12			*	O	●	O	●	O	●	O
[illegible]			*	O	●	O	●	O	●	O

x	Y
1.00000	0.00000
.99675	.00034
.98709	.00147
.97129	.00363
.94976	.00699
.92304	.01155
.89170	.01729
.85637	.02403
.81764	.03151
.77610	.03945
.73227	.04752
.68565	.05541
.63971	.06283
.59189	.06950
.54359	.07520
.49522	.07974
.44716	.08302
.39979	.08492
.35348	.08543
.30862	.08454
.26555	.08228
.22460	.07876
.18620	.07414
.15074	.06849
.11855	.06186
.08988	.05438
.06493	.04617
.04386	.03741
.02677	.02839
.01380	.01938
.00503	.01069
.00046	.00283
.00079	-.00320
.00681	-.00787
.01835	-.01209
.03499	-.01546
.05666	-.01780
.08328	-.01908
.11474	-.01932
.15085	-.01865
.19129	-.01724
.23565	-.01528
.28345	-.01292
.33413	-.01034
.38706	-.00772
.44159	-.00516
.49702	-.00279
.55265	-.00069
.60776	.00107
.66163	.00245
.71356	.00342
.76287	.00400
.80893	.00420
.85114	.00406
.88893	.00364
.92183	.00301
.94939	.00225
.97126	.00146
.98713	.00074
.99677	.00020
1.00000	.00000

S4061-096-84 COORDINATES

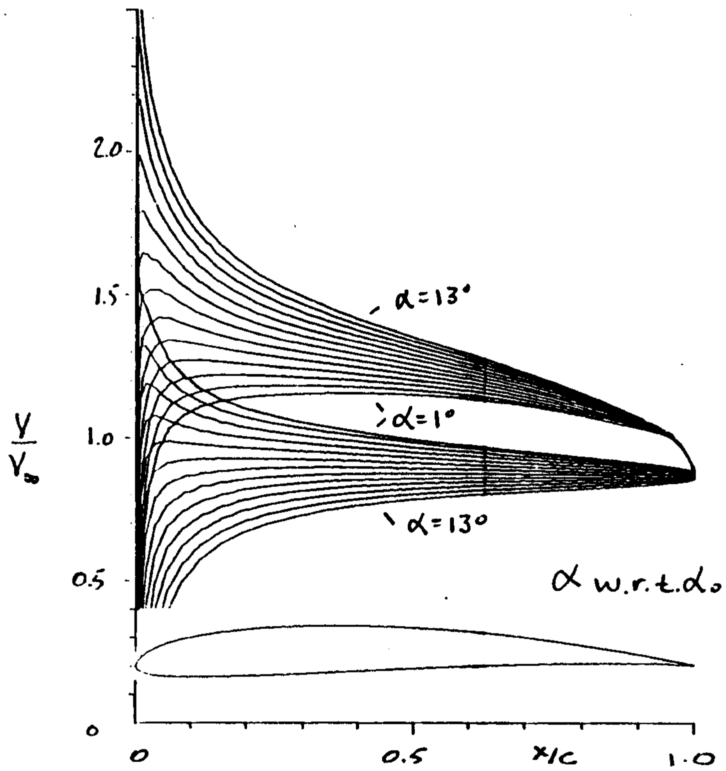

FIG. 38 · VELOCITY DISTRIBUTIONS FOR THE S4110-084-84.

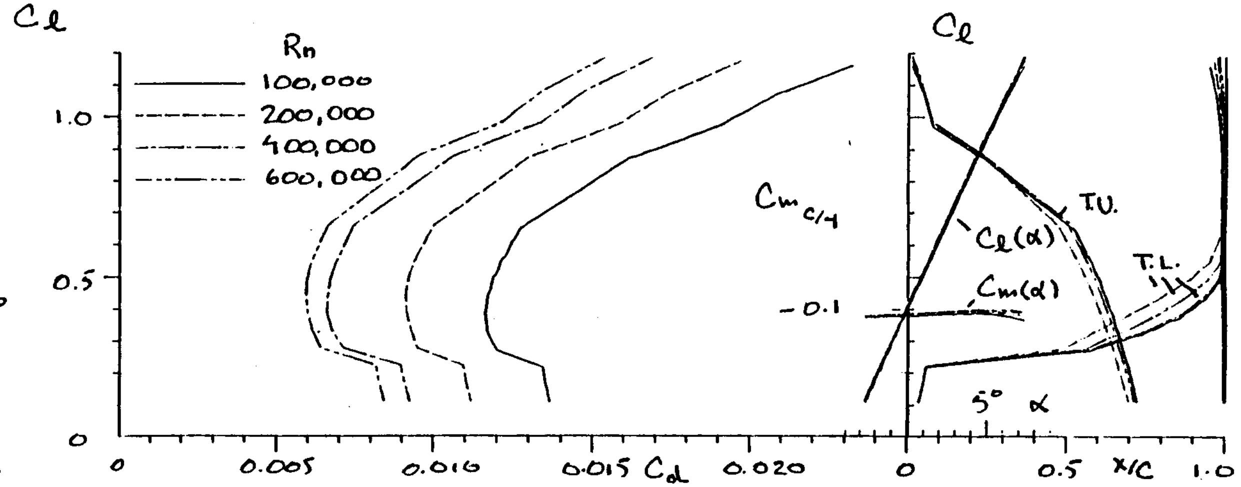

FIG. 39 · THEORETICAL SECTION CHARACTERISTICS FOR THE S4110-084-84.

THEORETICAL BOUNDARY-LAYER SUMMARY TABLE										
AIRFOIL 4110-084-84	*-LAMINAR SEPARATION BUBBLE WARNING O-NO SEPARATION BUBBLE WARNING ●-NO BUBBLE, TRANSITION BEFORE 0.05C --SEPARATION AT LEADING EDGE (STALL) +-ANGLE OF ATTACK WITHIN DRAG BUCKET									
ALPHA (deg)	REYNOLDS NUMBER									
			100000		200000		400000		600000	
	us	ls	us	ls	us	ls	us	ls	us	ls
1			*	*	*	*	*	●	*	●
2			*	*	*	O	*	O	*	O
+ 3			*	*	*	*	*	*	*	*
+ 4			*	*	*	*	*	*	*	*
+ 5			*	*	*	*	*	*	*	*
+ 6			*	O	*	O	*	O	*	O
+ 7			*	O	*	O	*	O	*	O
+ 8			*	O	*	O	O	O	O	O
+ 9			*	O	O	O	O	O	O	O
+10			*	O	O	O	O	O	O	O
11			*	O	●	O	●	O	●	O
12			*	O	●	O	●	O	●	O
13			*	O	●	O	●	O	●	O

X	Y
1.00000	0.00000
.99677	.00055
.98738	.00228
.97242	.00521
.95237	.00908
.92746	.01359
.89794	.01868
.86424	.02430
.82685	.03033
.78630	.03657
.74310	.04282
.69771	.04883
.65062	.05439
.60225	.05934
.55306	.06352
.50349	.06683
.45401	.06922
.40507	.07062
.35714	.07102
.31066	.07042
.26612	.06885
.22394	.06631
.18453	.06285
.14830	.05849
.11555	.05328
.08659	.04729
.06167	.04060
.04093	.03323
.02437	.02536
.01204	.01730
.00400	.00935
.00021	.00191
.00119	-.00408
.00755	-.00892
.01905	-.01317
.03554	-.01630
.05723	-.01820
.08413	-.01911
.11599	-.01920
.15247	-.01865
.19313	-.01757
.23751	-.01605
.28509	-.01417
.33537	-.01202
.38774	-.00970
.44162	-.00726
.49640	-.00487
.55145	-.00256
.60606	-.00053
.65957	.00121
.71127	.00260
.76051	.00360
.80665	.00418
.84906	.00436
.88717	.00416
.92046	.00363
.94843	.00285
.97068	.00193
.98686	.00102
.99670	.00029
1.00000	.00000

S4110-084-84 COORDINATES

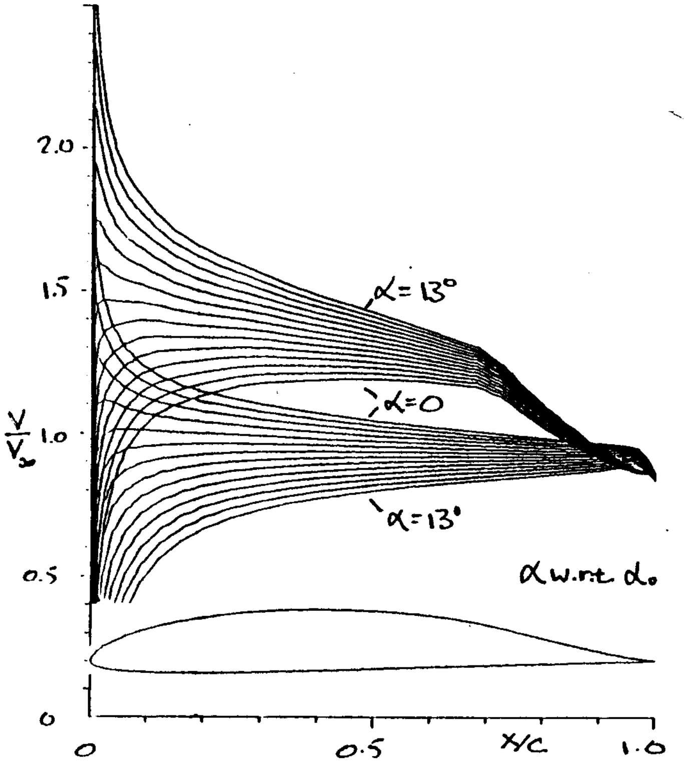

FIG. 40 – VELOCITY DISTRIBUTIONS FOR THE S4158-109-84.

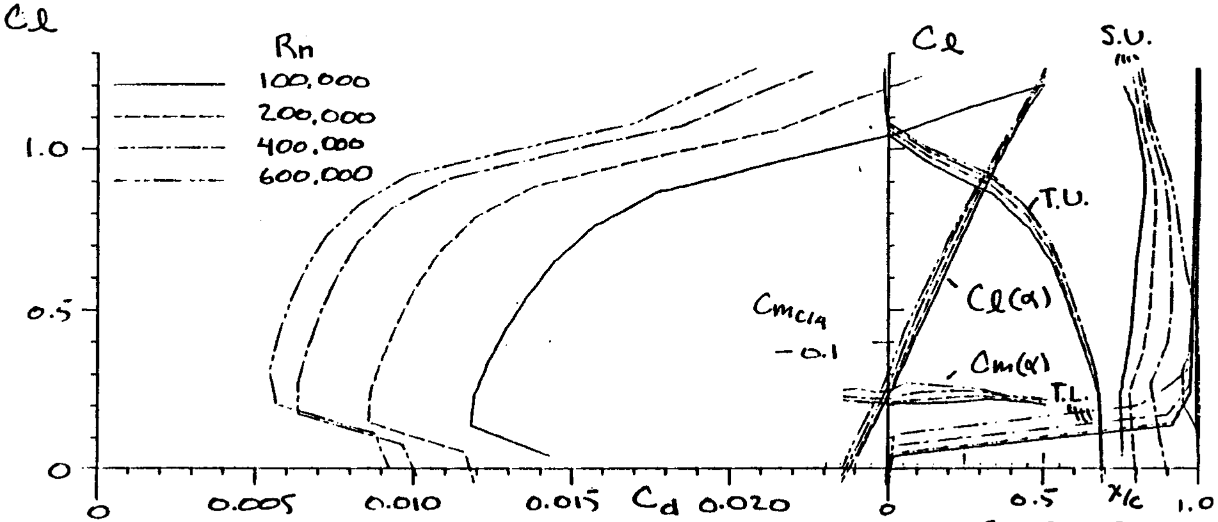

FIG. 41 – THEORETICAL SECTION CHARACTERISTICS FOR THE S4158-109-84.

THEORETICAL BOUNDARY-LAYER SUMMARY TABLE

AIRFOIL
*-LAMINAR SEPARATION BUBBLE WARNING
O-NO SEPARATION BUBBLE WARNING
●-NO BUBBLE, TRANSITION BEFORE 0.05C
--SEPARATION AT LEADING EDGE (STALL)
4158-109-84 +-ANGLE OF ATTACK WITHIN DRAG BUCKET

ALPHA (deg)	REYNOLDS NUMBER		100000		200000		400000		600000	
	us	ls	us	ls	us	ls	us	ls	us	ls
0			*	-	*	*	*	●	*	●
1			*	*	*	●	*	●	*	●
+ 2			*	*	*	*	*	*	*	*
+ 3			*	*	*	*	*	*	*	*
+ 4			*	*	*	*	*	*	*	*
+ 5			*	*	*	*	*	*	*	*
+ 6			*	*	*	*	*	*	O	*
+ 7			*	*	*	*	*	*	O	*
+ 8			*	*	*	*	*	*	*	*
+ 9			*	*	*	*	*	*	O	*
+10			*	*	*	*	O	*	O	*
11			*	*	●	*	●	*	●	*
12			*	*	●	*	●	*	●	*
13			*	*	*	*	●	*	●	*

X	Y
1.00000	0.00000
.99654	.00023
.98621	.00111
.96923	.00307
.94604	.00654
.91742	.01182
.88428	.01890
.84751	.02757
.80801	.03745
.76666	.04799
.72424	.05830
.68083	.06722
.63593	.07442
.58958	.08025
.54234	.08482
.49464	.08805
.44690	.08996
.39957	.09057
.35312	.08992
.30808	.08804
.26485	.08486
.22375	.08044
.18512	.07496
.14938	.06857
.11693	.06137
.08808	.05342
.06297	.04484
.04177	.03594
.02474	.02697
.01209	.01814
.00392	.00965
.00018	.00185
.00127	-.00429
.00801	-.00894
.02053	-.01294
.03845	-.01613
.06167	-.01849
.09001	-.02012
.12317	-.02113
.16075	-.02160
.20228	-.02159
.24730	-.02109
.29534	-.02016
.34590	-.01888
.39836	-.01735
.45218	-.01565
.50667	-.01385
.56120	-.01202
.61511	-.01022
.66775	-.00852
.71848	-.00696
.76666	-.00556
.81168	-.00437
.85297	-.00337
.88999	-.00257
.92225	-.00193
.94931	-.00140
.97083	-.00087
.98666	-.00035
.99659	-.00005
1.00000	.00000

S4158-109-84 COORDINATES

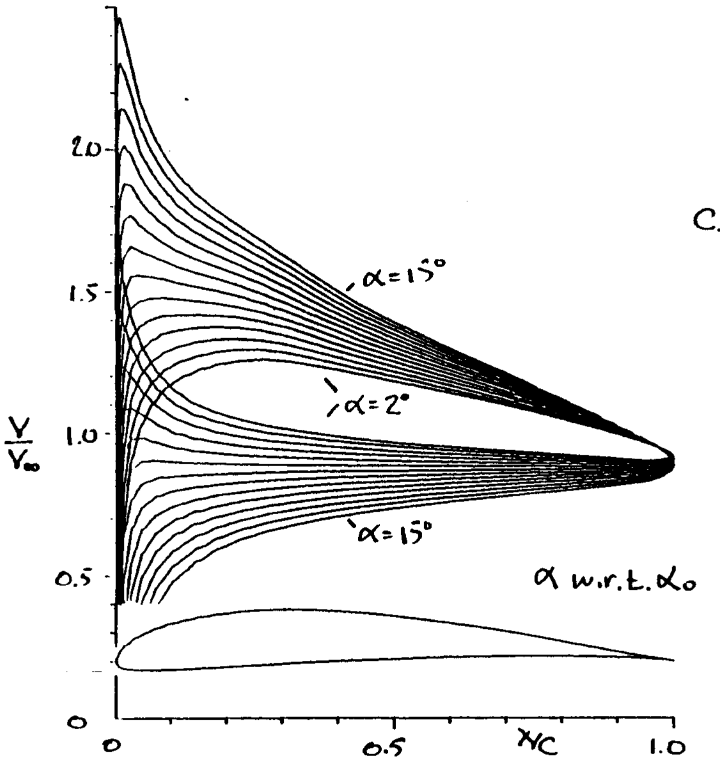

FIG. 42 - VELOCITY DISTRIBUTIONS FOR THE S4180-098-84.

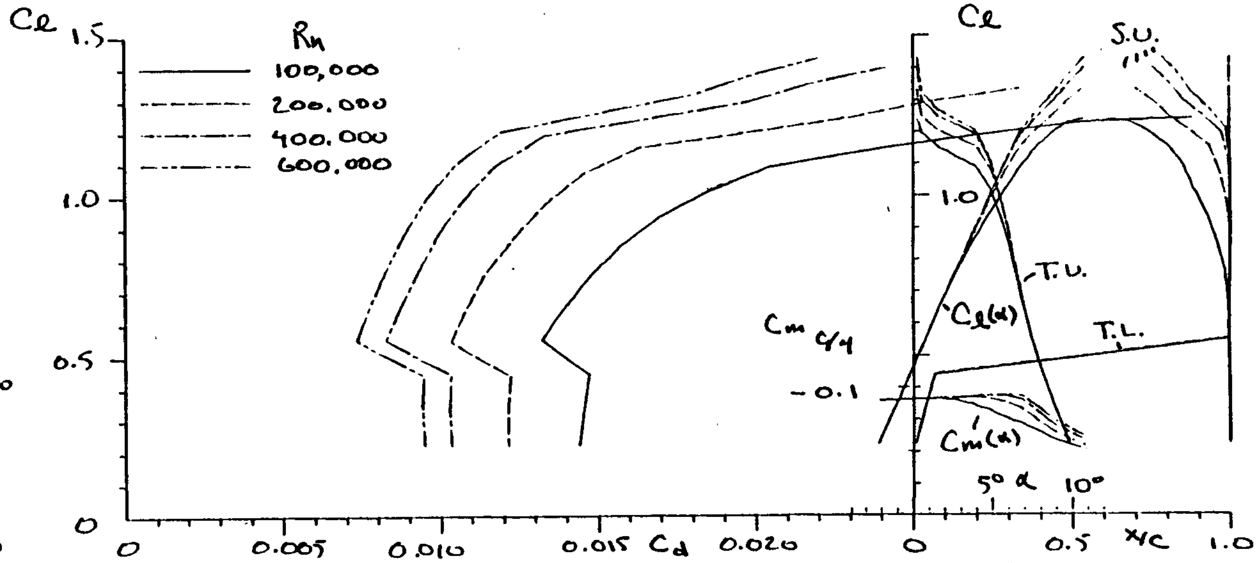

FIG. 43 - THEORETICAL SECTION CHARACTERISTICS FOR THE S4180-098-84.

THEORETICAL BOUNDARY-LAYER SUMMARY TABLE										
AIRFOIL	*-LAMINAR SEPARATION BUBBLE WARNING O-NO SEPARATION BUBBLE WARNING ●-NO BUBBLE, TRANSITION BEFORE 0.05C --SEPARATION AT LEADING EDGE (STALL)									
4180-098-84	+-ANGLE OF ATTACK WITHIN DRAG BUCKET									
ALPHA	REYNOLDS NUMBER									
(deg)			100000		200000		400000		600000	
	us	ls	us	ls	us	ls	us	ls	us	ls
2			*	*	*	●	*	●	*	●
3			*	*	*	*	*	●	O	●
+ 4			*	*	*	O	*	O	O	O
+ 5			*	O	*	O	*	O	O	O
+ 6			*	O	*	O	*	O	O	O
+ 7			*	O	*	O	*	O	O	O
+ 8			*	O	*	O	*	O	O	O
+ 9			*	O	*	O	*	O	O	O
+10			*	O	*	O	*	O	O	O
+11			*	O	*	O	O	O	O	O
+12			*	O	O	O	O	O	O	O
13			*	O	●	O	●	O	●	O
14			*	O	●	O	●	O	●	O
15			*	O	●	O	●	O	●	O

1.00000	0.00000
.99684	.00036
.98746	.00156
.97208	.00376
.95106	.00702
.92483	.01132
.89384	.01661
.85861	.02279
.81971	.02971
.77768	.03718
.73313	.04497
.68661	.05280
.63859	.06042
.58961	.06762
.54019	.07420
.49083	.07997
.44204	.08472
.39427	.08829
.34798	.09050
.30355	.09118
.26126	.09018
.22127	.08751
.18383	.08329
.14916	.07770
.11757	.07095
.08935	.06323
.06476	.05468
.04398	.04553
.02726	.03596
.01467	.02606
.00607	.01606
.00129	.00643
.00016	-.00200
.00377	-.00814
.01306	-.01234
.02779	-.01523
.04791	-.01670
.07351	-.01680
.10453	-.01584
.14065	-.01417
.18140	-.01202
.22624	-.00957
.27459	-.00696
.32585	-.00433
.37936	-.00178
.43445	.00060
.49043	.00273
.54656	.00455
.60221	.00601
.65660	.00708
.70908	.00774
.75897	.00800
.80564	.00786
.84847	.00735
.88692	.00652
.92046	.00540
.94862	.00407
.97093	.00262
.98703	.00131
.99674	.00035
1.00000	.00000

S4180-098-84 COORDINATES

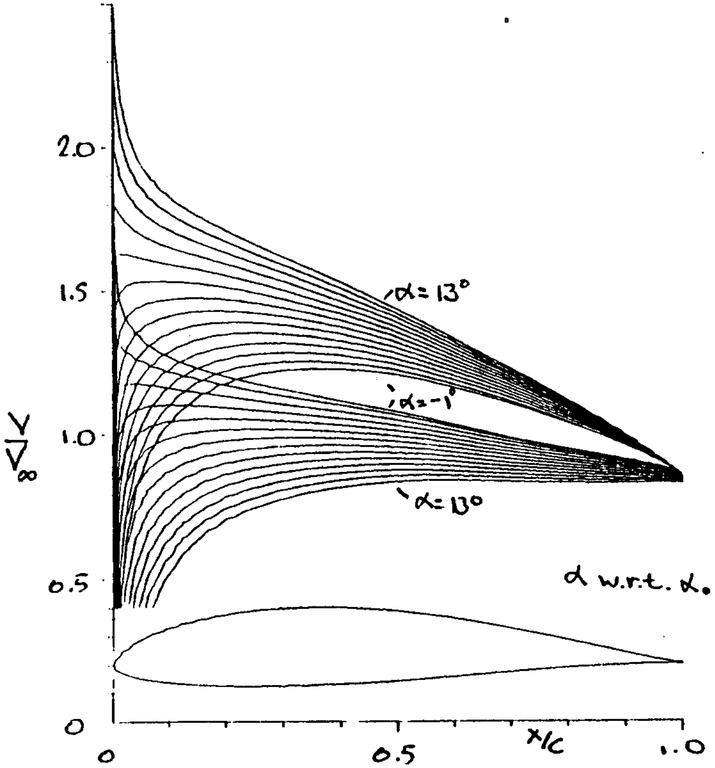

FIG. 44 - VELOCITY DISTRIBUTIONS FOR THE S4233-136-84.

THEORETICAL BOUNDARY-LAYER SUMMARY TABLE										
AIRFOIL 4233-136-84	*-LAMINAR SEPARATION BUBBLE WARNING O-NO SEPARATION BUBBLE WARNING ●-NO BUBBLE, TRANSITION BEFORE 0.05C --SEPARATION AT LEADING EDGE (STALL) +-ANGLE OF ATTACK WITHIN DRAG BUCKET									
ALPHA (deg)	REYNOLDS NUMBER									
			100000		200000		400000		600000	
	us	ls	us	ls	us	ls	us	ls	us	ls
-1			*	-	*	-	*	●	*	●
0			*	●	*	●	*	●	*	●
+ 1			*	*	*	*	*	*	*	*
+ 2			*	*	*	*	*	*	*	*
+ 3			*	*	*	*	*	*	*	*
+ 4			*	*	*	*	*	*	*	*
+ 5			*	*	*	*	*	*	*	*
+ 6			*	*	*	*	*	*	O	*
+ 7			*	*	*	*	*	*	O	*
+ 8			*	*	*	*	*	*	O	*
+ 9			*	*	*	*	*	*	O	*
+10			*	*	*	*	*	*	O	*
+11			*	O	*	O	*	O	O	O
+12			*	O	*	O	O	O	O	O
13			*	O	●	O	●	O	●	O

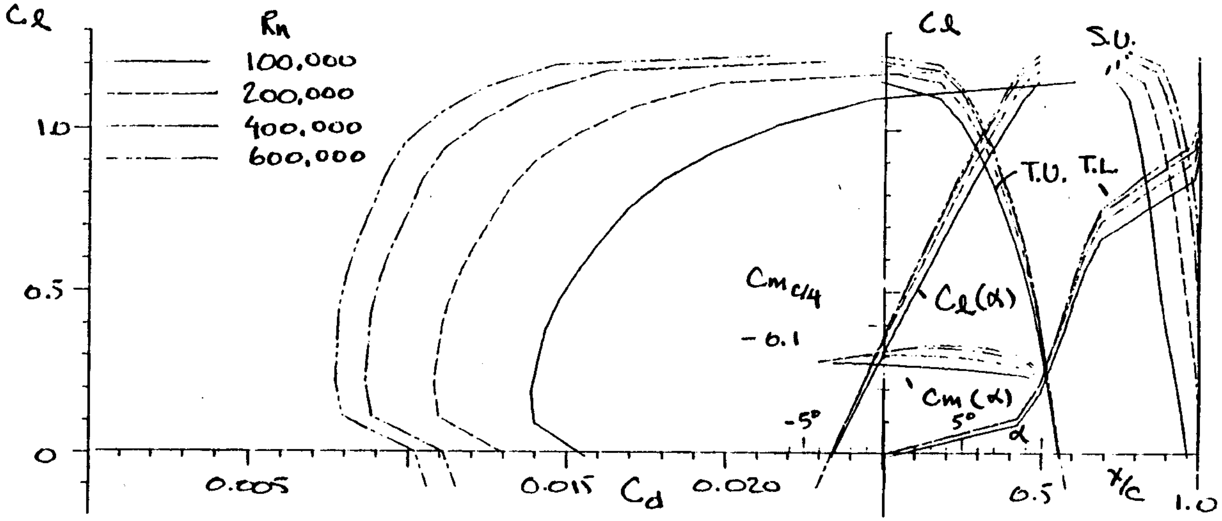

FIG. 45 - THEORETICAL SECTION CHARACTERISTICS FOR THE S4233-136-84.

X	Y
1.00000	0.00000
.99650	.00042
.98618	.00186
.96949	.00461
.94697	.00881
.91927	.01444
.88703	.02138
.85088	.02939
.81146	.03817
.76933	.04740
.72503	.05674
.67907	.06586
.63196	.07443
.58414	.08218
.53609	.08881
.48820	.09406
.44078	.09770
.39411	.09969
.34857	.10001
.30450	.09867
.26227	.09571
.22219	.09119
.18457	.08523
.14971	.07798
.11788	.06963
.08935	.06040
.06437	.05056
.04320	.04033
.02602	.03000
.01301	.01987
.00433	.01032
.00017	.00183
.00156	-.00488
.00916	-.01058
.02237	-.01621
.04069	-.02144
.06388	-.02609
.09171	-.03004
.12392	-.03322
.16018	-.03559
.20012	-.03714
.24337	-.03782
.28950	-.03768
.33802	-.03672
.38846	-.03497
.44031	-.03249
.49308	-.02934
.54625	-.02558
.59939	-.02139
.65199	-.01703
.70341	-.01286
.75289	-.00910
.79966	-.00591
.84299	-.00337
.88219	-.00149
.91664	-.00026
.94576	.00040
.96905	.00058
.98608	.00043
.99649	.00014
1.00000	.00000

S4233 - 136-84 COORDINATES

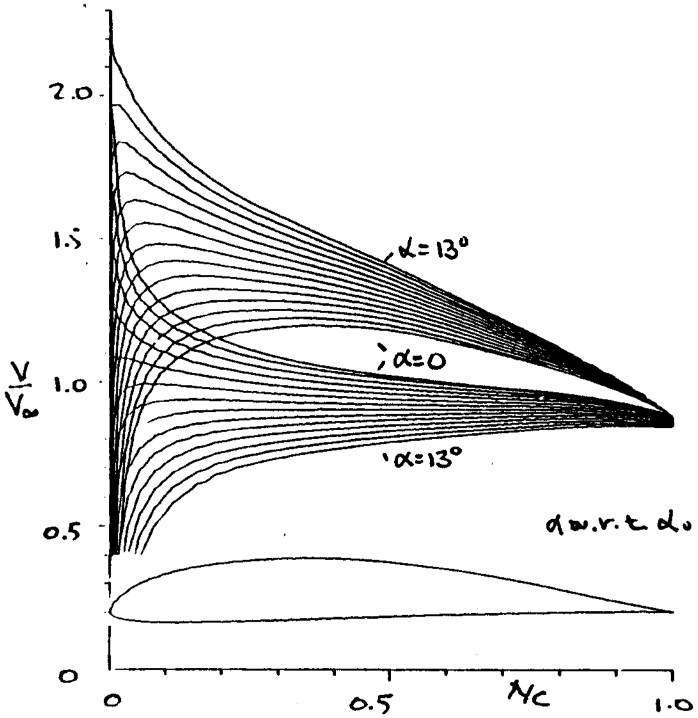

FIG. 46 - VELOCITY DISTRIBUTIONS FOR THE S4310-109-84.

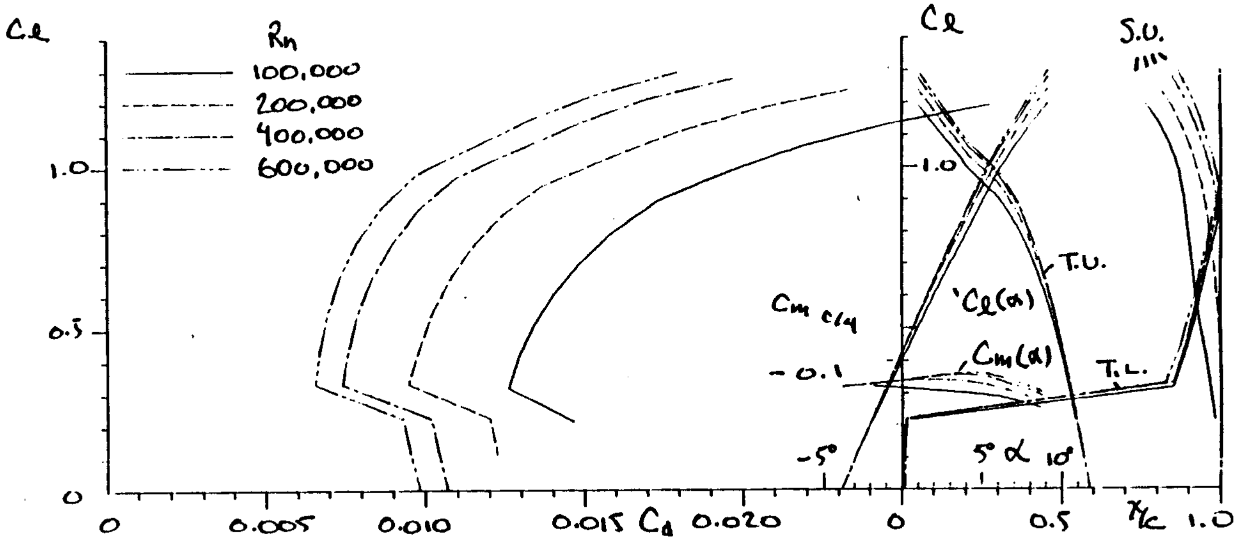

FIG. 47- THEORETICAL SECTION CHARACTERISTICS FOR THE S4310-109-84

THEORETICAL BOUNDARY-LAYER SUMMARY TABLE										
AIRFOIL	*-LAMINAR SEPARATION BUBBLE WARNING O-NO SEPARATION BUBBLE WARNING ●-NO BUBBLE, TRANSITION BEFORE 0.05C --SEPARATION AT LEADING EDGE (STALL)									
4310-109-84	+-ANGLE OF ATTACK WITHIN DRAG BUCKET									
ALPHA	REYNOLDS NUMBER									
(deg)			100000		200000		400000		600000	
	us	ls	us	ls	us	ls	us	ls	us	ls
1			*	-	*	*	*	●	*	●
2			*	*	*	●	*	●	*	●
+ 3			*	*	*	*	*	*	*	*
+ 4			*	*	*	*	*	*	O	*
+ 5			*	*	*	*	*	*	*	*
+ 6			*	*	*	*	*	*	O	*
+ 7			*	*	*	*	*	*	O	*
+ 8			*	*	*	*	*	*	O	*
+ 9			*	O	*	O	O	O	O	O
+10			*	O	*	O	O	O	O	O
+11			*	O	*	O	O	O	O	O
+12			*	O	O	O	O	O	O	O
+13			*	O	O	O	O	O	O	O

x	y
1.00000	0.00000
.99665	.00043
.98675	.00184
.97069	.00444
.94893	.00834
.92202	.01351
.89054	.01984
.85507	.02714
.81616	.03516
.77439	.04365
.73029	.05230
.68439	.06084
.63721	.06896
.58923	.07640
.54091	.08285
.49265	.08806
.44477	.09187
.39761	.09421
.35154	.09504
.30694	.09439
.26416	.09231
.22361	.08889
.18569	.08418
.15073	.07822
.11898	.07113
.09072	.06303
.06611	.05406
.04530	.04443
.02840	.03437
.01546	.02416
.00643	.01419
.00130	.00509
.00030	-.00210
.00498	-.00721
.01603	-.01117
.03260	-.01434
.05451	-.01664
.08156	-.01807
.11352	-.01869
.15011	-.01857
.19095	-.01784
.23562	-.01661
.28362	-.01503
.33437	-.01323
.38726	-.01133
.44162	-.00942
.49677	-.00758
.55203	-.00585
.60671	-.00428
.66013	-.00291
.71162	-.00175
.76053	-.00079
.80627	.00001
.84833	.00067
.88622	.00114
.91946	.00139
.94757	.00137
.97008	.00110
.98655	.00065
.99661	.00020
1.00000	.00000

S4310-109-84 COORDINATES

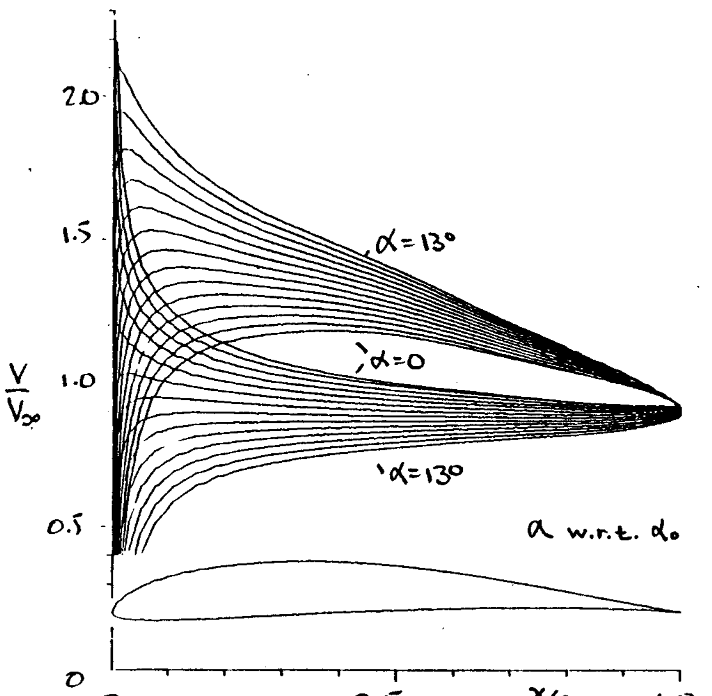

FIG. 48 - VELOCITY DISTRIBUTIONS FOR THE S4320-094-84.

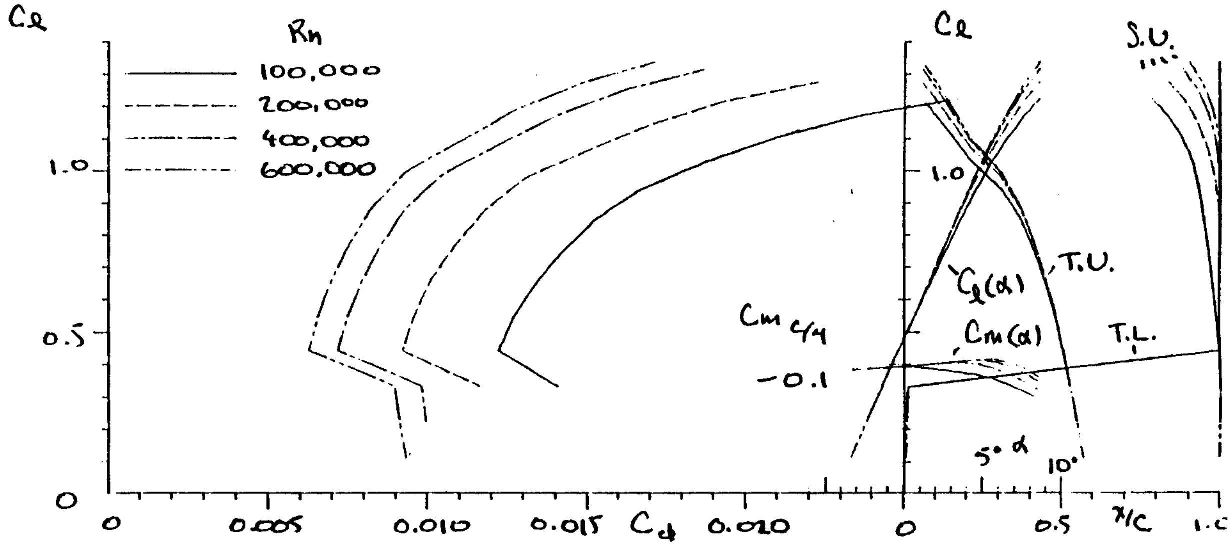

FIG. 49 - THEORETICAL SECTION CHARACTERISTICS FOR THE S4320-094-84

THEORETICAL BOUNDARY-LAYER SUMMARY TABLE										
AIRFOIL	*-LAMINAR SEPARATION BUBBLE WARNING O-NO SEPARATION BUBBLE WARNING ●-NO BUBBLE, TRANSITION BEFORE 0.05C --SEPARATION AT LEADING EDGE (STALL)									
4320-094-84	+-ANGLE OF ATTACK WITHIN DRAG BUCKET									
ALPHA (deg)	REYNOLDS NUMBER									
			100000		200000		400000		600000	
	us	ls	us	ls	us	ls	us	ls	us	ls
2			*	-	*	-	*	●	*	●
3			*	●	*	●	*	●	*	●
+ 4			*	O	*	O	*	O	*	O
+ 5			*	O	*	O	*	O	*	O
+ 6			*	O	*	O	*	O	*	O
+ 7			*	O	*	O	*	O	O	O
+ 8			*	O	*	O	*	O	O	O
+ 9			*	O	*	O	O	O	O	O
+10			*	O	*	O	O	O	O	O
+11			*	O	*	O	O	O	O	O
+12			*	O	O	O	O	O	O	O
+13			*	O	O	O	O	O	O	O

X	Y
1.00000	0.00000
.99682	.00044
.98739	.00182
.97202	.00426
.95108	.00780
.92500	.01242
.89426	.01804
.85937	.02454
.82088	.03175
.77933	.03946
.73529	.04746
.68931	.05550
.64198	.06333
.59384	.07063
.54538	.07709
.49698	.08242
.44898	.08642
.40169	.08902
.35549	.09018
.31075	.08991
.26783	.08826
.22712	.08530
.18903	.08108
.15387	.07563
.12192	.06906
.09342	.06147
.06855	.05300
.04745	.04385
.03022	.03425
.01690	.02445
.00744	.01483
.00179	.00598
.00009	-.00116
.00380	-.00601
.01372	-.00931
.02926	-.01168
.05023	-.01305
.07648	-.01348
.10780	-.01304
.14390	-.01186
.18445	-.01009
.22900	-.00788
.27707	-.00540
.32807	-.00283
.38137	-.00031
.43629	.00206
.49213	.00417
.54818	.00596
.60374	.00738
.65811	.00838
.71057	.00894
.76047	.00905
.80716	.00871
.85000	.00791
.88833	.00671
.92161	.00526
.94939	.00373
.97133	.00229
.98719	.00110
.99678	.00029
1.00000	.00000

S4320-094-84 COORDINATES

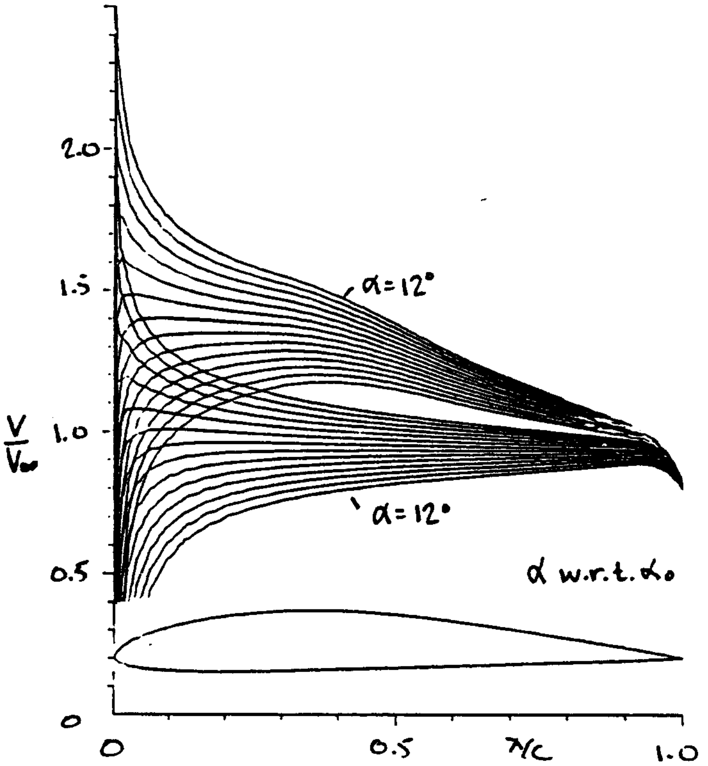

FIG. 50 - VELOCITY DISTRIBUTIONS FOR THE ANTARES AIRFOIL.

THEORETICAL BOUNDARY-LAYER SUMMARY TABLE										
AIRFOIL ANTARES	*-LAMINAR SEPARATION BUBBLE WARNING O-NO SEPARATION BUBBLE WARNING ●-NO BUBBLE, TRANSITION BEFORE 0.05C --SEPARATION AT LEADING EDGE (STALL) +-ANGLE OF ATTACK WITHIN DRAG BUCKET									
ALPHA (deg)	REYNOLDS NUMBER									
			100000		200000		400000		600000	
	us	ls	us	ls	us	ls	us	ls	us	ls
-1			*	-	*	-	*	●	*	●
0			*	*	*	●	*	●	*	●
+ 1			*	*	*	*	*	*	*	*
+ 2			*	*	*	*	*	*	*	*
+ 3			*	*	*	*	*	*	*	*
+ 4			*	*	*	*	*	*	*	*
+ 5			*	*	*	*	*	*	*	*
+ 6			*	*	*	*	*	*	*	*
+ 7			*	*	*	*	*	*	O	*
+ 8			*	*	*	*	*	*	*	*
+ 9			*	*	*	*	*	*	O	*
+10			*	*	*	*	*	*	O	*
11			●	*	●	*	●	*	●	*
12			*	*	●	*	●	*	●	*

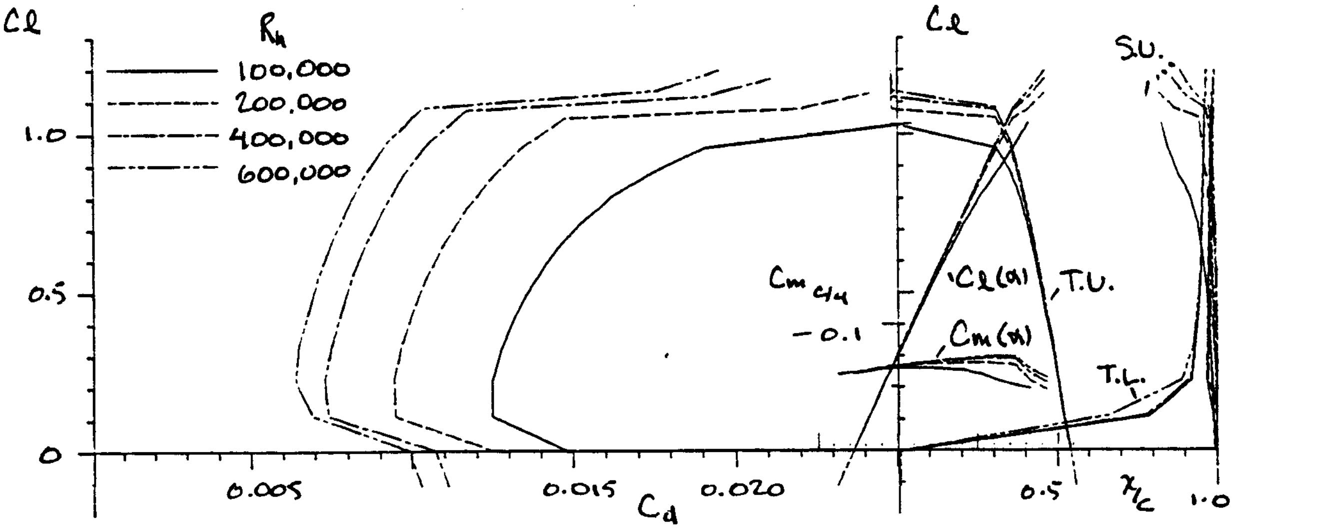

FIG. 51 - THEORETICAL SECTION CHARACTERISTICS FOR THE ANTARES AIRFOIL.

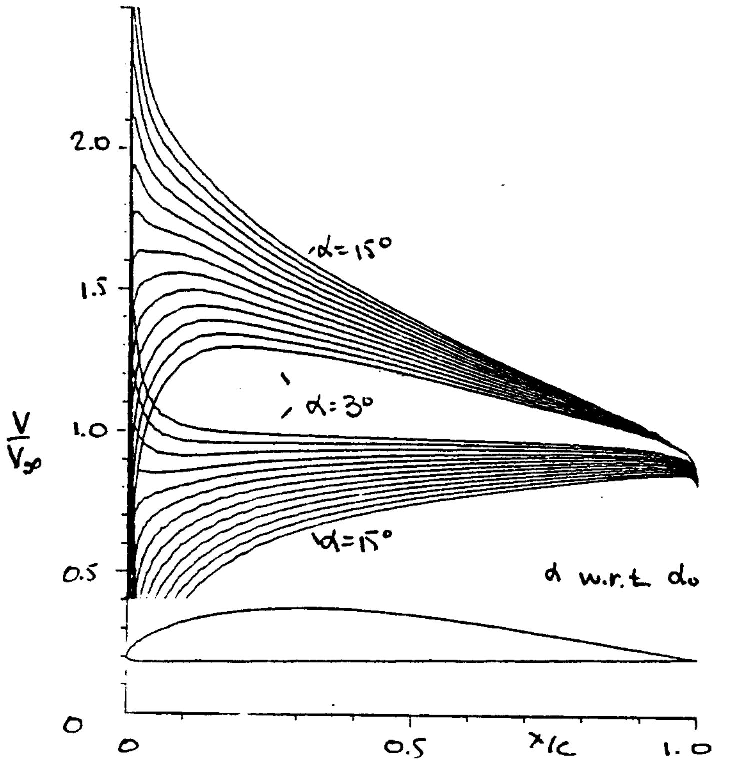

FIG. 52 - VELOCITY DISTRIBUTIONS FOR THE AQUILA AIRFOIL.

THEORETICAL BOUNDARY-LAYER SUMMARY TABLE

AIRFOIL: AQUILA

*-LAMINAR SEPARATION BUBBLE WARNING
O-NO SEPARATION BUBBLE WARNING
●-NO BUBBLE, TRANSITION BEFORE 0.05C
--SEPARATION AT LEADING EDGE (STALL)
+-ANGLE OF ATTACK WITHIN DRAG BUCKET

ALPHA (deg)	REYNOLDS NUMBER		100000		200000		400000		600000	
	us	ls	us	ls	us	ls	us	ls	us	ls
4			*	*	*	●	*	●	*	●
+ 5			*	*	*	*	*	*	O	*
+ 6			*	*	*	*	*	*	O	*
+ 7			*	*	*	*	*	*	O	*
+ 8			*	*	*	*	O	*	O	*
+ 9			*	*	*	*	O	*	O	*
+10			*	*	*	*	O	*	O	*
+11			*	*	*	*	O	*	O	*
+12			*	*	O	*	O	*	O	*
13			●	*	●	*	●	*	●	*
14			●	*	●	*	●	*	●	*
15			*	*	●	*	●	*	●	*

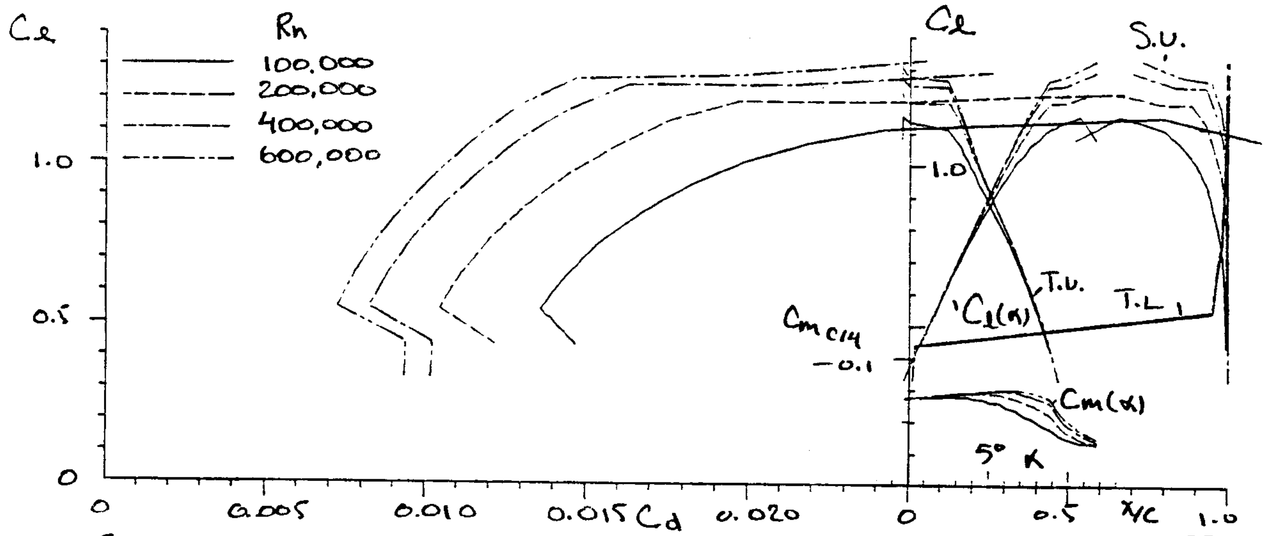

FIG. 53- THEORETICAL SECTION CHARACTERISTICS FOR THE AQUILA AIRFOIL

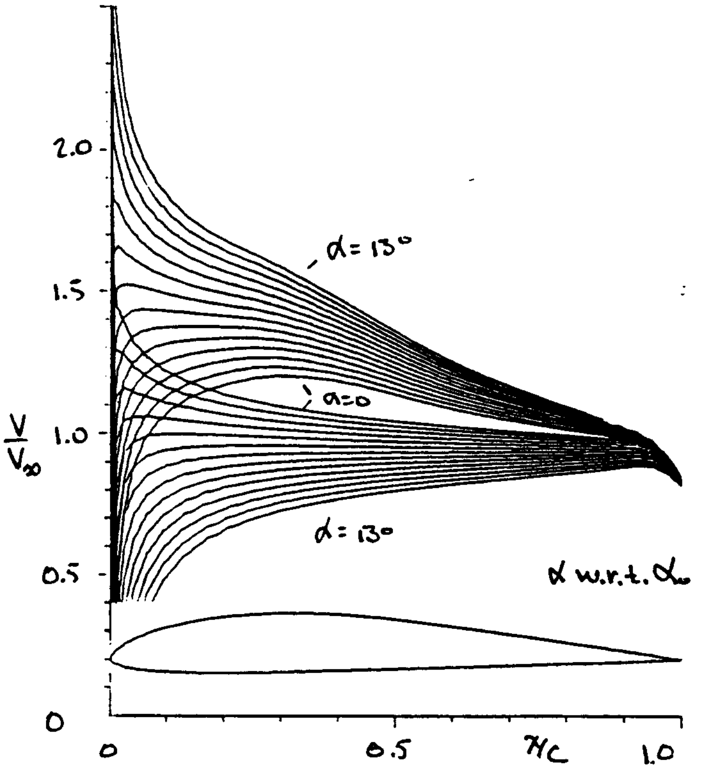

FIG. 54 – VELOCITY DISTRIBUTIONS FOR THE E205.

THEORETICAL BOUNDARY-LAYER SUMMARY TABLE										
AIRFOIL E 205	*-LAMINAR SEPARATION BUBBLE WARNING O-NO SEPARATION BUBBLE WARNING ●-NO BUBBLE, TRANSITION BEFORE 0.05C --SEPARATION AT LEADING EDGE (STALL) +-ANGLE OF ATTACK WITHIN DRAG BUCKET									
ALPHA (deg)	REYNOLDS NUMBER									
			100000		200000		400000		600000	
	us	ls	us	ls	us	ls	us	ls	us	ls
-1			*	●	*	●	*	●	*	●
0			*	●	*	●	*	●	*	●
+ 1			*	*	*	*	*	*	*	*
+ 2			*	*	*	*	*	*	O	*
+ 3			*	*	*	*	*	*	*	*
+ 4			*	*	*	*	*	*	O	*
+ 5			*	*	*	*	*	*	*	*
+ 6			*	*	*	*	*	*	O	*
+ 7			*	*	*	*	*	*	O	*
+ 8			*	*	*	*	*	*	O	*
+ 9			*	*	*	*	*	*	O	*
10			*	*	●	*	●	*	●	*
11			●	*	●	*	●	*	●	*
12			*	*	*	*	●	*	●	*

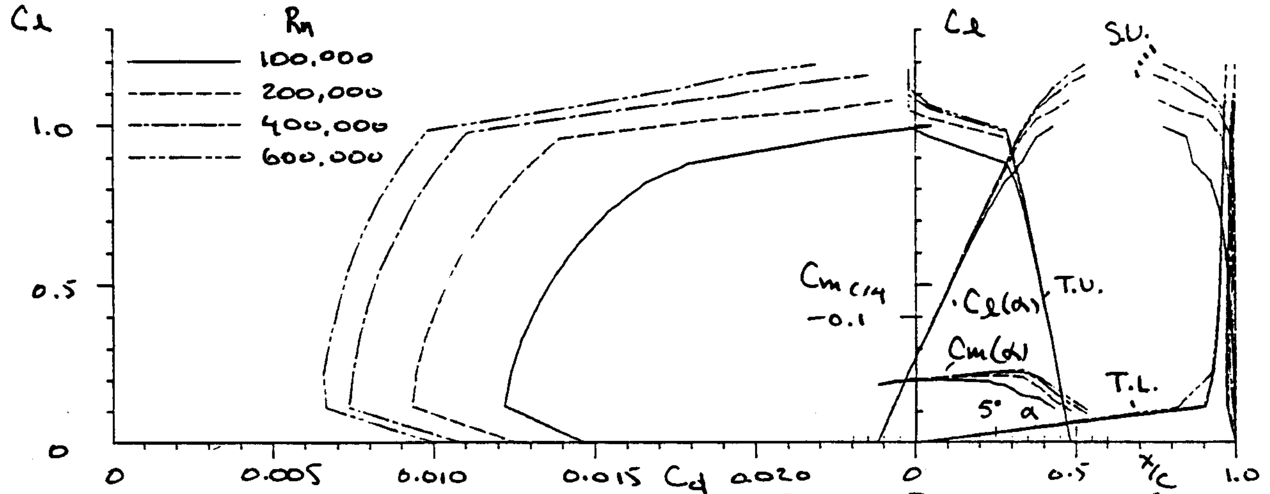

FIG. 55 – THEORETICAL SECTION CHARACTERISTICS FOR THE E205.

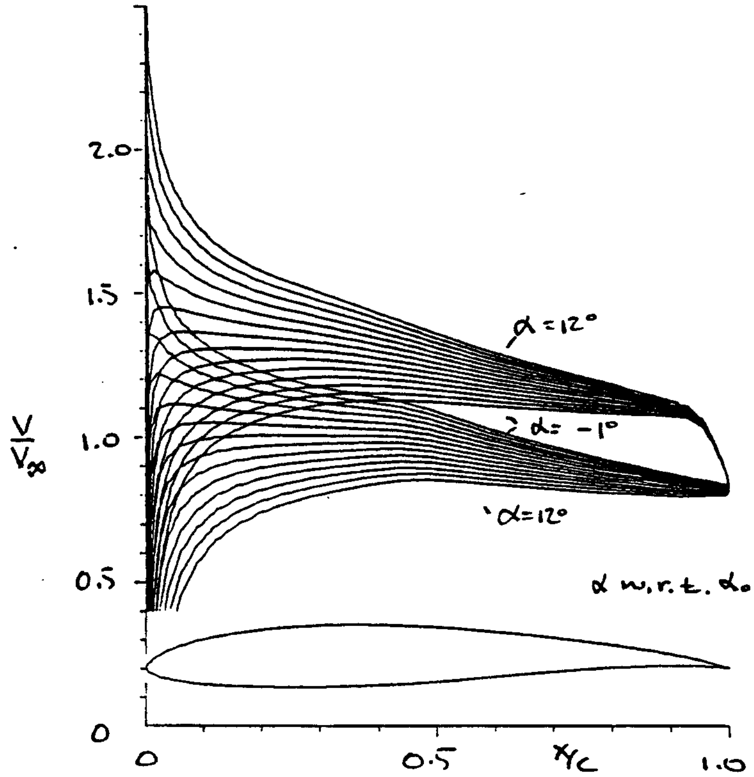

FIG. 56 - VELOCITY DISTRIBUTIONS FOR THE E211.

THEORETICAL BOUNDARY-LAYER SUMMARY TABLE										
AIRFOIL E211	*-LAMINAR SEPARATION BUBBLE WARNING O-NO SEPARATION BUBBLE WARNING ●-NO BUBBLE, TRANSITION BEFORE 0.05C --SEPARATION AT LEADING EDGE (STALL) +-ANGLE OF ATTACK WITHIN DRAG BUCKET									
ALPHA (deg)	REYNOLDS NUMBER									
			100000		200000		400000		600000	
	us	ls	us	ls	us	ls	us	ls	us	ls
-1			-	-	*	●	*	●	*	●
0			*	*	*	●	*	●	*	●
+ 1			*	*	*	*	*	*	*	*
+ 2			*	*	*	*	*	*	*	*
+ 3			*	*	*	*	*	*	*	*
+ 4			*	*	*	*	*	*	*	*
+ 5			*	*	*	*	*	*	*	*
+ 6			*	*	*	*	*	*	O	*
+ 7			*	*	*	*	*	*	*	*
+ 8			*	*	*	*	*	*	O	*
+ 9			*	*	*	*	*	*	O	*
+10			*	*	O	*	O	*	O	*
12			*	O	*	O	●	O	●	O
13			*	O	*	O	●	O	●	O

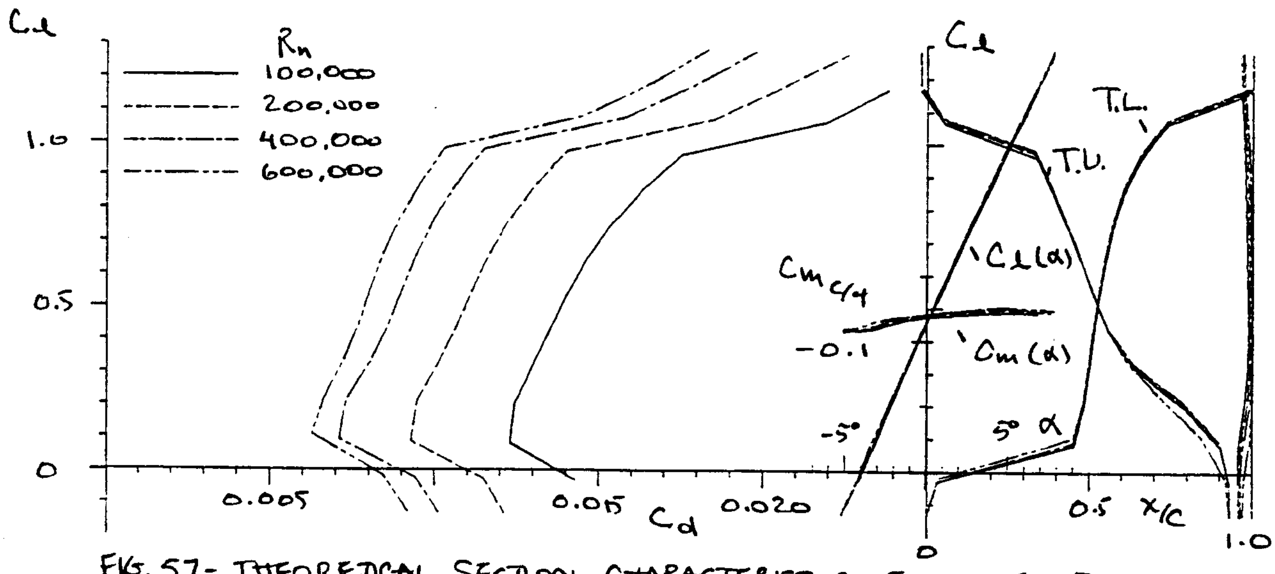

FIG. 57 - THEORETICAL SECTION CHARACTERISTICS FOR THE E211.

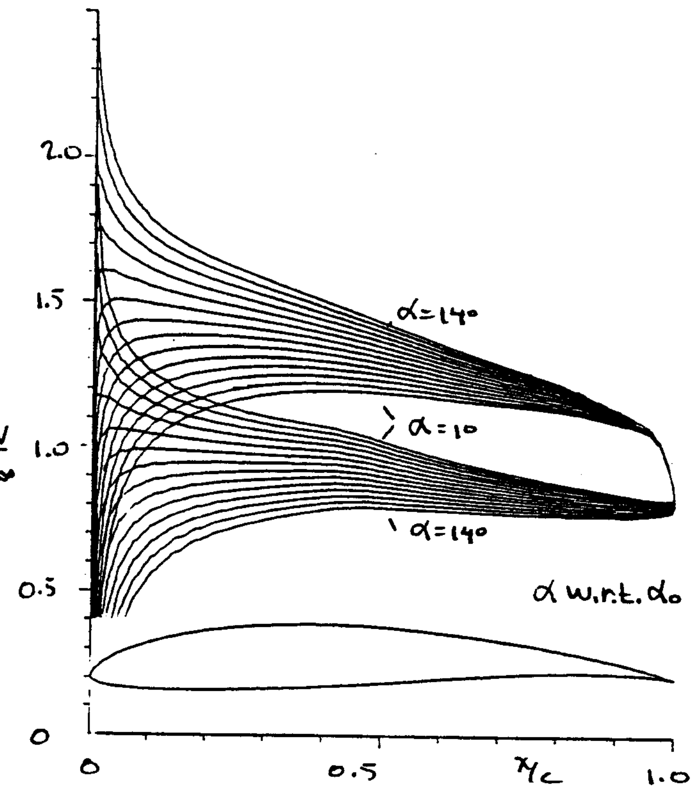

FIG. 58- VELOCITY DISTRIBUTIONS FOR THE E214.

THEORETICAL BOUNDARY-LAYER SUMMARY TABLE										
AIRFOIL E214	*-LAMINAR SEPARATION BUBBLE WARNING O-NO SEPARATION BUBBLE WARNING ●-NO BUBBLE, TRANSITION BEFORE 0.05C --SEPARATION AT LEADING EDGE (STALL) +-ANGLE OF ATTACK WITHIN DRAG BUCKET									
ALPHA (deg)	REYNOLDS NUMBER									
			100000		200000		400000		600000	
	us	ls	us	ls	us	ls	us	ls	us	ls
1			*	●	*	●	*	●	*	●
2			*	*	*	●	*	●	*	●
+ 3			*	*	*	*	*	*	*	*
+ 4			*	*	*	*	*	*	*	*
+ 5			*	*	*	*	*	*	*	*
+ 6			*	*	*	*	*	*	*	*
+ 7			*	*	*	*	*	*	*	*
+ 8			*	*	*	*	*	*	*	*
+ 9			*	*	*	*	*	*	O	*
+10			*	*	*	*	*	*	O	*
+11			*	O	*	O	*	O	O	O
+12			*	O	*	O	O	O	O	O
13			●	O	●	O	●	O	●	O
14			●	O	●	O	●	O	●	O

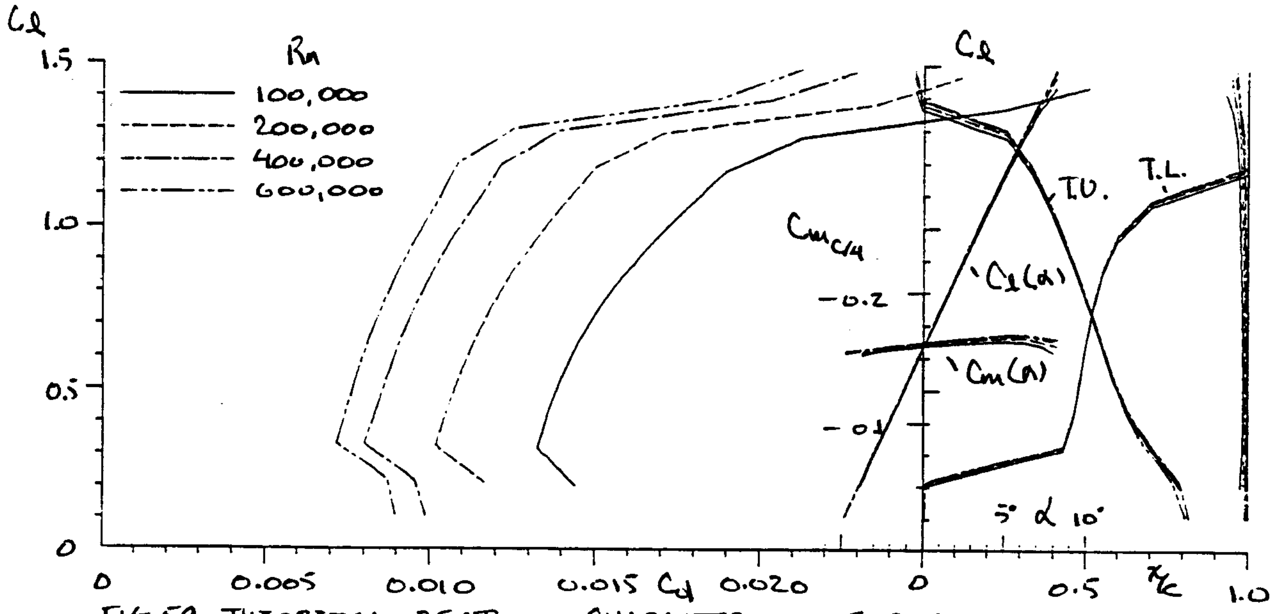

FIG. 59-THEORETICAL SECTION CHARACTERISTICS FOR THE E214.

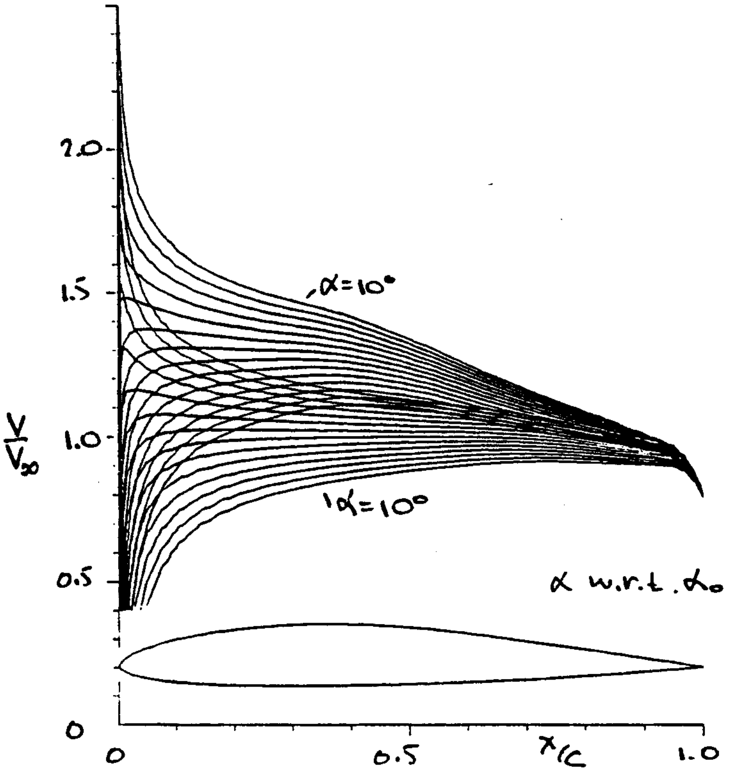

FIG. 60 - VELOCITY DISTRIBUTIONS FOR THE E374.

THEORETICAL BOUNDARY-LAYER SUMMARY TABLE											
AIRFOIL E374	*-LAMINAR SEPARATION BUBBLE WARNING O-NO SEPARATION BUBBLE WARNING ●-NO BUBBLE, TRANSITION BEFORE 0.05C --SEPARATION AT LEADING EDGE (STALL) +-ANGLE OF ATTACK WITHIN DRAG BUCKET										
ALPHA (deg)	REYNOLDS NUMBER										
			100000		200000		400000		600000		
	us	ls	us	ls	us	ls	us	ls	us	ls	
-3			*	-	*	*	*	●	*	●	
-2			*	*	*	●	*	●	*	●	
+-1			*	*	*	*	*	*	*	*	
+ 0			*	*	*	*	*	*	*	*	
+ 1			*	*	*	*	*	*	*	*	
+ 2			*	*	*	*	*	*	*	*	
+ 3			*	*	*	*	*	*	*	*	
+ 4			*	*	*	*	*	*	*	*	
+ 5			*	*	*	*	*	*	*	*	
+ 6			*	*	*	*	*	*	*	*	
+ 7			*	*	*	*	*	*	O	*	
8			●	*	●	*	●	*	●	*	

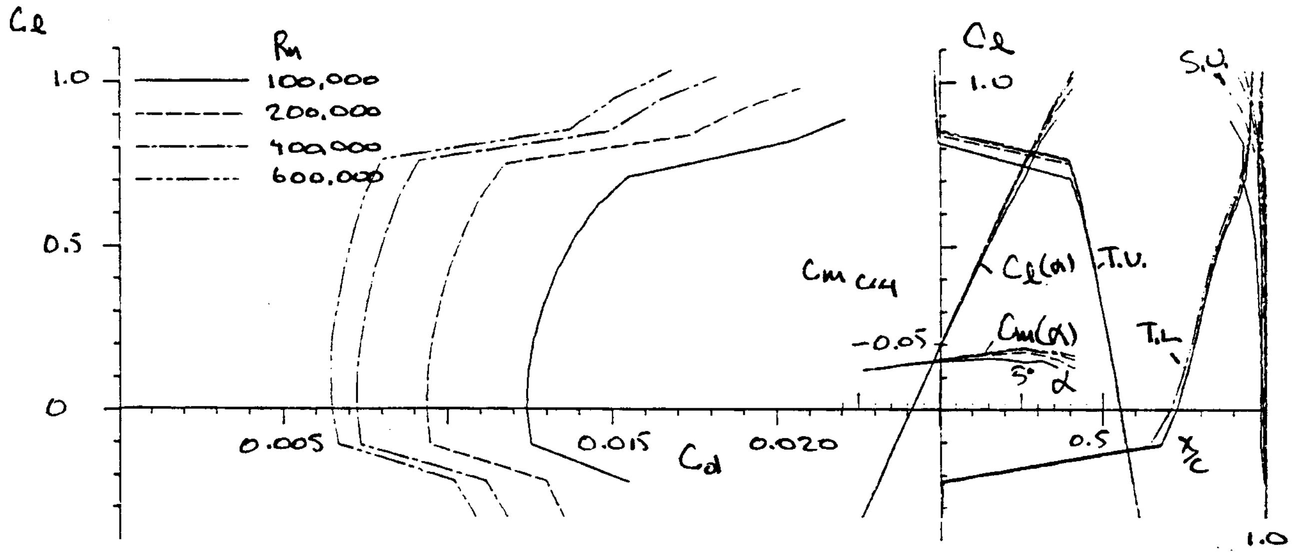

FIG. 61 - THEORETICAL SECTION CHARACTERISTICS FOR THE E374.

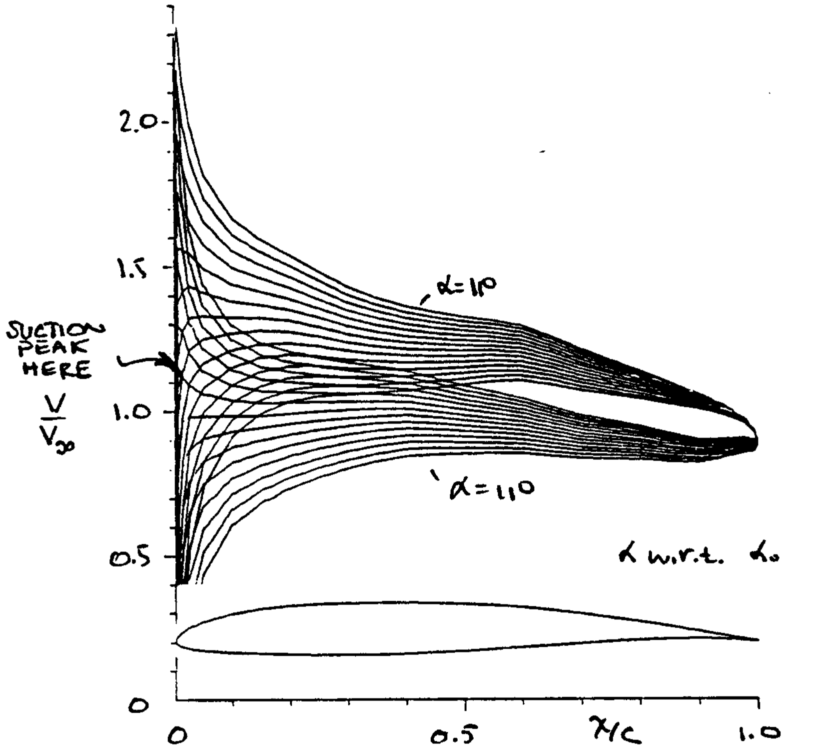

FIG. 62 - VELOCITY DISTRIBUTIONS FOR THE HQ 2.5/9.

THEORETICAL BOUNDARY-LAYER SUMMARY TABLE										
AIRFOIL HQ 2.5/9	*-LAMINAR SEPARATION BUBBLE WARNING O-NO SEPARATION BUBBLE WARNING ●-NO BUBBLE, TRANSITION BEFORE 0.05C --SEPARATION AT LEADING EDGE (STALL) +-ANGLE OF ATTACK WITHIN DRAG BUCKET									
ALPHA (deg)	REYNOLDS NUMBER									
	60000		100000		200000		400000		600000	
	us	ls	us	ls	us	ls	us	ls	us	ls
1	*	*	*	*	*	●	*	●	*	●
+ 2	*	*	*	*	*	*	*	*	*	*
+ 3	*	*	*	*	*	*	*	*	*	*
+ 4	*	*	*	*	*	*	*	*	*	*
+ 5	*	*	*	*	*	*	*	*	*	*
+ 6	*	*	*	*	*	*	*	*	*	*
+ 7	*	*	*	*	*	*	O	*	O	*
+ 8	*	*	*	*	*	*	O	*	O	*
+ 9	*	O	*	O	O	O	O	O	O	O
10	*	O	*	O	●	O	●	O	●	O
11	-	-	*	O	●	O	●	O	●	O

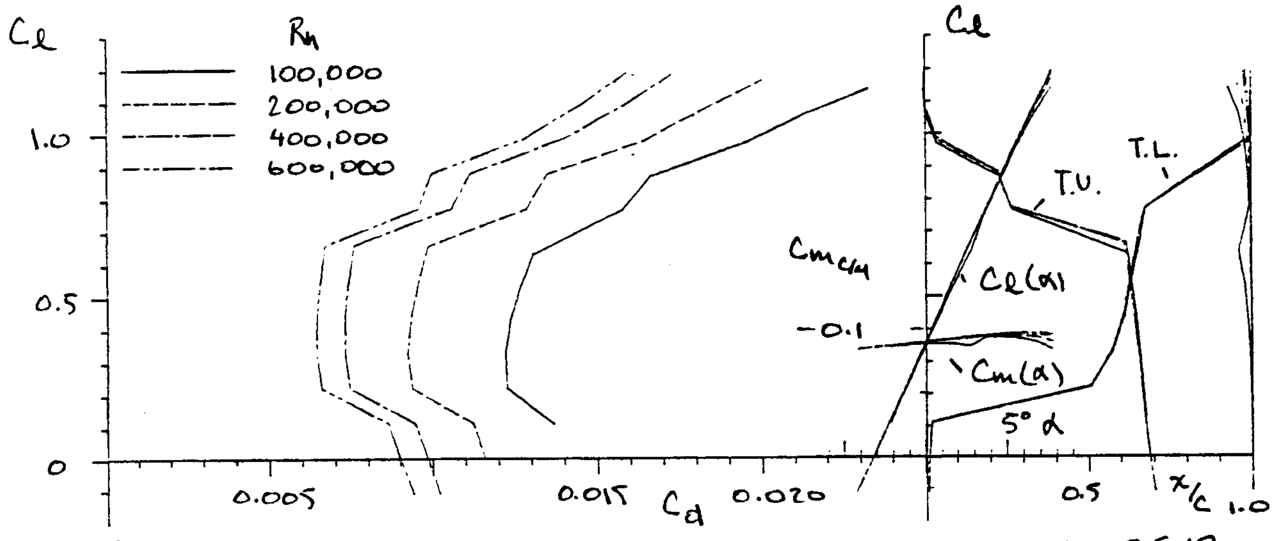

FIG. 63 - THEORETICAL SECTION CHARACTERISTICS FOR THE HQ 2.5/9.

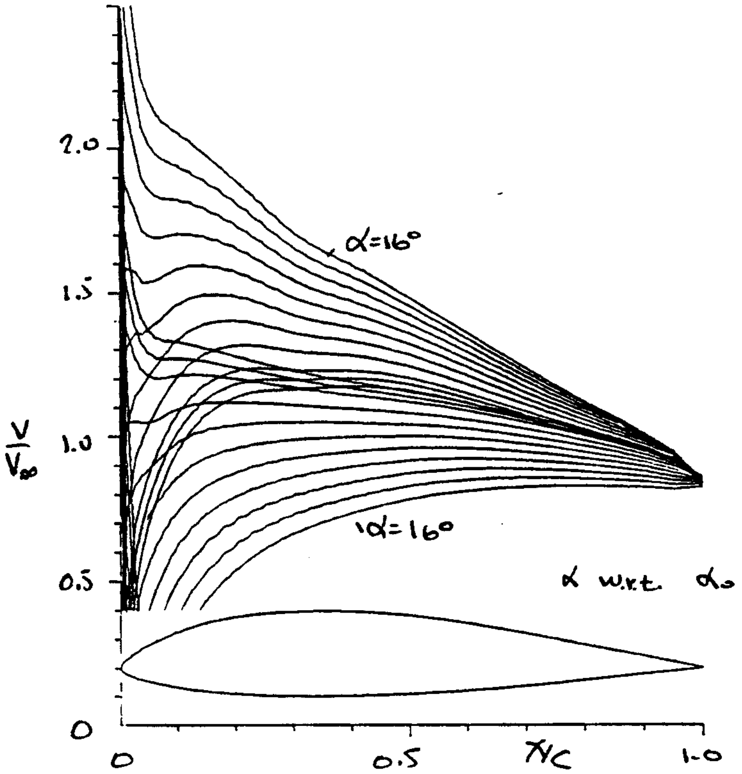

FIG. 64 - VELOCITY DISTRIBUTIONS FOR THE MB253515.

THEORETICAL BOUNDARY-LAYER SUMMARY TABLE										
AIRFOIL MB 253515	*-LAMINAR SEPARATION BUBBLE WARNING O-NO SEPARATION BUBBLE WARNING ●-NO BUBBLE, TRANSITION BEFORE 0.05C --SEPARATION AT LEADING EDGE (STALL) +-ANGLE OF ATTACK WITHIN DRAG BUCKET									
ALPHA (deg)	REYNOLDS NUMBER									
			100000		200000		400000		600000	
	us	ls	us	ls	us	ls	us	ls	us	ls
-2			-	-	*	*	*	●	*	●
-1			*	*	*	●	*	●	*	●
+ 0			*	*	*	*	*	*	*	*
+ 1			*	*	*	*	*	*	*	*
+ 2			*	*	*	*	*	*	*	*
+ 4			*	*	*	*	*	*	O	*
+ 5			*	*	*	*	*	*	*	*
+ 6			*	*	*	*	*	*	O	*
+ 7			*	*	*	*	O	*	O	*
+ 8			*	*	*	*	O	*	O	*
+ 9			*	*	*	*	O	*	O	*
10			●	*	●	*	●	*	●	*
11			●	*	●	*	●	*	●	*
12			*	*	●	*	●	*	●	*

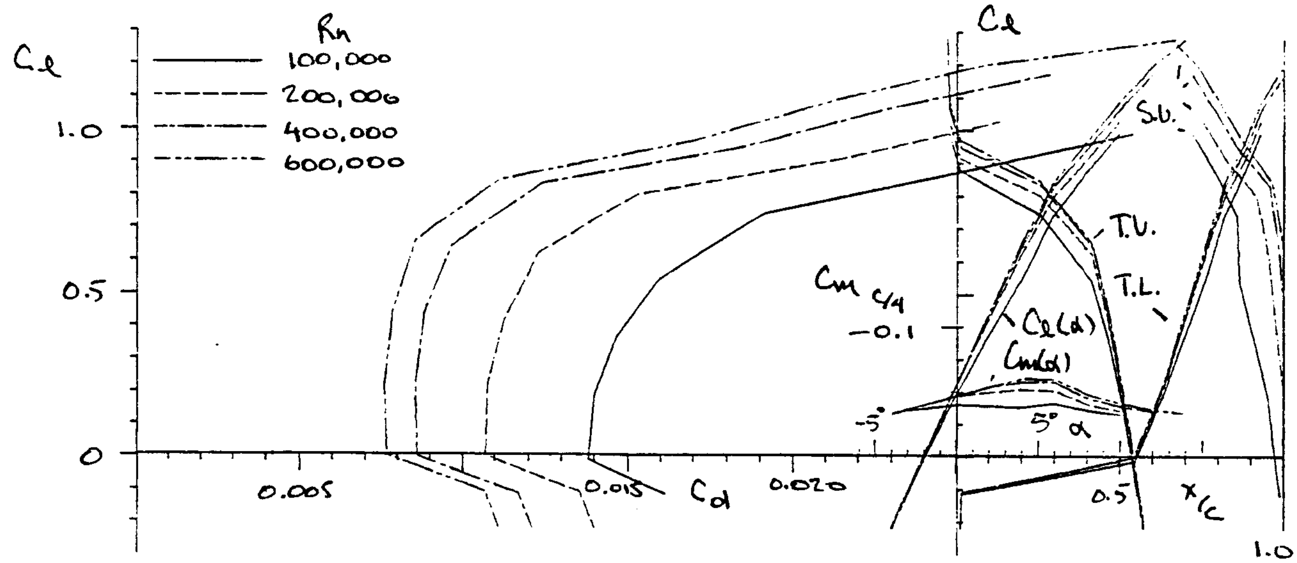

FIG. 65 - THEORETICAL SECTION CHARACTERISTICS FOR THE MB253515.

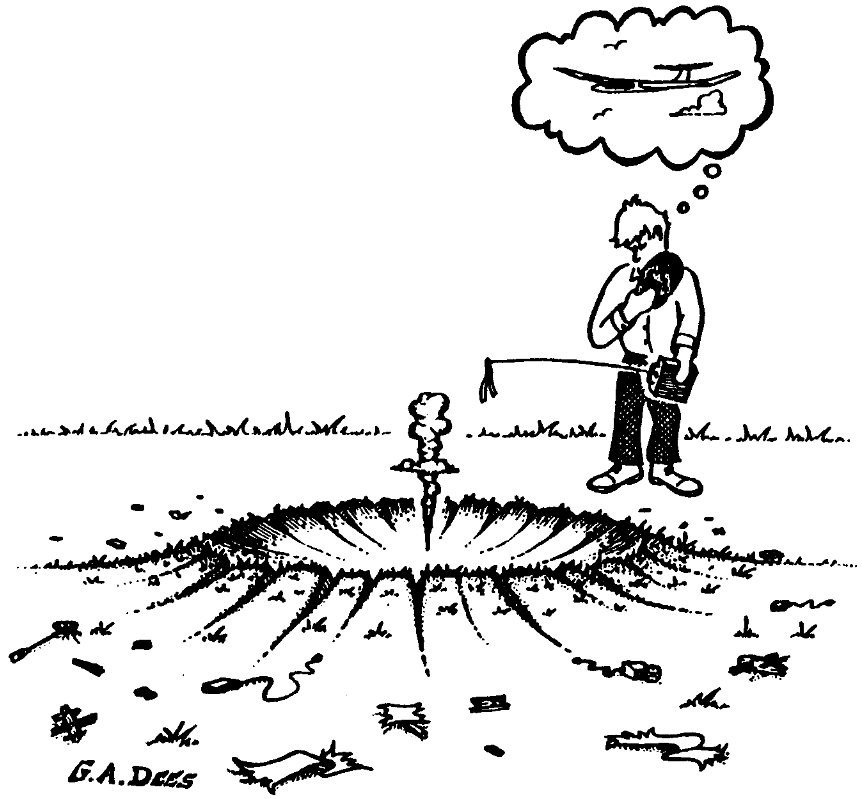
G.A.DEES

SOAR TECH

JANUARY 1985

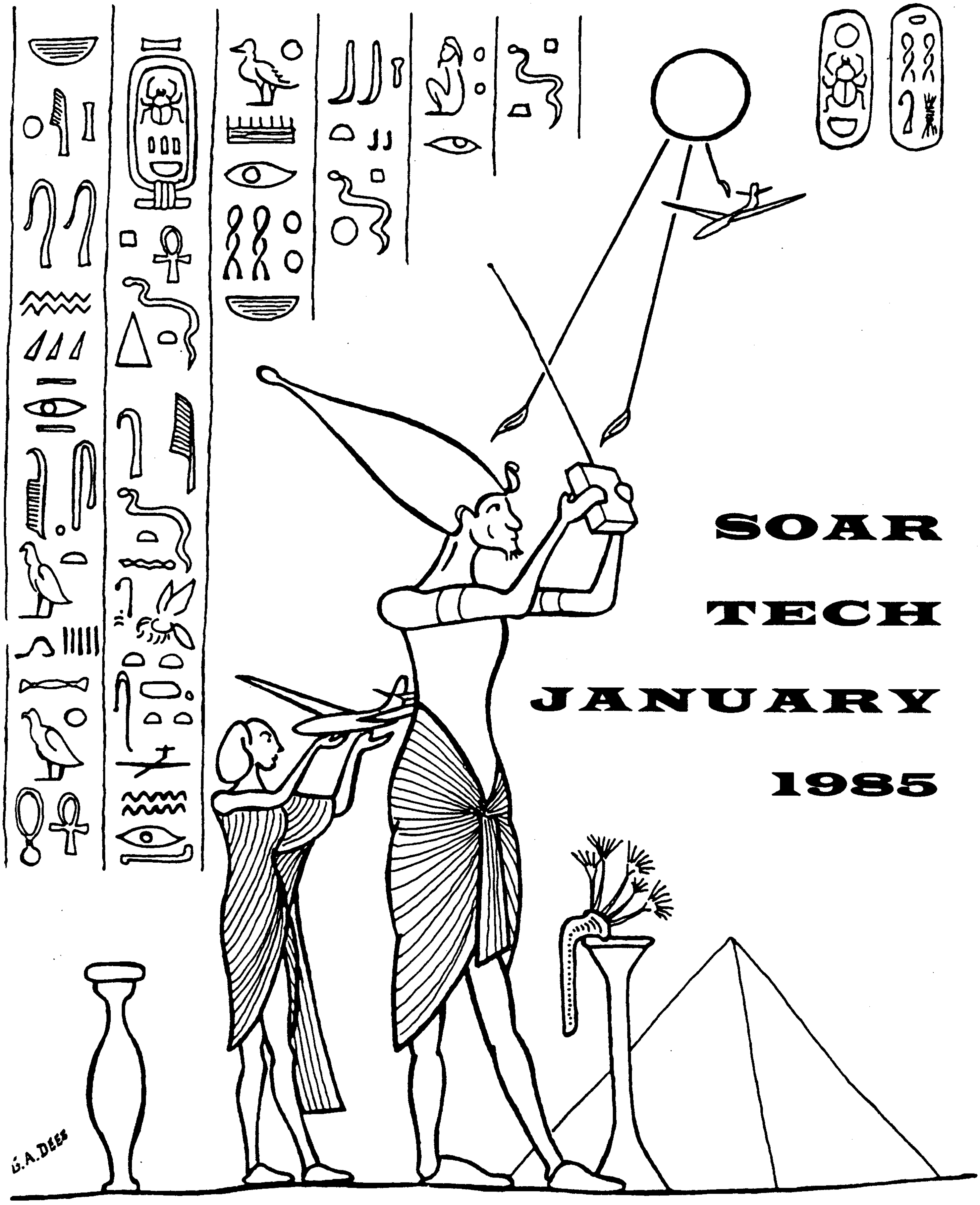

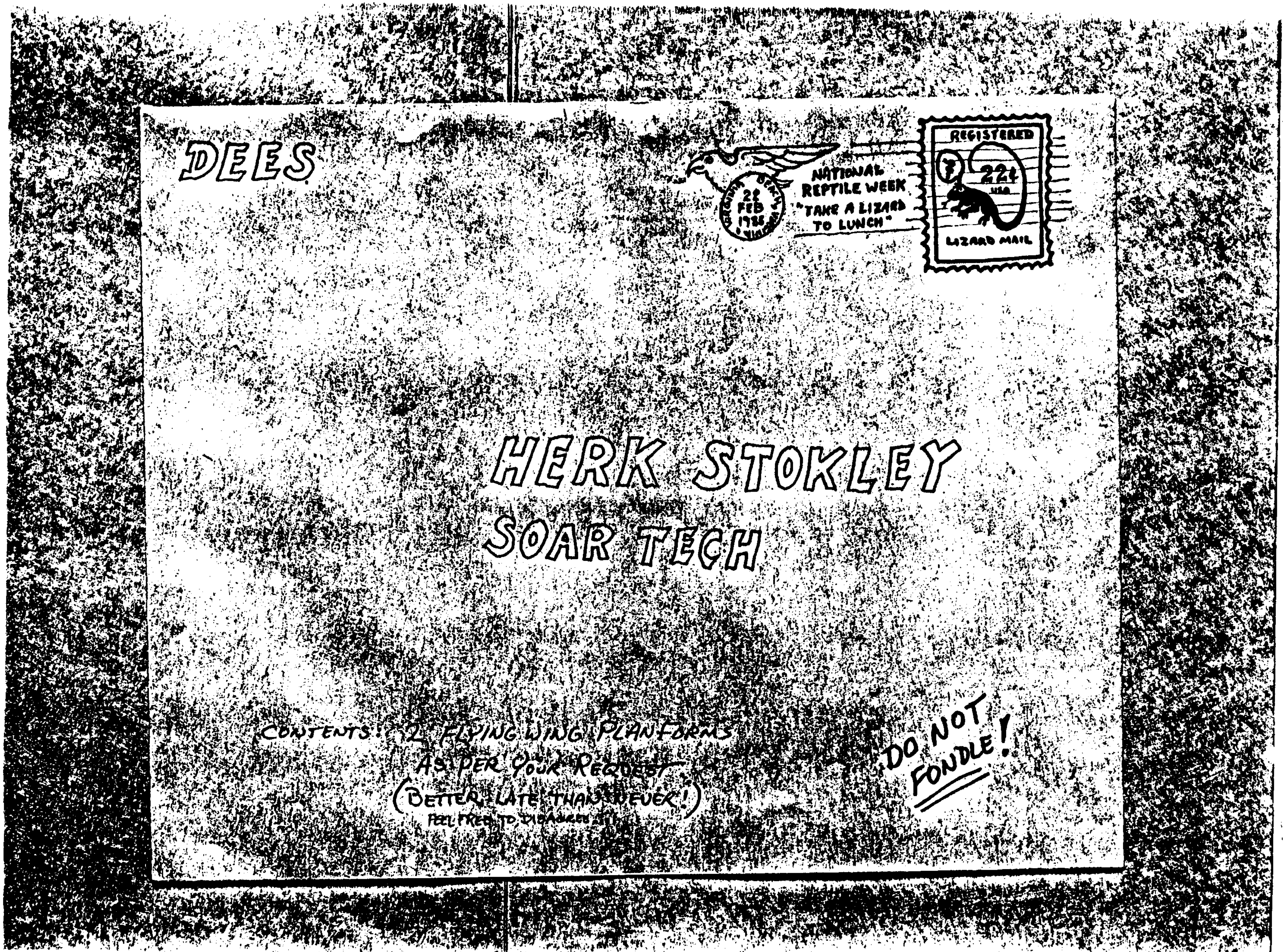
DEES
NATIONAL REPTILE WEEK
"TAKE A LIZARD TO LUNCH"
REGISTERED
22¢
LIZARD MAIL
HERK STOKLEY
SOAR TECH
CONTENTS: 2 FLYING WING PLANFORMS
AS PER YOUR REQUEST
(BETTER LATE THAN NEVER!)
DO NOT FONDLE!

January 1985

Thanks for your interest in SOARTECH. Soartech was an idea for an English language technical journal on the subject of Radio Controlled Soaring. It is similar to the ISF journals in Europe which are published in German. The material which we publish is generally too long or detailed technically to be suitable for publication in newsletters or in the model magazines. There is a very limited amount of this type of data, and it really interests only a small percentage of those who enjoy our sport. Because of this it is not suitable for a profit making project. Soartech then is provided to subscribers for the cost of producing it. Contributors are not paid for the material they offer, and the journal itself is not copywrited. In fact, copying and sharing or republishing of the material is encouraged.

I do not want the number of subscribers to Soartech to grow too large. Indeed if it gets too large it'll become necessary to have it published and distributed commercially. This makes the costs soar, and greatly increases the problems of the editor. For that reason I encourage you to interpret Soartech correctly; that is as a journal for the complex and technical aspects of RC soaring, and not as a popular "HOW TO" publication.

As to the Journals themselves, this is the fourth that I have produced to this date. Soartech I was dated Nov 82. Soartech II ran into printing delays. It was completed in December 83, but because of its size it was very difficult to complete the printing and distribution as a spare time operation, and it was not mailed out until 8 months later. If you subscribed to #1 you should have received #2 at no additional cost. Volume #3 is dated July 84. I went to a commercial printer for #3 which made it more expensive, but it was copied quickly. The cost of number 3 is the same as the earlier issues but it is smaller (about 90 pages where #1 and #2 were over 150) If you are one of those who had the long wait for #2, I apologize. I hope you found the result worth waiting for (it's 192 pages).

Many of you wrote for some or all of the journals. All are now available. #3 and #4 are still available in the original printing at $5 ($10 for foreign air mail). Because of the smaller numbers printed, the reproductions of #1 and #2 cost more to copy. Their price is $7.50 each for the USA, and foreign surface mail. Foreign airmail is $12. Checks or money orders should be in US dollars. Make them payable to H. A. Stokely.

Thanks again for your interest,

Herk Stokely editor

SOARTECH #4 CONTENTS AND AUTHORS

"Soartech" is a NO-PROFIT English Language journal which provides technical information on the subject of Radio controlled Soaring and Sailplanes. The papers included have been provided freely by their authors, and should be used freely by others. Copying and further use of this material is encouraged. Common courtesy indicate that where it is used in other publications, the author and the source be given credit. Contributions are requested, and the editor asks that you correspond with him on any of the material that is included.

H. A. (Herk) Stokely
1504 Horseshoe Circle
Virginia Beach, Va. 23451 USA

NOTE:

IF YOU WANT TO ORDER #5 (WHEN IT'S READY) SEND $5 FOR U.S. AND FOREIGN SURFACE MAIL OR $10 FOR FOREIGN AIR MAIL. MAKE CHECKS OR MONEY ORDERS TO H. A. STOKELY

PAPERS INCLUDED IN THE FOURTH ISSUE

COVER STORY

You may be able to tell that Gene Dees has joined me in producing SOARTECH. Gene is an excellent writer, illustrator, photographer, and cartoonist. You may not realize that he is also a well known and widely recognized amateur archaeologist of the same cut as Howard Carter etc.. The little known history of RC Soaring has been his specialty, and he is widely published in this obscure but fascinating little corner of the field. This issue he explores the Egyptian experience for us. His work is supplemented on the front and back covers with authentic reproductions of ancient Egyptian art work which he discovered during his historic 1981 expedition.

Receiving mail from Gene is not an ordinary experience. The inside covers are jackets from the envelopes in which he forwarded some of the material which he prepared for this issue.

Needless to say I am delighted to have Gene join me in this project. He is talented, humorous, unusual, wry, ironic, a tireless worker, and fun.

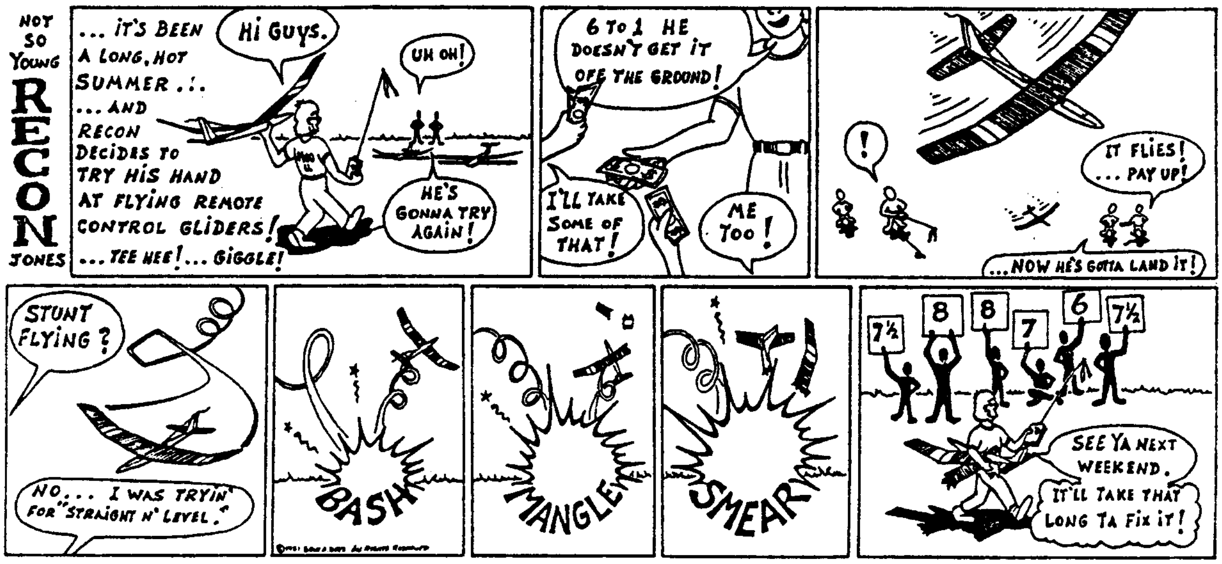

GENE DEES
2309 WALKE ST. APT B
VIRGINIA BEACH VA 2345:

A BRIEF HISTORY
OF THE
ANCIENT ART
OF
REMOTE CONTROL
SAILPLANES

As it turns out, thanks to some startling new evidence that has come to my attention, R/C sailplanes have been plying the skies of planet Earth for quite some time before the Wright Brothers and, in several cases, even before the birth of Christ ! The most shocking example of a recorded ancient R/C sailplane flight came from the discovery of a fresco on the wall of an obscure priest's tomb dating from the reign of Cheops II found recently in the low-rent district of the Valley of the Kings in Egypt. A drawing of this fresco appears on the cover of this issue of *Soar Tech.* as no photos have been allowed and a great deal of effort has been expended to keep this discovery quiet. It is only fitting that the discovery of man's first successful efforts in the direction of flight appear in an obscure journal such as this (no offense intended, Herk) since it is a fact that the first report of the Wright Brother's successful *POWERED* flight appeared in the *AMERICAN BEE JOURNAL*, a periodical devoted to the development of bee keeping* !

The pharaoh Cheops, it turns out, had a thing for flying. It seems that Egyptian pharaohs, being considered gods, were expected to hob-nob and otherwise rub elbows with Ra as he made his daily trip from east to west across the sky in his flaming chariot. This hob-nobbing and elbow-rubbing was made easier by the fact that Ra shed a hell of a lot of heat on those desert sands creating thermals that reached the pyramid-block sucking stage sometime just before noon, B.C.

Well, we ain't too sure exactly when some bright boy added up two-and-two and began hot-stuffing reeds together and covering them with papyrus dipped in embalming fluid, but it could have happened as early as 500 years before Cheops did his thing.

All this sounds just fine and dandy, but for the fact of *Just where did they get the radio equipment ?*

Now pardon me for being rude, but any idiot that has read Erich Von Daniken knows that the Ancient Astronauts passed out complementry samples just before checking out of the palace. They even left a "1-800" number just in case the pharaohs wanted to order more. This happened about 11:00 o'clock in the morning (regular check-out time),B.C.

The pharaohs had such a ball flying, hob-nobbing, and rubbing elbows with Ra, and, in general getting such a kick out their sailplanes, that they promptly declared it heresy for anyone else besides pharaohs and a few selected high priests to indulge (a note of interest: a few deaf and dumb eunuchs were allowed along--- after all, somebody had to shag chutes and fetch cold Coca-Colas because it's hot out there in the desert while Ra is making thermals.).

Everything was going just great for about a couple of hundred years when a pharaoh who shall remain nameless started having trouble with a dude named Moses. Moses, it seems, got mad because the pharaoh wouldn't let his people fly** and caused plagues and other bad stuff to happen to Egypt. Some of this "bad stuff" blocked out the sun and Ra couldn't make thermals anymore. Not only that, but the wind blew like the dickens all day long and some of the pharaohs' best birds got busted---one even got blown into the Nile only to be snarfed up by a crocodile !

Boy ! The pharaoh got really bent out of shape---you see, he wasn't himself with all this Moses business going on and everything---but, just then, a bright up-and-coming junior priest saved the day with an idea.

"Why not build a pyramid---a really BIG one--- and then you could slope soar no matter which way the wind blew and the lack of thermals wouldn't make any difference !" says the priest to the pharaoh.

"Great !" says the pharaoh to the priest.

So they built the Great Pyramid which stands to this day. Folks have got the wrong idea about what it was built for but then this story is a little hard to swallow too.

---and the only mummies found in that pyramid were of some long-gone cows* (we all know that they were the all-dried-out, left-overs from the "after-the-contest bar-b-que" that was held sometime after 4:30 in the afternoon, B.C.) !

There was a happy ending for Moses and his gang, though. The Pharaoh let his people fly and they all went over to the Siani so's there wouldn't be any frequency conflicts (you see, Moses had to "hob-nob" with someone up in the sky too !)

-G.A.Dees
Professor of Pseudo-History
Sally's Gas Station &
Charm School
Virginia Beach, VA US of A

*footnote: The remarks about the American Bee Journal & cow mummies being found in the Great pyramid are the only bits of truth to be found in this pack of lies !

**footnote: fly, flee, go---it's all in the way you want to translate it.

BATES ON WINGS

The following article from Ken Bates follows up earlier articles in SOARTECH numbers 1 & 2. Ken's development of this idea continues with new developments at each stage. One of the things I really like about this series is that Ken shares successes and failures equally. It is a real help to read about someone's efforts that didn't work out just the way he hoped. It's interesting, and it keeps others from having to explore the same paths all over again. The success of the Bates effort was demonstrated last year at the 1984 KRC Electric Fun Fly when Keith Shaw flew his remarkable Horten type wing with electric power. Keith and Ken had collaborated in working out the details of that very successful design.

P-4C A PROGRESS REPORT ON THE FLYING WING PROJECT

P-4C was constructed to test the upright-inverted airfoil concept which I proposed in SOARTECH 1. The root airfoil is the Eppler 205 upright, and the tip is the same airfoil inverted. The ribs were produced by "stack-sanding". Due to the taper, the symmetrical section is about 18 inches from the tip. Four degrees of geometric washout was built into the wing as it was built. I didn't remember that there was already a lot of aerodynamic washout because of the angles between the root and tip airfoil's zero lift angles. This gave a total of 8 to 10 degrees total washout (which was more than I wanted) - which may have caused some of the plane's later problems. The CG was placed at 19% of the mean aerodynamic chord.. The combined dihedral is 6 degrees. Spoilers were placed in the geometric center of area spanwise with two-thirds of the spoiler extending outboard and one-third inboard from that point.

P-4C exhibits some substantially different characteristics from the symmetrical airfoil wings. The model was built large (RISKY!) to more realistically explore the performance potential in using the cambered - non reflexed airfoil sections. The area was 1750 square inches with a loading of 8 ounces per square foot of planform. For a flying wing the effective loading is higher than this because the washed-out tips carry a down load.

The launch is slow and steep like a lightly loaded conventional ship, and requires only moderate line tension. On the first flights a high start was used. Coming off tow I found that, unlike the symmetrical ships, P-4C had bad adverse yaw. So bad in fact that I couldn't turn. I could steer a bit by holding full up and stalling which sometimes caused a spin. The spin would stop when I released the "up" and crude steering could be done this way. I missed the trees but not the curb! (Ken didn't mention diving to get aileron control. Adverse yaw is usually a high angle of attack problem. This plane is different though and it might not have helped -- Herk)

After repairs and adding 6 by 1 inch tip drag spoilers (coupled like coupled rudder-aileron on a conventional plane) handling was much more normal. The spoilers worked well and only caused a slight dragging of the nose into the turn. They greatly reduced the glide performance though. Landings on the "pod" underneath were arrow-straight with no problems, and control was positive at all times.

In soaring flight a little "turn-in" aileron had to be held. Using the drag rudders alone however, caused a steepening turn and they had to be closed periodically, or opposite aileron used. The crossed controls or use of up elevator in turns produced spins. This limited the circle size and circling speed I could use because, with little warning, an increasingly tight and slowing turn would degrade into a spin in the direction of the turn. The spin would break into a spiral when some of the "up" elevator was eased out and seldom exceeded one and one-half turns. The spin would start before I could slow the plane to what I felt was its optimum minimum sink speed in a turn.

During the first winch launch the winch switch stuck ON. After more repairs, testing resumed. Low power winch launches were OK, but high power launches tended to produce a directional "wander". This wander could have been an incipient spin. Moving the CG forward and using more "up elevator" during tow caused a genuine spin and another repair episode. Moving the tow-hooks forward didn't help - another repair. Going back to the original setup and lighter tow forces worked OK until a turn at the top of a launch resulted in a bad line angle for the towhooks mounted on the sides of the pod - jamming them. Wings seldom have enough control authority on tow to overcome the pull from the line, and this was not an exception. My attempt to unhook produced a spin resulting in a total crash - as the line, still attached, prevented recovery.

The performance of P-4C was most encouraging. It appeared to have competitive tow, L/D, and sink performance with conventional aircraft. The only "fly in the ointment" was the spin, landing, and my towhook location (also the fact that they weren't releasable. Towhooks are safest on the bottom of the wing; and releasable.

I suspected that the dihedral was involved with the spins but I want to keep it as it produced nice stable turns that, left alone, would gradually open rather than tighten. Experiments with small models and a conversation with someone named Herk provided some answers. The "OOPS" about forgetting zero lift angles meant I had much more washout than intended. This probably resulted in flow separation on the lower side of the tips - especially when "up elevator" was given. The worst case of this would be when turning - as both up and in elevon would be given at the same time. The resultant flow separation and drag on the inner wing produced the spin. The dihedral augments this by lifting the outboard wing. Unlike a conventional ship a tip stall does not drop the inner tip, but the drag increase does cause a sudden yaw. This yaw would have less effect on a flat wing than on a dihedraled wing. Small model tests, the book "NURFLUGEL", and various writings on the Horten's projects all point the same way. To reduce yaw instability, and yaw-roll coupling: minimize dihedral and washout and maximize sweep.

The next iteration is finding the optimum compromises as sweep must be reasonable, some dihedral is desirable, and aerodynamic washout is necessary. Maybe I can keep my dihedral if I use less washout, more taper to get more of the elevon in the negative lift area without getting too much negative lift area (to reduce adverse yaw). Maybe no drag rudders. Less washout to prevent flow separation under the tips. I might have to use a more stable airfoil section. I already know that a fully-stable reflexed section has bad reactions with spanwise flow ---- so it goes ___

No ballasted high speed runs were done, but unballasted dives showed none of the stability problems or excessive control forces that are sometimes present when reflexed airfoils are used on swept wings. The wing was not fully sheeted and had some flex, so these problems should have shown up if the upright/inverted system was prone to them.

Also of interest is the "SOMBRA DEL AQUILA" with moderate forward sweep, inverted section at the root (elevator area) and Eppler 178 airfoil outboard transitioned over two bays between the outboard end of the elevator and the rest of the wing. This design worked well although the controls were somewhat less effective than I'd have liked. The ailerons had differential, but they worked as pure roll control with no pitch coupling. Likewise rudder gave pure yaw with no roll coupling. The design is too stable in pitch which caused the elevator to be somewhat ineffective. This plane has good performance in some conditions. Its dead air time was 4 minutes from launch compared with 5 minutes for "pieceles" my 1983 Great Race winner. This plane is fatiguing to thermal because of the soft elevator control, and because cross coupling of the controls is required due to the forward sweep. It was also a bit overweight after all reasonable modifications had been tried. This weight (11.5#) is over the FAI limit so it can't be used for cross country racing. I sold it to a friend who was not interested in cross country racing.

KEN BATES, 738 N. HARRIS, SALINE, MICHIGAN 48176

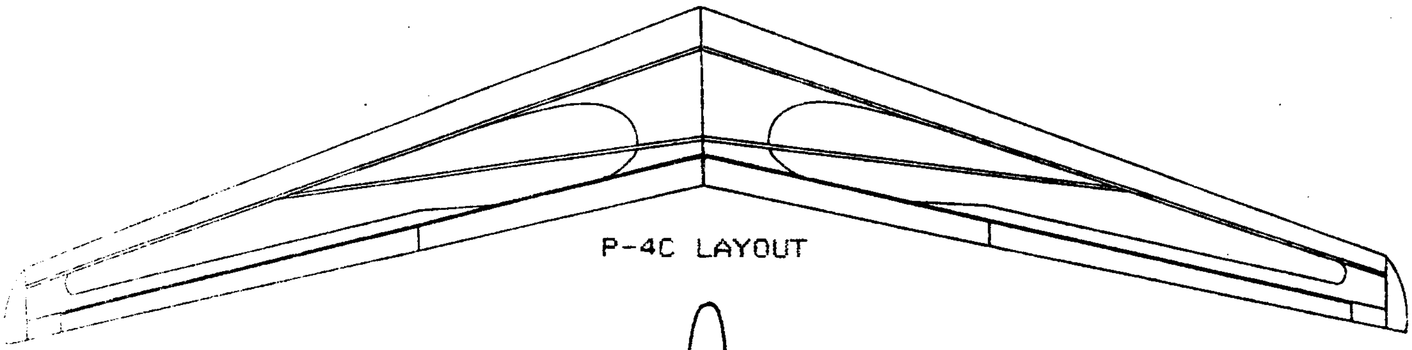

P-4C LAYOUT

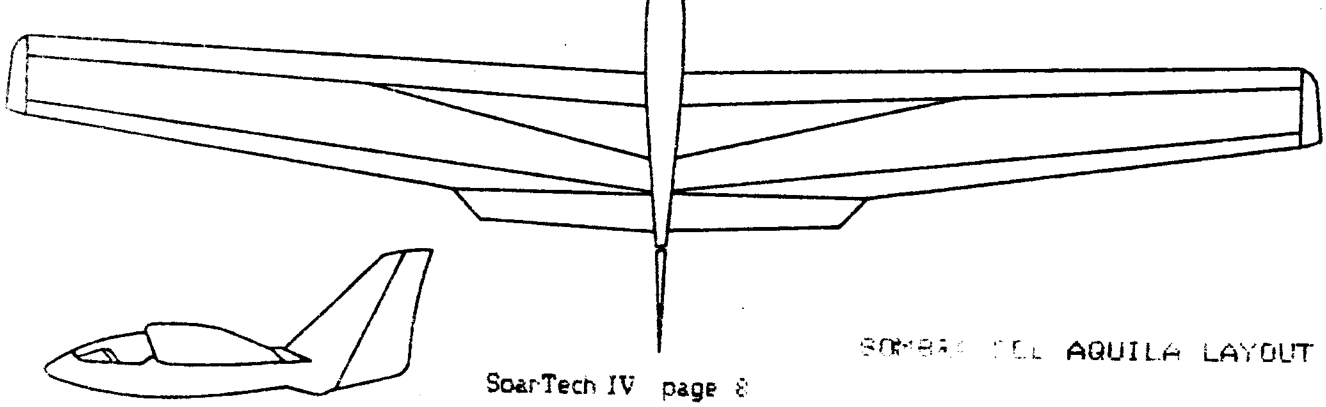

SOMBRA DEL AQUILA LAYOUT

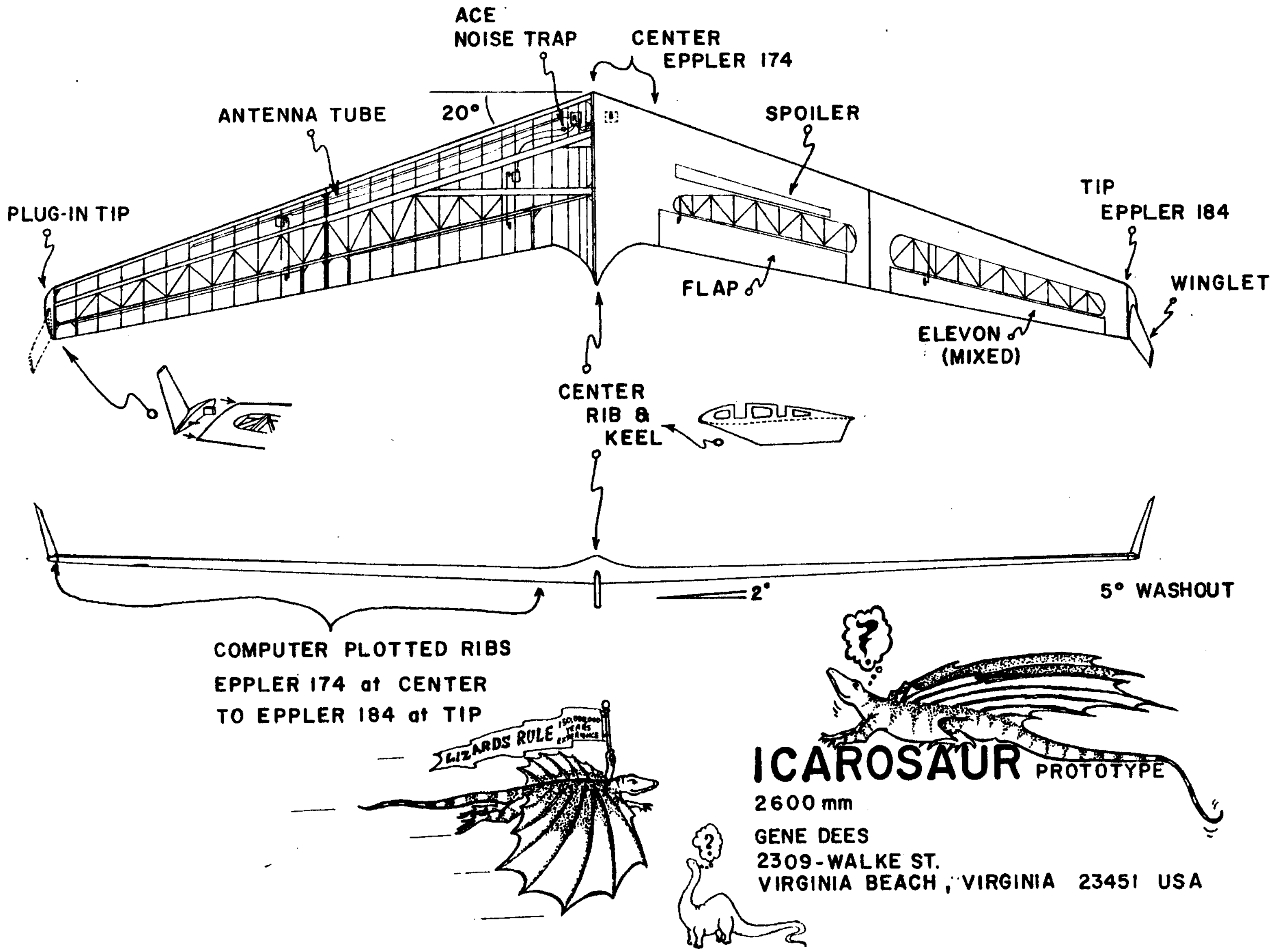
ACE
NOISE TRAP
CENTER
EPPLER 174
ANTENNA TUBE
20°
SPOILER
PLUG-IN TIP
TIP
EPPLER 184
WINGLET
FLAP
ELEVON
(MIXED)
CENTER
RIB &
KEEL
2°
5° WASHOUT
COMPUTER PLOTTED RIBS
EPPLER 174 at CENTER
TO EPPLER 184 at TIP
LIZARDS RULE
ICAROSAUR PROTOTYPE
2600 mm
GENE DEES
2309-WALKE ST.
VIRGINIA BEACH, VIRGINIA 23451 USA

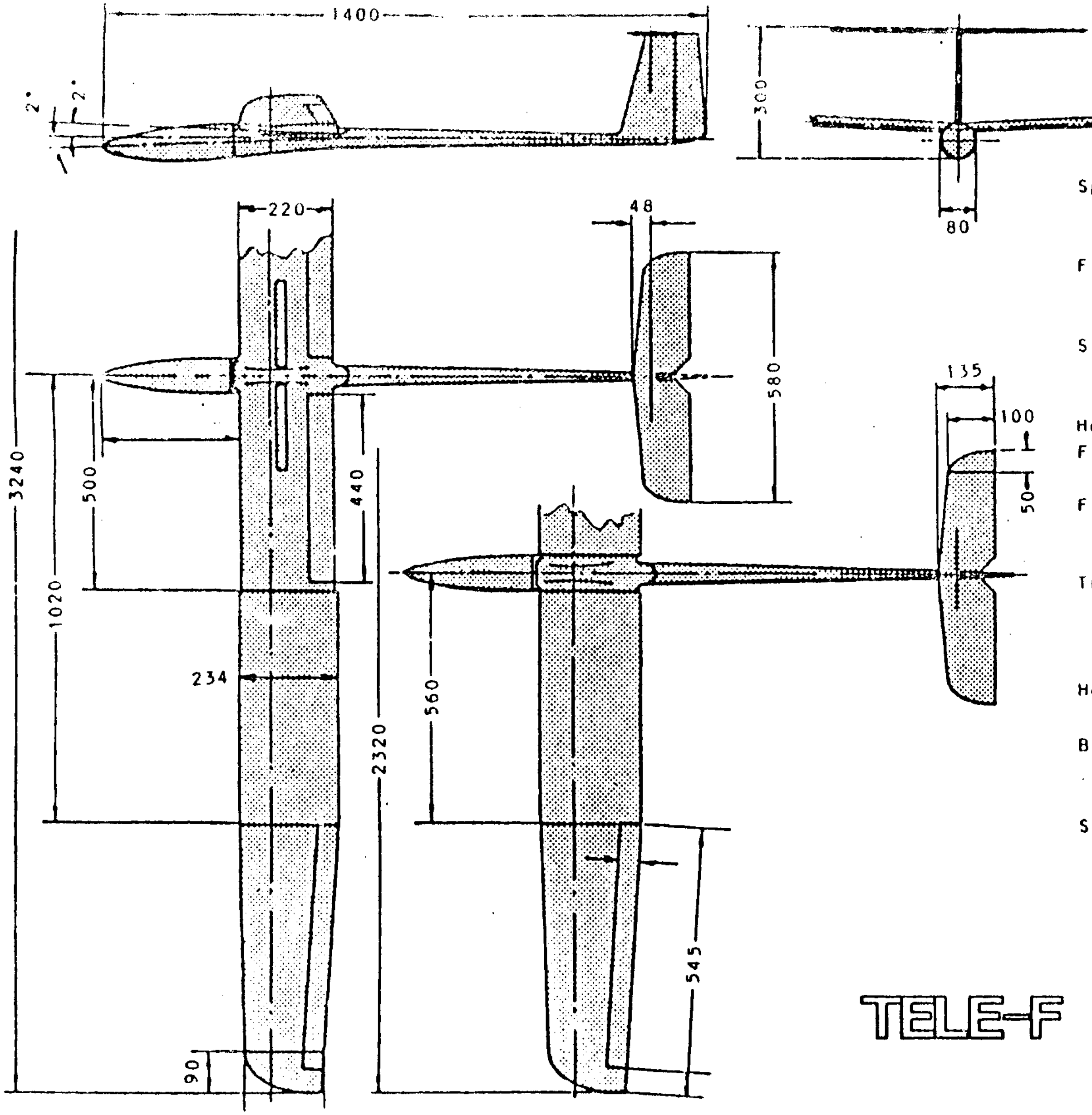

Spannweite:	max 3240 mm min 2320 mm
Flügelfläche:	max 70,48 dm^2 min 51,50 dm^2
Steckung:	max 14,89 min 10,45
Höhenleitwerksfläche:	6,6 dm^2
Fluggewicht:	2500 g
Flächenbelastung:	max 48,54 g/dm^2 min 35,47 g/dm^2
Tragflügelprofil:	Wurzel RG15/9,23% Mitte RG15/9,4% Außen RG15/9,44%
Höhenleitweksprofil:	NACA 63A006
Bauweise:	GFK, CFK, Balsa, Rohacell
Steuerung:	Höhenruder Seitenruder Querruder Wölbklappe Störklappe Teleskopantrieb

TELE-F F3B Modell 1984/85

von Dieter Pfefferkorn und Ralf Decker

FROSTY WINGS

The following paper is from one of the ISF seminar proceedings in which the Austrian F. Fritz reported some fascinating (but controversial) observations that were made during early morning performance testing of the now famous "DASSEL".

Because it is difficult to interpret this kind of observation, I asked Michael Selig to see if he could comment on the observations, if possible; put forward a hypothesis as to what they mean. Michael has given a lot of educated thought and study to the events taking place in the airflow around model wings, so his interpretation is educational in itself. I'm not going to say that I completely agree with all he says, but I'm going to keep my reservations to myself. You'll have to argue with Michael for yourself if your ideas are different.

This paper was graciously and expertly translated from German by J. Muller MD, of Indianapolis Indiana.

Incidentally, the term "Abb." on the illustrations from the ISF paper means "Figure". Thus Abb 1 means Figure 1.

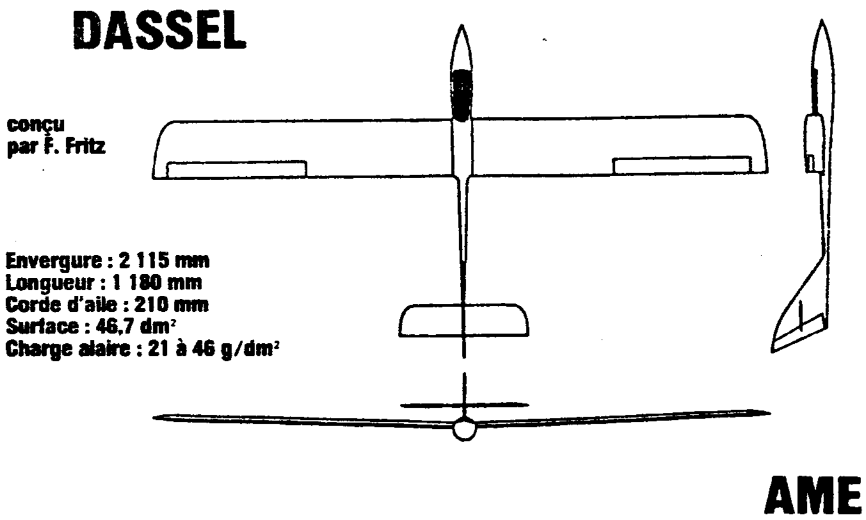

OBSERVATIONS ON FREE AIR-AIRFLOW OF THE EPPLER 193 PROFILE IN THE MIDDLE OF ITS C_L RANGE.

I. INTRODUCTION

The Innsbruck Workgroup for the Development of Model Soaring (AME) has conducted in the years from 1977 through 1979 a large series of measured flights in the open air (1). At the same time, as a byproduct, there were most interesting observations on the airflow on the upper surface of the wing of the experimental model, Dassel D 751. Unfortunately the collected results of these observations are not scientifically usable because the observations in general are incomplete and only portions of them were documented. The reason is that usually all the observations could only be made when they provided a disturbance in the course of the original measured flights: either in the morning between 4:00 and 5:00 A.M. when a series of measured flights had been started and its strict temporal sequence could not be interrupted by lengthly manipulations (documentation) or towards the end of the measured flights when everyone was happy to be able to make it home before night after putting away the extensive measuring apparatus.

II. OBSERVATIONS

On the upper surface of the E 193 wing there were almost over the entire span streak-like areas of dew (or, in quite cold weather, frost) deposits. These streaks or bands were at their front edge always quite sharply demarcated in a straight line parallel to the leading edge of the rectangular wing. The back margin of this condensation band was not so sharply demarcated as the forward edge but, with only slight variation was essentially also in a straight line, also parallel to the leading edge. The front band limit was from chord dimension $X_1/C=0$ to $X_1/C=0$ (Translator: in original, the same value is given twice.)

The rear limit was between $X_3/C=0$ and $X_3/C=0$ (see note above) (Figure 1).

The dew or frost strips did not really show any surface features, apart from the fact that about in the middle portions of these bands there was a zone, parallel to the wing span and quite narrow (about 1½ mm) in the middle of which there was a much reduced, with on both sides a much increased deposit of dew or frost. This quite narrow zone swings back and forth somewhat irregularly, overall again parallel to the leading edge; particularly in the case of the deposit of frost a "frost groove" (Figure 2) was formed, with particularly prominent elevated walls on both sides of the zone of thin deposit. Impressive was the amount of frost deposited; with the fingernail the frost could be swept together like snow.

The dew or frost deposits did not develop after a one mm thick whool string was glued along the immediate vicinity of the leading edge. Zones of "spurious" development also could be seen where, in the inner portions of the wing, ribs were in contact with the wing covering. As a generality it should be remarked that this whole phenomenon could be shown so beautifully, because the entire wing construction (spar-less foam core; only one rib in the inner portion of the wing) provides ideal conditions for a uniform distribution of temperature on the upper wing surface sheeting and therefore an extensive true picture.

III. DEVELOPMENT OF THE DEPOSIT OF DEW OR FROST

All observations were made during twilight before sun-up or after sun-down. Obviously it is of importance that at this time of day there often are only small differences between dew point and air temperature in the layers of air close to the ground. In flowing around the wing the almost water-saturated air is cooled in the low pressure zone on the upper surface of the wing below the dew point which results in immediate condensation of water vapor. It seems that the mentioned narrow strip in the middle of the condensation field, the groove, marks the transition from a laminar into a turbulent boundary zone flow.

IV. THE SIGNIFICANCE AND THE OBJECTIVE OF THE OBSERVATIONS

The observations of these phenomona can be instructive. He who for instance would like to know more about the quality of the construction of his wing (contour fidelity; surface (micro) waviness) can from such observations develop important information on the aerodynamic quality of his wing. Thus, particularly he who is interested in the quality of the construction of the leading edge of his wing can derive many conclusions.

Much more interesting however is the possibility to compare the transition of the laminar to the turbulent boundary zone flow with the calculated characteristics of the wing section. (The "transition" which depends on the Re number and the angle of incidence, Figure 3).

Finally, the dew or frost deposit also marks the dead water zone of the unloved so-called separation bubble, a phenomenon that particularly at low Re numbers and high lift values results in high additional section drag and can result in cases in enormous losses in performance. It is probably not possible to visualize the problems of slow flow any cheaper.

IV. DOCUMENTATION

In almost all the flights in question the pilot will try to use the rudder as little as possible so that the phenomenon is the result of one particular attitude and type of flight. Immediately after landing the condensation strip is documented with a felt tip pen directly on the wing. This has to be done quite quickly, since the condensation usually (particularly in the marginal zones) starts to evaporate rather rapidly. At home one can then transfer the outlines established at the flying field to transparent paper.

Unfortunately systematic documentation by photography was not successful, in part due to poor light circumstances during twilight, in part because the necessary photographic apparatus due to oversight was left at home. Therefore there are as of today only a quite small series of useful photographs but there are a considerable series of graphic protocols.

In part the test flights were done with greater details (metereology, height on leaving the high start, duration of flight, speed of flight, rudder deflections) laid down in protocols, rather than just the contour protocols, unfortunately never all the data together. This circumstance makes the observations, from a scientific standpoint useless.

However the demonstrated observations relevant to the Eppler 193 ongoing research can be of interest because it is not being done in a wind tunnel but in free flight. It is to be emphasized that the actual wing used in terms of its section corresponds 100% with the one used in the wind tunnel of the ETH-Innsbruck and also corresponds 100% with the one used in the laminar flow wind tunnel of the TU-Stuttgart.

Due to shortage of time, I was unable to prepare the protocols that were available for publication but perhaps this will occur at some future date.

SOURCES:

1. F. Fritz: Unpublished protocols of the Research into Distance and Speed Flights.

2. D. Althaus: Profil polaren fuer den Modellflug.Neckar-Verlag, Villingen.

Abb.1,2u.3

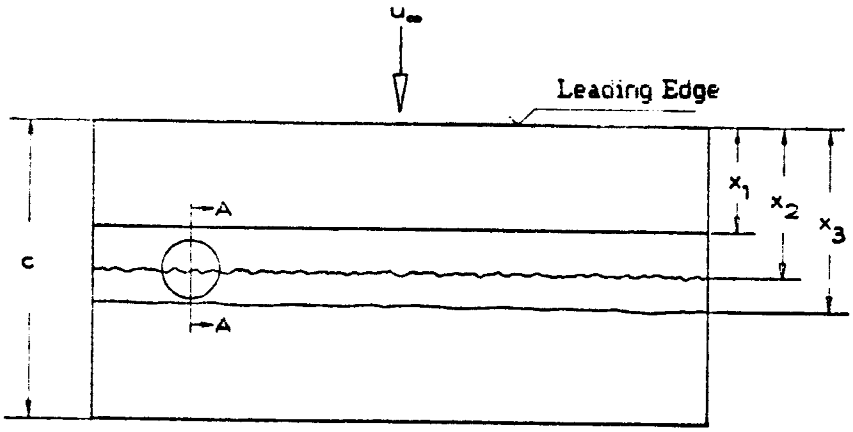

◁ Abb. 1

SECTION A-A (enlarged; not to scale)

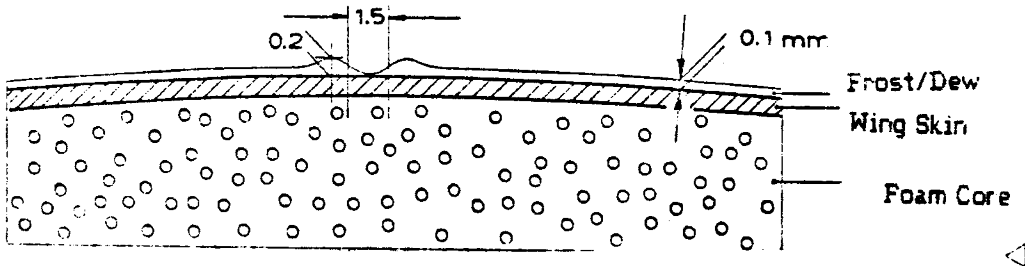

◁ Abb 2

estimated measurements in mm.

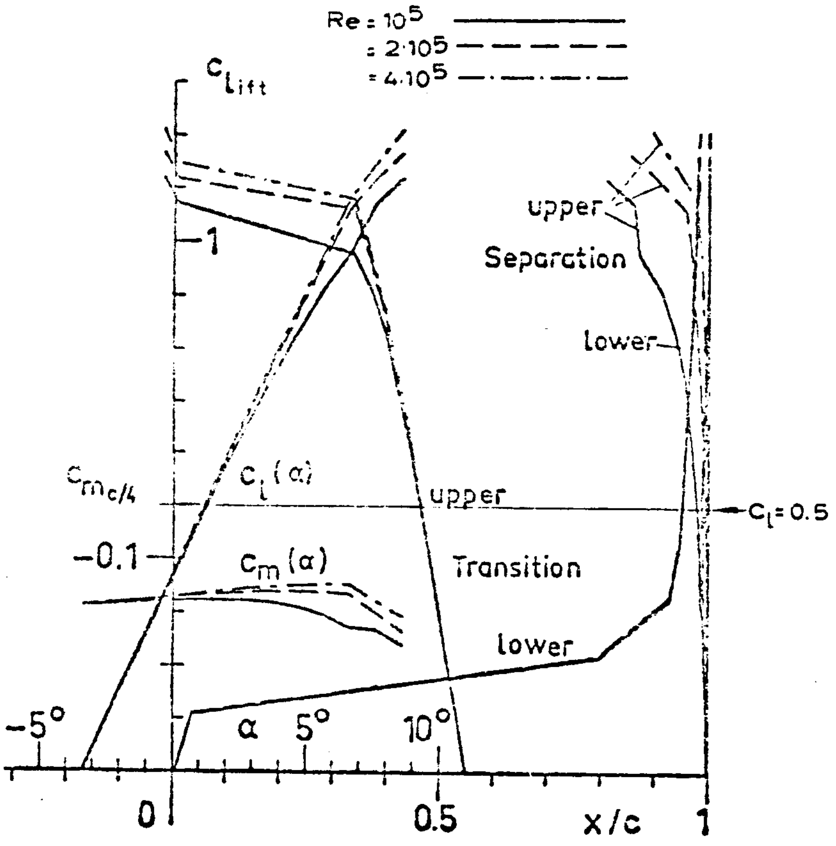

Relative Wing Chord X/C

◁ Abb. 3

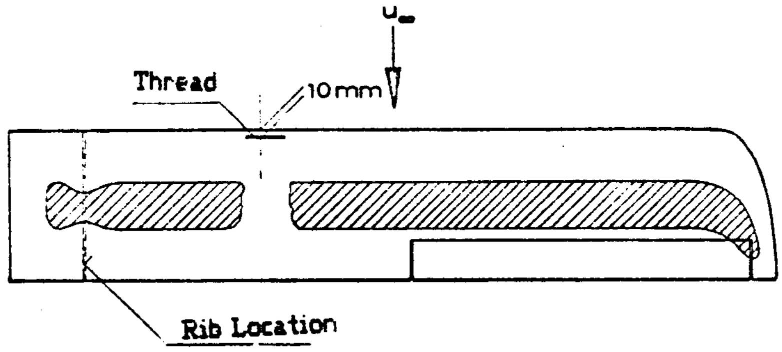

△ Abb.4.1 DASSEL D751 Wing Planform With Condensation (////)

▽ Abb. 4.2 Wing Section With Condensation

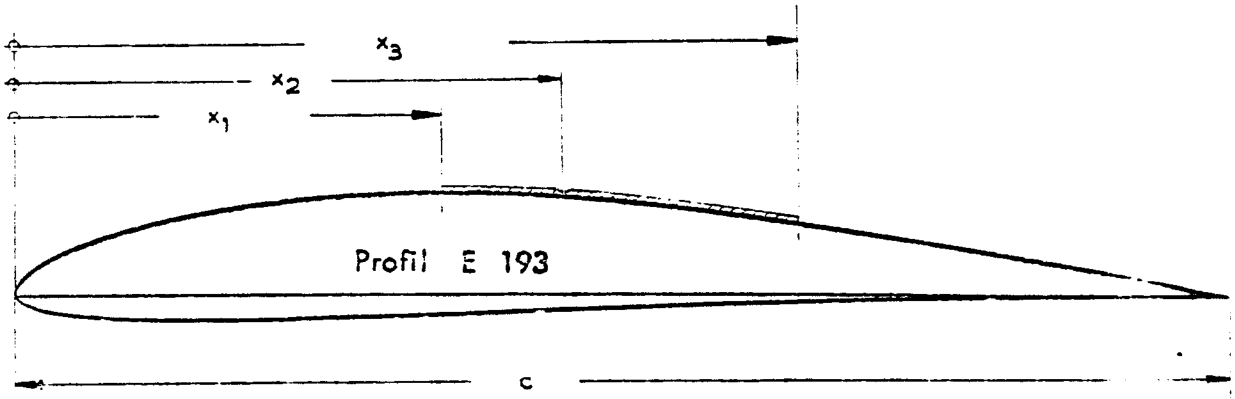

Observations from March 12, 1978

Starting time.......1836 LMT
Model weight........1.128 kg.
CG position.........34.4%C
Launch height.......140 M(agl)
Flight duration.....316 sec.
Air TEmperature.....+6 deg C
Surface wind........0.5 - 1.0 m/s
Dimensions...x1=71mm(36%C), x2=86mm(43%C), x3=130mm(65%C)

COMMENTS: by Michael Selig

Dept. of Mechanical and Aero Engineering
Princeton University
Princeton, NJ 08544

For the Eppler 193 airfoil, Mr. Fritz has located point x1 at about the point where the adverse pressure gradient of the recovery begins (see Abb 4.2). On page 4 he states that this seems to be the point of transition from laminar to turbulent flow. I think it is more likely that this is the point of laminar separation, or the leading edge of the laminar separation bubble, because it is so clearly defined. The beginning of the adverse pressure gradient or the "recovery area" (the point where the air begins to slow after speeding up over the forward part of the airfoil) is very clearly defined on most Eppler airfoils. When testing airfoils in the wind tunnel at Reynolds Numbers around 100,000 to 400,000 some investigators put a dark colored oil film on the surface to locate the transition point. In these tests, transition takes place over definite distance, not suddenly. The point of transition is seen as a band of oil that looks different from the oil in the laminar region, and from that in the completely turbulent boundary layer. If transition on the "Dassel" wing did take place on the surface there should be some appearance of a band of a different sort of texture in the frost. You would also this band to be longer at low Re than it is at higher. That's why I conclude that the sharp beginning of the frost band at x1 is the "laminar separation point".

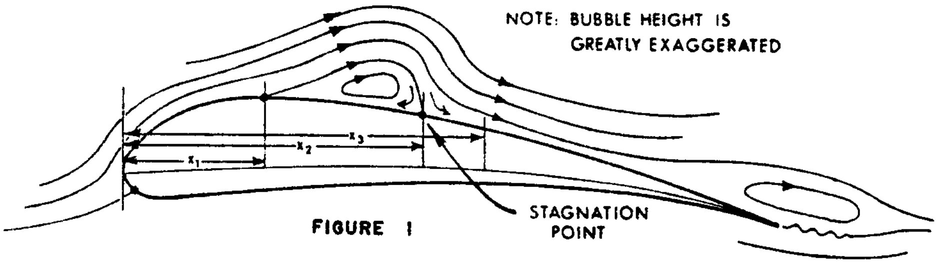

FIGURE 1

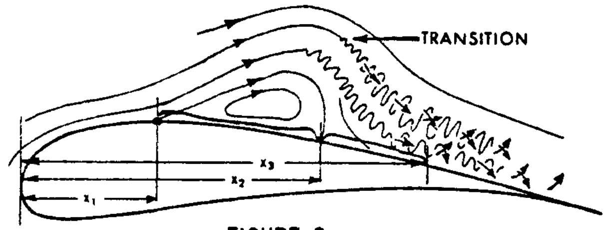

FIGURE 2

Figure 1 is a drawing of the laminar separation bubble's mean streamlines. That is, it doesn't include the unsteadiness in the flow that's always present. In Figure 2 I try to picture it more realistically. Notice that the streamlines at the reattachment point (aft end of the bubble) are almost perpendicular to the wing surface.

This summer at NASA Langley, I got my hands on a NASA document dated July 84 that discusses a method of calculating the flow of a transitional separation bubble. A copy of a Figure 7 from that document is included. Notice how the streamlines approach the surface at the reattachment point (almost perpendicular). This is the continental divide of the bubble. The flow aft of this point goes aft, and ahead of it; forward. I think this point is x2.

The frost or dew continues to collect after reattachment until the boundary layer becomes fully turbulent a bit before x3. When the turbulent boundary layer is fully developed, no frost collects. Why not? The first question is "why does the frost collect to begin with?". Mr. Fritz conjectured that the water saturated air is cooled on the suction side of the airfoil due to the low pressure zone, and as a consequence of this - frost forms. But wait! didn't he say that the wool string turbulator stopped the collection? Actually the low pressure zone is well forward of the frost area, and would still occur even with the turbulator, and if it caused the frost, it would still form. My conclusion is that in the boundary layer, the shear forces are enough to scrub away any frost that forms, however; in the bubble area the flow velocity is small, the shear stresses are low, and thus nothing scrubs away the condensation. Flow visualization oil collects in a laminar separation bubble during wind tunnel tests because there is very little boundary flow pushing on the oil - it just sits there in the bubble. At the time of the tests there was probably frost on the cars and other exposed surfaces like the wing. The phenomenon described by Mr. Fritz may be more frost removal than formation. Or at least its formation was prevented in areas where the boundary layer forces were high enough to remove it as it formed.

This summer at Langley one of the researchers described an experiment he was conducting. In order to see areas of high shear stress he sprayed the model with a subliming chemical. After some hours of running the wind tunnel, the model could then be examined. Areas of high shear stress (good flow attachment) were scrubbed clean, but areas of low stress (poor flow attachment) were still coated. I think the frost is behaving the same way.

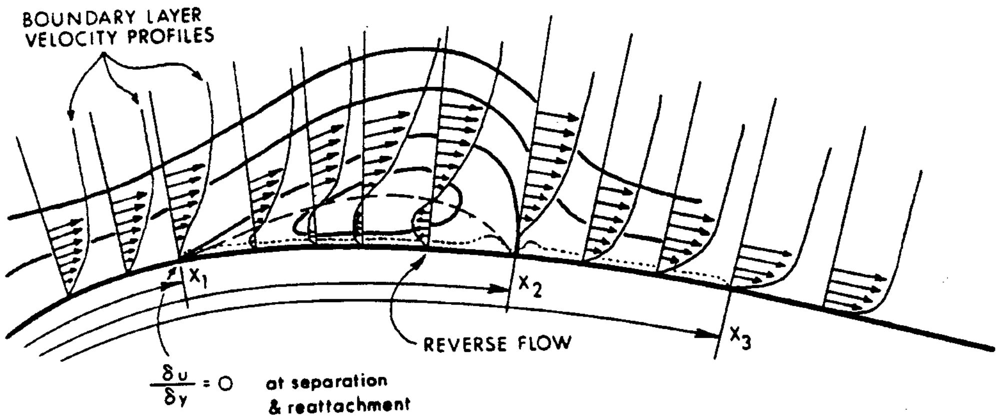

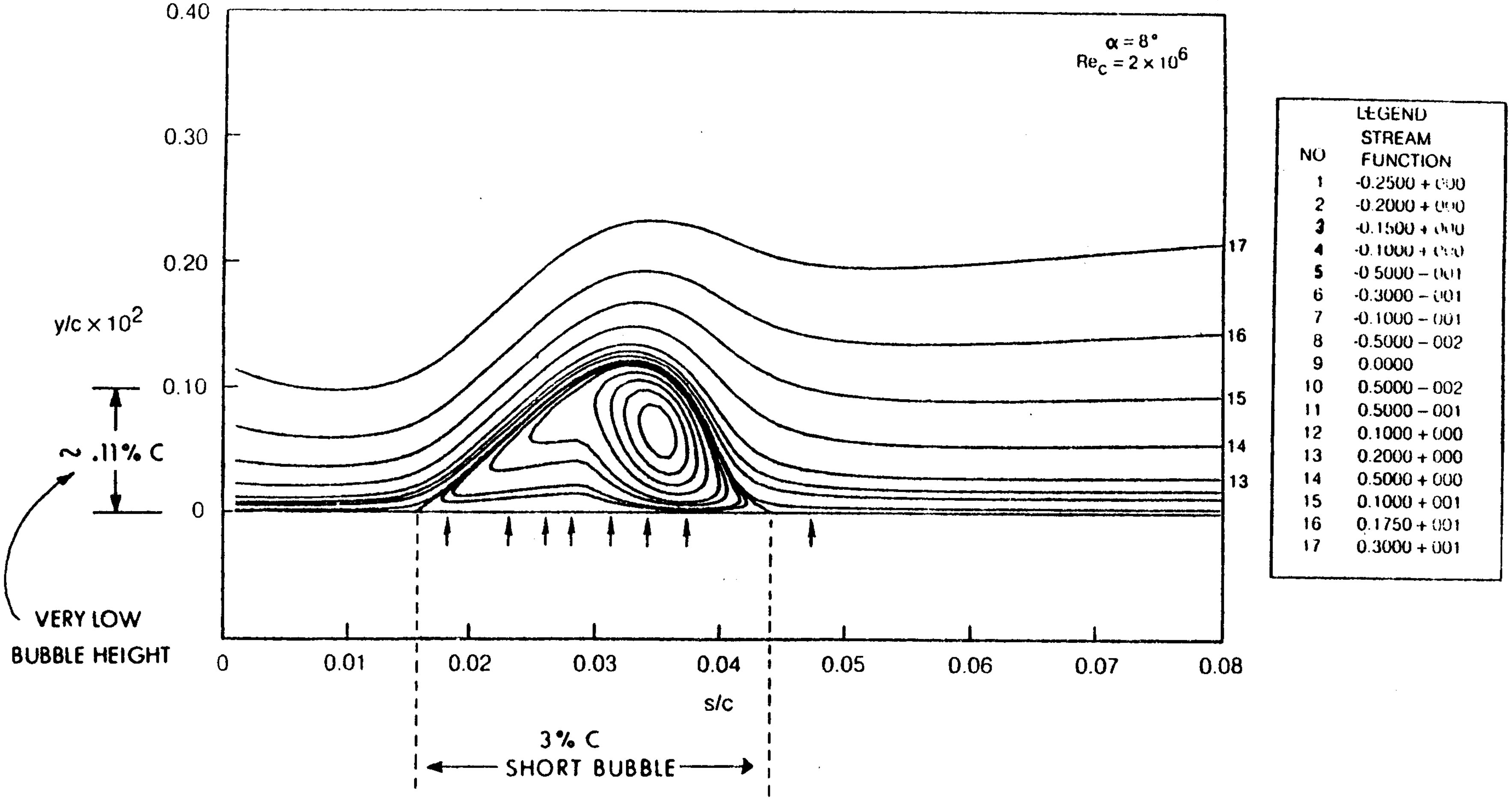

Fig. 7 Transitional separation bubble streamline pattern — NACA-0010 airfoil (modified).
(b) FLARE approximation

ALL-MOVING WINGS FOR LATERAL CONTROL

In SOARTECH 1 Preben Norholm from Denmark told about flying on the volcanoes in Iceland. He also has described to me the handling qualities of what he calls "SWING-WING" gliders. This design has been very popular in Europe for some time, and it is gaining popularity in the USA now as well. We've changed "swing-wing" to "all-moving" wing in order to prevent some confusion with the variable sweep "swing-wing" arrangement as seen on the F-14 Tomcat fighter and B-1 bomber. Using wing rotation instead of ailerons is attractive because it eliminates the drag and complexity of aileron installations. I suggested that a mixer could be used and both pitch and roll controlled by wing swing alone. That way the elevator linkage could be eliminated as well.

If you decide to try this arrangement, be advised that all-moving wings still create much adverse yaw, so coupled rudder with aileron (wing twist) is essential. Preben describes it well. The plane is his "PLY-BOY" which is the one he flew on the volcanoes. It is pictured in SOARTECH 1 This arrangement might also require a small gap between the wing and fuselage, so take a look at Steve McLellon's article on the penalty of gaps.

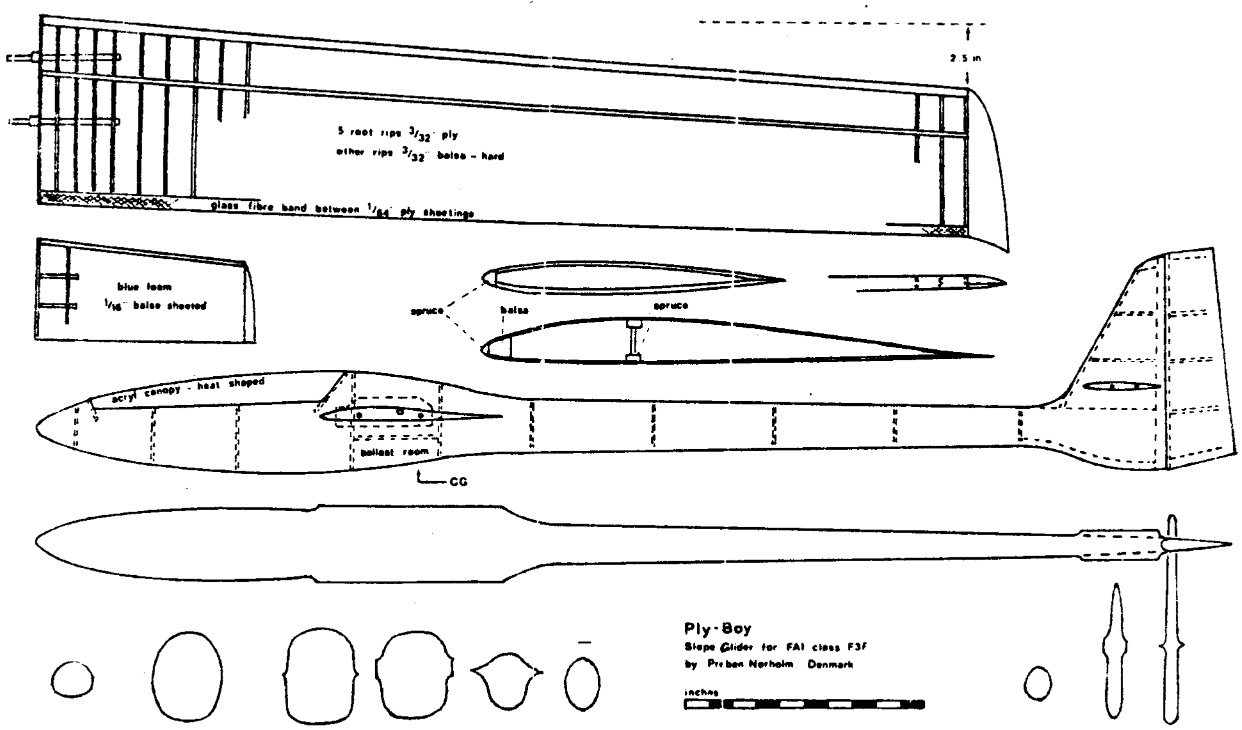

HANDLING OF "ALL-MOVING WING" GLIDERS

By Preben Norholm

About handling of an all-moving wing aileron glider. At high speed (CL 0.2/0.3 or lower) the handling characteristics are very good with very quick response - no problems at all - only very little rudder is needed for making clean maneuvers. At low speed it is very different, so rather long landing approaches are convienient when they are possible. All talk about differential ailerons on an all-moving wing glider is, of course, nonsense, and it is a problem. At CL 0.5 the ailerons stop working. They only produce side slip. At higher CL values the side slip tendency becomes so violent that the ailerons seem to be connected the wrong way --- this has rekitted many good gliders. The procedure when turning at low speed (when rudder-only movement is too little) is to initiate the turn with a little up-elevator followed by a little down-elevator at the same time as moving ailerons. This is not so difficult to learn. But many pilots forget to use exactly the same procedure when leaving the turn. Because the ailerons seemed to be coupled the wrong way around, the glider continued its turn into a spiral dive, which of course, often got worse by using "panic" up-elevator.

You may have stopped reading a long time ago, because all-moving wings are not good for a F3B ship, even if you may be able to increase handling characteristics considerably by using an airfoil with a higher CL-max and some wash-out. But for a slope racer on the slope, all-moving wings are perfect.

Spoilers could make life much easier, but they are almost banned on a slope glider. You know--- spoilers are devices that increase sinking speed which they accomplish in two positions--- "open" and "closed" !

You (Herk) proposed to mix elevator and all-moving wing controls. One of my friends, Niels Hassing (61 years old - placed 26th in F3B in Sacramento) not only proposed that, but built such a glider with fixed stab back in 1974. This of course eliminated the inertia of the tail boom and this was found to be good but also there seemed to be too much "nervous elevator" at high speed. The idea was forgotten for 5 years, but is now half-way back in a few designs. This means that some of our best pilots use both a normal all-moving elevator and mixing of all-moving wing and elevator function. In addition some pilots have wide flaps on the all-moving wing mixed with the elevator for increasing the CL-max in the sharp turns. The flaps are only moved to a maximum of one-quarter of an inch and are mixed through an exponential function in the transmitter so half-up-elevator only means about 1/16th inch flap movement. In a mechanical way flaps-up at down-elevator is eliminated making the elevator control less "nervous". Flaps are actuated by micro servos buried in the wing.

PREBEN NORHOLM, GODTHAABSVEJ 7, DK-7400 HERNING, DENMARK

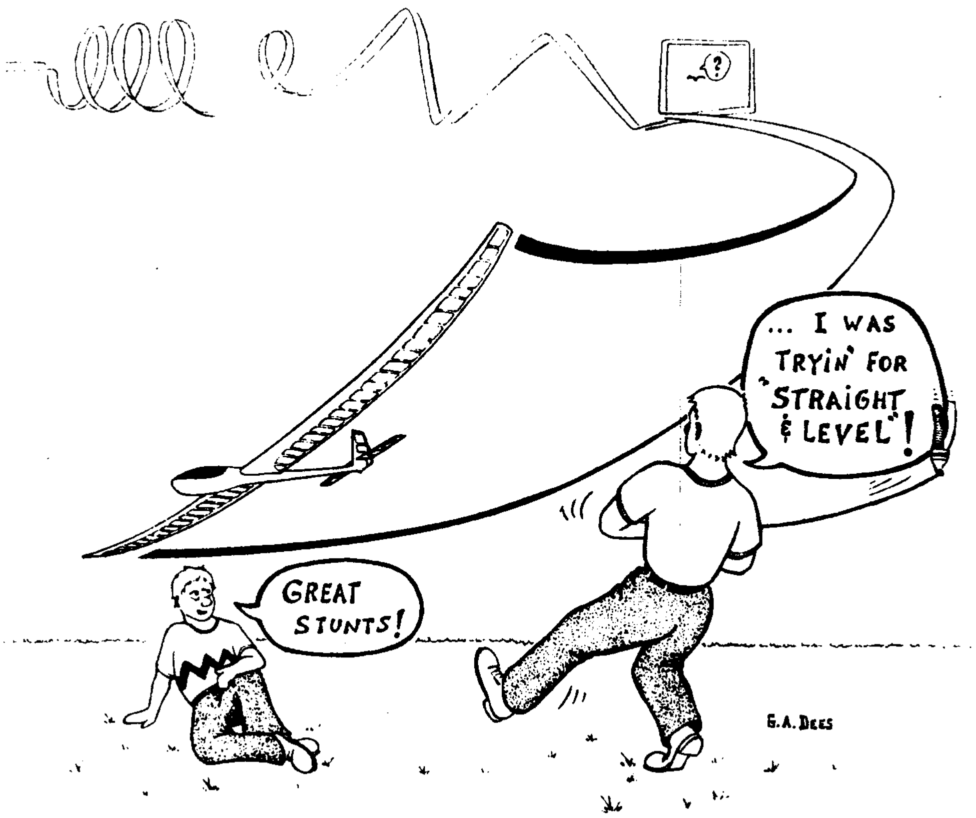

FROM "FLYING MODELS"

MCLELLON ON GAPS

Instinctively we all know that high pressure air leaking through from the bottom of the wing into the low pressure lifting flow on top of the wing will spoil some of the lift, and add to the drag. However, when I go to the field, I still see people attach their wing with a bit of tape here and there with rather large open gaps in between. I also have a plane of my own where the wing seating against the side of the fuselage isn't very precise; but I haven't done anything about it.

Steve goes beyond telling us to seal the gap, he gives us a bit of a tool to calculate the effect of the gap if we can't close it - or won't.

FROM "MODEL AVIATION"

STEVE MCLELLON
... C CHELSEA PL.
NEWPORT NEWS VA 23603

WHY GAPS HURT FLYING CHARACTERISTICS

by Steve Mclellon

Anyone who has spent some time at a winch or just hanging around model gliders would probably have noticed the gaps that exist on many models at the joint between the wing and fuselage or where tip panels join the center part of the wing. Many fliers make a point of taping these joints carefully, usually to hold things together, but I personally have seen plenty of untaped gaps at the joint the fuselage and plug-in wing panels and quite large gaps between plug-in stabilizers and the fuselage or vertical fin.

The less gap you have the better your model will fly but, I have seen little written about the reasons why. I came across a good explaination in *Aerospace Vehicle Design, Vol I*, by K.D.Wood and decided it would be worthwhile to pass the information along. There is some math involved but the example given later should show the effects without personally touching a calculator.

The major point to be made is that gaps reduce the effective aspect ratio of the wing or horizontal stabilizer and the panels on either side of the gap start to act independently. Air also leaks through the gap. Glider designers have known the advantages of a high aspect ratio wing for years and there are plenty of long, skinny, fragile wings on designs trying to squeeze out that last bit of performance. Higher aspect ratios improve maximum lift-to-drag ratios (L/D) and reduce sinking speed. By leaving gaps in the wing you reduce the effective aspect ratio which has the opposite effect and reduces performance. Even small gaps can cause rather drastic reductions.

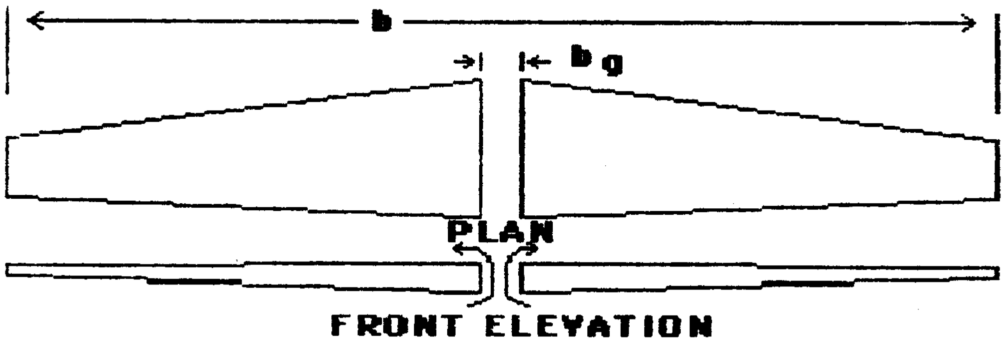

figure 1

Figure 1 is an illustration of a wing with a gap showing the two important dimensions: b_g the width of the gap and **b** the span of the wing. These will be related to the effective aspect ratio by the Munk "span factor" which will be called **K** . The effective aspect ratio, **Ae**, is determined by the formula:

$$Ae = (Kb)^2/s$$

where **s** is the wing area. If you were already fimiliar with the formula for the aspect ratio, **A** , of the wing;

$$A = b^2/s$$

then you would notice that this is simply a modified form with the correction factor K^2 added.

The only thing we need to know at this point is how Munk's "span factor", **K** , relates to the wing gap. Figure 2 relates the ratio of the wing gap to the wing span (b_g/b) to **K**. At this point we have enough information to try an example.

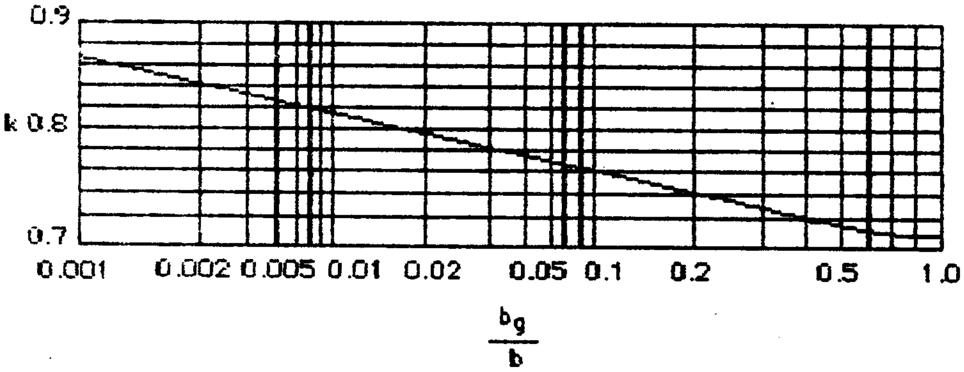

Figure 2. Effect of chordwise slot on Munk span factor

Assume your model has a wing span of 99 inches (standard class) and has a sixteenth (1/16) inch gap on either side of the fuselage where the wings plug on.

$$b_g/b = \frac{2 \times 1/16}{99} = \frac{.125}{99} = .0013$$

(We added the two gap widths since they would most likely have the effect of a single larger gap). The grap h (Figure 2) may be pretty difficult to read so I'll do it for you:

$$k = .86$$

If your model has about 900 square inches of wing area, its aspect ratio without the gap is:

$$A = \frac{99^2}{900} = 10.9$$

The effective aspect ratio with the two 1/16 inch gaps is:

$$Ae = (.86)^2\ 10.9 = 8.06$$

or less than three-quarters of the aspect ratio the model was designed with. It doesn't matter what the aspect ratio of your model was originally. Two 1/16 inch gaps on a 99 inch standard class model will cause the wing to act like one with an aspect ratio 74% as great as it was designed with.

Decreasing the effective aspect-ratio of your wing that much by leaving gaps can really hurt your model's performance. Even if you are just a Sunday flyer you want your model to stay up as long as it can, and taping over gaps helps.

Horizontal Stabilizers and Gaps

The previous example dealt with gaps in a wing. You may think that the same things happen when there are gaps where a horizontal stabilizer meets the fuselage or rudder but there are some differences.

The effective aspect-ratio of the horizontal stabilizer is reduced the same as for the wing. Two 1/16 inch gaps on a 25 inch stabilizer give a ratio of the equivalent single gap to the span (b_g/b) of:

$$b_g = \frac{2x1/16}{25} = \frac{.125}{25} = .005$$

and, from Figure 1 $K = .77$

$$K^2 = .77^2 = .60$$

Since your design aspect-ratio is multiplied by this factor to get your effective aspect-ratio, you have reduced the aspect-ratio of the horizontal stabilizer by 40% just by leaving those gaps !

The aspect-ratio really effects the induced drag of a wing, which is the drag resulting from the lift the wing is generating. Since horizontal stabilizers aren't usually producing much lift (their purpose is to stabilize the model) this type of drag increase really isn't a problem...**BUT**... if you think that means the reduced aspect-ratio doesn't affect your model, you're wrong !

The aspect-ratio of the horizontal stabilizer has a very large effect on its contribution to the longitudinal stability of a model. Technically it changes the amount of lift the stabilizer produces at a given stabilizer angle of attack. Horizontal stabilizers with higher aspect-ratios definitely increase the longitudinal stability of a model. The aspect-ratio of most horizontal stabilizers is down around 6 or less and reductions in aspect-ratio below this have severe effects. You can't afford to reduce model stability by allowing gaps if you're designing models with smaller horizontal stabilizers for slight increases in performance.

Gaps in the Real World

Most models don't have gaps of 1/16 inch while sitting on the ground. If the wing rods are soft this tends to change on hard launch when the wings flex up and the top of the root rib pushes the wing away from the fuselage. Still, wing rods help prevent this. If you use tape with flexible rods the tape has to be flexible or it will tend to pull away.

Don't underestimate the effects od smaller gaps. A 1/32 inch gap does not have half the effect of a 1/16 inch gap. The effects aren't that simple (study figure 2). Any gap really hurts.

Models that have their two-piece wings rubber banded on top of the fuselage don't have any problems because the fuselage blocks airflow through the joint. All Paragon, Bird of Time, and Wind Drifter owners can breathe a sigh of relief !

Two-meter models are especially susceptible to these problems. Most two-meter gliders have fairly low aspect-ratios to start with and any effective reductions caused by gaps will really hurt performance.

Some European gliders have used sliding monocoat seals on their flaps. Something like that should work on flat stabilizers at the root. Anything you can do to reduce the gaps at the horizontal stabilizer root will help. The further forward the gap is in the joint the worse its effect.

While this article may not deplete all the stock of electrical tape and 3M plastic tape at the corner store, it should have emphasized the care needed in designing wing fuselage joints. If you end up taping, a permanent layer of Scotch Magic Mending Tape on the surfaces under the tape used to cover the gaps will prevent the monocoat from pulling up or tearing when you rip the tape off. Remember, keep some good flexible tape handy and use it !

SOME MORE OF MICHAEL SELIG

Michael did most of his airfoil work while he was a student at the University of Illinois. The year after he graduated, he had a chance to do some work at NASA Langley. While there he did more thinking and research on his favorite subject. The result is here in the form of a progress report. Relating the behavior of groups of airfoils in the wind tunnel, to the Eppler program velocity distributions, Michael reaches some exciting conclusions. Thinking about his conclusions can lead us to some of our own.

One that I'll point out for you is that any wing with a sheeted leading edge and open - bay structure aft, will be prone to hysteresis and would probably benefit from a turbulator near the leading edge.

Michael also includes for us some more data on popular airfoils. Some of this was supposed to be in his article in Soartech #3 but was accidentally omitted. This should make it complete. If you read and digest this paper, it'll make your study of his earlier paper much more effective.

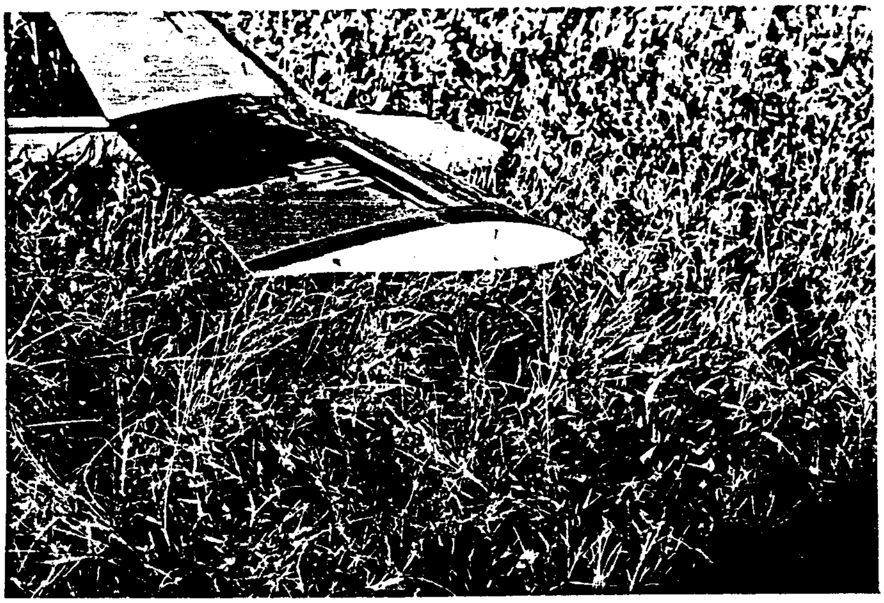

MICHAEL SELIG
OLD GRADUATE COLLEGE
PRINCETON NJ 08544

ADDENDUM TO THE DESIGN OF AIRFOILS AT LOW REYNOLDS NUMBERS

Michael Selig

Department of Mechanical and Aerospace Engineering

Princeton University, Princeton, New Jersey

LOW REYNOLDS NUMBER AIRFOILS/COANDA EFFECT/HYSTERESIS

Of particular interest to me is the design of airfoils at low Reynolds numbers (RN<500,000). The flow over an airfoil operating in this RN regime commonly supports a transitional separation bubble which for increasing angle-of-attack behaves differently than for decreasing angle-of-attack, accounting for the hysteresis shown in experimental lift, drag, and moment curves. It was suggested by Dr. Mangalam of NASA-Langley that there may exist a physical relationship between the hysteresis of an airfoil at low RNs and the hysteresis of the Coanda effect - the adherence of a fluid blown tangentially over a highly convex surface. If such a relationship were found, it may give insight into the peculiar behavior of the transitional separation bubble and may then lead to analytical or numerical prediction methods. After a literature search some evidence of a correlation has emerged. Study in this area will continue.

LOW REYNOLDS NUMBER AIRFOIL HYSTERESIS

Two common types of airfoil lift hysteresis are found at low RNs: (1) pre-stall hysteresis and (2) stall hysteresis show in figures 1 and 2. Previously in ref. 1 pre-stall was referred to as moderate-lift hysteresis and stall hysteresis as high-lift hysteresis. The change is made here because moderate-lift and high-lift imply that the hysteresis is associated directly with the lift when in fact it is not. In the case of pre-stall hysteresis for increasing angle-of-attack, a long transitional separation bubble, formed near the airfoil mid-chord, grows larger and can extend into the wake. As this happens the lift begins to level off - a process which can be thought of as a trailing-edge stall. Further increasing the angle-of-attack "unstalls" the airfoil by causing the long bubble to collapse into a short bubble near the leading edge. This occurence can be identified by a sharp increase in lift. Through decreasing angle-of-attack, a sharp decrease in lift occurs due to the reformation of the long bubble at a angle-of-attack lower than that at which the sharp increase occurred.

In contrast to pre-stall hysteresis caused by a long transitional separation bubble, stall hysteresis involves a short transitional separation bubble. Near stall for increasing angle-of-attack, a short bubble exists on the leading-edge of the airfoil. Further increasing the angle-of-attack causes the airfoil to stall either by the bursting of the bubble or by turbulent separation rapidly migrating towards the leading-edge. Through decreasing angle-of-attack, the short bubble reattaches at an angle-of-attack lower than that of stall for increasing angle-of-attack.

Figure 3 depicts an airfoil with pre-stall hysteresis and without stall hysteresis. Figure 4 shows an airfoil with stall hysteresis and without pre-stall hysteresis. And an airfoil with both pre-stall and stall hysteresis is shown in figure 5. Some airfoils, for example those shown in figures 6 and 7, have no hysteresis.

It was observed that airfoils with pre-stall hysteresis have a concave potential flow velocity recovery on the upper surface while airfoils with no pre-stall hysteresis have a convex to linear velocity recovery, summarized in figures 8 and 9. Airfoils with stall hysteresis commonly at stall have near constant, small velocity gradients beyond the suction peak, and airfoils without stall hysteresis have decreasing, large gradients beyond the suction peak as illustrated in figures 10 and 11.

In view of this four different combinations of airfoil suction peak/recovery design are conceivable, each of which would have a different lift curve hysteresis. Using the Eppler computer program [2], four such airfoils have been designed with the criterion: $9\%<t/c<10\%$, $0.3<Cl<1.2$. These airfoils (designated S4410-097-84, S4411-096-84, S4412-093-84, and S4413-098-84), velocity distributions, design input data, theoretical section characteristics, expected lift curve hysteresis, and coordinates are all shown in figures 12 through 15.

Regarding the theoretical section characteristics, they should be viewed with caution as to the validity of the theoretical results since:

1. Upon prediction of laminar separation, quick reattachment of the flow is assumed. Thus no account is made of the gain in drag and loss in lift due to a transitional separation bubble of any size. Another implication of this assumption is that the program cannot predict the stall characteristics of the airfoil since at stall a bubble may play a major role.
2. In case of turbulent separation, a small correction is made in the lift, drag, and pitching moment coefficients; however, this correction is not emperically founded.
3. The lift is based on potential flow theory which for high RNs is a good approximation, but it is not good at low RNs due to thick boundary layers, and laminar and turbulent separation.

It is recommended that these four airfoils be tested in a low-speed wind tunnel to study the hysteresis.

A COMMENT ON THE EPPLER BUBBLE PREDICTION CRITERION

The version of the Eppler computer program used by the author during the writing of "The Design of Airfoils at Low Reynolds Numbers" [1] is that version discussed in ref. 2. It should be pointed out that since the documentation of ref. 2, the transitional (or laminar) separation bubble criterion has apparently been changed without, the author believes, further documentation. Consequently, before one compares the Theoretical Boundary-Layer Summary Table data, published in ref. 1, with data generated by another program, it is necessary to know which version of the program was used. As a helpful guide, the later version of the program has a bubble prediction criterion which predicts bubbles less frequently on the upper surface than the earlier version. This modification of the program does not effect the calculation of the drag coefficient. Drag polars then may still be compared.

REFERENCES

2. Eppler, Richard and Somers, Dan M., "A Computer Program for the Design and Analysis of Low-Speed Airfoils," NASA TM-80210, August, 1980.

1. Selig, Michael S., "The Design of Airfoils at Low Reynolds Numbers," SOARTECH III, c/o H. A. Stokely, 1504 Horseshoe Circle, Virginia Beach, Virginia, 23451, July 1984.

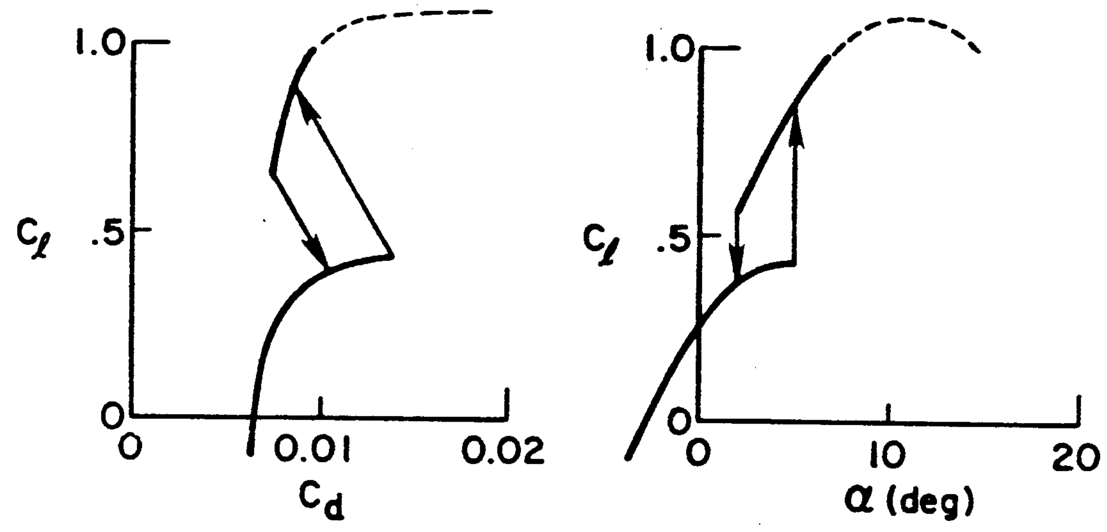

FIG 1 - PRE-STALL HYSTERESIS.

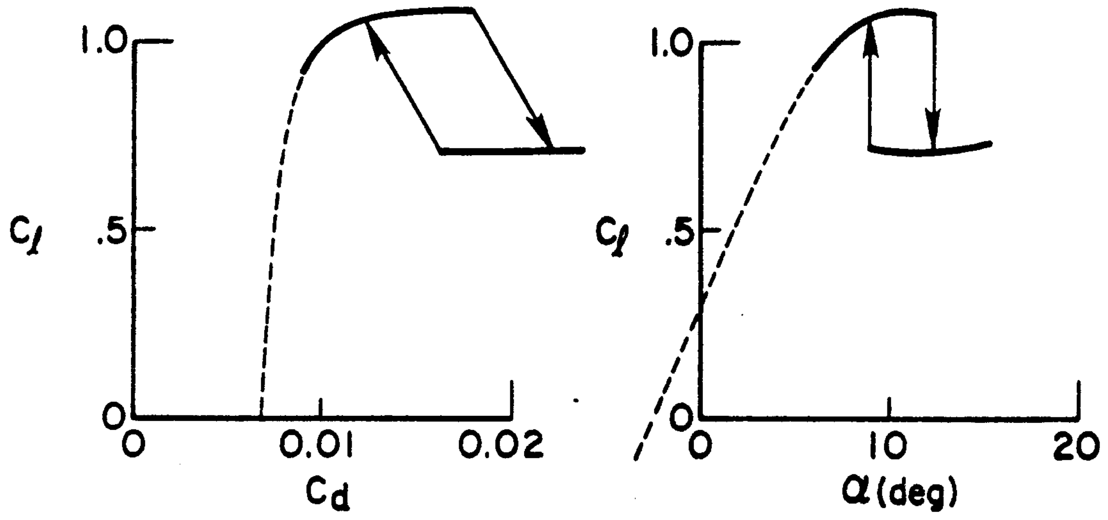

FIG 2 - STALL HYSTERESIS.

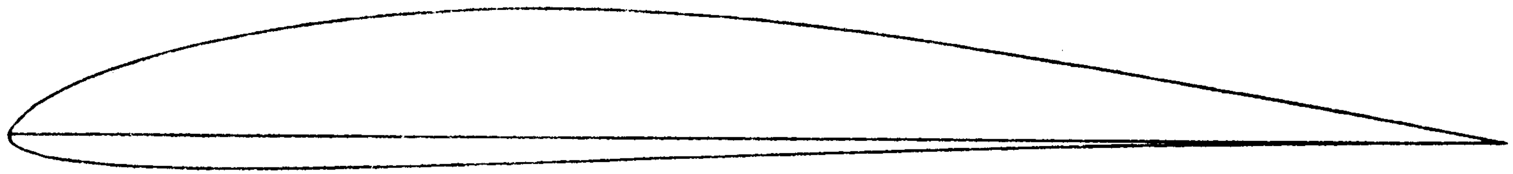

E 193

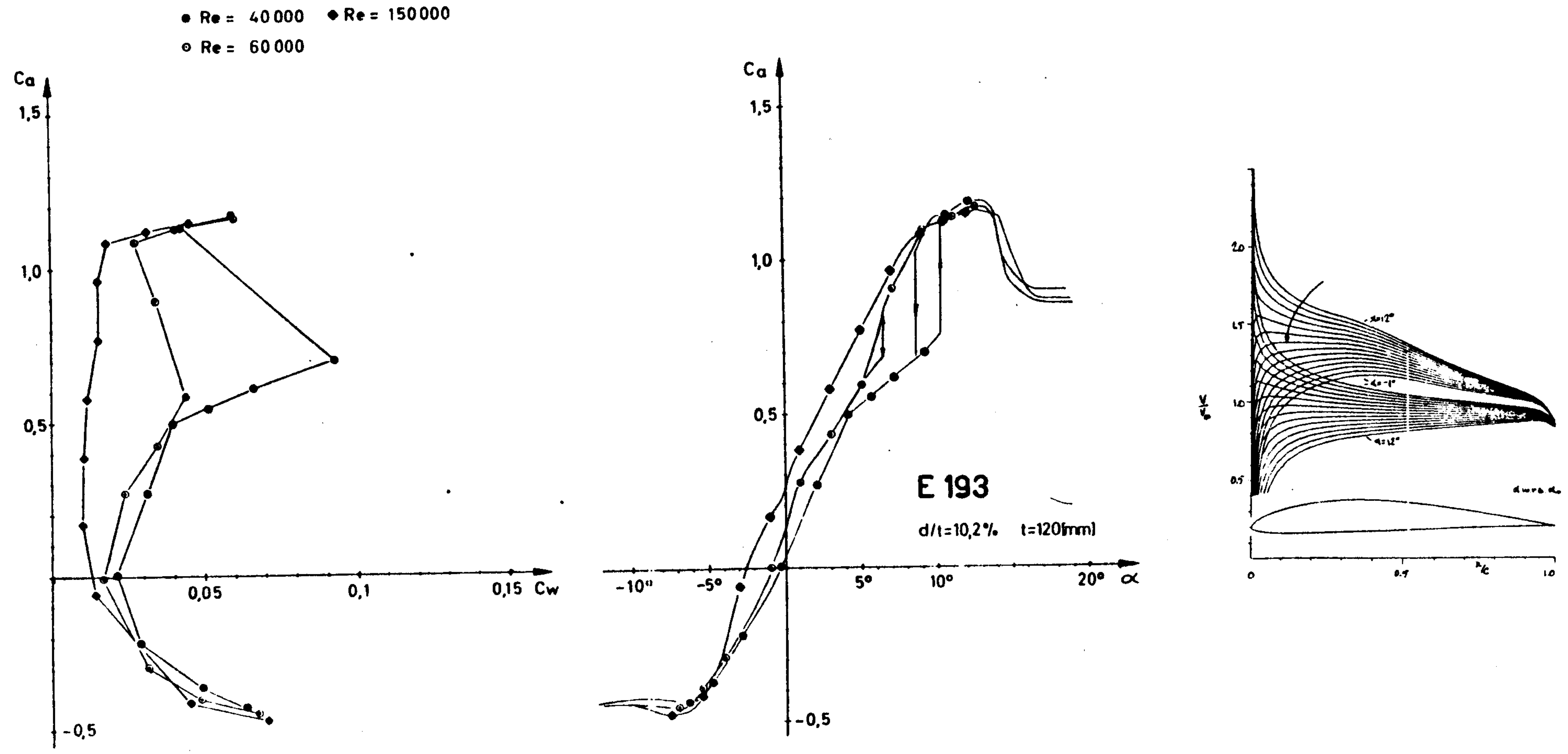

FIG 3 - E193

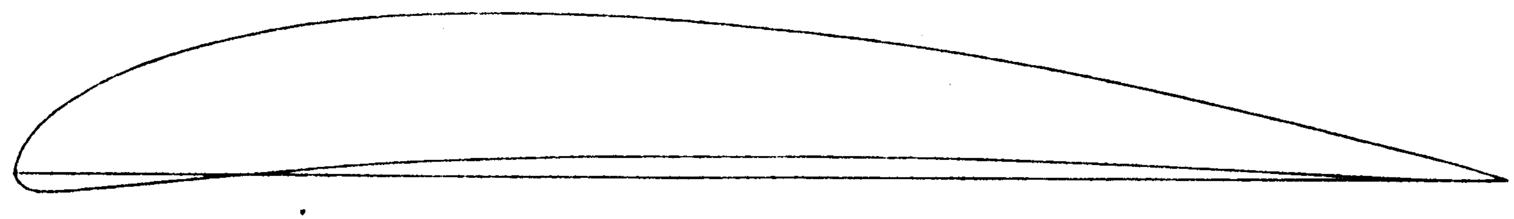

GOE 801

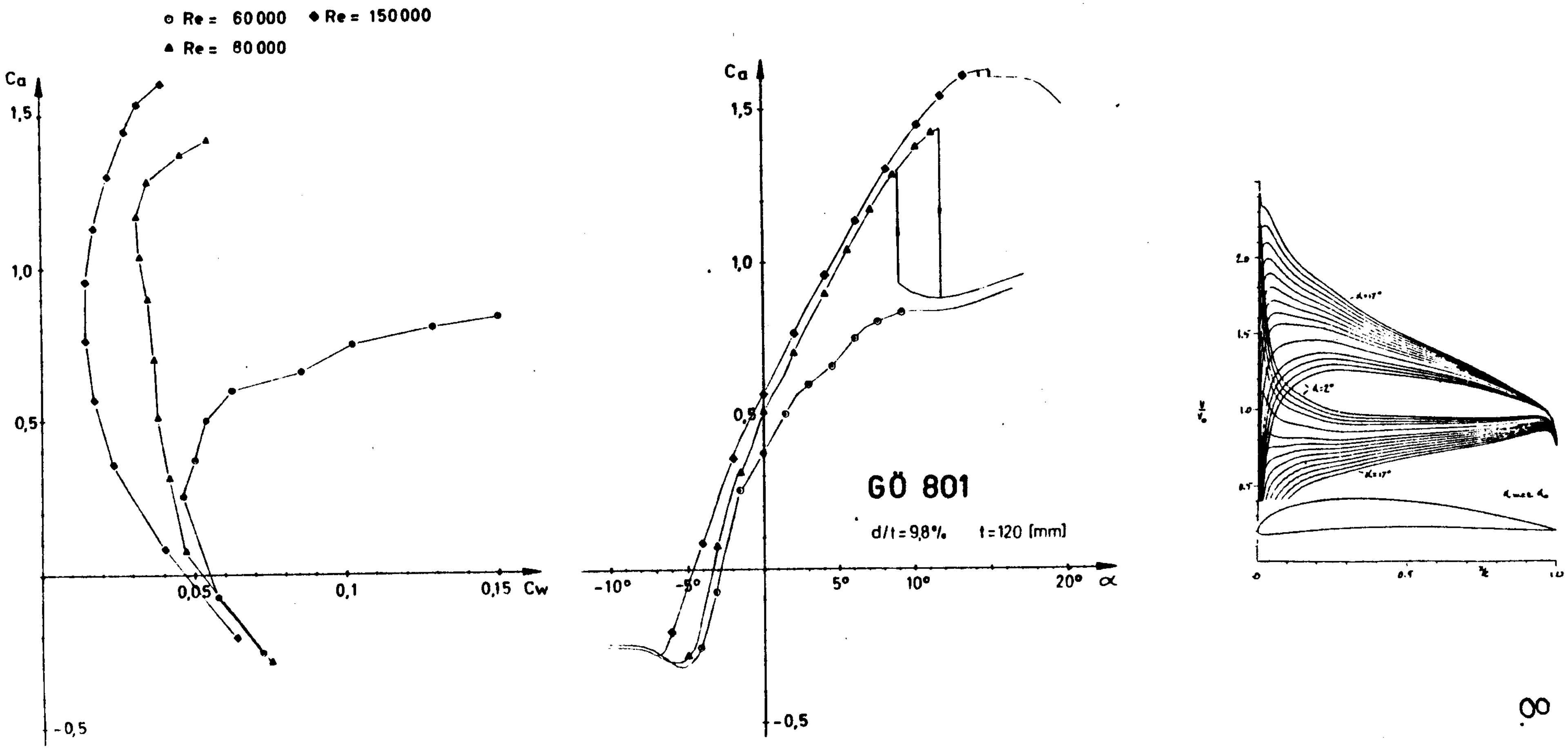

FIG 4 - GOE 801

8.

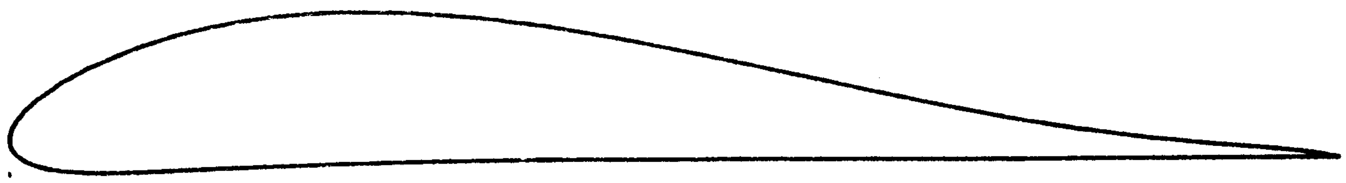

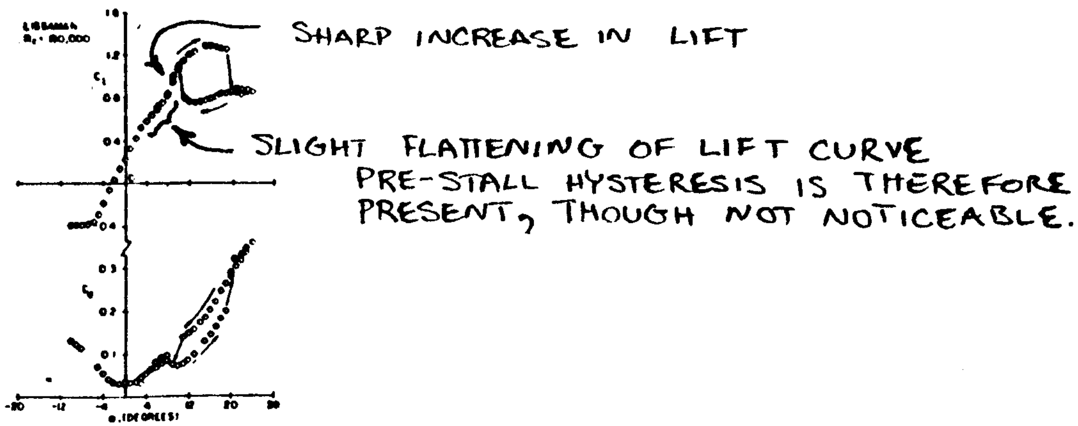

FIG 5 - LISSAMAN 7769

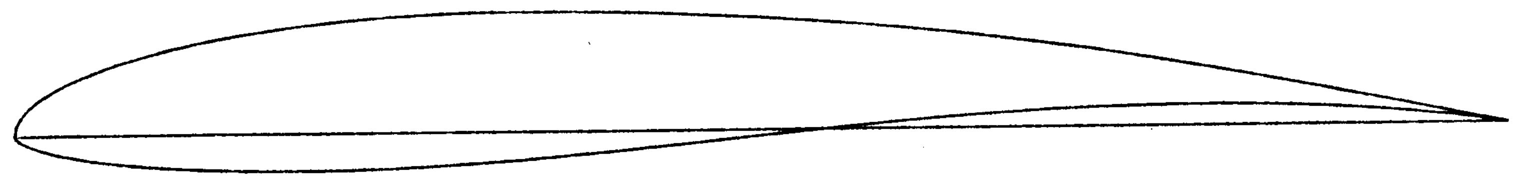

FX 60-100

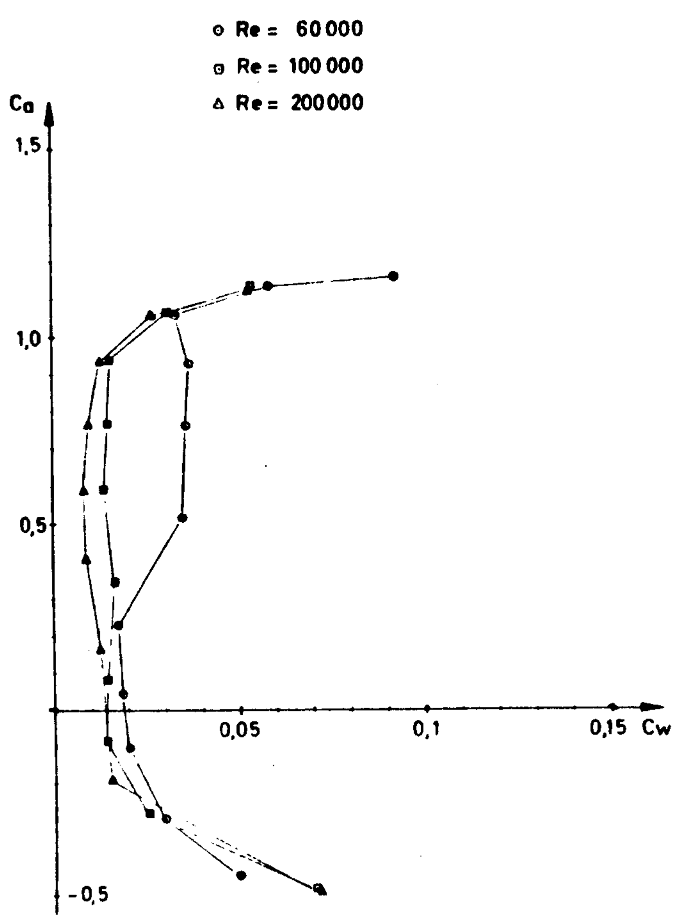

○ Re = 60 000
⊡ Re = 100 000
△ Re = 200 000
Ca
1,5
1,0
0,5
-0,5
0,05
0,1
0,15 Cw

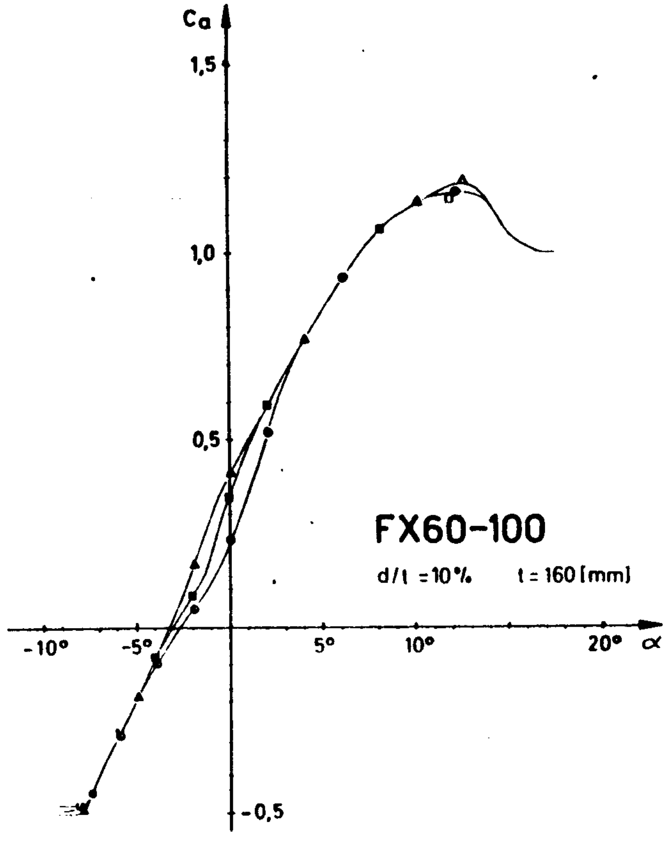

Ca
1,5
1,0
0,5
-0,5
-10°
-5°
5°
10°
20° α
FX60-100
d/t = 10%   t = 160 [mm]

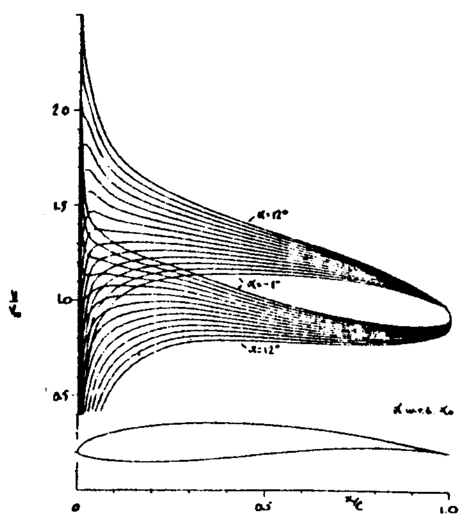

10.

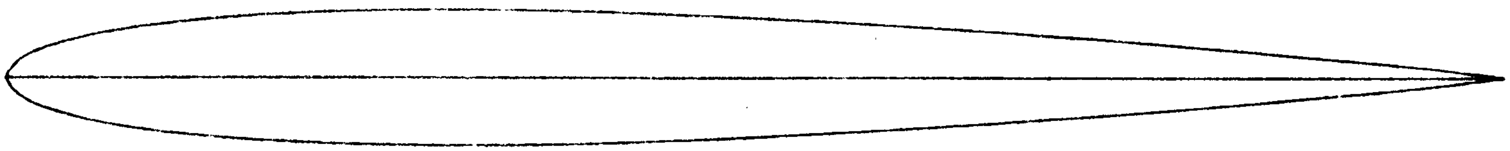

NACA 0009

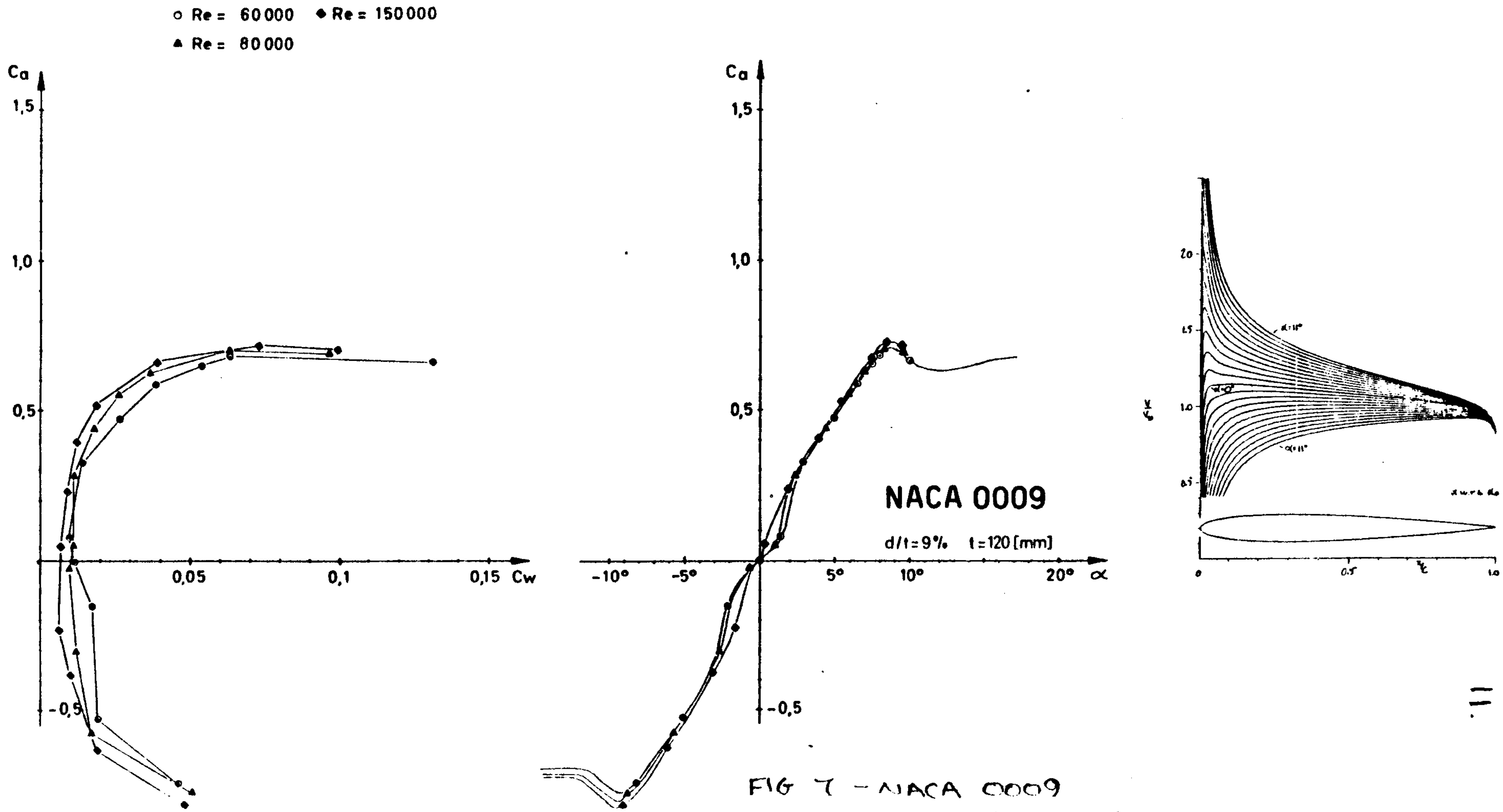

FIG 7 - NACA 0009

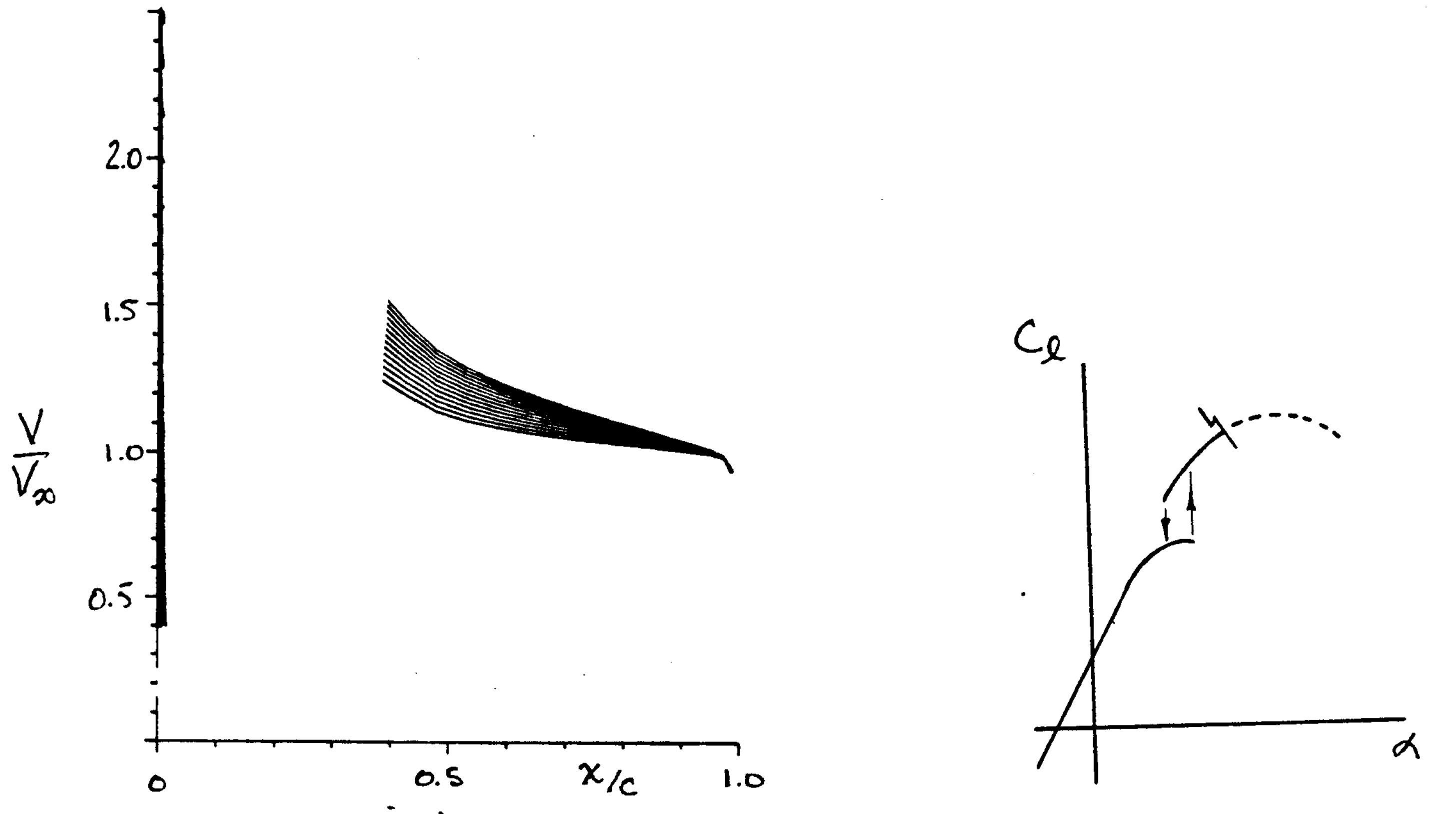

FIG 8 – PRE-STALL HYSTERESIS.

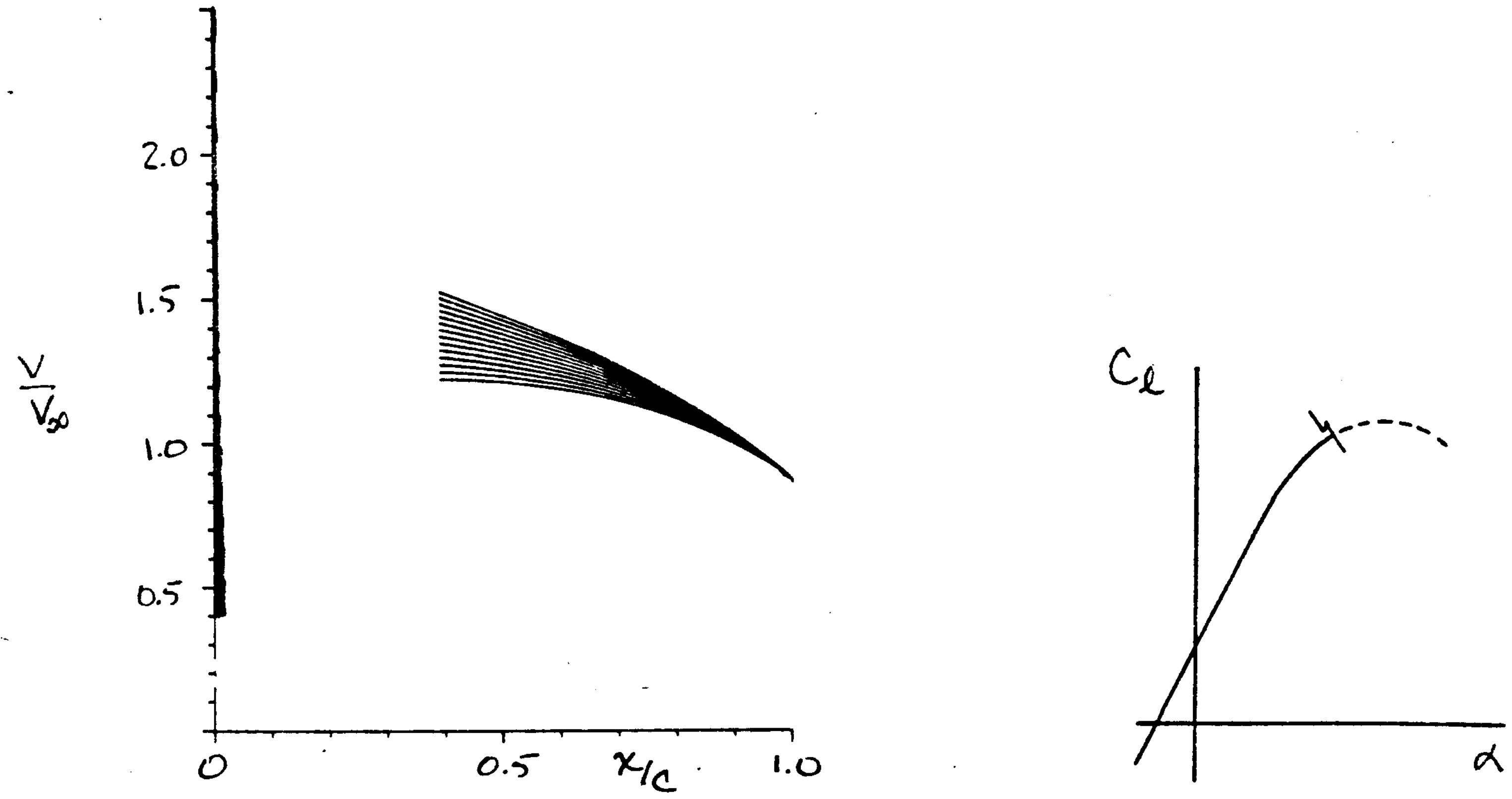

FIG 9- NO PRE-STALL HYSTERESIS

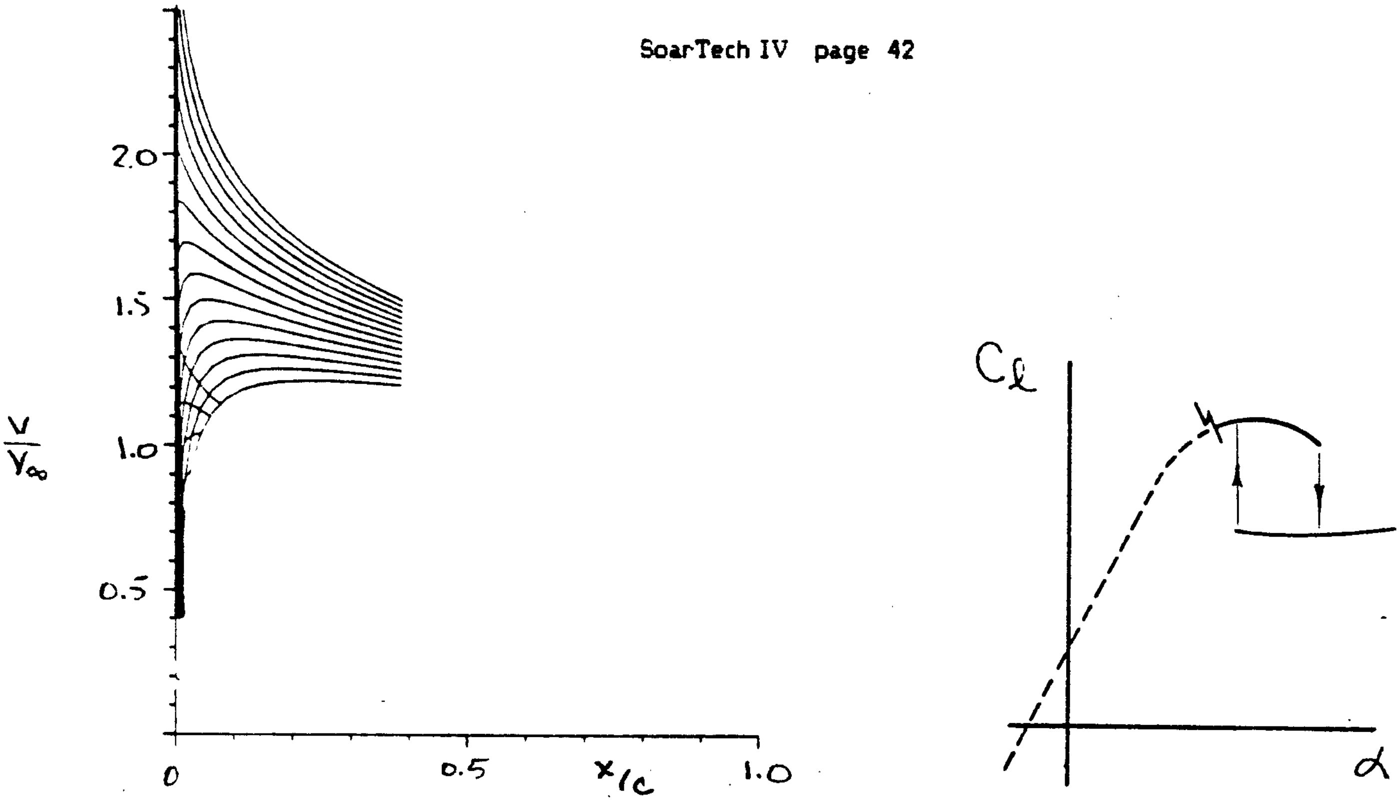

FIG 10- STALL HYSTERESIS

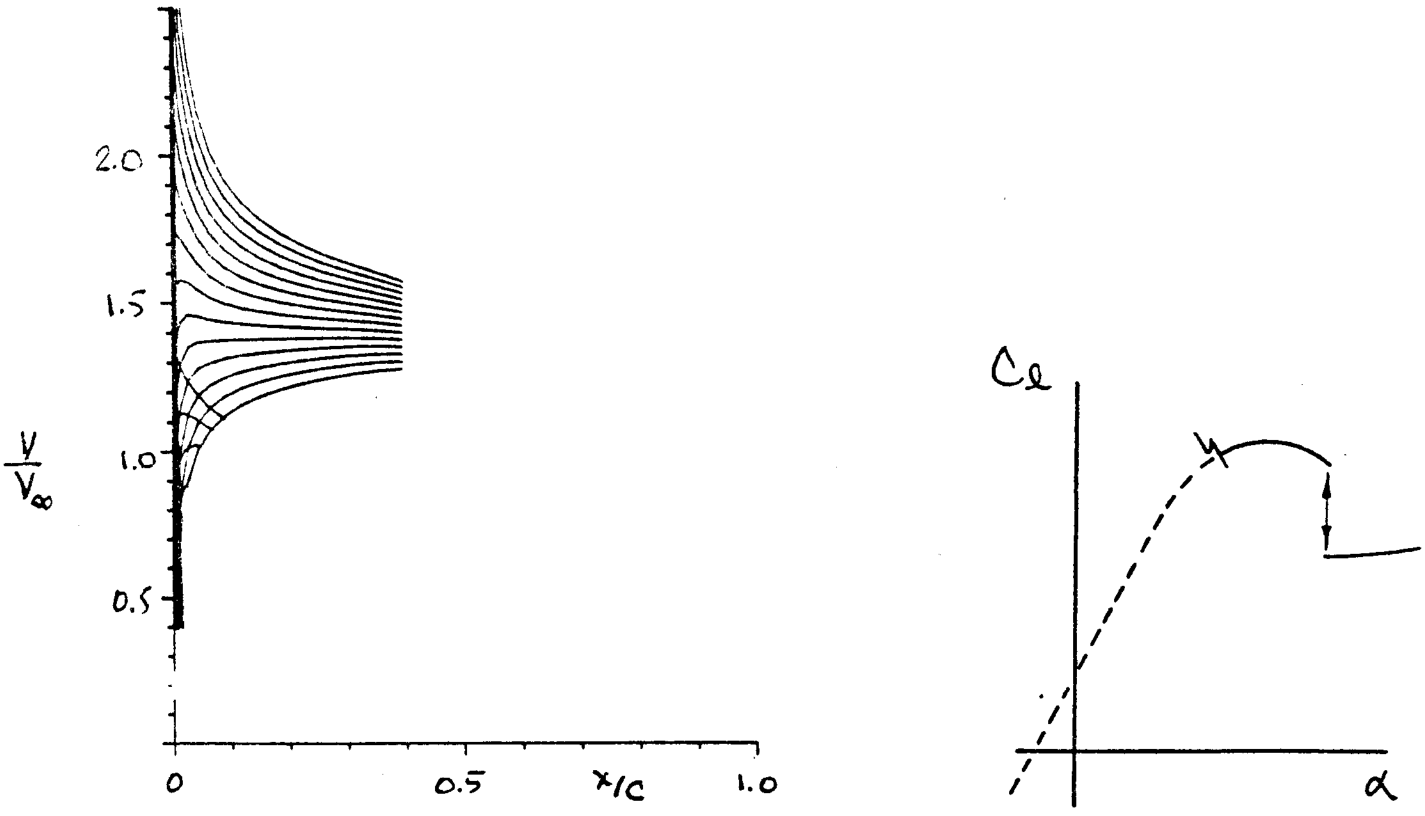

FIG 11- NO STALL HYSTERESIS

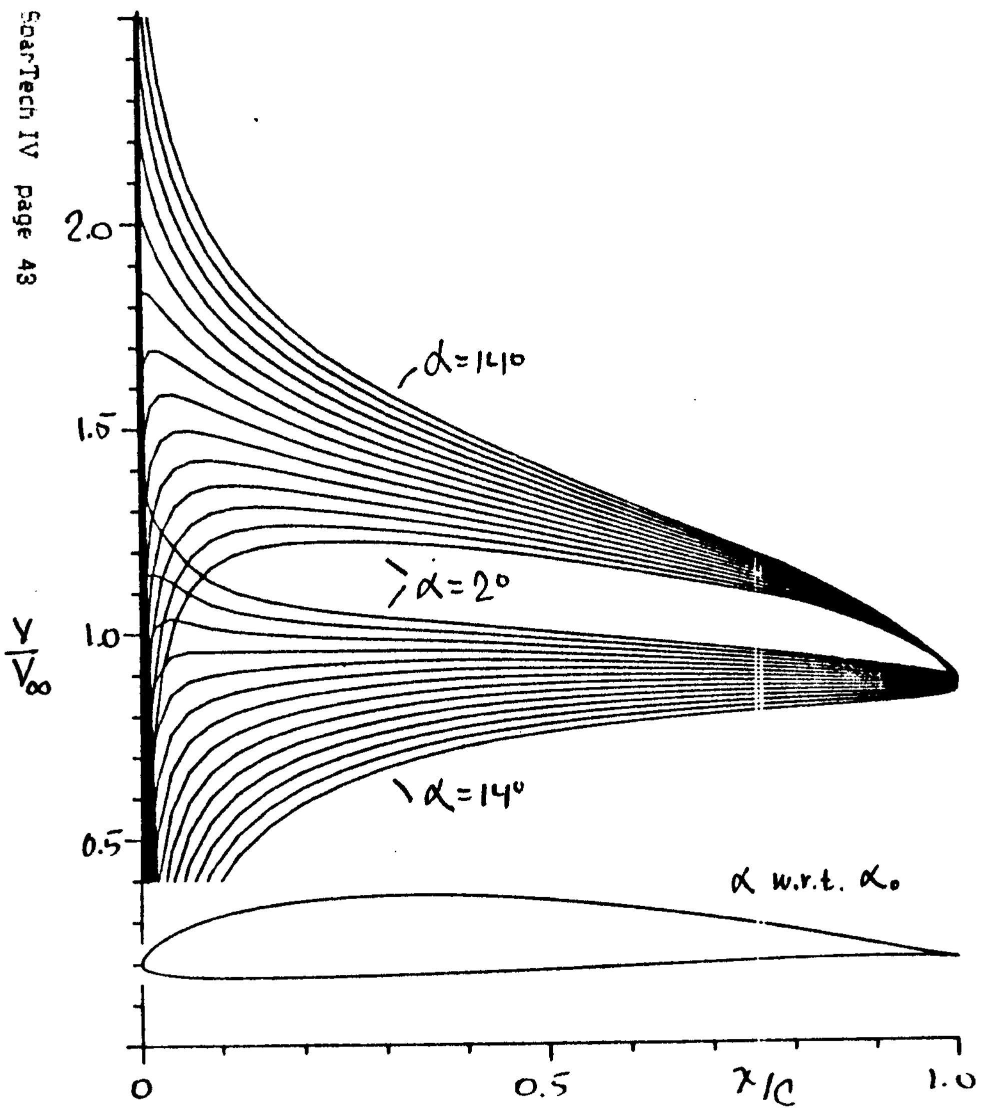

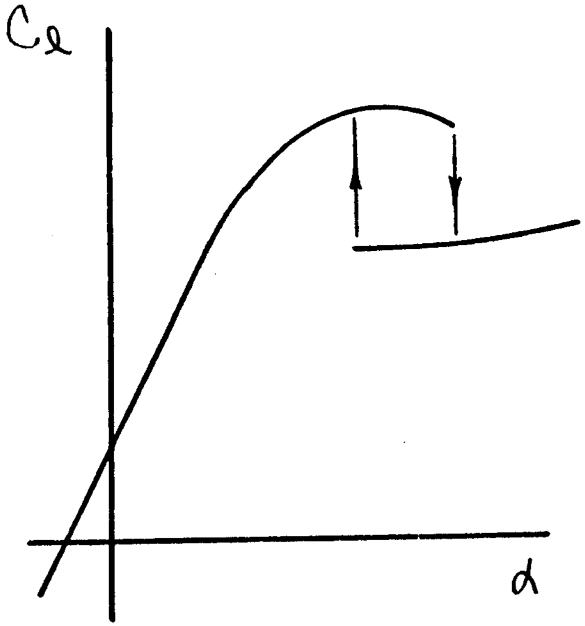

FIG 12 - S4410-097-84

```
TRA1  0010 1150-0950 1350 -750 1550 -500 1750 -200 1950  030 2150  200 2250

TRA1  0010 2350  400 2450  490 2550  580 2650  670 2750  760 2850  850 2950

TRA1  0010 3050 1030  000 1120 3350  300 3450  300 3550  400 3650  500 4250

TRA1  0010 6000  500 6000  500 6000  500 6000  500 6000  500 6000  500 6000

TRA2  0010  950  950  000  020 1000 1650 1650  000  020 1000  000 0550
ALFA100 14  200  300  400  500  600  700  800  900 1000 1100 1200 1300 1400

DIAG
RE  110   03      10003      20003      40003      600
CDCL
ALFA110  1
ENDE
```

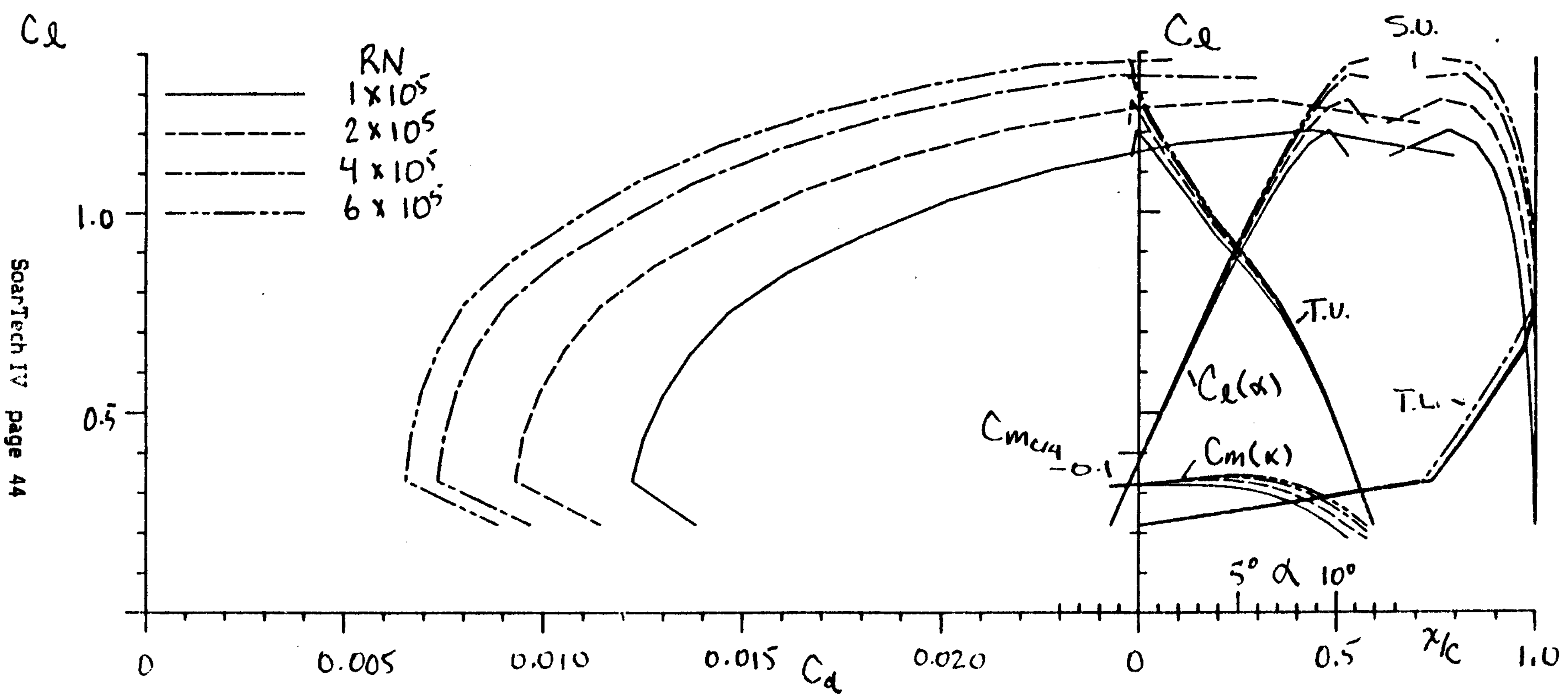

FIG 12 - (CONT) S4410-097-84

15.

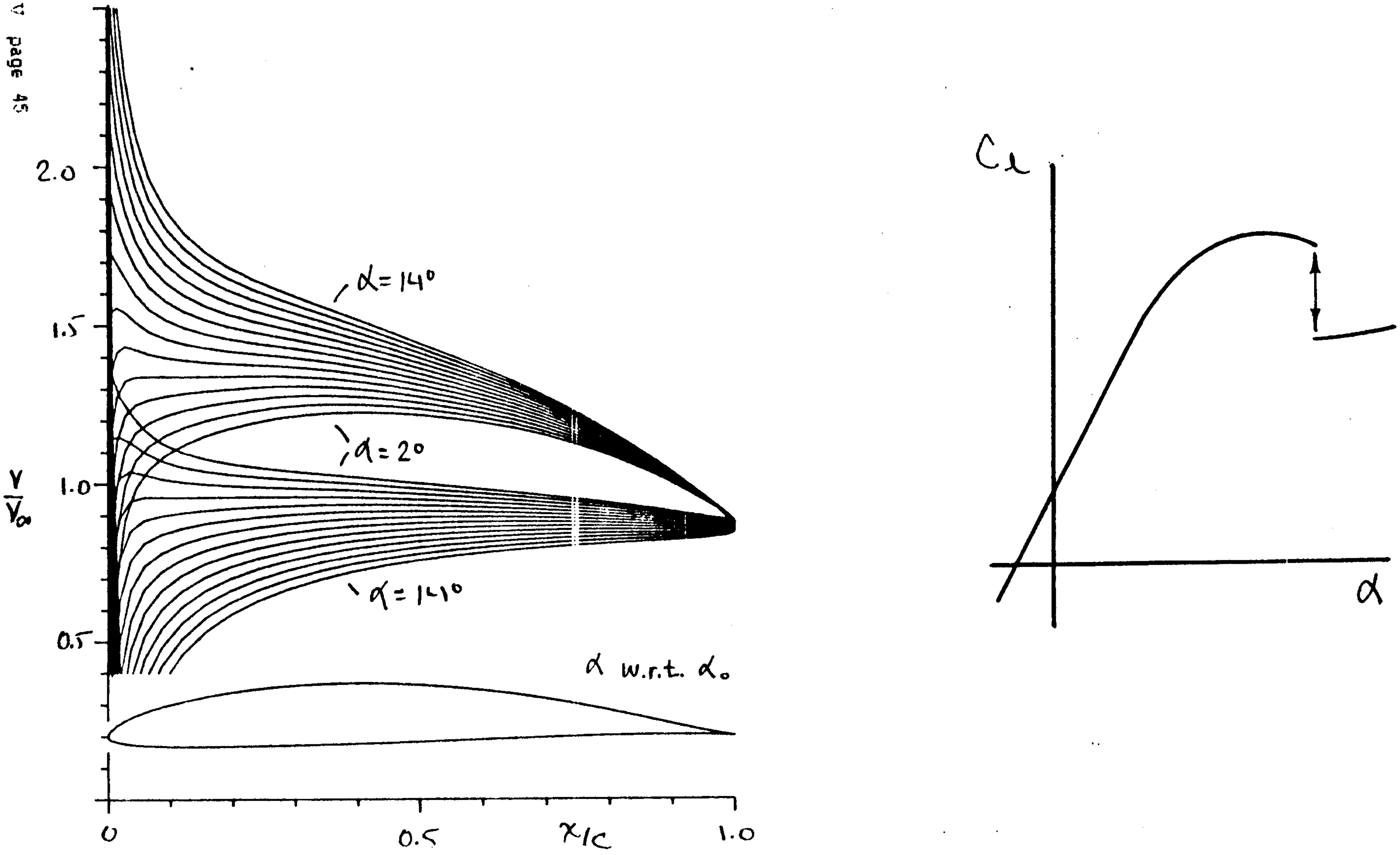

FIG 13 - S4411-096-84

```
TRA1  0011 1350-9900 1350 -900 1550 -600 1750 -200 1950  100 2150  300 2250

TRA1  0011 2350  300 2450  300 2550  300 2650  300 2750  300 2850  400 2950

TRA1  0011 3050  550  000  600 3350  300 3450  300 3550  400 3650  500 4250

TRA1  0011 6000  500 6000  500 6000  500 6000  500 6000  500 6000  500 6000

TRA2  0011 1250 1250  000  020 1000 1650 1650  000  020 1000  100 0550
ALFA100 14  200  300  400  500  600  700  800  900 1000 1100 1200 1300 1400

DIAG
RE  110   03      10003      20003      40003      600
CDCL
ALFA110  1
ENDF
```

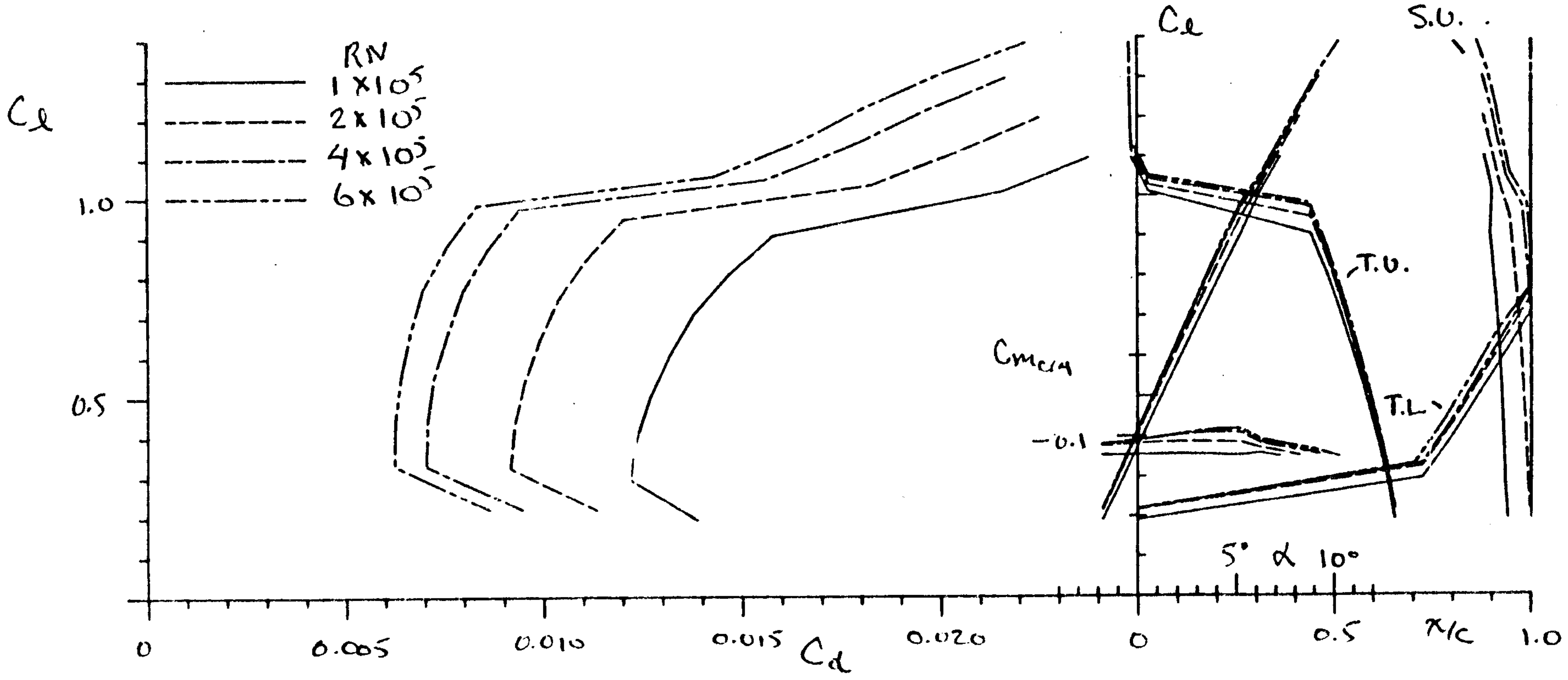

FIG 13 - (CONT) S4411-096-84

Soar Tech IV page 47

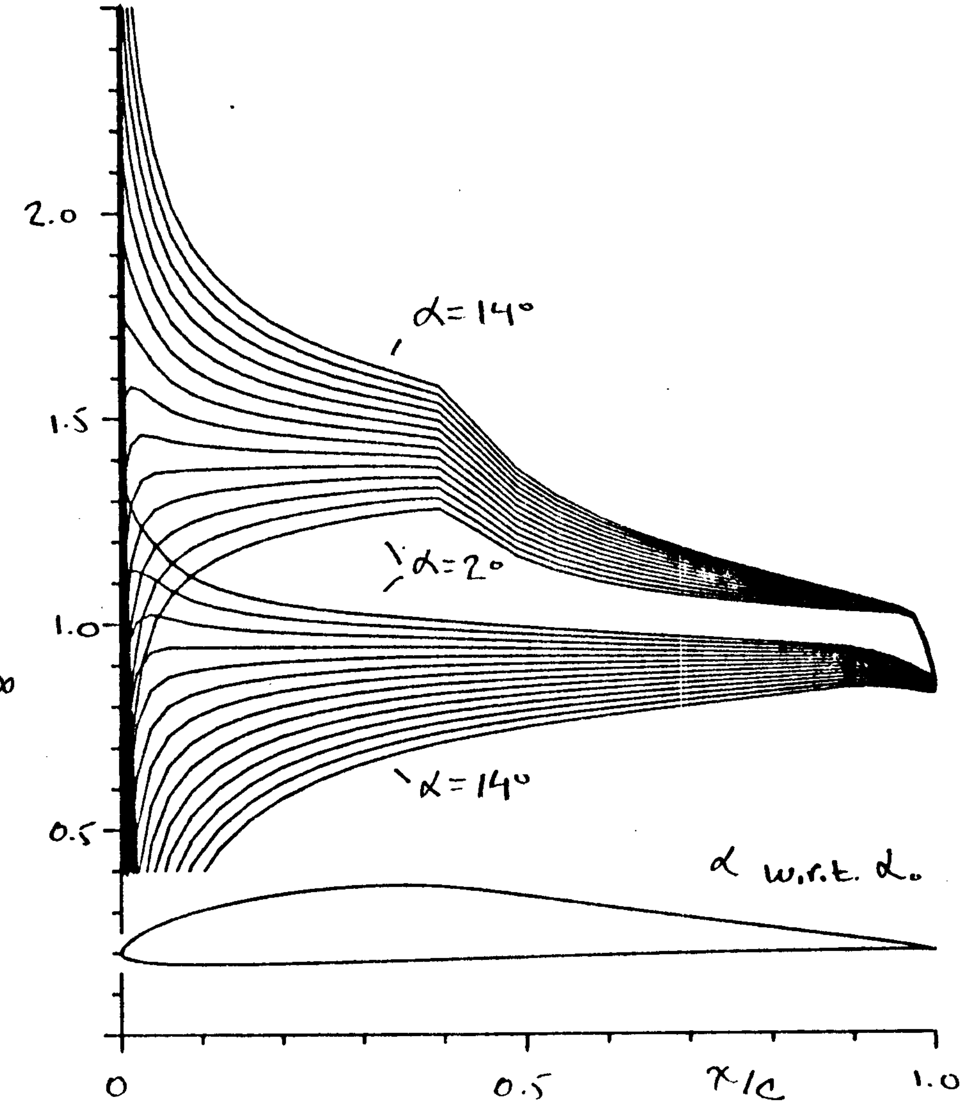

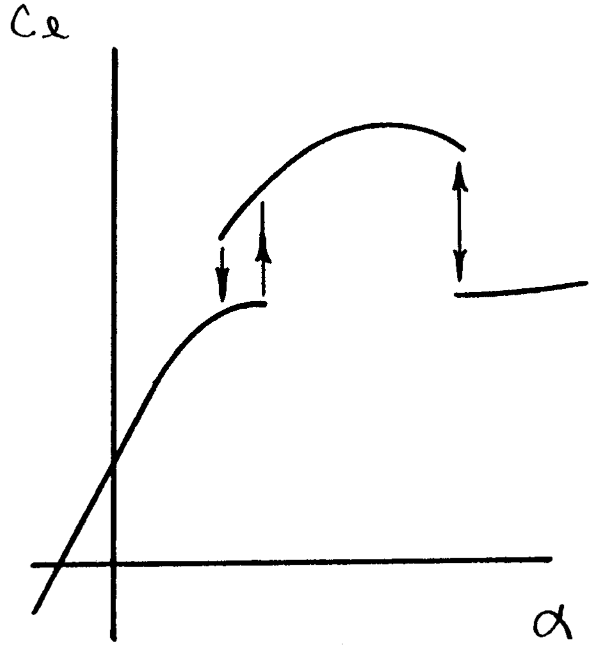

FIG 14 - 54412-093-84

```
TRA1   0012 1750 0375 1750 0375 1850  525 1950  625 2050  625 2150  625 2250

TRA1   0012 2350  625 2450  625 2550  625 2650  625 2750  625 2850  725 2950

TRA1   0012 3050  875  000  925 3350  300 3450  300 3550  400 3650  500 4250

TRA1   0012 6000  500 6000  500 6000  500 6000  500 6000  500 6000  500 6000

TRA2  0012  350 1650  000 3000 0100  650 1650  000  020 1000  400 0550
ALFA100 14  200  300  400  500  600  700  800  900 1000 1100 1200 1300 1400

DIAG
RE  110   03      10003     20003     40003     600
CDCL
ALFA110  1
ENDE
```

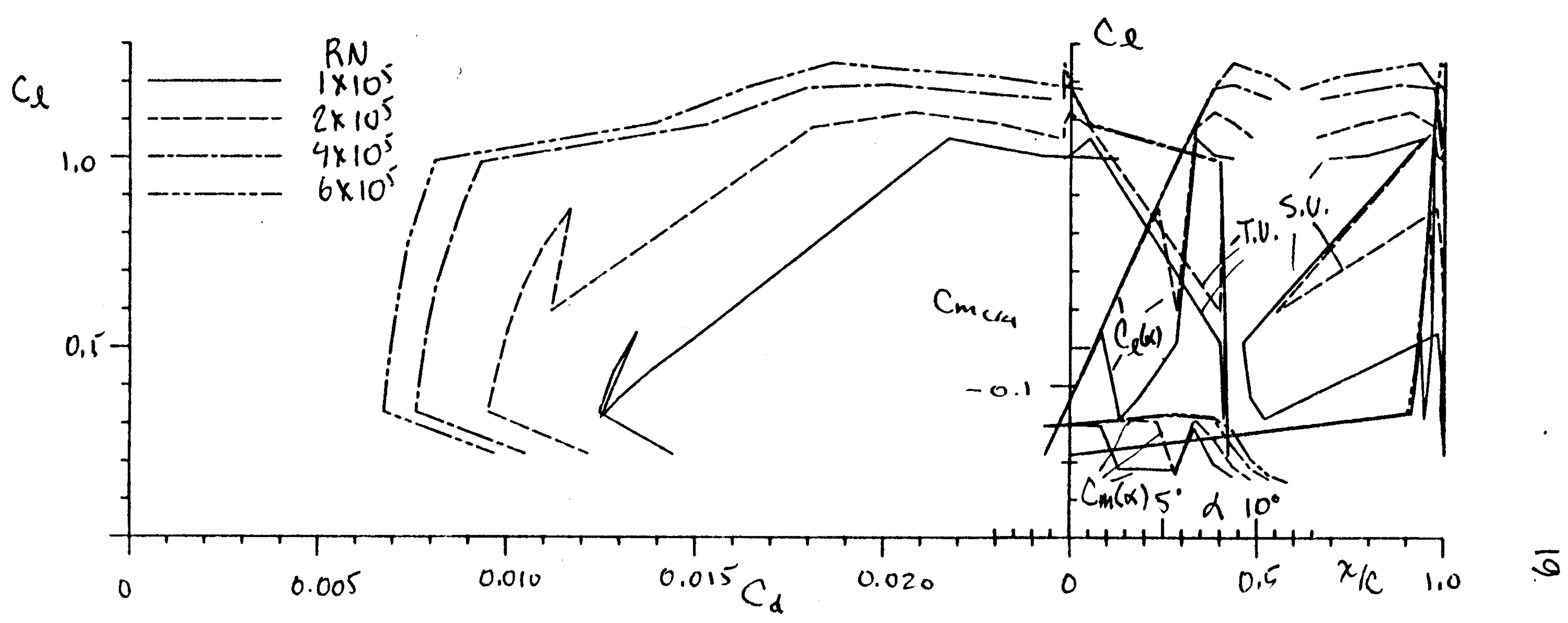

FIG 14 - (CONT) S 4412-093-84

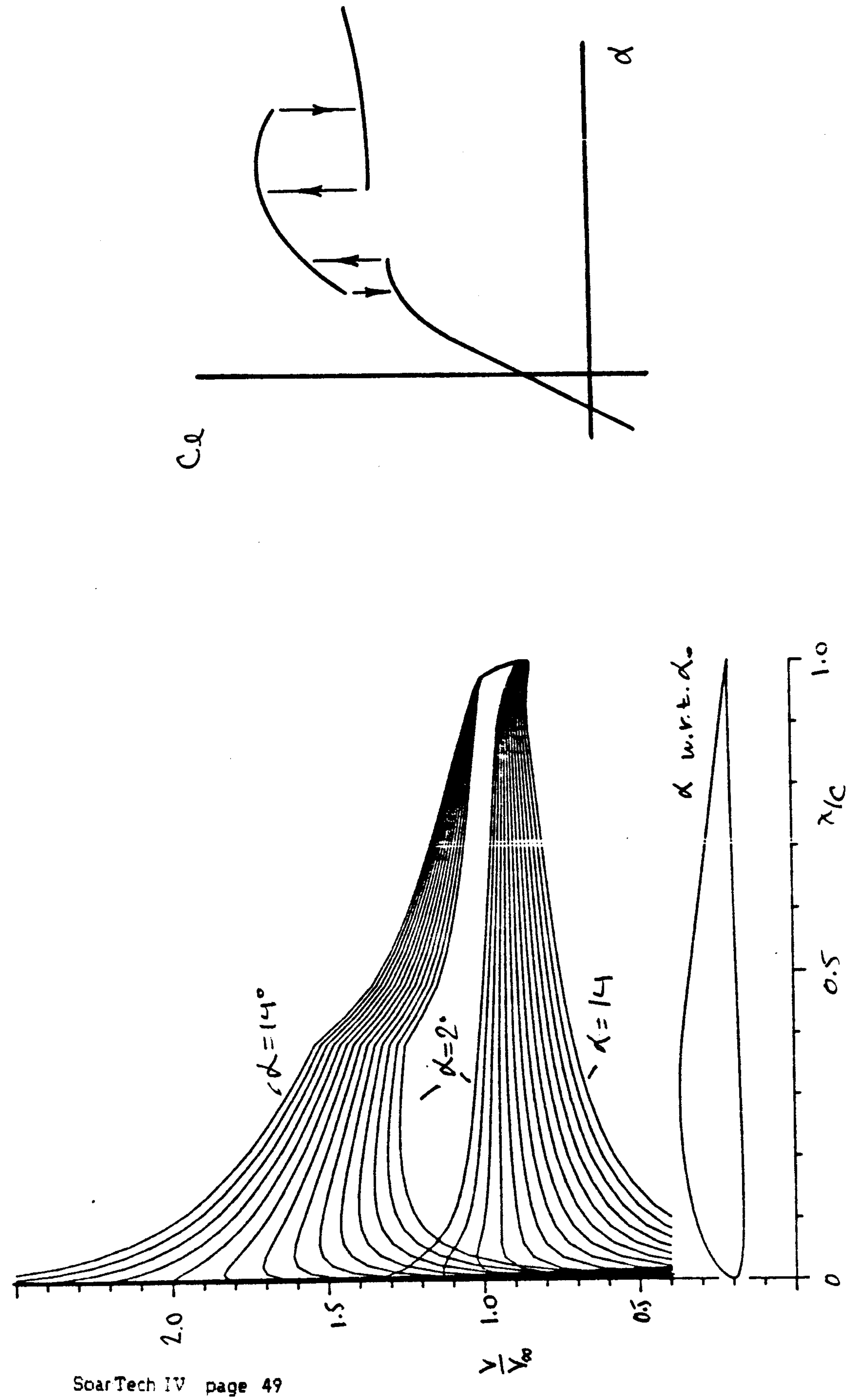

FIG 15 - S4413-098-84

```
TRA1  0013 1750 -150 1750 -150 1850 -050 1950  050 2050  150 2150  250 2250

TRA1  0013 2350  450 2450  540 2550  630 2650  720 2750  810 2850  900 2950

TRA1  0013 3050 1080  000 1170 3350  300 3450  300 3550  400 3650  500 4250

TRA1  0013 6000  500 6000  500 6000  500 6000  500 6000  500 6000  500 6000

TRA2  0013  350 1650  000 3000 0050  650 1650  000  020 1000  400 0150
ALFA100 14  200  300  400  500  600  700  800  900 1000 1100 1200 1300 1400

DIAG
RE  110   03     10003      20003      40003      600
CDCL
ALFA110  1
ENDE
```

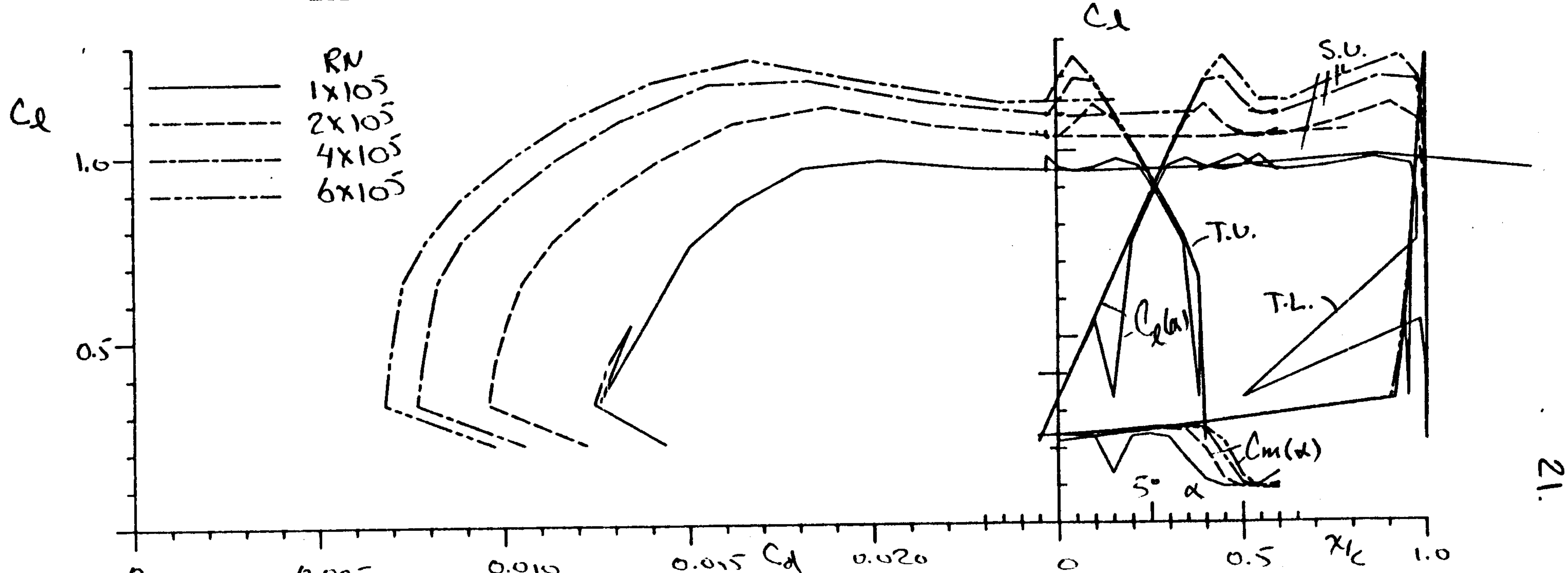

FIG 15 - (CONT) S4413-098-84

AIRFOIL 4410 9.66%

N	X	Y
0	1.00000	0.00000
1	.99671	.00042
2	.98701	.00181
3	.97131	.00436
4	.95010	.00812
5	.92392	.01299
6	.89331	.01880
7	.85877	.02529
8	.82078	.03219
9	.77976	.03921
10	.73609	.04618
11	.69023	.05295
12	.64274	.05938
13	.59411	.06528
14	.54485	.07046
15	.49552	.07477
16	.44649	.07804
17	.39823	.08016
18	.35115	.08109
19	.30567	.08078
20	.26219	.07923
21	.22110	.07648
22	.18279	.07255
23	.14758	.06748
24	.11573	.06132
25	.08747	.05420
26	.06298	.04626
27	.04239	.03768
28	.02580	.02871
29	.01328	.01964
30	.00482	.01085
31	.00046	.00290
32	.00069	-.00298
33	.00671	-.00720
34	.01873	-.01093
35	.03603	-.01390
36	.05861	-.01590
37	.08644	-.01709
38	.11922	-.01769
39	.15652	-.01783
40	.19788	-.01758
41	.24278	-.01701
42	.29068	-.01615
43	.34098	-.01503
44	.39311	-.01364
45	.44654	-.01198
46	.50070	-.01014
47	.55490	-.00820
48	.60880	-.00622
49	.66149	-.00430
50	.71247	-.00251
51	.76109	-.00095
52	.80676	.00033
53	.84886	.00126
54	.88681	.00180
55	.92007	.00197
56	.94811	.00178
57	.97047	.00133
58	.98676	.00075
59	.99667	.00022
60	1.00000	-.00000

ALPHA0 = 3.45 DEGREES

AIRFOIL 4411 9.61%

N	X	Y
0	1.00000	0.00000
1	.99669	.00045
2	.98692	.00195
3	.97110	.00473
4	.94976	.00888
5	.92351	.01435
6	.89295	.02095
7	.85866	.02839
8	.82119	.03636
9	.78102	.04450
10	.73858	.05247
11	.69430	.05996
12	.64855	.06669
13	.60167	.07246
14	.55406	.07715
15	.50613	.08064
16	.45830	.08285
17	.41094	.08369
18	.36444	.08316
19	.31917	.08129
20	.27550	.07815
21	.23378	.07385
22	.19439	.06858
23	.15774	.06247
24	.12422	.05569
25	.09417	.04838
26	.06791	.04070
27	.04574	.03280
28	.02788	.02478
29	.01440	.01677
30	.00525	.00907
31	.00045	.00227
32	.00091	-.00271
33	.00736	-.00650
34	.01943	-.00993
35	.03674	-.01266
36	.05928	-.01450
37	.08705	-.01557
38	.11976	-.01609
39	.15699	-.01619
40	.19827	-.01595
41	.24307	-.01540
42	.29086	-.01461
43	.34106	-.01356
44	.39309	-.01226
45	.44642	-.01070
46	.50048	-.00897
47	.55468	-.00711
48	.60842	-.00524
49	.66107	-.00340
50	.71201	-.00171
51	.76064	-.00022
52	.80633	.00096
53	.84848	.00180
54	.88650	.00225
55	.91982	.00232
56	.94794	.00203
57	.97037	.00149
58	.98671	.00082
59	.99666	.00024
60	1.00000	-.00000

ALPHA0 = 3.77 DEGREES

AIRFOIL 4412 9.30%

N	X	Y
0	1.00000	0.00000
1	.99673	.00060
2	.98742	.00247
3	.97286	.00531
4	.95316	.00852
5	.92825	.01205
6	.89835	.01602
7	.86387	.02047
8	.82524	.02540
9	.78299	.03079
10	.73767	.03665
11	.68990	.04290
12	.64038	.04951
13	.58982	.05638
14	.53904	.06338
15	.48896	.07032
16	.44072	.07663
17	.39488	.08086
18	.35053	.08220
19	.30712	.08131
20	.26508	.07881
21	.22486	.07491
22	.18687	.06986
23	.15154	.06382
24	.11921	.05698
25	.09025	.04952
26	.06495	.04162
27	.04361	.03346
28	.02644	.02517
29	.01352	.01692
30	.00482	.00902
31	.00035	.00207
32	.00102	-.00294
33	.00762	-.00660
34	.01989	-.00982
35	.03742	-.01226
36	.06021	-.01376
37	.08827	-.01446
38	.12130	-.01461
39	.15890	-.01434
40	.20057	-.01375
41	.24581	-.01291
42	.29407	-.01189
43	.34475	-.01069
44	.39729	-.00936
45	.45111	-.00791
46	.50561	-.00646
47	.56013	-.00506
48	.61402	-.00377
49	.66663	-.00263
50	.71729	-.00167
51	.76540	-.00090
52	.81033	-.00033
53	.85152	.00009
54	.88846	.00042
55	.92079	.00073
56	.94820	.00093
57	.97029	.00092
58	.98659	.00064
59	.99661	.00021
60	1.00000	-.00000

ALPHA0 = 3.35 DEGREES

AIRFOIL 4413 9.77%

N	X	Y
0	1.00000	0.00000
1	.99673	.00049
2	.98731	.00205
3	.97238	.00450
4	.95214	.00742
5	.92662	.01077
6	.89609	.01463
7	.86097	.01900
8	.82172	.02388
9	.77985	.02924
10	.73292	.03503
11	.68453	.04121
12	.63435	.04770
13	.58306	.05442
14	.53142	.06128
15	.48025	.06814
16	.43066	.07467
17	.38346	.07974
18	.33816	.08241
19	.29436	.08308
20	.25249	.08214
21	.21294	.07966
22	.17605	.07574
23	.14211	.07049
24	.11138	.06404
25	.08410	.05654
26	.06046	.04817
27	.04059	.03916
28	.02460	.02976
29	.01256	.02029
30	.00448	.01115
31	.00041	.00291
32	.00069	-.00316
33	.00671	-.00741
34	.01889	-.01105
35	.03639	-.01385
36	.05920	-.01564
37	.08730	-.01658
38	.12038	-.01692
39	.15804	-.01679
40	.19977	-.01629
41	.24509	-.01549
42	.29341	-.01446
43	.34417	-.01323
44	.39679	-.01181
45	.45068	-.01025
46	.50526	-.00865
47	.55986	-.00708
48	.61383	-.00560
49	.66650	-.00425
50	.71724	-.00308
51	.76541	-.00209
52	.81041	-.00130
53	.85167	-.00068
54	.88966	-.00018
55	.92102	.00026
56	.94841	.00058
57	.97044	.00067
58	.98667	.00050
59	.99663	.00017
60	1.00000	-.00000

ALPHA0 = 3.03 DEGREES

COORDINATES

THEORETICAL BOUNDARY-LAYER SUMMARY TABLE											
AIRFOIL CLARK-Y	*-LAMINAR SEPARATION BUBBLE WARNING O-NO SEPARATION BUBBLE WARNING ●-NO BUBBLE, TRANSITION BEFORE 0.05C --SEPARATION AT LEADING EDGE (STALL) +-ANGLE OF ATTACK WITHIN DRAG BUCKET										
ALPHA (deg)	REYNOLDS NUMBER										
	60000		100000		200000		400000				
	us	ls	us	ls	us	ls	us	ls	us	ls	
-1	-	-	-	-	*	*	*	●			
0	-	-	*	*	*	*	*	●			
1	*	*	*	*	*	●	*	●			
+ 2	*	*	*	*	*	*	*	●			
+ 3	*	*	*	*	*	*	*	*			
+ 4	*	*	*	*	*	*	*	*			
+ 5	*	*	*	*	*	*	*	*			
+ 6	*	*	*	*	*	*	*	*			
+ 7	*	*	*	*	*	*	*	*			
+ 8	*	*	*	*	*	*	O	*			
+ 9	*	*	*	*	*	*	O	*			
+10	*	*	*	*	*	*	O	*			
11	*	*	*	*	●	*	●	*			
12	*	*	*	*	●	*	●	*			

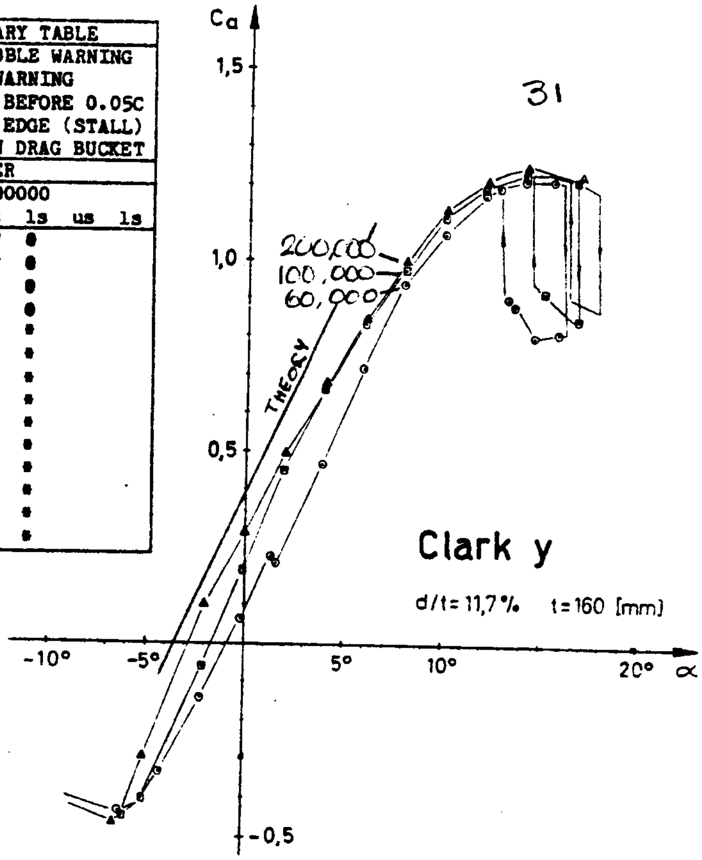

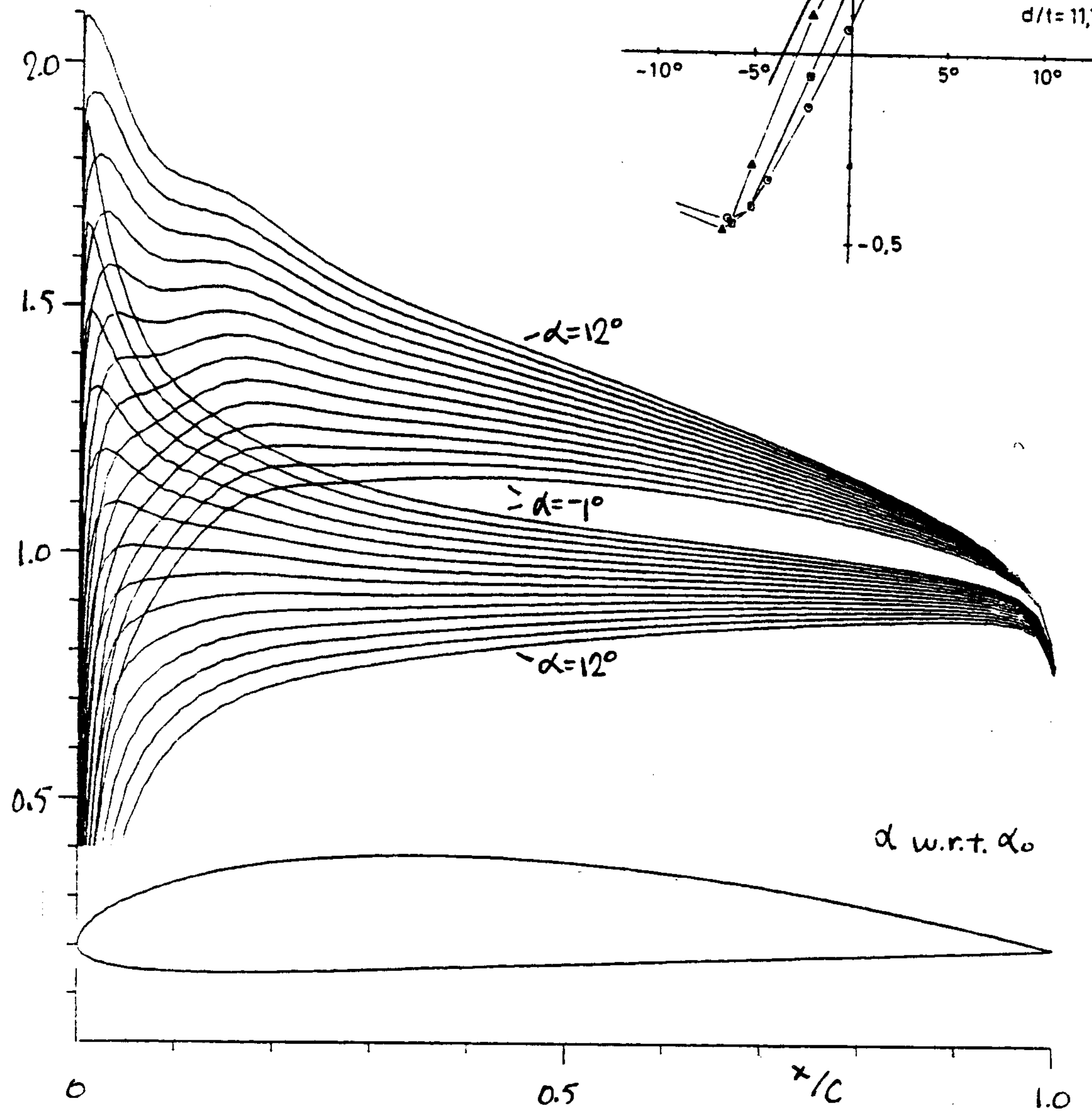

FIGURE 7. - VELOCITY DISTRIBUTIONS FOR THE CLARK-Y AIRFOIL.

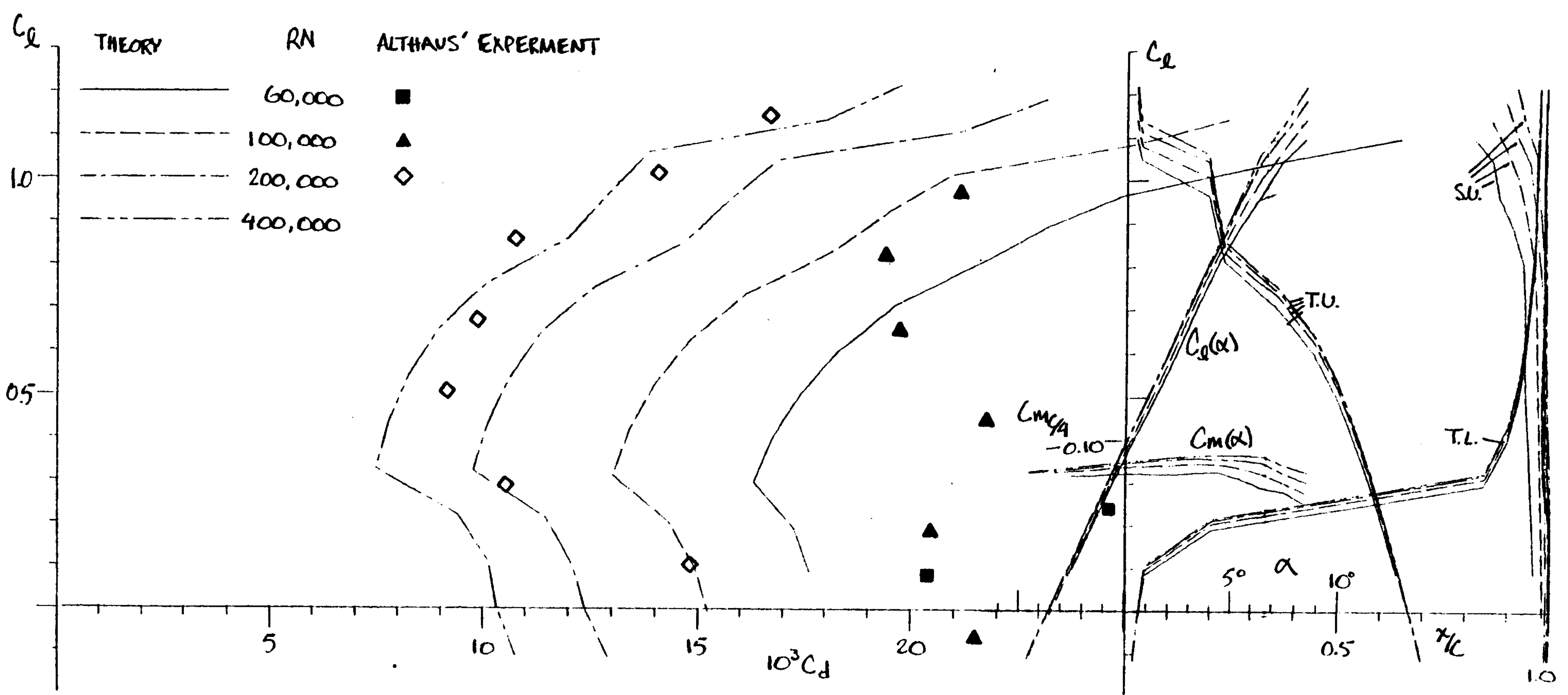

FIGURE 8.- COMPARISON OF THE THEORETICAL AND EXPERIMENTAL SECTION CHARACTERISTICS FOR THE CLARK-Y AIRFOIL.

THEORETICAL BOUNDARY-LAYER SUMMARY TABLE										
AIRFOIL GOE 801	*-LAMINAR SEPARATION BUBBLE WARNING O-NO SEPARATION BUBBLE WARNING ●-NO BUBBLE, TRANSITION BEFORE 0.05C --SEPARATION AT LEADING EDGE (STALL) +-ANGLE OF ATTACK WITHIN DRAG BUCKET									
ALPHA (deg)	REYNOLDS NUMBER									
	60000		80000		150000		400000			
	us	ls	us	ls	us	ls	us	ls	us	ls
5	-	-	-	-	-	-	*	*		
7	*	*	*	*	*	*	*	●		
+ 9	*	*	*	*	*	*	O	*		
+10	*	*	*	*	*	*	O	*		
+11	*	*	*	*	*	*	O	*		
+12	*	*	*	*	*	*	O	*		
+13	*	*	*	*	*	*	O	*		
+14	*	*	*	*	*	*	O	*		
+15	*	*	*	*	O	*	O	*		
16	*	*	*	*	●	*	●	*		
17	*	*	*	*	●	*	●	*		

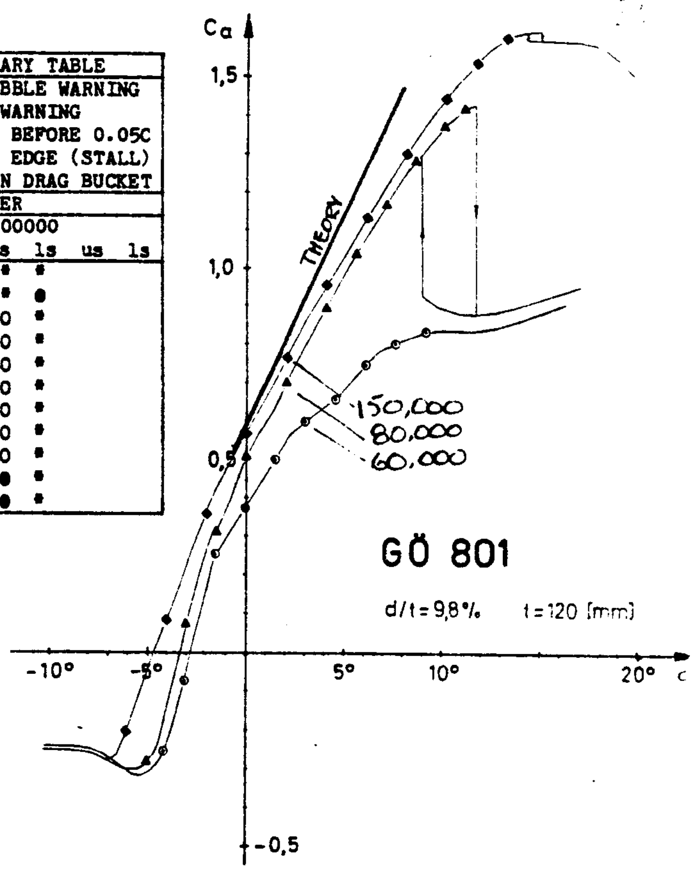

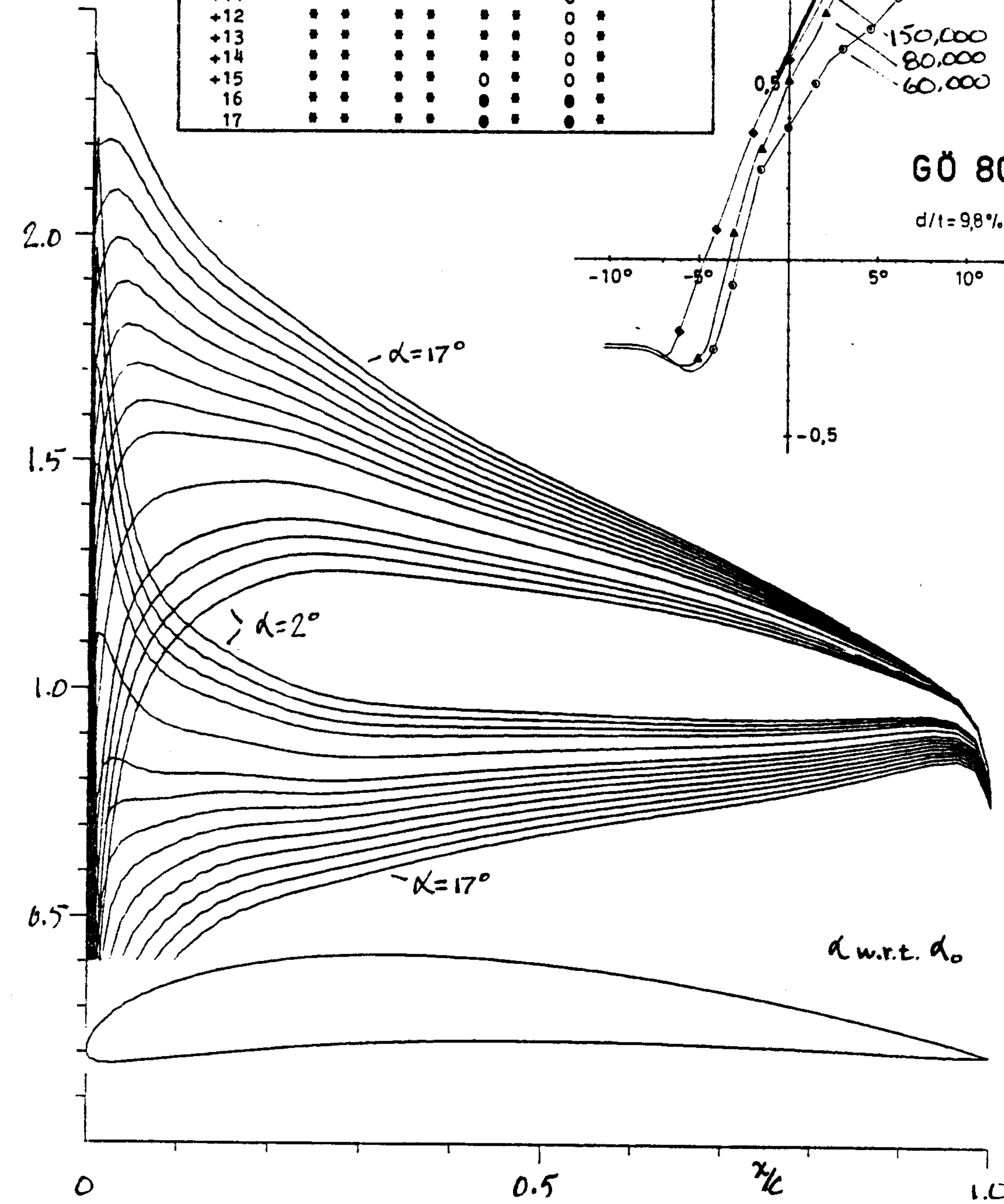

FIGURE 11. - VELOCITY DISTRIBUTIONS FOR THE GOE 801 AIRFOIL.

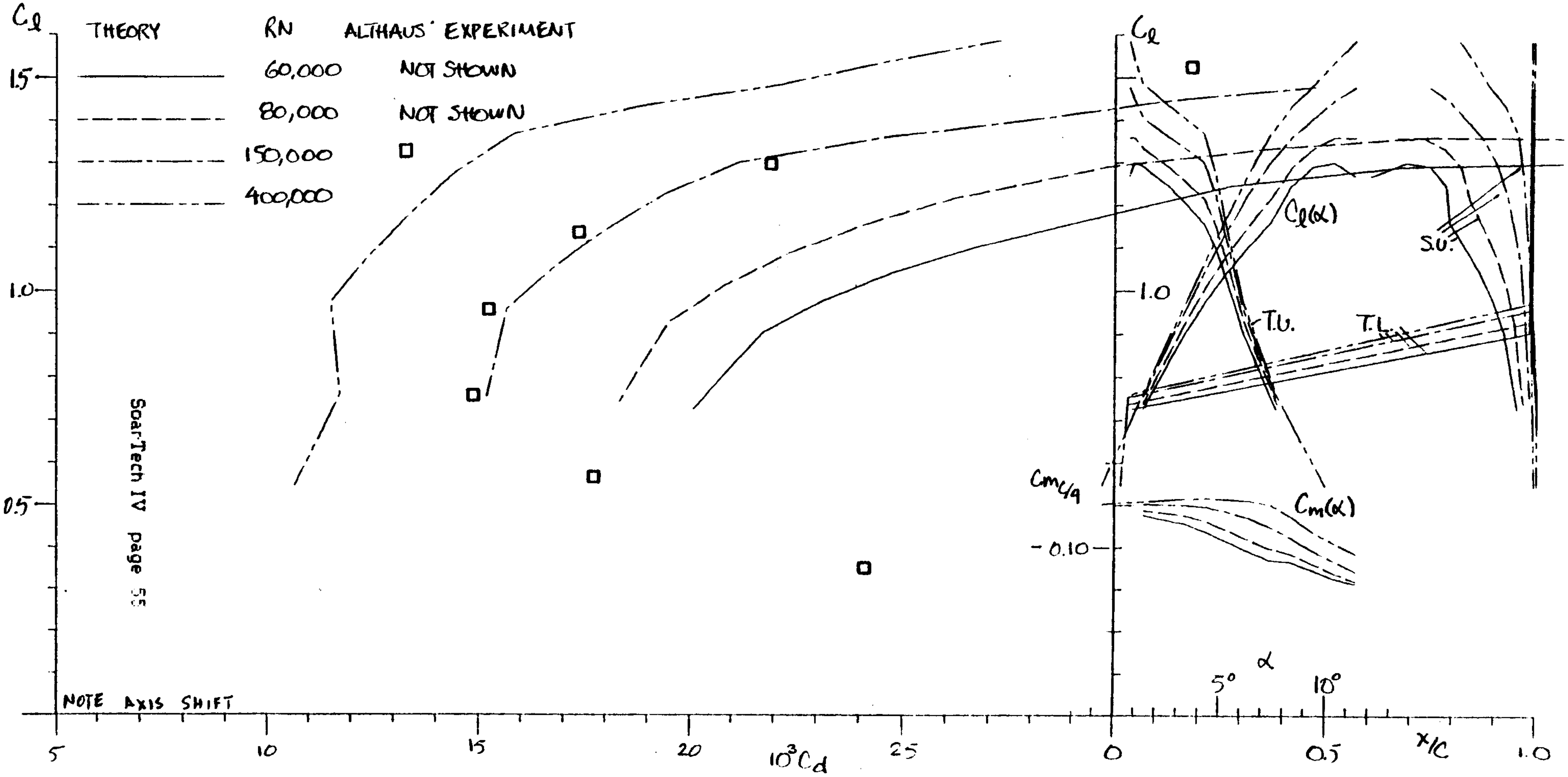

FIGURE 12.- COMPARISON OF THE THEORETICAL AND EXPERIMENTAL SECTION CHARACTERISTICS FOR THE GOE 801 AIRFOIL.

THEORETICAL BOUNDARY-LAYER SUMMARY TABLE										
AIRFOIL FX 61-140	*-LAMINAR SEPARATION BUBBLE WARNING O-NO SEPARATION BUBBLE WARNING ●-NO BUBBLE, TRANSITION BEFORE 0.05C --SEPARATION AT LEADING EDGE (STALL) +-ANGLE OF ATTACK WITHIN DRAG BUCKET									
ALPHA (deg)	REYNOLDS NUMBER									
	60000		100000		200000		400000			
	us	ls	us	ls	us	ls	us	ls	us	ls
0	-	-	-	-	-	-	*	*		
1	-	-	-	-	*	●	*	●		
+ 2	*	*	*	*	*	*	*	*		
+ 3	*	*	*	*	*	*	*	*		
+ 5	*	*	*	*	*	*	*	*		
+ 7	*	*	*	*	*	*	*	*		
+ 9	*	*	*	*	*	*	*	*		
+10	*	*	*	*	*	*	*	*		
11	●	*	●	*	●	*	●	*		
12	●	*	●	*	●	*	●	*		
13	*	*	*	*	●	*	●	*		
14	*	*	*	*	*	*	●	*		

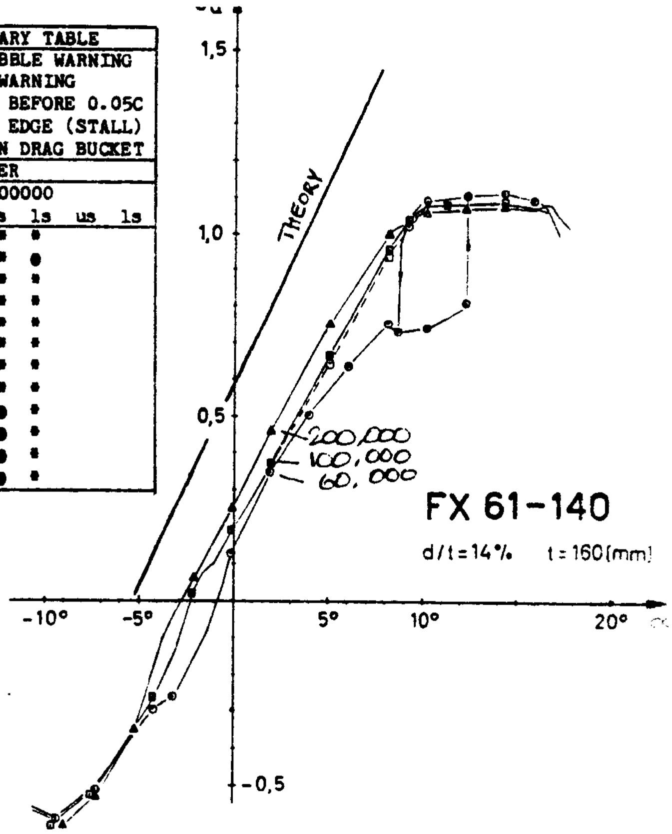

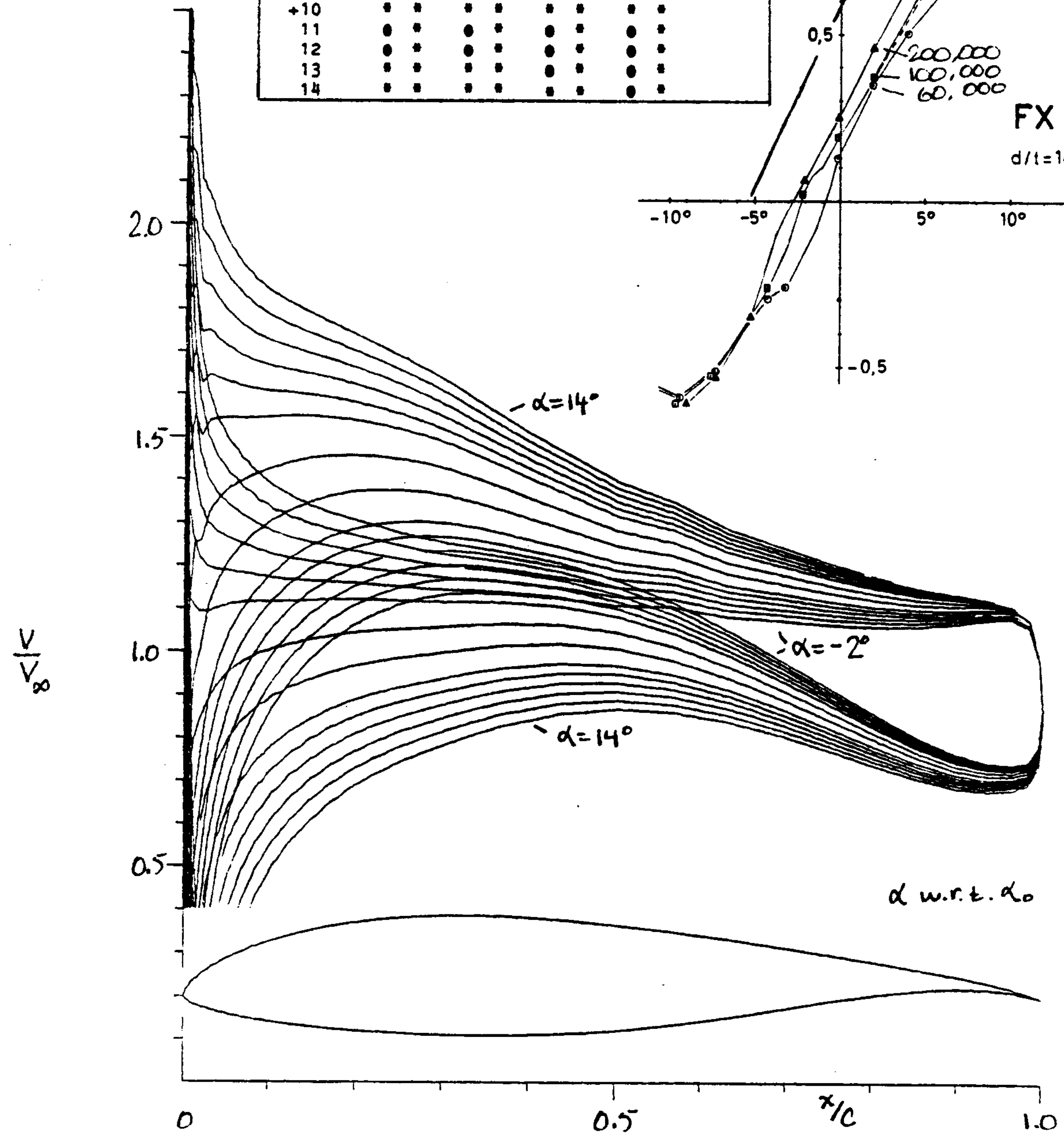

FIGURE 13.- VELOCITY DISTRIBUTIONS FOR THE FX 61-140 AIRFOIL.

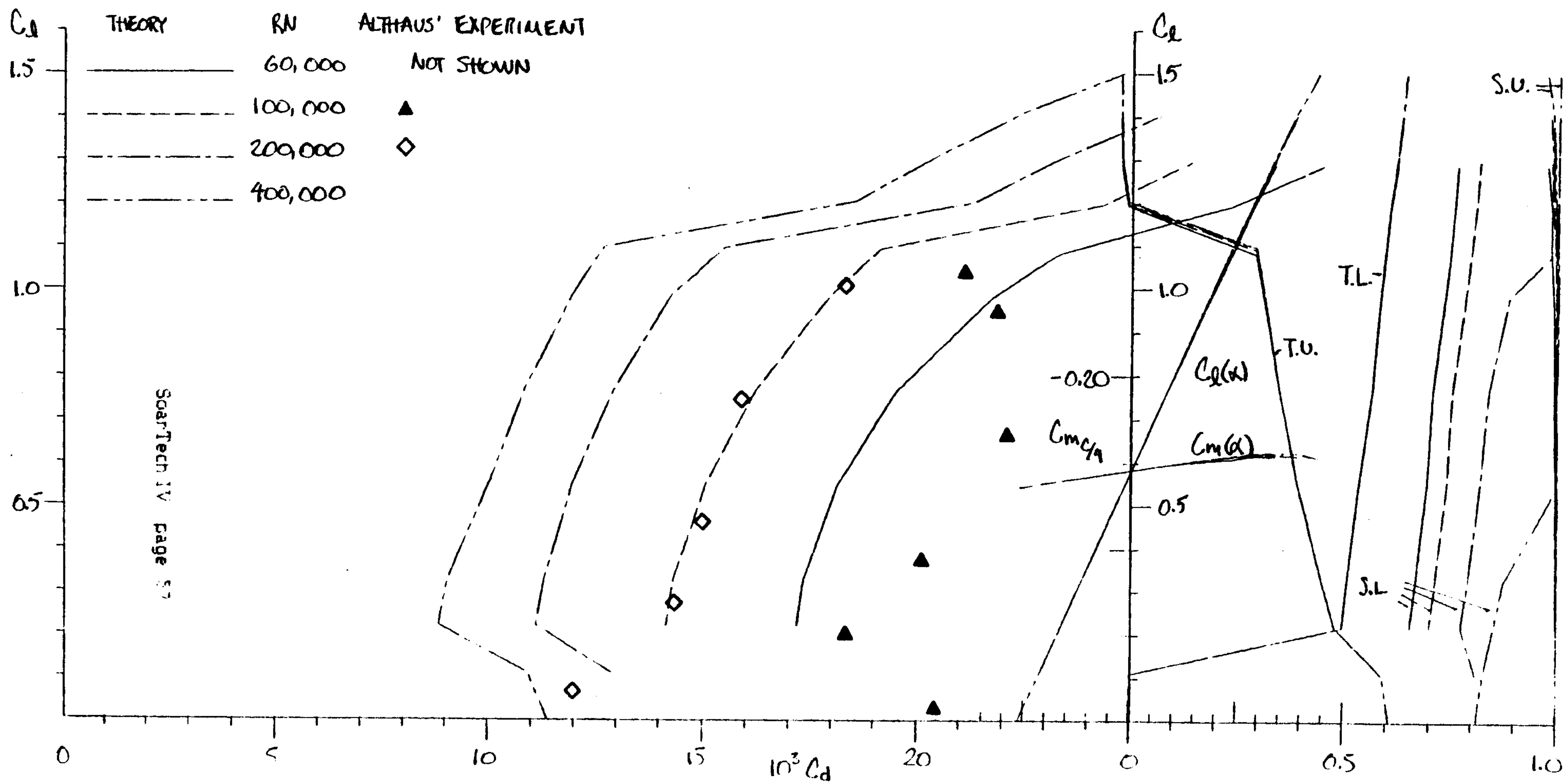

FIGURE 14. - COMPARISON OF THE THEORETICAL AND EXPERIMENTAL SECTION CHARACTERISTICS FOR THE FX 61-140 AIRFOIL.

THEORETICAL BOUNDARY-LAYER SUMMARY TABLE										
AIRFOIL E 392	*-LAMINAR SEPARATION BUBBLE WARNING O-NO SEPARATION BUBBLE WARNING ●-NO BUBBLE, TRANSITION BEFORE 0.05C --SEPARATION AT LEADING EDGE (STALL) +-ANGLE OF ATTACK WITHIN DRAG BUCKET									
ALPHA (deg)	REYNOLDS NUMBER									
	60000		100000		200000		400000			
	us	ls	us	ls	us	ls	us	ls	us	ls
1	*	*	*	*	*	●	*	●		
+ 2	*	*	*	*	*	*	*	*		
+ 3	*	*	*	*	*	*	*	*		
+ 4	*	*	*	*	*	*	*	*		
+ 5	*	*	*	*	*	*	*	*		
+ 6	*	O	*	O	*	O	*	O		
+ 7	*	O	*	O	*	O	*	O		
+ 8	*	O	*	O	*	O	*	O		
+ 9	*	O	*	O	*	O	*	O		
+10	*	O	*	O	*	O	*	O		
11	●	O	●	O	●	O	●	O		
12	●	O	*	O	●	O	●	O		
13	*	O	*	O	*	O	●	O		
14	*	O	*	O	*	O	●	O		

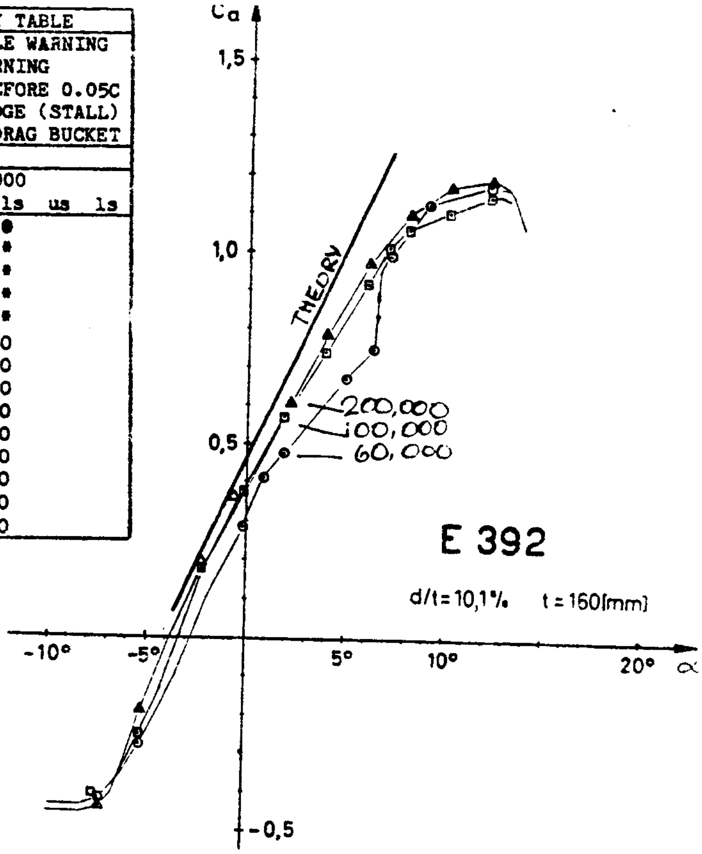

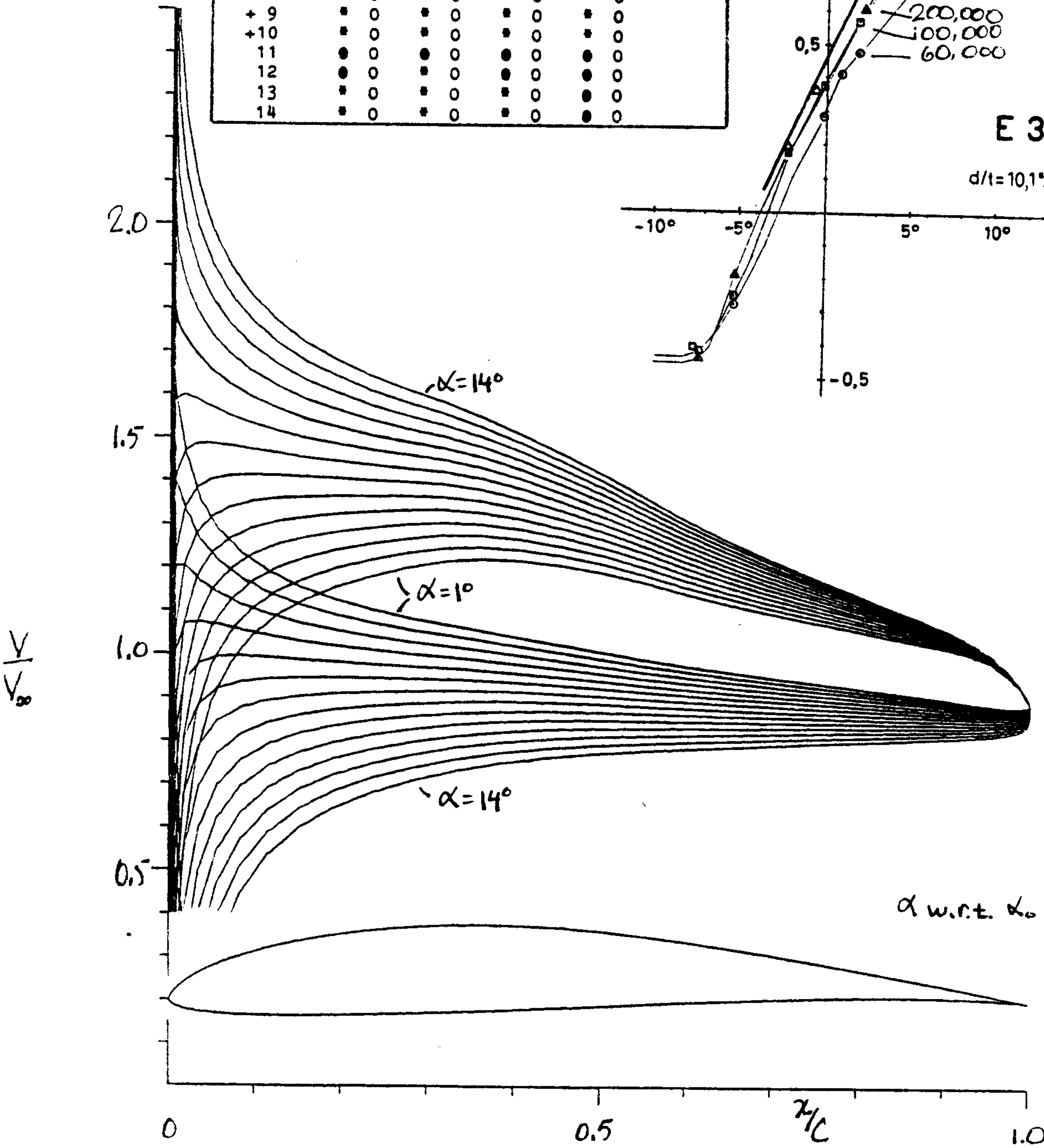

FIGURE 19.- VELOCITY DISTRIBUTIONS FOR THE E392 AIRFOIL.

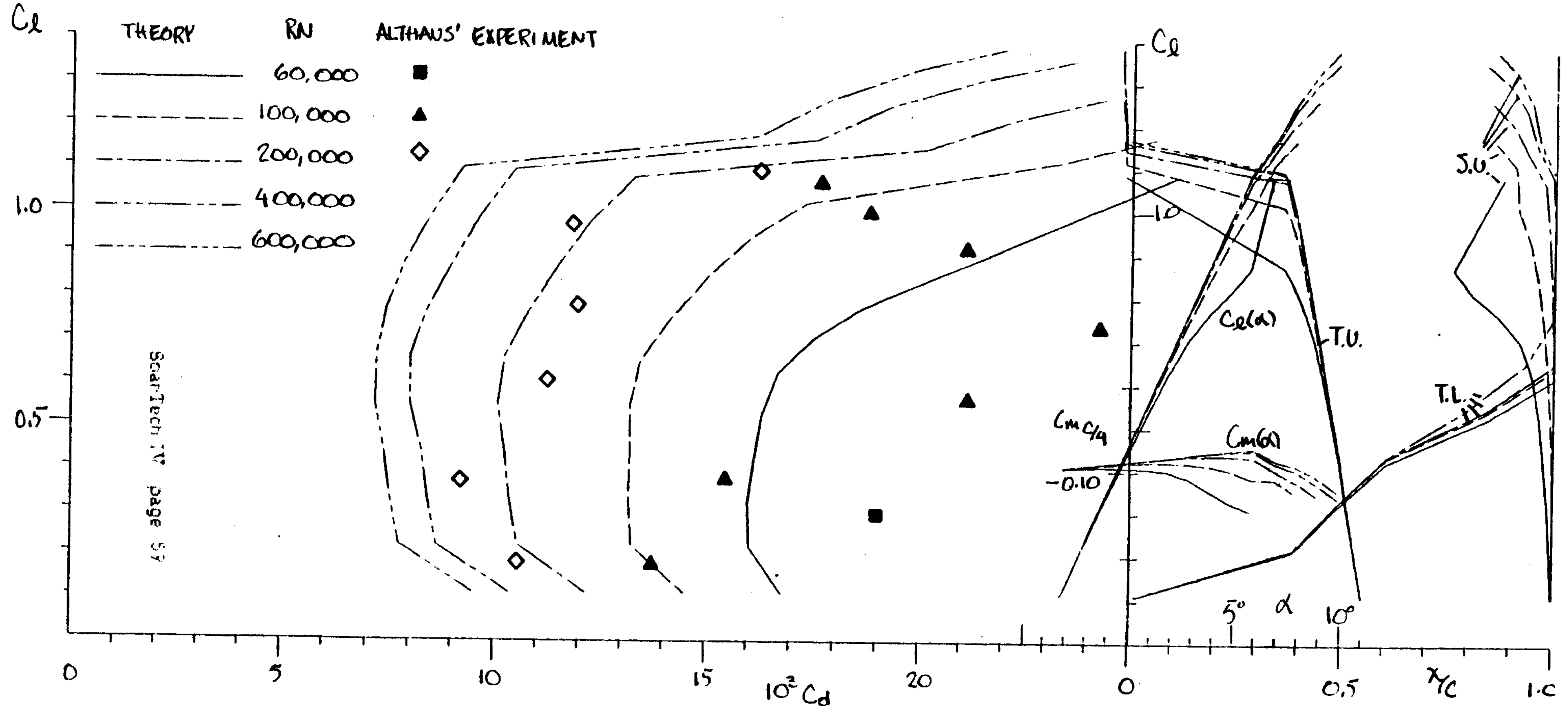

FIGURE 20. - COMPARISON OF THE THEORETICAL AND EXPERIMENTAL SECTION CHARACTERISTICS FOR THE E392 AIRFOIL.

THEORETICAL BOUNDARY-LAYER SUMMARY TABLE										
AIRFOIL	*-LAMINAR SEPARATION BUBBLE WARNING									
	O-NO SEPARATION BUBBLE WARNING									
	●-NO BUBBLE, TRANSITION BEFORE 0.05C									
	--SEPARATION AT LEADING EDGE (STALL)									
GOE 795	+-ANGLE OF ATTACK WITHIN DRAG BUCKET									
ALPHA	REYNOLDS NUMBER									
(deg)	40000		60000		80000		400000			
	us	ls	us	ls	us	ls	us	ls	us	ls
-2	-	-	-	-	-	-	*	●		
-1	-	-	-	-	-	-	*	●		
0	-	-	*	*	*	*	*	●		
+ 1	*	*	*	*	*	*	*	O		
+ 2	*	*	*	*	*	*	*	*		
+ 3	*	*	*	*	*	*	*	*		
+ 4	*	*	*	*	*	*	*	*		
+ 5	*	*	*	*	*	*	*	*		
+ 6	*	*	*	*	*	*	*	*		
+ 7	*	*	*	*	*	*	*	*		
8	*	*	*	*	*	*	●	*		
9	●	*	●	*	●	*	●	*		
10	●	*	●	*	●	*	●	*		

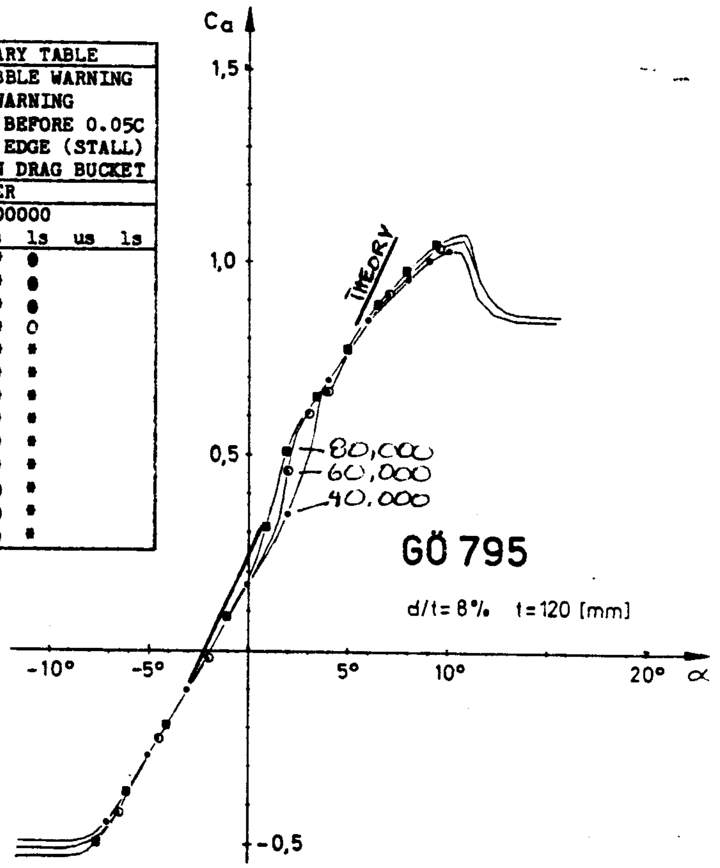

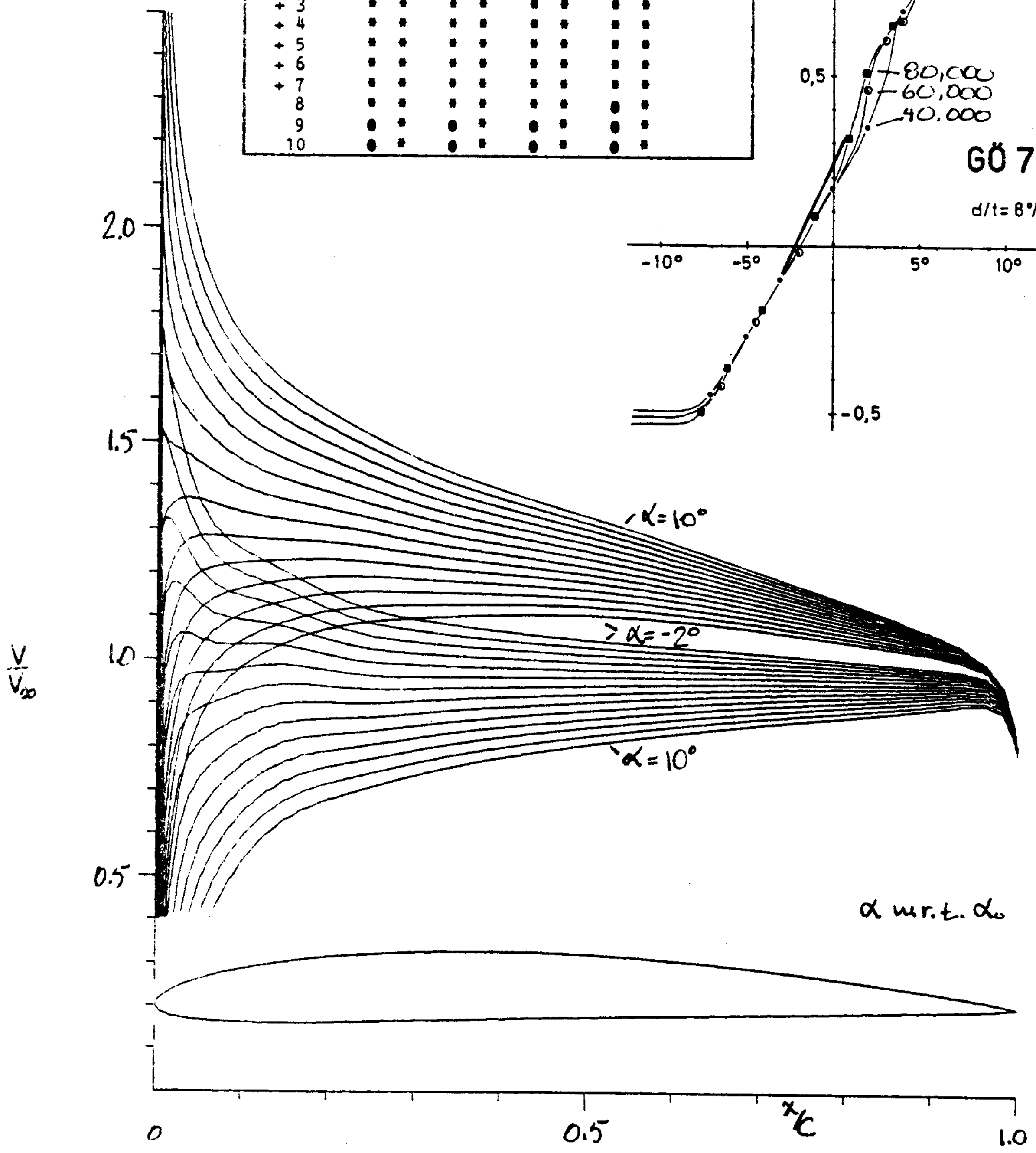

FIGURE 21.- VELOCITY DISTRIBUTIONS FOR THE GOE 795 AIRFOIL.

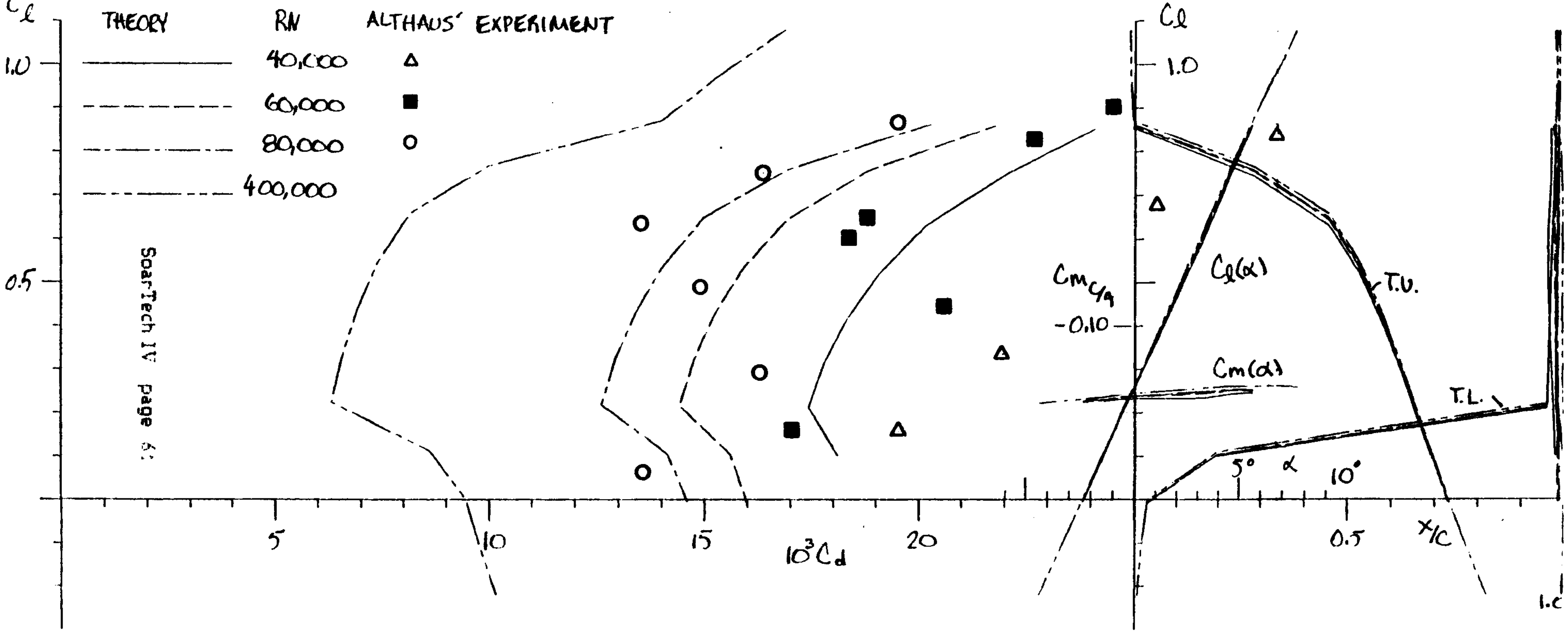

FIGURE 22.- COMPARISON OF THE THEORETICAL AND EXPERIMENTAL SECTION CHARACTERISTICS FOR THE GOE 795 AIRFOIL.

THEORETICAL BOUNDARY-LAYER SUMMARY TABLE										
AIRFOIL AH 79-100A	*-LAMINAR SEPARATION BUBBLE WARNING O-NO SEPARATION BUBBLE WARNING ●-NO BUBBLE, TRANSITION BEFORE 0.05C --SEPARATION AT LEADING EDGE (STALL) +-ANGLE OF ATTACK WITHIN DRAG BUCKET									
ALPHA (deg)	REYNOLDS NUMBER									
	60000		100000		200000		400000			
	us	ls	us	ls	us	ls	us	ls	us	ls
1	*	*	*	*	*	●	*	●		
+ 2	*	*	*	*	*	*	*	*		
+ 3	*	*	*	*	*	*	*	*		
+ 4	*	*	*	*	*	*	*	*		
+ 5	*	*	*	*	*	*	*	*		
+ 6	*	*	*	*	*	*	*	*		
+ 7	*	*	*	*	*	*	*	*		
+ 8	*	O	*	O	*	O	*	O		
+ 9	*	O	*	O	*	O	*	O		
+10	*	O	*	O	*	O	O	O		
11	*	O	●	O	●	O	●	O		
12	-	-	*	O	●	O	●	O		
13	-	-	-	-	*	O	●	O		

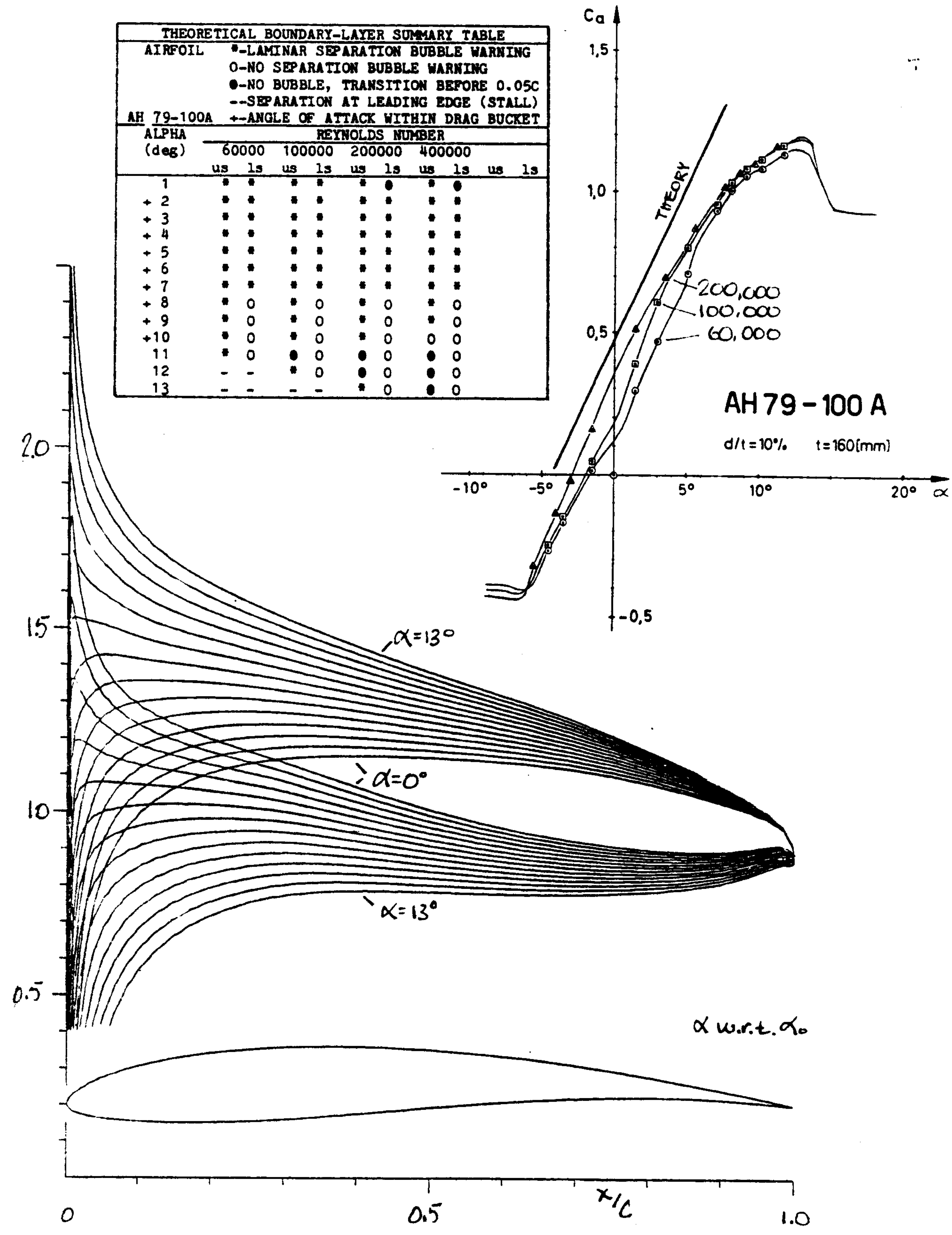

FIGURE 27.- VELOCITY DISTRIBUTIONS FOR THE AH 79-100 A AIRFOIL.

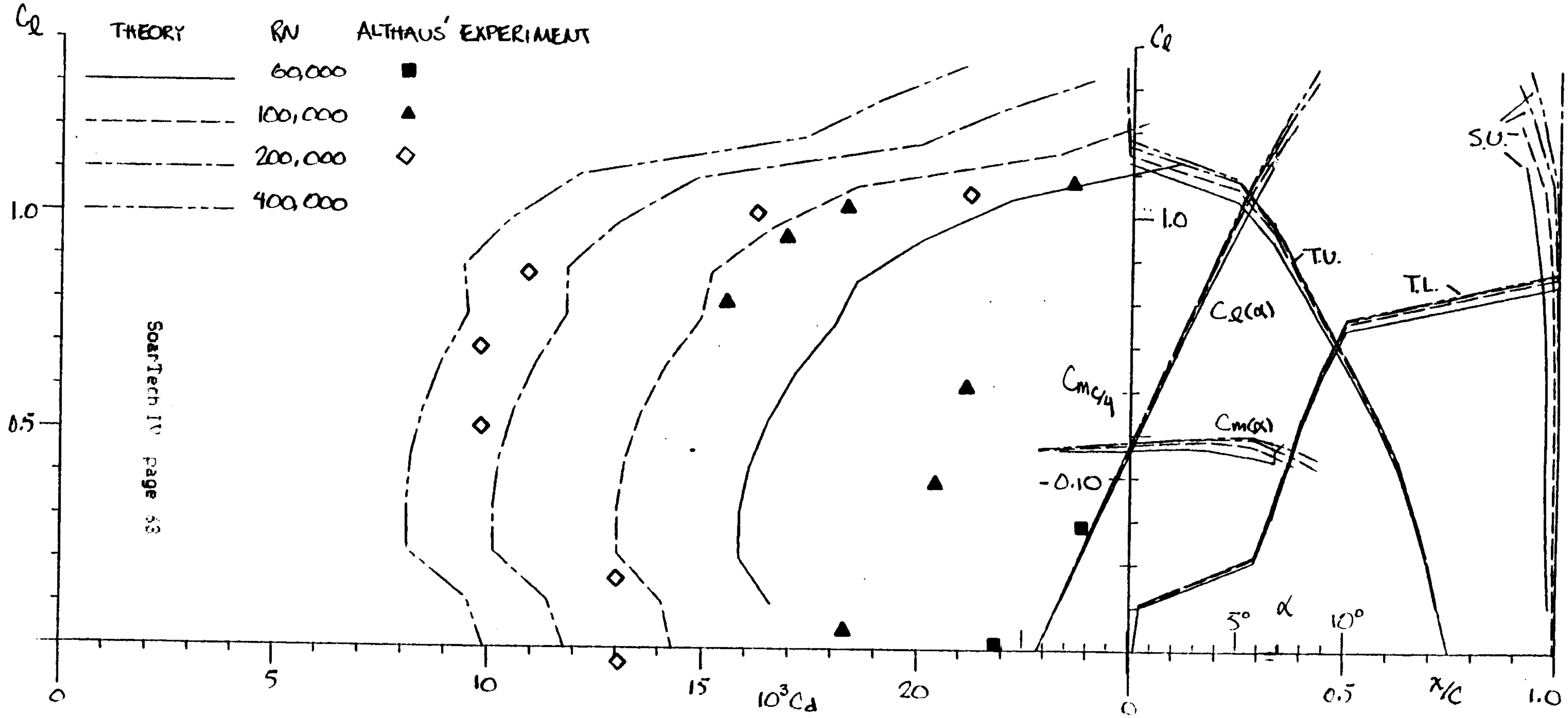

FIGURE 28. - COMPARISON OF THE THEORETICAL AND EXPERIMENTAL SECTION CHARACTERISTICS FOR THE AH79-100A AIRFOIL.

THEORETICAL BOUNDARY-LAYER SUMMARY TABLE										
AIRFOIL ME214F	*-LAMINAR SEPARATION BUBBLE WARNING O-NO SEPARATION BUBBLE WARNING ●-NO BUBBLE, TRANSITION BEFORE 0.05C --SEPARATION AT LEADING EDGE (STALL) +-ANGLE OF ATTACK WITHIN DRAG BUCKET									
ALPHA (deg)	REYNOLDS NUMBER									
			100000		200000		400000		600000	
	us	ls	us	ls	us	ls	us	ls	us	ls
-2			-	-	-	-	-	-	*	*
-1			-	-	-	-	*	●	*	●
0			*	*	*	●	*	●	*	●
+ 1			*	*	*	*	*	*	*	*
+ 3			*	*	*	*	*	*	*	*
+ 5			*	*	*	*	*	*	*	*
+ 6			*	*	*	*	*	*	*	*
+ 7			*	*	*	*	*	*	O	*
+ 8			*	*	*	*	*	*	O	*
+ 9			*	*	*	*	*	*	O	*
+10			*	*	*	*	O	*	O	*
11			*	*	●	*	●	*	●	*
12			*	*	●	*	●	*	●	*

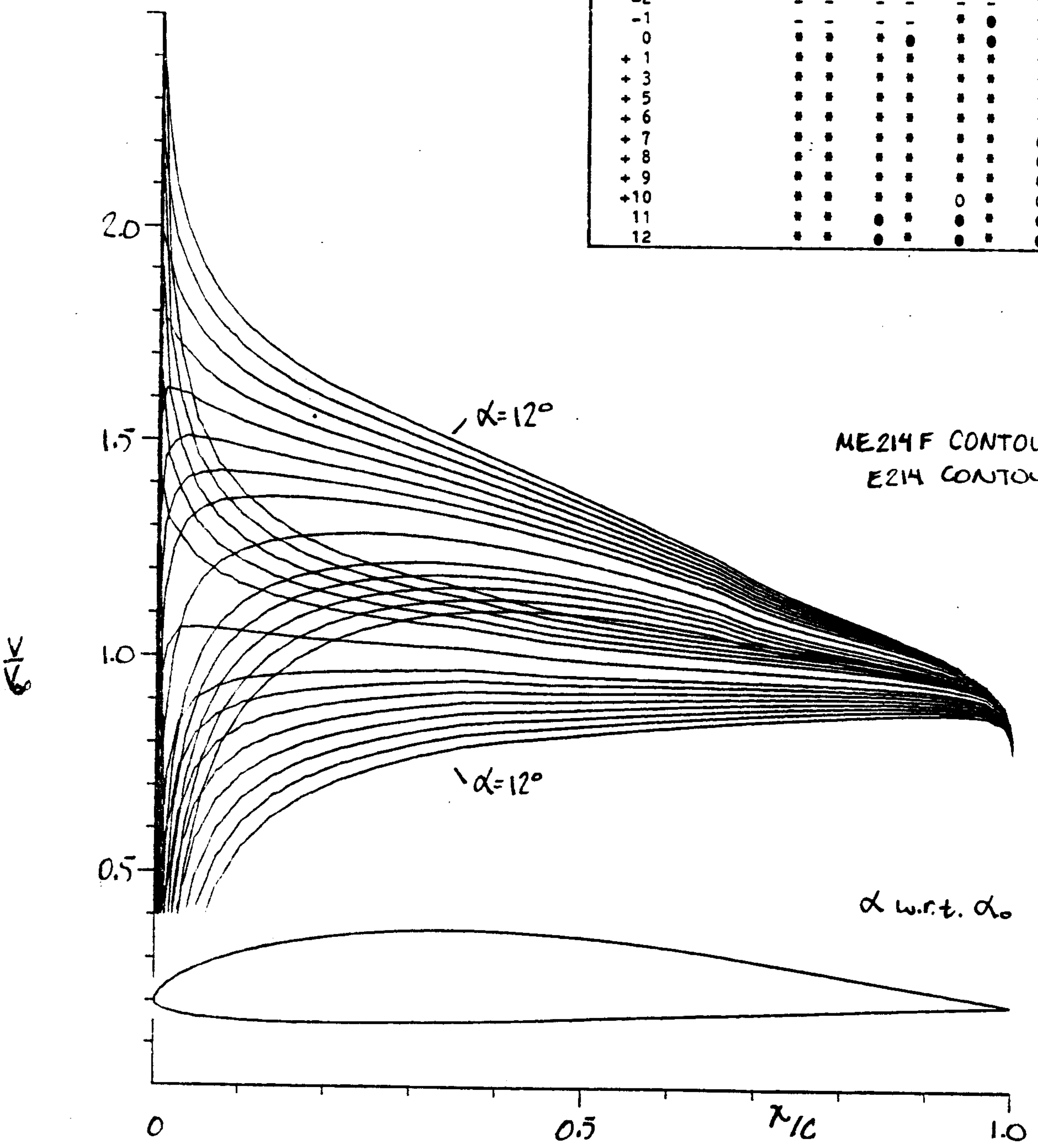

FIGURE 46.- VELOCITY DISTRIBUTIONS FOR THE ME214 F AIRFOIL.

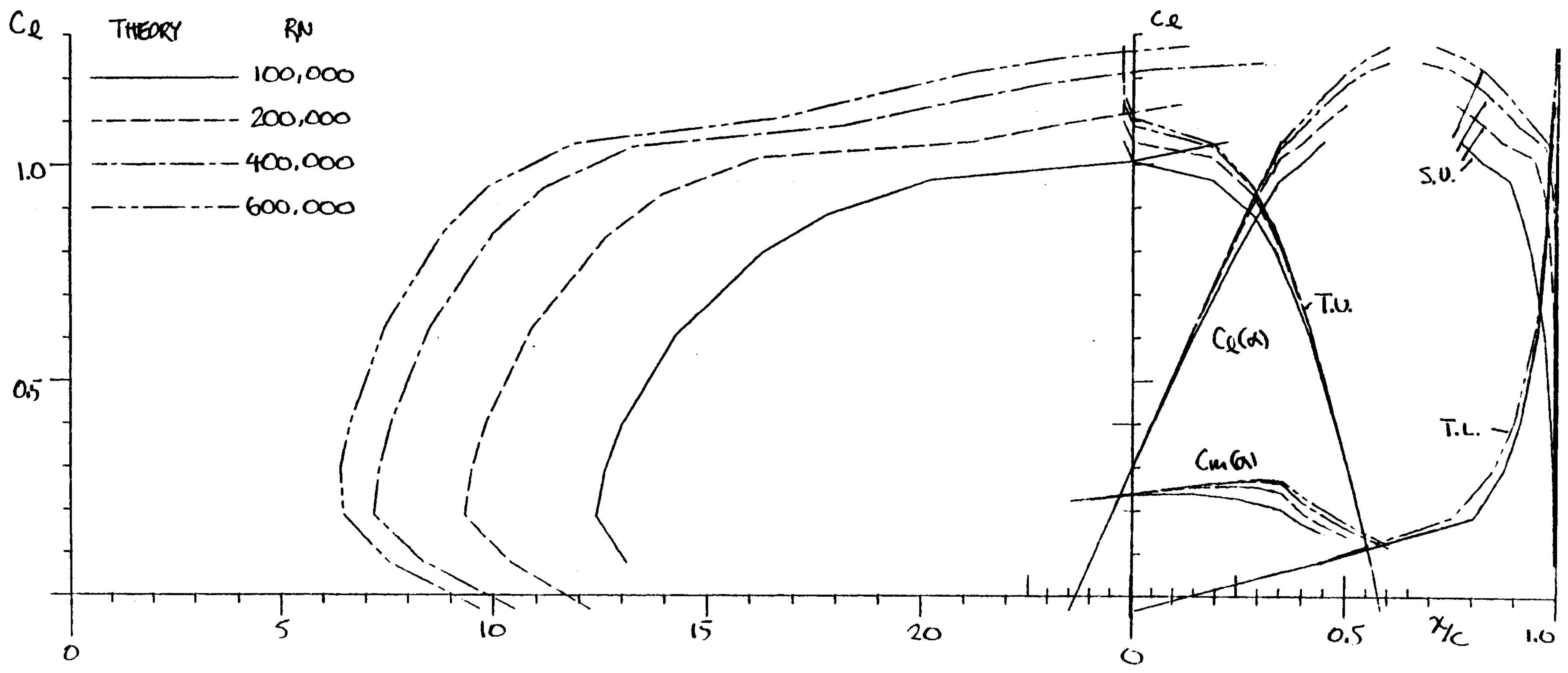

FIGURE 47. - THEORETICAL SECTIONS CHARACTERISTICS FOR THE ME 214 F AIRFOIL.

HEWITT PHILLIPS

When a flap type of control is deflected, the control force is nearly proportional to the deflection angle - up to a point. Beyond that point, the linearity of the response is lost with control force increasing less and less and drag becoming much higher. Double hinged controls have been used on several aircraft to get more control force than is possible with single surfaces.

The offering here is an update of a paper Hewitt did earlier for the Journal of the old East Coast Soaring Society. Hewitt has a plane with a double hinged rudder. It's a big sailplane with a fairly long tail moment - but the fin and rudder are tiny in comparison to the rest of the model. Hewitt flys the model very well, and the control available is a testimony to the effectiveness of this scheme. Its use isn't limited to rudders; any control surface's response can be improved by this arrangement. Rudders and flaps are the places it's most usually used. Careful attention to design details is necessary because this kind of arrangement is sometimes more prone to flutter.

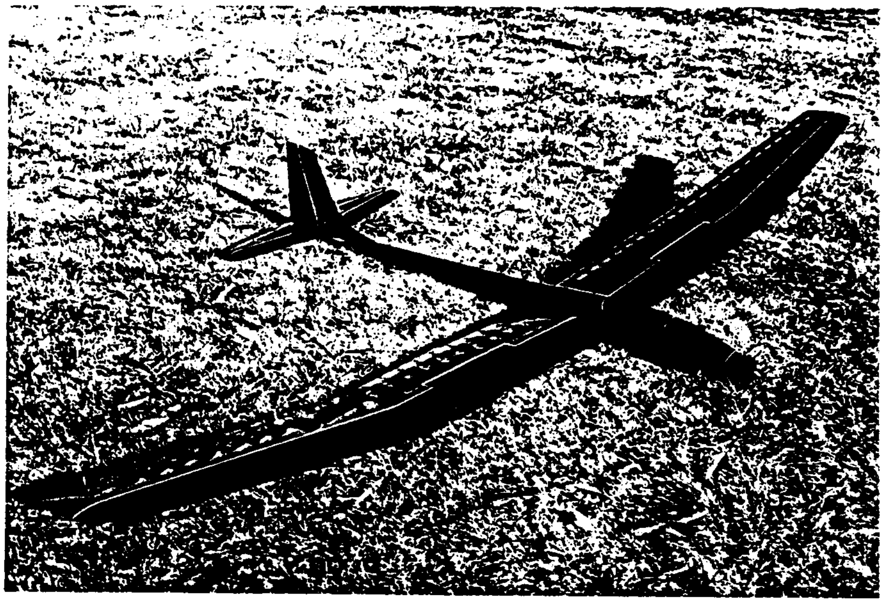

HEWITT PHILLIPS
310 MANTEO AV.
HAMPTON, VA. 23661

THE DOUBLE-HINGED RUDDER

By Hewitt Phillips

Hardly anyone objects to having more rudder effectiveness on an R/C glider. Most popular designs are sporting large, slab-sided rudders. The author's own models usually have ended up with several strips glued on the rudder to extend the chord, span, or both.

The need for rudder effectiveness arises in part from the usual short tail length and the need to overcome the large inertia in yaw of the large-span wing when initiating or recovering from a turn. Increasing the rudder area increases the drag, however. The rudder should, therefore, be as effective as possible for a given area.

One way to increase the effectiveness of a rudder without increasing its size is to use a double-hinged rudder. This method is used on some well-known transport airplanes, such as the Boeing 727 and the McDonnell-Douglas DC-10, to obtain the maximum cross-wind landing capability with a given size tail. (Figure 1)

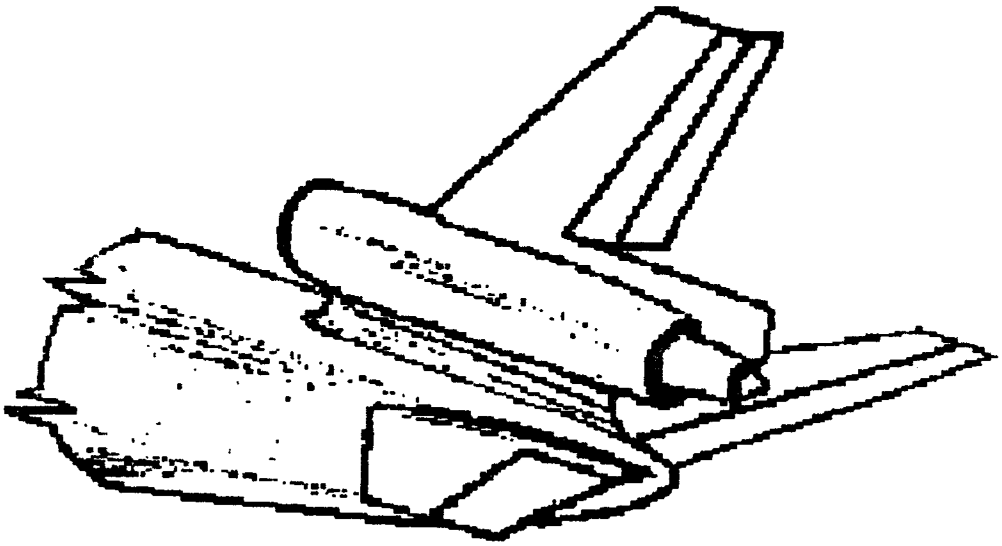

Figure 1: Double-hinged rudder on the McDonnell-Douglas DC-10

The principle of the double-hinged rudder is shown in figure 2, along with three possible mechanisms for obtaining the desired action. The "crossed-thread" mechanism seems particularly easy to apply to models.

The double-hinged rudder is more effective than a single-hinged rudder for two reasons. First, the lift on the rear segment carries forward onto the rest of the vertical tail, causing an increased side force far greater than that on the rear segment itself. Second, the rear segment acts like a trailing edge flap, allowing at least as great a deflection of the forward segment to be reached before the rudder stalls as with a conventional rudder. The effectiveness is thereby increased while keeping the rudder in the region of unstalled, low drag operation.

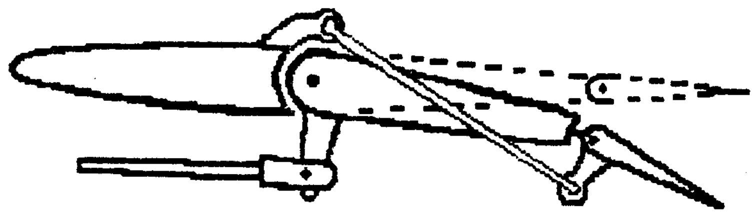

PUSHROD

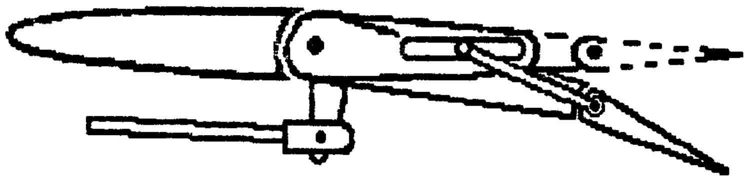

CRANK and SLOT

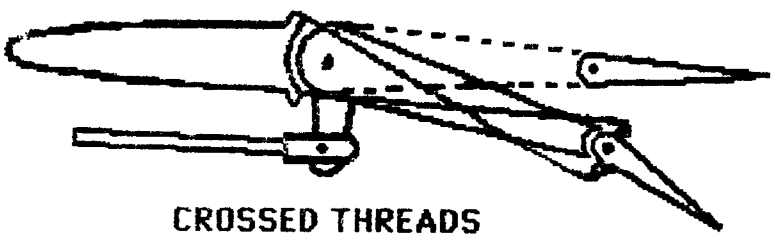

CROSSED THREADS

FIGURE 2; Three possible mechanisms for operating a double-hinged rudder.

Calculation of the effectiveness of a rudder in terms of the tail lift produced per degree deflection of the rudder can be made with the aid of two curves, Figures 3 and 4, obtained from the reference report in these calculations, the tail is assumed to be unstalled. The rudder effectiveness therefore applies to the case of moderate maneuvers or corrections to the flight path which do not involve maximum rudder deflection or large side slip angles.

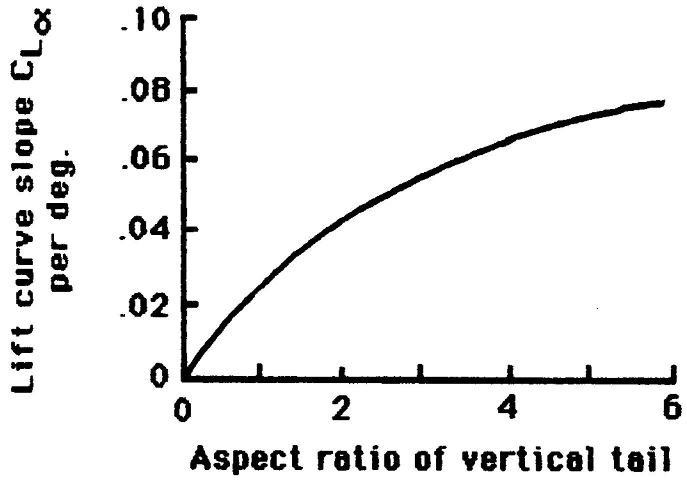

Figure 3.- Lift curve slope of vertical tail as a function of aspect ratio.

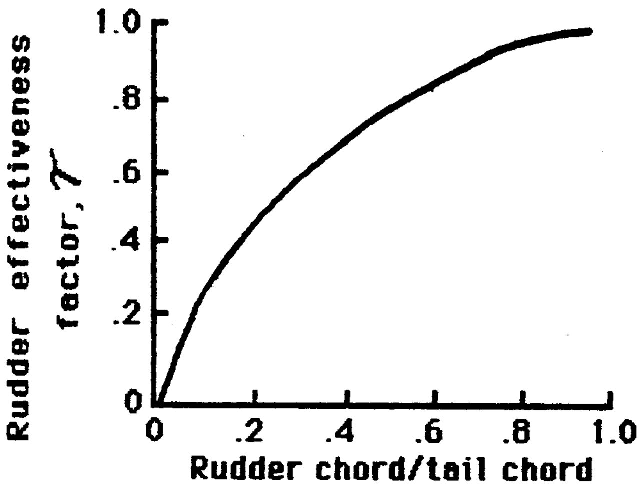

Figure 4.- Ratio of lift of tail due to rudder deflection to lift due to change in angle of attack of tail.

As will be shown later, the same curves may be used to calculate the effectiveness of a double-hinged rudder. These curves apply to the case of sealed hinge gaps between the surfaces. Sealed gaps themselves often increase the effectiveness of rudders by about 20 percent. The first curve gives the lift curve slope,

$$C_{L_\alpha}$$

,of the vertical tail as a function of its aspect ratio. The second gives the factor,

$$\tau$$

, which is the ratio of the lift produced by a given deflection of a rudder to that produced by the same change in angle of attack of the whole tail. This factor is given as a function of the ratio of rudder chord to tail chord. For a given change in rudder deflection, the tail lift is given by the formula:

$$L_t = C_{L_t} \frac{\rho}{2} V^2 S_t = \delta\, C_{L_\alpha} \tau \frac{\rho}{2} V^2 S_t$$

Where:

C_{L_t} = **lift coefficient of tail**

δ = **rudder deflection, degrees**

C_{L_α} = **lift curve slope of tail (figure 3)**

τ = **rudder effectiveness factor (figure 4)**

ρ = **air density (.00238 sl/ft^3)**

V = **airspeed, ft/sec**

S_t = **total vertical tail area, ft^2**

The aspect ratio of the vertical tail should be increased by a factor of 1.4 if the horizontal tail is located at the base or at the tip of the vertical tail. The effective aspect ratio in these cases is increased by the end plate effect of the horizontal tail.

A hinged flap or rudder is seen to be surprisingly effective even when it is quite narrow. Thus, a flap of only 20 percent the total chord deflected through a given angle is 47 percent as effective as the whole tail deflected through the same angle. This high effectiveness of trailing-edge control, of course, accounts for their universal use on all types of airplanes.

For unstalled conditions, the effects of the two surfaces on a double-hinged rudder are additive. Thus, the effect of having the front segment of the rudder deflected 10^0 and the rear segment deflected 10^0 with respect to the front segment is the sum of the effect of 10^0 deflection of each segment considered separately. The formula given previously may, therefore, be used to calculate the effectiveness of a double-hinged rudder by adding the effects of each segment.

Two examples are given to illustrate the gains to be expected from double-hinging. In the first, consider a rudder having 60 percent of the tail chord. The rear 15 percent of the chord is sliced off and geared to deflect with a 1:1 gear ratio. For this case, the area and aspect ratio of the tail do not change, so the gain in effectiveness is simply that due to the gearing of the rear segment. The effectiveness is calculated as the lift per degree deflection of the forward segment.

For the original tail, the effectiveness is proportional to,

$$\tau$$

which for the 60 percent chord rudder is **.84** .

For the modified tail, the effectiveness is proportional to the sum of the values of,

$$\tau$$

for the two segments, which is:

$$.84 + .37 = 1.21$$

Thus, the ratio of effectiveness of the double-hinged rudder to the single-hinged rudder is:

$$\frac{1.21}{.84} = 1.44$$

A second case, which may represent a more likely possibility, is that the flyer wishes to increase the effectiveness of his rudder by adding to the chord. A comparison is made between the effect of addition of a fixed segment of 15 percent original tail chord or a geared segment of 15 percent original tail chord with a 1:1 gear ratio. In this case, we will consider the aspect ratio of the original vertical tail to be 2.0 with a "T" tail horizontal stabilizer so that the effective aspect ratio of the vertical tail is $1.4 \times 2 = 2.8$. The original ratio of rudder chord to tail chord is 0.6.

For the tail with the fixed addition to the chord, the rudder effectiveness is increased in proportion to the product of the changes in area,

C_{L_α}, and τ.

Thus, the ratio of the effectiveness of the modified tail to the original tail is:

$$\frac{S_{t_2}}{S_{t_1}} \times \frac{C_{L_{\alpha_2}}}{C_{L_{\alpha_1}}} \times \frac{\tau_2}{\tau_1} = \frac{1.15}{1} \times \frac{.049}{.054} \times \frac{.86}{.84} = 1.07$$

For the case of double-hinged rudder, the increase in effectiveness is this same ratio plus the effect of deflection of the rear segment. Thus, the ratio of effectiveness of the modified tail to the original tail is:

$$1.07 + \frac{1.15}{1} \times \frac{.049}{.054} \times \frac{.34}{.84} = 1.07 + .42 = 1.49$$

Finally, the ratio of the effectiveness of the geared addition to the effectiveness of the fixed addition is:

$$\frac{1.49}{1.07} = 1.39$$

Again, these values are for a given deflection of the front segment. These calculations do not take into account the possible effect of the larger unstalled deflection range of the double-hinged rudder. The conclusion drawn from these examples is that a double-hinged rudder provides a much more powerful method of increasing rudder effectiveness than simply an addition to the rudder chord.

As pointed out previously, the curves of figures 3 and 4 apply only for unstalled flow conditions on the vertical tail. A second problem of interest is to determine the maximum possible yawing moment produced by the vertical tail or the maximum sideslip angle which can be obtained with full rudder deflection. The sideslip angle, for a glider without ailerons, then produces rolling moment through the action of the wing dihedral. Unfortunately, these maximum maneuvers almost always involve stalled flow conditions. When the rudder is first moved to full deflection, the flow separates at the rudder hinge line. Thus, as the sideslip angle increases, the flow separates on the leeward side from the leading edge of the vertical tail and may re-attach at the hinge line. No general rules exist for calculating rudder effectiveness under these conditions, inasmuch as many factors are involved, including tail planform, airfoil section, and Reynold's number. The double-hinged rudder appears favorable, however, because the flap effect of the rear portion of the rudder serves to increase the maximum lift due to rudder deflection.

Reference: Sears, Richard L. : WIND-TUNNEL DATA ON THE AERODYNAMICS CHARACTERISTICS OF AIRPLANE CONTROL SURFACES. NACA ACR 3608 (Wartime Report L-663) Dec.,1943

THREE OFFERINGS FROM THE TIDEWATER MODEL SOARING SOCIETY TECHNICAL JOURNAL

by Herk Stokely

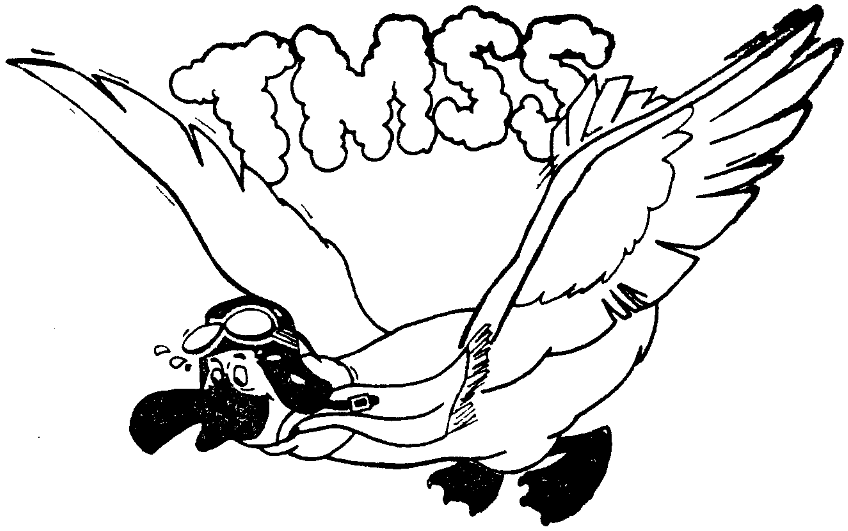

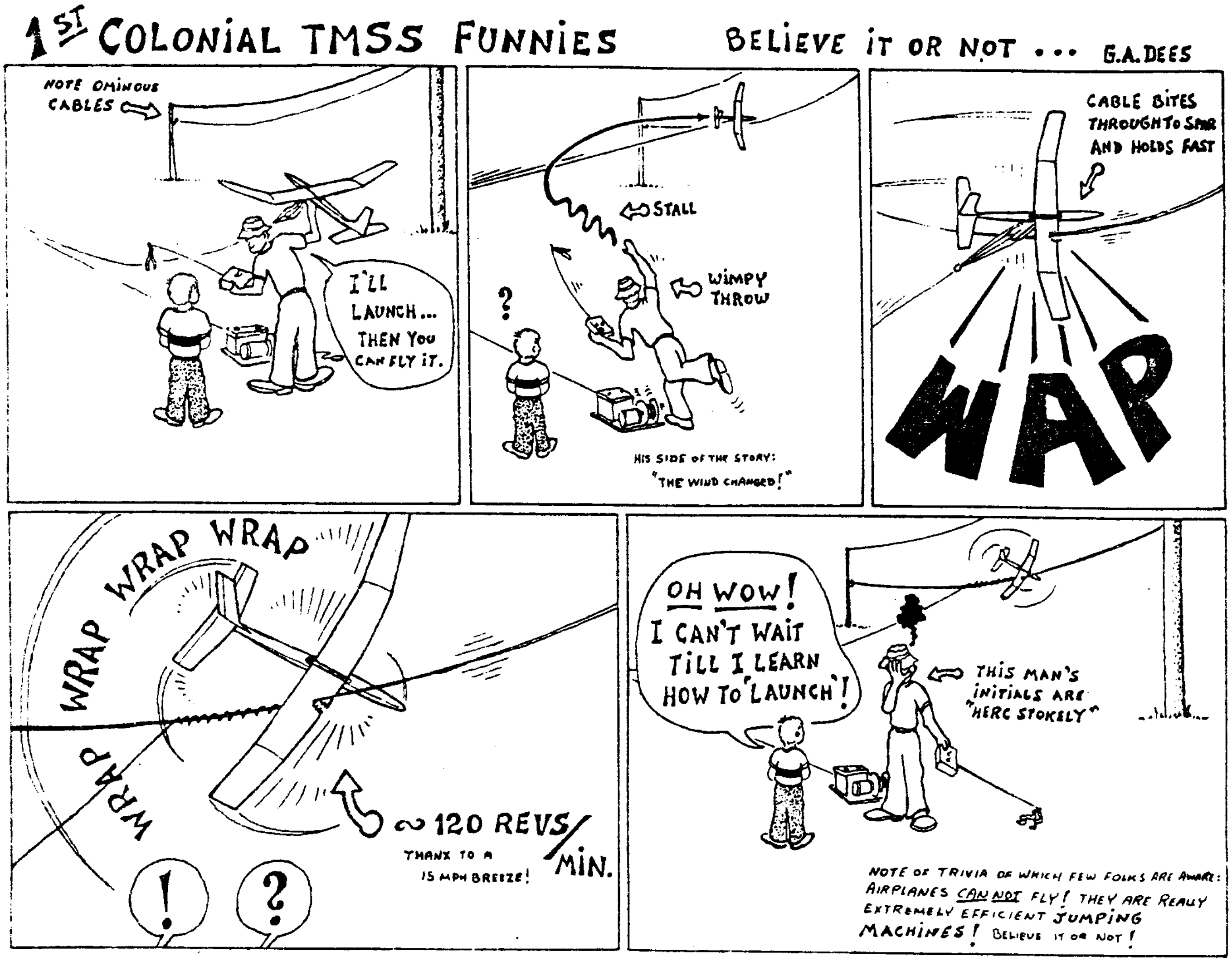

TIDEWATER MODEL SOARING SOCIETY

TECHNICAL JOURNAL # 16

MOUNTING DESIGNS FOR ALL-MOVING HORIZONTAL STABILIZERS

ALL-MOVING HORIZONTAL STABILIZER MOUNTING AND CONTROL DOESN'T USUALLY CAUSE MUCH TROUBLE ON THERMAL-SOARING MODEL DESIGNS. POKE A COUPLE OF WIRES THROUGH A HORN IN THE FUSELAGE, AND MOUNT THE STAB-HALVES ON THE WIRES IN SOME REASONABLE CONVENIENT WAY, AND "PRESTO" YOU HAVE AN EFFECTIVE PITCH CONTROL THAT WILL REQUIRE VERY LITTLE ADDITIONAL ATTENTION. MULTI-TASK MODEL DESIGN (FAI/F3B, 2-METER WORLD CUP, ETC) HOWEVER, CREATES A NEED FOR PLANES THAT CAN ROUTINELY FLY AT MUCH HIGHER SPEEDS. THIS KIND REQUIRE MORE CAREFUL CONSIDERATION OF THE DETAILS OF THE DESIGN.

THERE ARE TWO BASIC PROBLEMS THAT NEED ATTENTION WHEN YOU ARE LAYING OUT THIS KIND OF PLUG-IN STAB ARRANGEMENT. THE FIRST IS THE LOCATION OF THE PIVOT POINT ON THE CHORD OF THE STAB. HERE IT IS IMPORTANT TO MINIMIZE THE EFFECTS OF THE AIRLOAD ON THE STAB IN RELATION TO THE LINKAGE AND THE SERVO. BY MOUNTING THE PIVOT POINT AT JUST THE RIGHT SPOT, YOU CAN PRACTICALLY ELIMINATE ANY LOADS ON THE SERVO AND PUSHROD. THIS IS TRUE REGARDLESS OF HOW LARGE THE STAB IS OR HOW HIGH THE AIRSPEED, AND IS VERY IMPORTANT TO SMOOTH CONTROL OF THE MODEL. IF THE PIVOT POINT IS TOO FAR FOREWARD ON THE STAB THE HIGH AIRLOADS CAN OVERPOWER THE LINKAGE AND SERVO, DRIVING THE STAB TOWARD NEUTRAL, AND MAKING IT DIFFICULT TO MAKE TIGHT TURNS, OR PULL OUT OF HIGH SPEED DIVES. ON THE OTHER HAND IF THE PIVOT POINT IS TOO FAR AFT ON THE STAB AIRLOADS CAN MAKE THE STAB DEFLECT FURTHER THAN THE PILOT INTENDED. DEFLECTIONS CAN IN FACT OCCURR EVEN WHEN THE PILOT HASN'T PUT IN ANY CONTROL MOTIONS. PLANES WITH THIS KIND OF PROBLEM GET VERY FUNNY (OR NOT-FUNNY) TO FLY AT HIGH SPEED. THE SOLUTION FOR THIS PART OF THE DESIGN PROBLEM IS TO MOUNT THE PIVOT ROD WITH ITS ALIGNMENT AS NEAR AS POSSIBLE TO THE 1/4 CHORD POINT ON THE MEAN CHORD OF THE STAB. OF COURSE, IF YOU'RE INTO AERODYNAMICS, YOU KNOW THAT THE MEAN AERODYNAMIC CHORD ISN'T THAT SIMPLE TO LOCATE---BUT FOR SIMPLICITY, IF YOU LAY OUT THE STAB-HALF ON PAPER, ACT AS IF THE RUDDER CUTOUT IS PART OF THE STAB, AMPUTATE WHAT-EVER KIND OF TIP YOU'VE PUT ON IT, AND FIND THE AVERAGE CHORD LOCATION FOR THE REMAINDER. THAT'LL BE CLOSE ENOUGH FOR SUB-SONIC SAILPLANES.

THE SECOND DESIGN FACTOR HAS AN EFFECT WHICH IS NOT QUITE AS EASY TO SEE. THIS TIME WE'RE DEALING WITH THE PROBLEM OF AERO-ELASTICITY AND WE FIND THE IDEAL DESIGN ARRANGEMENT SANDWICHED BETWEEN FLUTTER ON THE ONE HAND, AND DIVERGENCE ON THE OTHER. MOUNTING THE STAB WITH ONLY ONE ROD AT THE 1/4 CHORD POINT OF THE MEAN AERODYNAMIC CHORD IS NOT THE USUAL DESIGN. WE ORDINARILY PUT ANOTHER ROD EITHER FOREWARD OR AFT OF THE PIVOT ROD TO TIE THE STAB SOLIDLY TO THE ACTUATING HORN WHICH CONTROLLS THE

MOVEMENT OF THE STAB. FOR CLARITY I'LL CALL THIS THE ACTUATING ROD. (I'M ALREADY CALLING THE OTHER ONE THE PIVOT ROD) THE PROBLEM DEVELOPS BECAUSE ONCE THE STAB IS INSTALLED ON THE RODS, IT DOESN'T KNOW WHICH OF THE TWO IS THE PIVOT ROD. (STABS ARE DUMB) THE STAB SEES THESE TWO RODS AS WORKING TOGETHER EQUALLY, AND THE AEROELASTIC AXIS FOR TWISTING AND FLEXING IS BASICALLY THE AVERAGE OF THE TWO WIRES. WHAT ALL OF THIS MEANS IS; IF YOU HAVE THE PIVOT ROD AT THE 1/4 CHORD OF THE M.A.C. (25%MAC), AND YOU INSTALL THE ACTUATING ROD FOREWARD OF THE PIVOT ROD, THE ELASTIC AXIS OF THIS CONNECTION IS 1/2 WAY BETWEEN THE WIRES. THIS IS EASILY SEEN TO BE WELL FOREWARD OF THE 25%MAC POINT. SO WHAT!---RIGHT? WELL, IF THE WIRES ARE STIFF ENOUGH, THE STAB SMALL ENOUGH, AND THE SPEED LOW ENOUGH---IT'S NO PROBLEM. BUT HAVING THIS ELASTIC AXIS AHEAD OF THE 25%MAC IS A SET-UP FOR FLUTTER. IT'S NOT WITHIN THE SCOPE OF THIS PAPER TO EXPLAIN WHY THIS LEADS TO FLUTTER, BUT IF YOU WANT TO, YOU CAN TAKE MY WORD FOR IT. THE OTHER ARRANGEMENT WITH THE ACTUATING ROD BEHIND THE PIVOT ROD MOVES THE ELASTIC AXIS BEHIND THE 25%MAC IS MUCH MORE DESIRABLE BECAUSE THIS KIND OF ARRANGEMENT TENDS TO PREVENT FLUTTER. IT CAN (TECHNICALLY) LEAD TO A HIGH-SPEED CONDITION KNOWN AS DIVERGENCE WHERE THE STAB TWISTS OFF, BUT THIS IS VERY MUCH LESS LIKELY THAN FLUTTER ON A REASONABLY WELL DESIGNED MODEL.

WHAT IS THE BEST ARRANGEMENT? KEEP IN MIND THAT THE PIVOT ROD SHOULD BE AT THE 25%MAC POINT FOR SMOOTH CONTROLLABILITY AT HIGH SPEED. MY SUGGESTION IS THAT YOU MAKE THIS ROD LARGER IN DIAMETER THAN ORDINARY DESIGN PRACTICE. INSTALL THE ACTUATING ROD BEHIND THE PIVOT ROD AND MAKE IT SOMEWHAT SMALLER IN DIAMETER. (ABOUT THE SIZE USED ORDINARILY FOR BOTH WIRES) THIS BIASES THE ELASTIC AXIS CLOSER TO THE PIVOT ROD, AND STILL KEEPS IT BEHIND THE 1/4 CHORD POINT TO SUPRESS FLUTTER. WILL THIS PREVENT STAB FLUTTER? IN A WORD ---- NO! (NOT BY ITSELF)-- THE BENDING AND TWISTING STIFFNESS OF THE STAB ITSELF (NOT JUST THE CONNECTION TO THE HORN) CONTROLS FLUTTER TOO, AND THAT IS A DIFFERENT SUBJECT. I'VE ALSO SEEN STAB FLUTTER CAUSED BY A VERY FLEXIBLE FUSELAGE ON A POD-AND-BOOM DESIGN. NOTHING YOU DO TO THE STAB CAN DO MUCH TO PREVENT THAT.

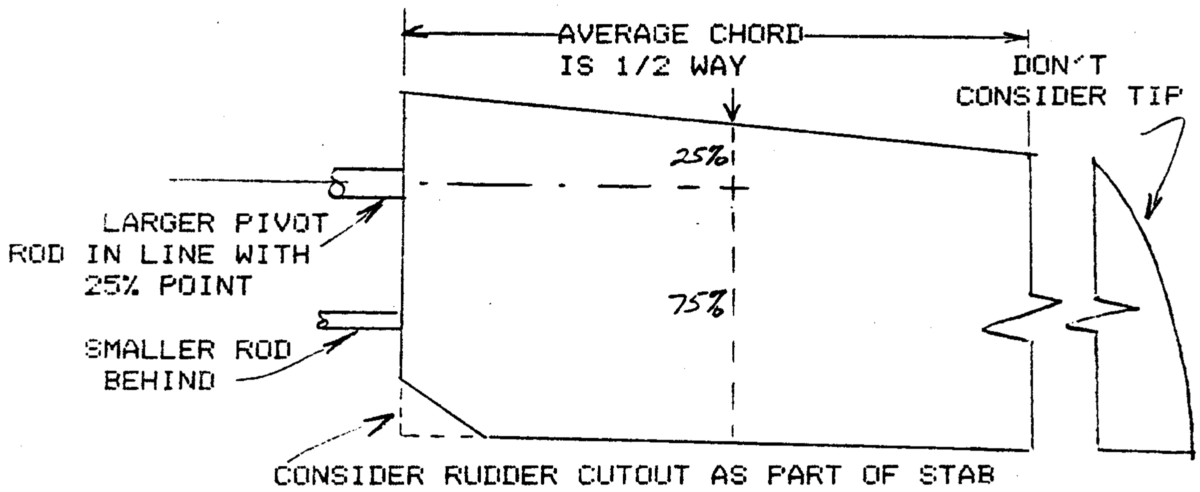

TIDEWATER MODEL SOARING SOCIETY

TECHNICAL JOURNAL NUMBER 18

RUDDER AND FIN DESIGN

THE FOLLOWING IDEAS ARE BASED ON YEARS OF OBSERVATION OF VARIOUS RC SAILPLANE RUDDER ARRANGEMENTS AND THEIR EFFECTS ON THE HANDLING AND PERFORMANCE OF THE MODELS. IN PUTTING TOGETHER THE FIRST "SOARTECH" JOURNAL, I HAVE ALSO HAD AN OPPORTUNITY TO LOOK THROUGH A NUMBER OF OLD NACA REPORTS IN WHICH CONTROL SURFACE ARRANGEMENTS WERE STUDIED AND TESTED FOR BOTH EFFECTIVENESS AND EFFICIENCY . PUT TOGETHER, THESE HAVE MADE ME LOOK CRITICALLY AT THE FIN AND RUDDER DESIGNS OF MY OWN PLANES AND OTHERS, AND I'VE DECIDED THAT I GENERALLY DON'T LIKE WHAT I SEE.

IN ALMOST EVERY RESPECT, A FIN AND RUDDER COMBINATION WORKS JUST LIKE A WING WITH A FLAP, OR AN AILERON. THE FEATURES OF A WING/AILERON COMBINATION THAT MAKE IT EFFICIENT AND EFFECTIVE APPLY WITH SOME SPECIFIC EXCEPTIONS TO THE DESIGN OF A GOOD FIN/RUDDER. THE FIRST POINT HAS TO DO WITH THOSE RUDDER BALANCE AREAS WHICH ARE A STYLE ON SO MANY OF THE DESIGNS IN USE TODAY. THERE IS SELDOM A GOOD REASON FOR THIS KIND OF RUDDER DESIGN ON AN RC SAILPLANE DESIGN. IT IS VERY INEFFICIENT BECAUSE WHEN YOU WANT THE FIN/RUDDER TO DEVELOP LIFT (READ THAT YAW THE MODEL), IT HAS THE EFFECT OF WASH-IN WHICH CAUSES A LOT OF UNNECESSARY DRAG. THIS KIND OF BALLANCE WAS USED IN FULL SIZE AIRCRAFT TO GET THE RIGHT FORCES IN THE CONTROL SYSTEM FOR PROPER PILOT FEEL. FOR AERODYNAMIC EFFICIENCY HOWEVER, THEY ARE USUALLY VERY UNDESIRABLE ON A CONTROL SURFACE THAT GETS USED MUCH BY THE PILOT.

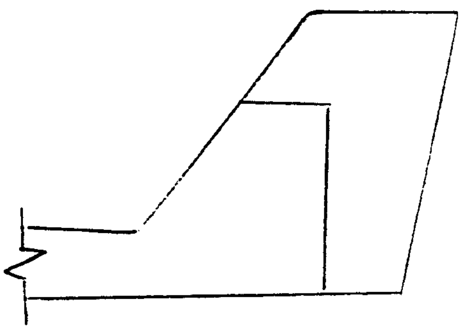

THE SECOND DESIGN FEATURE THAT NEEDS A CRITICAL LOOK IS THE RUDDER CHORD. THE OLD NACA DATA I MENTIONED HAS REPORTS WHICH SHOW THAT WHEN THE CHORD OF THE CONTROL SURFACE (RUDDER) GETS LARGER THAN ABOUT 35-40% OF THE CHORD OF THE WHOLE SURFACE, IT PRODUCES MORE DRAG WITHOUT A CORRESPONDING INCREASE IN EFFECTIVENESS. THE BASIC GEM OF KNOWLEDGE HERE IS THAT THE SPAN OF A CONTROL SURFACE (RUDDER) IS MORE IMPORTANT THAN ITS CHORD. IF YOU LOOK AROUND YOU'LL SEE THAT MOST OF OUR DESIGNS HAVE GONE THE OTHER WAY.

WHERE ? YOU ASK, DOES THIS KIND OF THINKING SEND US, AND WHAT ARE THE NEW PROBLEMS TO BE AVOIDED THERE? FIRST IT SHOULD INFLUENCE US TO USE HIGHER SPANS RATHER THAN GREATER CHORDS TO GET THE AMOUNT OF CONTROL AND STABILITY WE WANT FROM THE FIN/RUDDER DESIGN. BE CAREFUL THOUGH, BECAUSE HIGH ASPECT RATIO SURFACES STALL AT LOWER ANGLES OF ATTACK (YAW) THAN LOW ASPECT RATIO SURFACES. IT'S BEST TO AVOID DESIGNS WHERE THE A/R OF THE

FIN RUDDER COMBINATION IS LARGER THAN 2.5 TO 3. A/R=SPAN OR HEIGHT DIVIDED BY THE AVERAGE CHORD. (OR SPAN SQUARED DIVIDED BY AREA) THEN, USE A SMALLER RUDDER CHORD THAN WHAT YOU'RE USED TO SEEING. I THINK THAT THE 35-40% FIGURE IS RIGHT. NEXT GO FOR A BIT OF WASHOUT, RATHER THAN THE WASHIN THAT COMES FROM USING HORN BALANCE AREA. DO THIS BY STOPPING THE RUDDER SHORT OF THE FIN TIP. THIS METHOD HAS BEEN USED ON ALIERON DESIGN FOR QUITE A WHILE. ANOTHER METHOD IS TO REDUCE THE PERCENTAGE CHORD OF THE RUDDER AS IT APPROACHES THE TIP. THUS IT MIGHT BE 40% CHORD AT THE FUSELAGE, AND ONLY 25% AT THE TIP.

THERE ARE SOME REAL INEFFICIENCIES INDUCED AT THE LOWER END OF THE RUDDER WHEN WE HAVE A LARGE CHORD RUDDER EXTENDING ALL THE WAY TO THE BOTTOM OF THE FUSELAGE. HERE THE EFFECT OF SMALL DESIGN REFINEMENTS WILL NOT MAKE SO MUCH DIFFERENCE BECAUSE THE AREA IS ALREADY INEFFICIENT DUE TO THE AIRFLOW IRREGULARITIES IN THE WAKE OF THE FUSELAGE AND THE WING ROOT. STILL, IF YOU WANT TO GO ALL THE WAY, THE MOST EFFICIENT ARRANGEMENT (FROM THE VIEWPOINT OF MINIMIZING MANEUVERING DRAG) WOULD BE TO STOP THE RUDDER AT THE TOP OF THE FUSELAGE.

A WELL DESIGNED T-TAIL ARRANGEMENT WILL ALSO IMPROVE RUDDER EFFICIENCY. TO GET THE BENEFIT OF THIS HOWEVER, THE RUDDER TOP MUST BE FITTED CLOSELY TO A NON-MOVING STABILIZER SURFACE. THUS THE ELEVATOR WOULD HAVE TO BE LOCATED BEHIND THE RUDDER. NOT AN EASY ARRANGEMENT TO BUILD. THIS DESIGN INCREASES THE EFFECTIVE ASPECT RATIO OF THE FIN/RUDDER, AND IF YOU USE IT YOU SHOULD PROBABLY LIMIT THE A/R TO THE RANGE OF 2.5 OR LESS.

HOW ABOUT THE IDEA OF AN ALL-MOVING VERTICAL TAIL? NOT A BAD IDEA, BUT NOT SO EASY TO BUILD WITH GOOD CONTROL AND STIFFNESS. REMEMBER TOO THAT AN ALL-MOVING SURFACE CANNOT DEVELOP AS MUCH LIFT (YAW) AS A CONVENTIONAL FIN AND RUDDER DESIGN. (JUST AS A WING WITHOUT A FLAP CAN'T DEVELOP AS MUCH LIFT AS A WING WITH A FLAP) IF YOU WERE SUCCESSFUL IN PUTTING TOGETHER A GOOD STRUCTURAL AND CONTROL ARRANGEMENT, A TRUE ALL-MOVING DESIGN WOULD HAVE THE LEAST DRAG (FOR SMALL CONTROL DEFLECTIONS).

DON'T FORGET IT'S FOR FUN--HERK

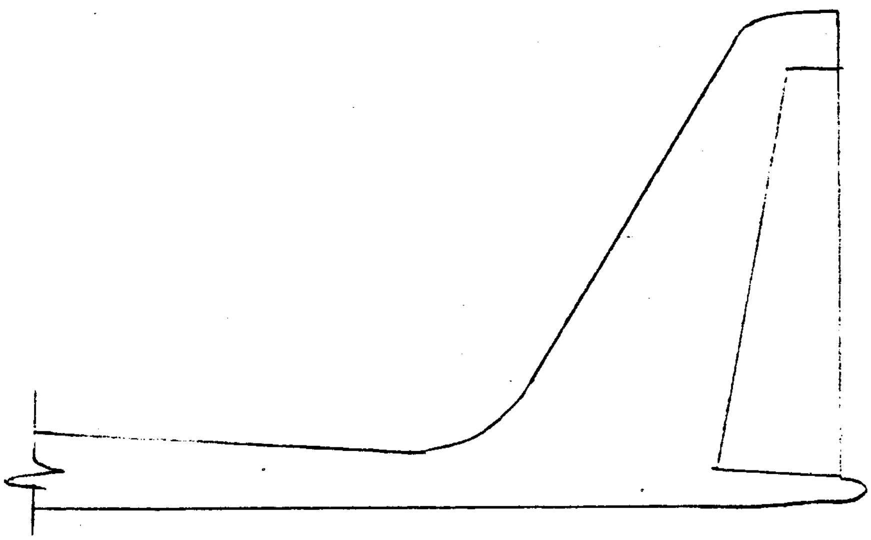

TIDEWATER MODEL SOARING SOCIETY

TECHNICAL JOURNAL #23

SOME IDEAS ON THE AERODYNAMICS OF FUSELAGE DESIGN

Fuselage design doesn't have nearly the effect on overall sailplane performance that some people think it does. Because it's a small effect you can almost ignore the aerodynamics of the fuselage and still get pretty good performance from any reasonable thermal - soaring type sailplane. In fact I've seen a few models over the years where I was sure that the designer ignored aerodynamics when he designed his fuselage! Some of them flew pretty well too.

My personal interest in the subject was triggered about a year ago by Preben Norholm of Denmark when he wrote me that Ralf Decker (current world champion) had designed what he (Preben) thought was exactly the best fuselage. Preben had even written an article on the subject for the Danish model magazine which he sends to me. Sorry to say I couldn't get much out of the article, - boy! talk about language barriers - but I did give a lot of thought and a bit of study to the subject. More recently, I was contacted by Ray Olson of Mesa Arizona who; Working with Lee (laser cut airfoils) Murray of Appleton Wisconsin, Was trying to design a new optimized sailplane fuselage. This is getting to be a bit of a cosmopolitan project as you can see. I predict that if this fuselage becomes available, you'll hear a lot more about it.

For a conventional model design, there is one big area of TROUBLE in the aerodynamics of the fuselage. The airflow interactions between the wing and the fuselage are ALWAYS bad. The boundary layer sweeping up over the nose of the fuselage thickens and slows until, when it encounters the wing, it's in bad shape, unable to follow the complex curves and intersections around the canopy, fuselage, and wing root fillet. This results in wedge shaped separations over the top of the wing as higher pressure slow moving air spills out into the low pressure lifting flow over the top of the wing.

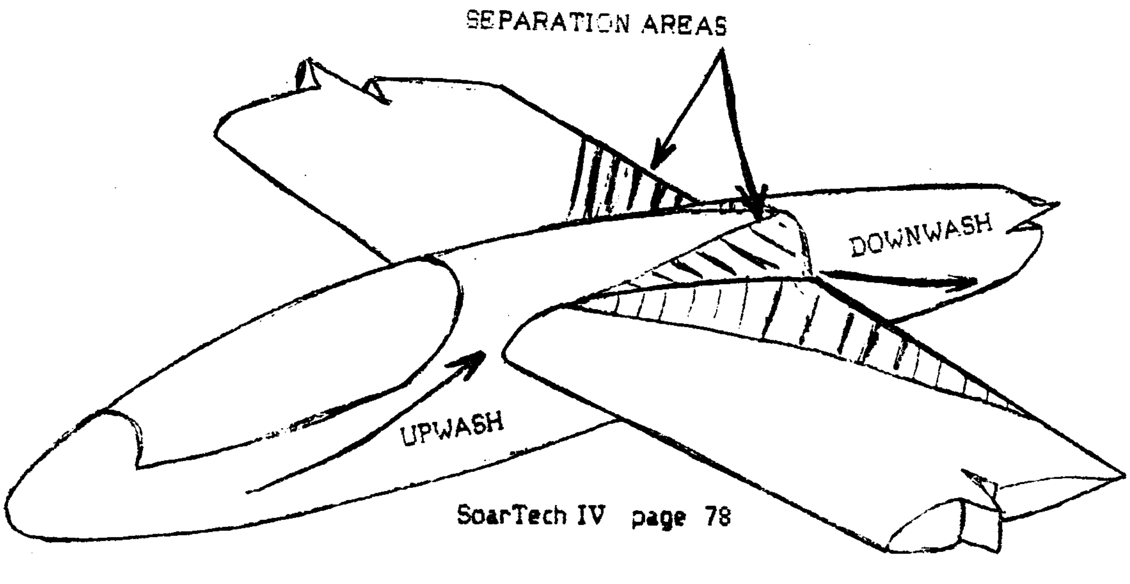

Bob Champine solves this problem by putting the wings of his Red Bird on a high pylon so that the leading edge is flying in clean undisturbed airflow, and the top of the wing has no fuselage intersections to spill bad air into the lifting flow. He gets more drag from the pylon, and its intersections with the fuselage and wing bottom, but he still is probably more efficient. Ray McGowan, from Napa California, and Eugenio Pagliano from Italy (and others) have built and flown Noseless designs where the front center of a swept back wing is the nose of the plane. Here again the wing is entering clean air - but there are losses due to the sweept wing and here again there is both gain and loss.

If however you really want a conventional looking design, how would you try to handle the aerodynamics to minimize the losses? Smooth curving fillets at the wing fuselage joint is the conventional approach. By avoiding sharp corners, and tight curves, the airflow has a better chance of being able to follow the surfaces. That still doesn't work very well, and to get the best results, you have to give the air itself more "sticking power". A freshly formed turbulent boundary layer sticks to the compicated contours and intersections better than any other kind of airflow. For that reason alone, we want to keep the boundary layer over the whole nose completely laminar. Then, just an inch or so before the flow gets to the area of the wing root, we must positively trip it into turbulent flow. The inch is to let the separation bubble form, transition the flow, and then reattach ahead of the wing.

To do this you have to have a laminar flow body with no seams or projections all the way back to the trip point. Further the laminar body must continue to increase in diameter back to that point. Then, at the right place, there must be a definite turbulator to make the boundary layer change to turbulent at that point. Notice that the laminar flow that's preserved over the whole nose isn't to reduce friction drag, but only to be sure that the turbulent transition starts where we want it. This is a real problem to manned sailplanes, because they <u>must</u> have a canopy --- but we don't. That's right the canopy seam (no matter how tight it is) trips the boundary layer in the wrong place. That's why Preben liked the Decker nose so much. In case you didn't notice, the Australians had a one piece removable nose like that too.

Now, with the flow transitioned to turbulent just an inch, or a bit more, ahead of the wing, those smooth fillets and intersections have the best chance of keeping the airflow attached through the wing root area.

Behind the wing there is a strong field of downwash. That means that the fuselage behind the wing has an airflow with a top to bottom velocity component. To get the best flow around the fuselage it should be a bit airfoil shaped itself with the leading edge at the top and the trailing edge at the bottom. Most designers just make the cross section elliptical with the long axis vertical and the short axis horizontal. This part of the plane should be narrowed to the maximum possible (structrual strength and stiffness requirements take over here) to reduce friction drag.

Few people realize that there is a similar field of upwash ahead of the wing. It is there though, and it's about as strong as the downwash. For that reason, the nose of the plane is drooped a few degrees to aim it into this upswept airflow. How much to droop it is a bit complicated. At slow speeds (high angle of attack) the upwash at its strongest, while at high speeds, it almost goes away. Therefore, a plane that's designed for optimum performance at high speed has less droop than one that's set up for thermalling. Nature helps us a bit here though, because the droop angle is set up to the wing's zero lift angle which is much higher (negatively speaking) for a highly cambered thermalling airfoil, than it is for a low camber airfoil used for high speed designs. Just set up the nose droop so that it's about 3 to 4 degrees below the wing chord line, and the airfoil you choose for the plane's designed purpose will take care of the rest.

Drooped symmetrical laminar flow body for a nose cone extending almost to the wing; intentional turbulator ringing the aft end of it; smoothly filleted wing root area contracting in cross section to a thin tapering boom just aft of the wing. Just a bit different than anything you're likely to see at the field, but certainly not radical. The smooth skidless nose will make a bit of a problem on landing (unless you make it strong enough to STICK-IT). You will have another problem if you try to build one of these. The low drag laminar flow body designs will all have too small a nose radius to meet the FAI minimum requirement. It'll have to be enlarged, and great care taken to assure that it meets the nose body smoothly. Any sharp change of radius in this area can cause the boundary layer to transition too soon. You might also like to look at the earlier Tech Journal article on the vertical fin and rudder. It suggests extending the boom to the aft end of the rudder.

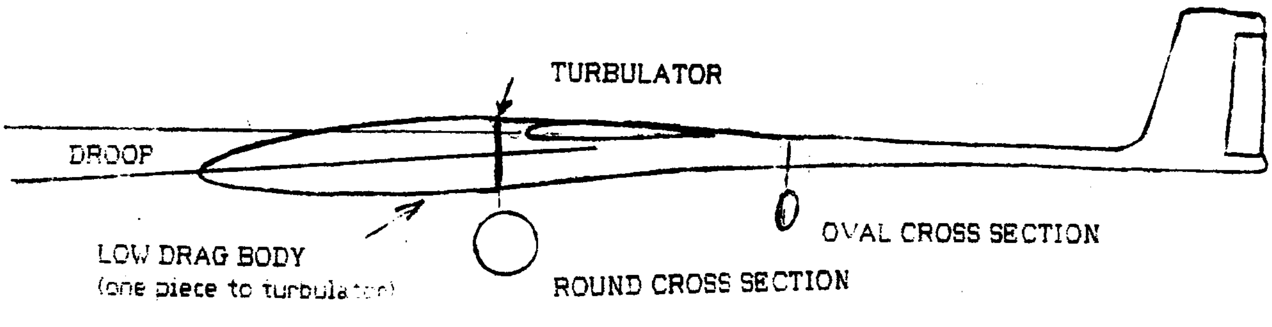

Low Drag Body nr. 1.
Laminarstrøm til 30% korde.
Næseradius 1.562% af korde.

X-akse	Y-akse
.000	.000
.100	.600
.200	.860
.300	1.050
.400	1.210
500	1.340
1.000	1.880
1.500	2.270
2.000	2.690
2.500	2.882
5.000	4.075
10.000	5.847
15.000	7.243
20.000	8.363
25.000	9.194
30.000	9.732
35.000	9.992
40.000	10.000
45.000	9.795
50.000	9.413
55.000	8.891
60.000	8.258
65.000	7.528
70.000	6.706
75.000	5.783
80.000	4.749
85.000	3.603
90.000	2.343
95.000	1.104
97.500	.513
100.000	.000

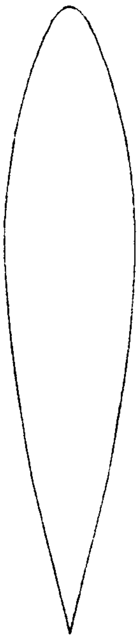

Low Drag Body nr. 4
Laminarstrøm til 60% korde.
Næseradius 0,986% af korde.

X-akse	Y-akse
.000	.000
.100	.335
.200	.620
.300	.770
.400	.899
.500	1.000
1.000	1.460
1.500	1.800
2.000	2.100
2.500	2.336
5.000	3.405
10.000	4.938
15.000	6.085
20.000	7.002
25.000	7.781
30.000	8.462
35.000	9.048
40.000	9.520
45.000	9.845
50.000	9.991
55.000	9.921
60.000	9.612
65.000	9.047
70.000	8.223
75.000	7.150
80.000	5.860
85.000	4.399
90.000	2.860
95.000	1.314
97.500	.613
100.000	.000

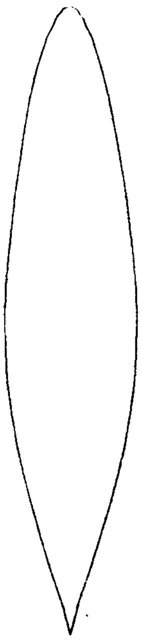

Wortmann FX-71-L-150/K25
Optimeret for 25% flap.
Næseradius 2,0% af korde.

X-akse	Y-akse
.000	.000
.107	.821
.428	1.455
.961	1.903
1.704	2.446
2.653	2.941
3.896	3.457
5.158	3.944
6.699	4.431
8.427	4.880
10.332	5.326
12.408	5.724
14.645	6.105
17.033	6.438
19.562	6.742
22.221	6.991
25.000	7.204
27.886	7.355
30.866	7.463
33.928	7.501
37.059	7.463
40.245	7.396
43.474	7.377
46.730	6.998
50.000	6.689
53.270	6.320
56.526	5.891
59.755	5.457
62.941	4.949
66.072	4.949
69.134	3.854
72.114	3.299
75.000	2.771
77.779	2.265
80.438	1.921
82.967	1.628
85.355	1.377
87.592	1.140
91.573	.731
94.844	.425
97.347	.223
99.039	.087
99.893	.010
100.000	.000

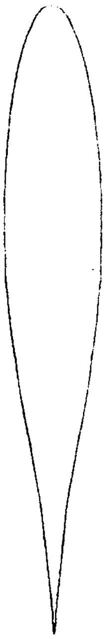

Low Drag Body nr. 2
Laminarstrøm til 40% korde.
Næseradius 1.465% af korde.

X-akse	Y-akse
.000	.000
.100	.570
.200	.780
.300	.970
.400	1.120
.500	1.240
1.000	1.770
1.500	2.140
2.000	2.440
2.500	2.679
5.000	3.776
10.000	5.373
15.000	6.640
20.000	7.716
25.000	8.601
30.000	9.280
35.000	9.738
40.000	9.968
45.000	9.968
50.000	9.753
55.000	9.339
60.000	8.752
65.000	8.028
70.000	7.190
75.000	6.269
80.000	5.278
85.000	4.209
90.000	3.017
95.000	1.659
97.500	.874
100.000	.000

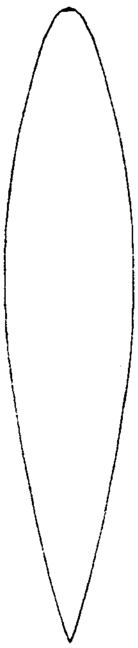

NACA 65 006

X-akse	Y-akse
.000	.000
.500	.476
.750	.574
1.250	.717
2.500	.956
5.000	1.310
7.500	1.589
10.000	1.824
15.000	2.197
20.000	2.482
30.000	2.852
40.000	2.988
50.000	2.900
60.000	2.518
70.000	1.935
80.000	1.233
90.000	.510
95.000	.195
100.000	.000

Wortmann FX-71-L-150/K30
Optimeret for 30% flap.
Næseradius 2,0% af korde.

X-akse	Y-akse
.000	.000
.107	.813
.428	1.437
.961	1.896
1.704	2.442
2.653	2.945
3.896	3.465
5.158	3.958
6.699	4.450
8.427	4.902
10.332	5.354
12.408	5.753
14.645	6.136
17.033	6.467
19.562	6.774
22.221	7.014
25.000	7.229
27.886	7.369
30.866	7.477
33.928	7.500
37.059	7.486
40.245	7.372
43.474	7.219
46.730	6.969
50.000	6.667
53.270	6.271
56.526	5.845
59.755	5.363
62.941	4.850
66.072	4.264
69.134	3.729
72.114	3.140
75.000	2.742
77.779	2.347
80.438	2.040
82.967	1.709
85.355	1.448
87.592	1.177
91.573	.756
94.844	.435
97.347	.227
99.039	.089
99.893	.010
100.000	.000

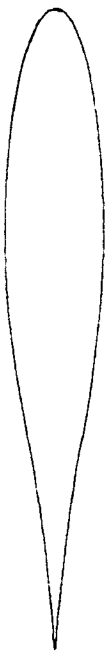

Low Drag Body nr. 3.
Laminarstrøm til 50% korde.
Næseradius 1.026% af korde.

X-akse	Y-akse
.000	.000
.100	.340
.200	.625
.300	.775
.400	.920
.500	1.030
1.000	1.500
1.500	1.850
2.000	2.150
2.500	2.388
5.000	3.480
10.000	5.039
15.000	6.197
20.000	7.154
25.000	7.987
30.000	8.715
35.000	9.313
40.000	9.743
45.000	9.967
50.000	9.959
55.000	9.709
60.000	9.224
65.000	8.528
70.000	7.662
75.000	6.676
80.000	5.610
85.000	4.483
90.000	3.258
95.000	1.827
97.500	.978
100.000	.000

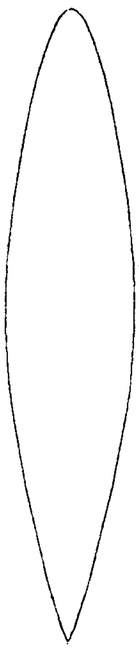

NACA 65 A 008

X-akse	Y-akse
.000	.000
.500	.615
.750	.746
1.250	.951
2.500	1.303
5.000	1.749
7.500	2.120
10.000	2.432
15.000	2.926
20.000	3.301
30.000	3.791
40.000	3.995
50.000	3.895
60.000	3.456
70.000	2.763
80.000	1.898
90.000	.960
95.000	.489
100.000	.018

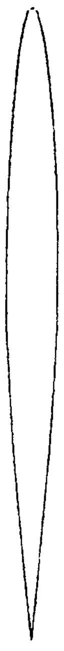

TWO POSTSCRIPTS BY GENE DEES

LITTLE KNOWN FACT! --- INSECTS LOVE FLYING TOO.

R/C SAILPLANES: **An Artist's View**

by Gene A. Dees

If I were not an artist, I probably would not ever have learned to fly R/C sailplanes. Sounds odd, but it's true.

In the summer of 1980, I was invited to be guest artist at a comic book and science fiction convention in Raleigh, NC. I was invited because of my comic strip then running in a newspaper at N.C.State University. It was a fantasy strip of sorts and a recent episode involved ritual combat on a planet where high technology and/or destructive warfare had been outlawed. Rules of combat were very similiar to medieval jousting excepting for the fact that the "jousts" were held between sailplanes in mid-air while riding cinder-block-sucking thermals that occured with regularity over vast grass plains. The closest thing to a powered aircraft was a "contraption-class" barrage balloon driven by a crude, but efficient steam engine. Combat between opposing balloons looked like a cross between mid-air rugby and a 2-for-1 Washington's Birthday Ladies' Lingerie Sale. Native inhabitants (six-foot tall bipedal lizards with incredible senses of humor) watched from below with binoculars or from balloons of their own and wagered on the outcome. It seems that the transplanted human civilization has supplied the lizards with straight-lines, punch-lines, and belly-laughs of heretofore unequalled magnitude. The sailplanes were not considered humorous though---they were regarded as the greatest contribution to art and aesthetics ever conceived . And a race that was able to produce such beauty and such frivolity in almost the same stroke was worth having around because every lizard worth his scales remembers how dull things were on Saturday nights before the humans showed up.

Well, to make a long story even longer--- Two guys approach me at the convention and ask to see the original art for the comic strips with the sailplanes in them. I complied immediately while asking if they were interested in sailplanes (I had, as yet, never flown in a sailplane and I had hopes of mooching a ride !). No. They didn't fly full-scale planes, they flew R/C sailplanes.

"What?" I had seen and had been interested at one time in R/C planes (the ones that drilled their way through the sky sounding like irritated, 100 pound bumblebees) but could never seem to get a straight answer from the high priesthood as to what a lowly outsider like myself had to know to get in on the fun. R/C sailplanes seemed fascinating but there were no mountains available locally to throw them off of.

I was given a quick verbal run-down on the particulars of launching, radios, construction, and piloting of R/C sailplanes.

This I had to see since the description of the launch sounded to me as though some laws of physics were being seriously violated.

I was invited to come out and watch the next afternoon.

Upon arrival at the field I found several people relaxing in lawn chairs, radios in hand, and staring straight up at what looked like nothing. I was welcomed and then the planes were pointed out.

"You have got to be kidding !" Those two dots were planes ?

After a half-hour the thermal petered out and the planes came down. That's all it took. I was hooked !

These contraptions were a marriage of beauty and serenity and watching one slip silently overhead on landing approach was too much. Besides the obvious parallels drawn with soaring birds in flight, I recalled whales gliding through crystal seas, polar birds in tuxedos that "fly" underwater, walrus and seals while ungainly on land, were graceful in water. Nothing seemed to fit precisely in comparison since buzzards in flight were beautiful but, close-up, were ugly as sin. Seals and walrus though graceful in water moved like animated water balloons on land and hawks and eagles, when not flying, walked as if their crotches hurt.

An R/C sailplane at rest is beautiful and I looked at them with my mind running wild.

My first efforts at building sailplanes and flying them were seriously handicapped. Someone would launch my plane for me then hand over the transmitter. After all, sailplanes were supposed to be easier to learn to fly than power planes and anyone can do it. Since I had demonstrated that I was proficient at chewing gum and walking at the same time, I would have no trouble that afternoon.

WRONG !

The artist in me was too busy tripping out on the sight of my new plane gliding silently against a royal blue sky that he didn't see the tree.

Well, this went on all summer long---FLY IT, BUST IT, REPAIR IT, etc. This sequence recurred from July until February of the following year. I just could not concentrate on the business at hand and would be content to lie in the grass and watch the three-dimensional poetry going on around me. If I did manage to snag another more experienced pilot to land it for me, I would consider myself to be one up for the week and anything more would be tempting the fates---so it was back down on the grass for some more "poetry".

Seven months later on one of those unseasonable pre-spring days, something snapped. I silently (uncharacteristic of me) got up off the grass and launched my plane, flew it, and landed it unassisted. Not long after that, it was suggested that I put a mail box at the field since I was there more than I was at home. I even put velcro on my wing tips to hold cyalume glow tubes so I could fly at night (it was considered cheating to fly during a full moon---it was too easy to see the plane). Seeing two green lights (that's all you can see of your plane) slipping through the darkness while someone who is ready to launch, calls to you; "I'm ready to launch. Where are you ?"

"I'm in Aries heading for Capricorn !"

A whooshing sound with green lights moving closer together overhead and there are now two more stars in the summertime sky.

All of this happened a number of years back before I moved to Virginia Beach but I haven't shed the artist's view of this sport. I don't fly with the same purpose as other pilots. My planes tend to reflect their "lizard planet" ancestry in their coloration and markings and my soon-to-be-completed "Icarosaur" flying wing is like nothing that ever flew around here (also bearing "Lizard Marks"). Hell ! It doesn't have to even fly all that well. I will be insufferably pleased with myself if all it does is blunder through circles and land for it will be incredibly beautiful in the air !

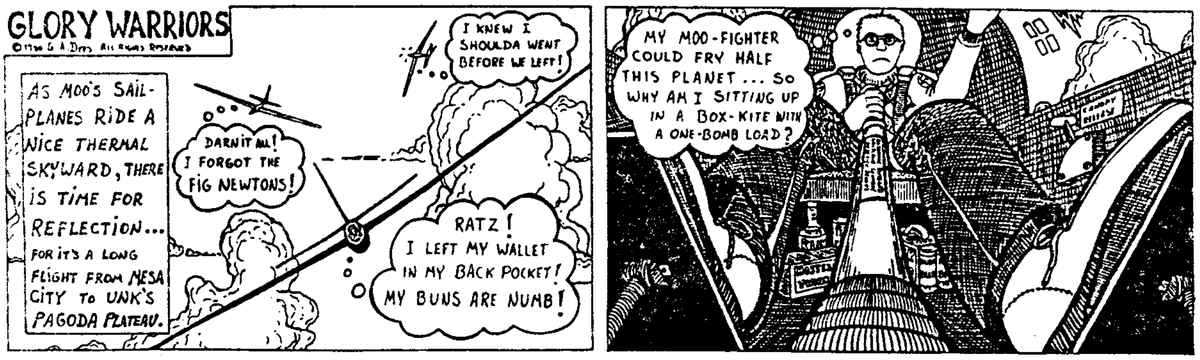

LSF: AN ARTIST'S VIEW

BY GENE A. DEES

Being an artist got me into flying sailplanes, and it's what keeps me at it after five years. I got into LSF for the simple reason that a couple of friends in Raleigh, NC needed "Level II or higher" witnesses. Level I was simple since I had already been flying a while when I got started. I blundered my way through Level II contests and was thrilled by a 19 minute thermal flight that reached the dizzying altitude of 30 feet ! Level III was fun (I still was blundering my way through contests, however). It took the better part of twenty minutes to fly the out-leg of my goal-and-return only to encounter the leading edge of a storm that got me back to my starting point in all of thirty seconds. It was exciting riding in a truck going 65 mph trying to keep up with a Drifter II !

I had budgeted two years for completing Level IV (you see, LSF IV actually requires that you do well in a few contests.) I completed it in one summer--- I hear a lot of good flyers had a bad year that summer. Well, I worried the contests to death, and, lo and behold ! I had the contests out of the way before I completed the " fun stuff" ! It was a bad year for thermals too.

My Level IV goal-and-return was done under conditions I haven't seen since desert survival training. Petersburg, VA was a mite on the hot side that day (104^0 and no shade). I told the guy driving the truck that if I wasn't doing well by the time I got down the road to the federal prison, I was going to abort the cross-country event and go for my Level IV. I made it---milking gopher belches at twenty feet for the last 3/4 of a mile.

After squeaking through most of LSF IV, I found myself needing one more hour thermal flight and the sky full of fifty-nine minute air for the remainder of the summer---until that day that I received special permission to over-fly a nuclear power plant that was under construction in North Carolina. After lizarding my way through most of LSF IV, I wind up with a 2 hour and thirty-eight minute flight and 160 witnesses (there was a power company picnic going on where I was flying and at least 60 of the people had stop watches on me !) It was sort of like swatting flys with an H-bomb---over-kill to several orders of magnitude. You see, nukes are good for something after all.

So here I am trying the same "worry-it-to-death" technique on Level V, and you know something? It ain't working out so hot. I did get three contests out of the way. I flew at the CASA meet in Washington last September and there is a lot to be said for contests with that many entrants--- I can place 15th and still walk away with more than 3,000 points! However, now I have to actually WIN three and that may take awhile! I did make a two-hour flight last May---with my wife and a guy working a bush-hog as witnesses. Sorry about that ! It doesn't count, but, what the Hell, I had fun doing it.

All of this may sound like I don't have much respect for LSF and contests in general. Well, you are half right. I think LSF captures the spirit of flying R/C sailplanes quite nicely while I still consider it somewhat of a blasphemy to dump out of a God-given thermal just to make a 10-minute max with landing points. I still remember the first contest I ever flew in---in the third round, I found a thermal and managed to stay in it ! Nothing noteworthy excepting that I had only been flying a short while and that had never happened to me before. My timer kept yelling at me to get it down or I'd loose points. By this time I had attracted a cheering section hollering in unison to get down in time. Well, there was no one else on my frequency so I responded: "TO HELL WITH THE CONTEST ! I FOUND A THERMAL! " And I was going to ride it out for what it was worth. I got an eleven minute flight out of it and was insufferably pleased with myself for at least a week. I had built a flyable sailplane, launched it, found a thermal all by myself, and stayed in it with no help or coaching. Up until then, my main objective was to launch the plane and try to get it back down intact (I took alot longer to learn to fly than anyone else that I know of).

Now, I'm considered at least competent in the skills of flying and some even consider me to be good. I'd known that I'd reached some sort of plateau when a total stranger (beginner) hands me his transmitter and asks me to "save it". Part of me is still delighted that I am able to do it. I do have trouble trying to instruct new pilots though since my flying skills are now entirely resident in the right half of my brain and the left half has trouble verbalizing the actions of the right half. I have the same trouble at work when someone sees me staring at a blank sheet of paper and asks what I'm doing. Why I'm composing an illustration and when I'm done, all I have to do then is ink in the lines---I've got to quit telling the truth and think up a plausible lie, because all the truth gets me are expressions that make me think the person is mentally measuring me for a "laughing jacket".

There is something to be said for the exquisite feeling one gets during a formation flight with a hawk or an hours-long cloud-hopping soar while lying in the grass. All this without feeling the need to drill a noisy hole in the sky. A spectator would see nothing but a slight movement of the pilot's thumb---but, my God ! If he could only see and feel what's going on in my mind !

G.A. Dees, Esq. Head Test Pilot
Lizard-Rip-Off Aeronautics
2309-B Walke Street
Virginia Beach, VA
23451

Herk Sore-Tech

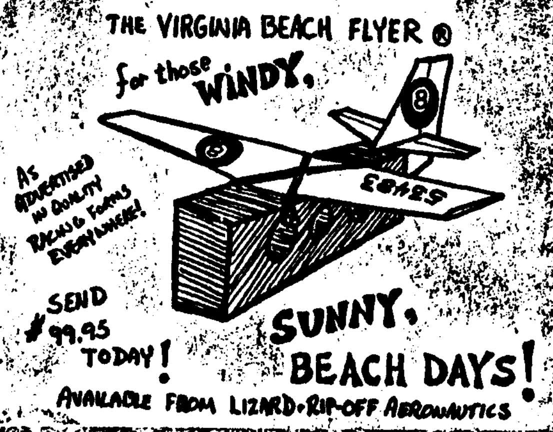

CONTENTS: 3 SELIG DRAWINGS
+ ORIGINALS


G.A.DEES